INVESTIGATIONS ON BISMUTH(III) AND LANTHANIDE(III) COMPLEXES- COORDINATION POLYMERS, MONOMERIC MOLECULES AND SECONDARY INTERACTIONS

A THESIS

SUBMITTED FOR THE DEGREE OF

DOCTOR OF PHILOSOPHY

BY

ORUGANTI ANJANEYULU

SCHOOL OF CHEMISTRY

UNIVERSITY OF HYDERABAD

HYDERABAD - 500 046

INDIA

November 2012

Dedicated to

My parents &

Uncle

(late) Ch.Venkateswarlu

CONTENTS

PART B

STATEMENT

I hereby declare that the matter embodied in this thesis is the result of investigations carried out by me in the School of Chemistry, University of Hyderabad, Hyderabad, under the supervision of Prof. K. C. Kumara Swamy.

In keeping with the general practice of reporting scientific observations, due acknowledgements have been made wherever the work described is based on the findings of other investigators.

Hyderabad

November 2012.

Oruganti Anjaneyulu

CERTIFICATE

This is to certify that the work described in this thesis entitled *''Investigations on Bismuth(III) and Lanthanide(III) Complexes-Coordination Polymers, Monomeric Molecules and Secondary Interactions"* has been carried out by Mr. Oruganti Anjaneyulu, under my supervision and the same has not been submitted elsewhere for any degree.

Hyderabad

November 2012.

Prof. K. C. Kumara Swamy

(Thesis supervisor)

Dean

School of Chemistry
University of Hyderabad
Hyderabad 500 046
INDIA.

ACKNOWLEDGEMENTS

I express my profound thanks to Prof. **K. C. Kumara Swamy**, my research supervisor, for his valuable guidance, encouragement and cooperation. He has been caring and quite helpful in improving my confidence, patience and communication skills.

I thank Prof. M. V. Rajasekharan, Dean, School of Chemistry for providing me the facilities needed for my research. I extend my sincere thanks to former Deans and all the faculty members for their cooperation on various aspects.

I would like to thank Prof. Anunay Samantha and Prof. Abani K. Bhuyan for their valuable suggestions and the moral support they gave me throughout my research work.

Special words of thanks to Prof. G. Umamaheswara Rao, Prof. P. Appa Rao, Prof. Anantha Krishnan, Prof. B. Rajasekhar, Prof. R. S. Sarraju, Dr. Vasuki, Dr. Satya Prakash, Dr. Ansari, Dr. Rajagopal, Dr. Debasish Acharya, Dr. Rajasree, Srinivas (Asst. Registrar), Sudhakar, Prasanna Kumar (Dy. Registrars) and Surya Narayana Raju for their support and personal rapport I had shared with them.

I am deeply indebted to all my teachers right from my school to the University for the excellent training I received throughout my academic career, especially to my teachers Profs. V. B. Mahale, B. Badami, V. K. Revankar, M. V. Kulkarni, I. M. Khazi, Rev. Fr. P. Anthony s.j., Drs. G. Sambasiva Rao, Balasundar Reddy, S. Prabhakar Rao, K. Subramanyeswara Rao, (*Late*) Sri Venkat Reddy, Pitchi Reddy, T. Venkat Rao and B. Rangaiah.

I also thank all the non-teaching staff of the School of Chemistry for their help in many ways. It is my privilege to acknowledge Dr. P. Raghavaiah, Mr. Sharma, Mr. Sai, Mr. Kumar, Mr. Jangaiah, Mr. Durgesh, Mr. Vara Prasad, Mr. Satyanarayana, Mr. Dilip, Mr. Bhaskar Rao, Mrs. Aisa Parwez, Mrs. Vijaya Lashmi, Mr. Vijaya Bhaskar and Krishna Rao.

I fondly cherish the company of my lab seniors Drs. Pavan, Manab, Balaraman, Prasad, Bhuvan, Phani, Venu, Rama Suresh and Sajna for all the good times we shared. I extend my special thanks to my current labmates Ramesh, Nagarjuna, Gangadhar, Srinivas, Prasad, Leela, Anitha, Siva Reddy and Dr. Anasuya for their help and cooperation whenever sought. My heart-felt thanks to my

beloved brother Dr. K. R. Roy, School of Life Sciences, UoH for his support, care and help in studying the biological activity for my compounds.

I would like to express my sincere gratitude to my friends Rev. Fr. Anand s.j., Surendranath Reddy, Bujji Reddy, Dr. Harish, Yugandhar, Dileep Reddy, Dr. Nageswara Rao, Ravi Kumar, Kishore, Sunkanna, Satya Narayana, Shakir Bilal, Maddileti, Deepthi, Sharada, Annapurna, Nivedita, Yedukondalu, Mallikarjuna Reddy, Peeraiah, Raghavendra Bakale, Santosh Surgond, Suresh Kulkarni, Deepak Hiremath, Sheetal Batakurki, Shobha Saidapur, Mamatha Hegde, Sudhakar Reddy, Subba Rao, Rammohan Reddy, Srikanth, Malli, Ranjith, Sumalatha Reddy, Ravi Kumar, Rajasekhar Reddy, Kasi Ramulu, Govindaih, Y. V. Ramesh, Venkata Ramulu, Manikyam, Nirmal Kumar, Wahab, Bhagath, Naga prasad, Chaitanya, Syam, Sandip and Pandu Ranga Reddy.

I thank all research scholars (seniors and present) of School of Chemistry and friends in UoH for the cheerful and enlivening atmosphere they maintained and for making my stay in the campus unforgettable.

I am grateful to the Council of Scientific and Industrial Research (CSIR, New Delhi) and Department of Science and Technology (DST, New Delhi) for financial support. I also thank DST for the Single Crystal X-ray Diffractometer Facility at the University of Hyderabad and UGC for providing many other research facilities.

I acknowledge with gratitude the unconditional love and support received from my cousins, M. Venkateswara Rao, C. V. Rama Krishna, C. V. Murali Krishna, Sujatha, Mukunda, Jayasimha and Govardhan right from my childhood.

I thank my wife, Padmavathi, for her love and support and for her patience to bear me during my thesis writing.

Words fail to express my gratitude and heartfelt indebtedness both on personal and professional fronts to Prof. Ramakrishna Ramaswamy for his encouragement and moral support.

Finally, yet importantly, I would like to express my heartfelt thanks to my beloved parents **O. Venkatalaxmi and O. Seshaiah,** my uncles C. V. Ramanaiah (*Late*) Ch. Venkateswarlu and Ch. Narasaiah for the blessings and to my sister (Anjali) for their kindness and support.

Oruganti Anjaneyulu

LIST OF PUBLICATIONS

1. Coordinatively polymeric and monomeric bismuth(III) complexes with pyridine carboxylic acids

   O. Anjaneyulu, T. K. Prasad and K. C. Kumara Swamy*

   Dalton Trans., 2010, **39**, 1935–1940.

2. Tris(4-oxy-pyridinium)nitrato lanthanide complexes $[M(4\text{-}O\text{-}C_6H_4NH)_3(NO_3)_2(H_2O)_2][NO_3]$ {M = La, Ce, Pr, Nd, Eu, Gd} – Synthesis, properties and structural characterization

   O. Anjaneyulu, T. K. Prasad and K. C. Kumara Swamy*

   Inorg. Chim. Acta, 2010, **363,** 2990–2995.

3. Studies on bismuth carboxylates- Synthesis and characterization of a new structural form of bismuth(III) dipicolinate

   O. Anjaneyulu and K.C. Kumara Swamy*

   J. Chem. Sci., 2011*,* **123**, 131-137

4. Structural motifs in phenylbismuth heterocyclic carboxylates – secondary interactions leading to oligomers

   O. Anjaneyulu, D. Maddileti and K. C. Kumara Swamy*

   Dalton Trans., 2012, **41**, 1004-1012

5. Investigations on synthesis, characterization and anti-tumor activity of lanthanide dipicolinates

   O. Anjaneyulu, K. R. Roy and K. C. Kumara Swamy*

   (Manuscript under preparation)

POSTERS PRESENTED IN SYMPOSIA

1. Secondary Interactions in Phenylbismuth Heterocyclic Carboxylates

   O. Anjaneyulu, D. Maddileti and K. C. Kumara Swamy*

   MTIC-XIV (December 10 – 13, 2011**)**, University of Hyderabad, Hyderabad.

2. Synthesis and Characterization of Bismuth/ Lanthanide Pyridine Carboxylates- Investigations on Gadolinium Dipicolinate as Anticancer Agent

   O. Anjaneyulu, D. Maddileti and K. C. Kumara Swamy*

   "CHEMFEST 2011", School of Chemistry, University of Hyderabad, Hyderabad.

3. Preparation, characterization and emission spectral studies of $Ln_{2/3}ZnP_2O_7$ (Ln = Pr, Sm, Nd, Dy, Eu)

   O.Anjaneyulu , B.Vijaya Kumar, M.Vithal and K.C.Kumara Swamy*

   MTIC-XII (December 6 - 8, 2007), IIT Madras, Chennai.

Synopsis

This thesis is divided into two parts: **Part-A** and **Part-B**. **Part-A** deals with (a) novel bismuth pyridine-carboxylates (coordination polymers and monomeric/ dimerc structures) using bismuth nitrate or ammonium bismuth citrate, (b) phenylbismuth heterocyclic carboxylates using $BiPh_3$– secondary bonding interactions in the products, and (c) synthesis and characterization of $BiVO_4$. In **Part-B**, (a) synthesis and structural characterisation of lanthanide oxopyridinium/ dipicolinate complexes, (b) anticancer activity of gadolinium dipicolinate so obtained, and (c) synthesis of lanthanide(III)-zinc(II) pyrophosphates $Ln_{2/3}ZnP_2O_7$ are discussed. Each part is subdivided into three chapters: (a) Introduction (literature survey), (b) Results and Discussion, and (c) Experimental Section. The compounds obtained in the present study are, in general, characterised by mp, IR and UV-Vis (solid/ solution), NMR (^1H) and TGA techniques followed by elemental analyses and single crystal X-ray structure determination, where possible. References are compiled at the end of each part.

PART-A

In Chapter 1, a review of literature on aspects relevant to this part is presented. In Chapter 2, the results obtained on these aspects are discussed while in Chapter 3, the experimental details are presented. Important results of this part are outlined here.

(i) Synthesis and structures of bismuth carboxylates from bismuth nitrate

In an attempt prepare the alternatives to bismuth metal based drugs available in the market, we made an attempt to synthesise three bismuth carboxylates $[Bi(2\text{-}O_2C\text{-}C_5H_4N)_3]_n$ (**1**), $\{Bi[(2,6\text{-}O_2C)_2C_5H_3N)][(2\text{-}HO_2C\text{-}6\text{-}O_2C)C_5H_3N].H_2O\}_n$ (**2**) and $Bi(O_2CC_9H_6N)_2(O_3N)(O_2CC_9H_6NH).2H_2O$ (**3**) [Fig. 1] by treating bismuth nitrate with the appropriate ligand in 1:3 molar ratio.

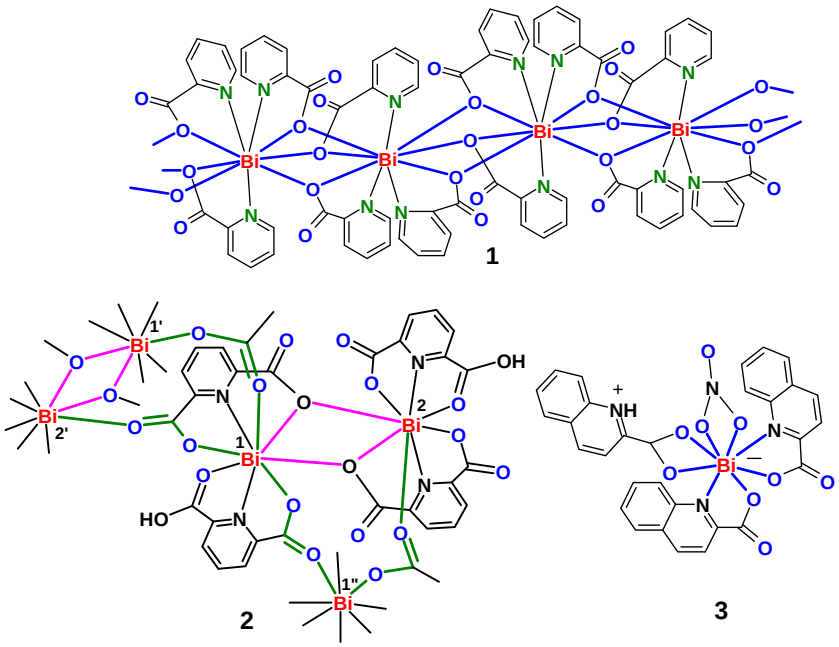

Figure 1. Structural drawings of **1**-**3** highlighting the coordination around bismuth atoms [water molecules are not shown].

Compound **1** crystallised in the space group $P2_1/n$. The central bismuth has a tricapped trigonal prismatic coordination [Fig. 2]. The lone pair of electrons on bismuth appears to be stereochemically inactive. Overall, the compound is a coordination polymer with three bridging oxygen atoms between adjacent bismuth centres.

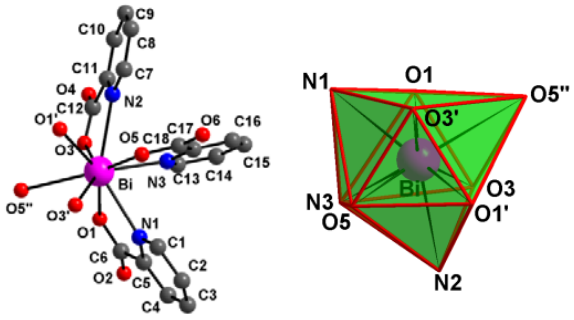

Figure 2. X-ray structure of **1**. Asymmetric unit showing the coordination around bismuth and polyhedron showing tricapped trigonal prismatic bismuth centre.

Compound **2** [Fig. 3] is also a coordination polymer but the structural motif is quite different from that observed in **1**. Although there are two distinct bismuth atoms in the asymmetric unit, both exhibit eight coordination with dodecahedral geometry. A major difference between the two bismuth atoms lies in the longest

bond length: While for Bi(1), it is the coordinate bond to the carboxylic acid C=O [i.e. Bi(1)-O(6)], for Bi(2) it is a bridging oxygen of the [Bi_2O_2] skeleton [Bi(2)-O(2)]. Also, two Bi(1) and only one Bi(2) form a larger ring as mentioned before.

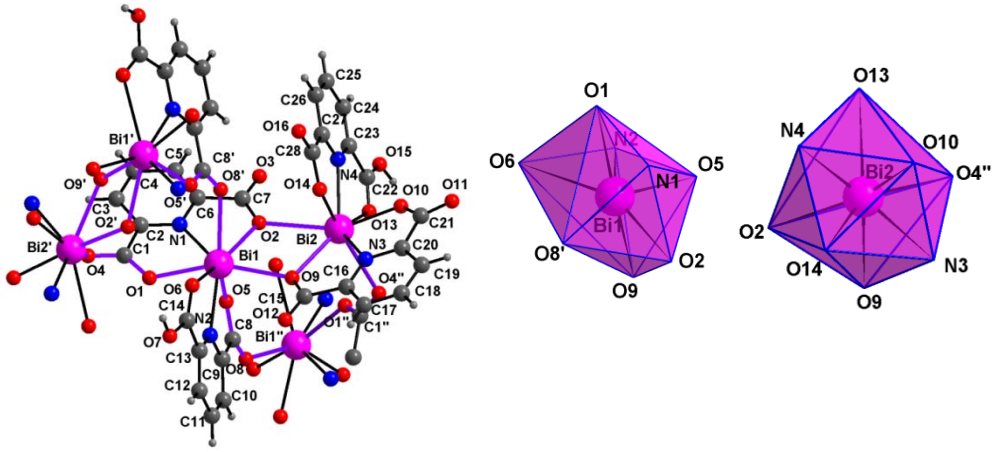

Figure 3. Drawings representing the X-ray structure of **2**. Left: Asymmetric unit along with parts of other units to show the overall skeleton. Right: Polyhedra showing dodecahedral geometry around the two bismuth atoms of the asymmetric unit.

Unlike **1** and **2**, compound **3** is monomeric [Fig. 4], most likely because of the sterically bulkier quinoline carboxylate moiety not permitting the oligomerization/polymerization. The distortion in geometry from the more regular dodecahedron may, at least in part, be due to the lone pair of electrons on bismuth.

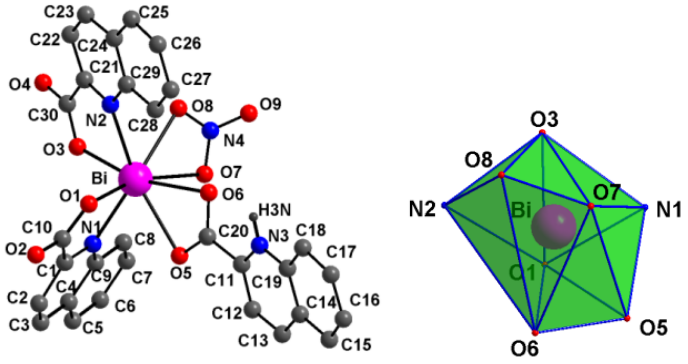

Figure 4. Drawings representing the X-ray structure of **3**. Left: asymmetric unit. Right: polyhedron showing slightly distorted dodecahedral geometry.

The TGA data show that compound **1** is perfectly stable up to ~360 ^{o}C, while compound **2** behaves differently, with the non-coordinated water molecules coming

off before the decomposition sets in. Compound **3** shows a more interesting behaviour with its melting point almost coinciding with decomposition/sublimation at ca ~220 ^{o}C (consistent with its lower melting point). Decomposition of all the compounds leads to Bi_2O_3.

(ii) Bismuth- dipicolinate prepared from ammonium bismuth citrate

The reaction of ammonium bismuth citrate with dipicolinic acid in water led to compound $\{[Bi((2,6\text{-}O_2C)_2C_5H_3N)((2\text{-}HO_2C\text{-}6\text{-}O_2C)C_5H_3N)(H_2O)]_2.5H_2O\}_n$ (**5**) which is different from $\{Bi[(2,6\text{-}O_2C)_2C_5H_3N)][(2\text{-}HO_2C\text{-}6\text{-}O_2C)C_5H_3N].H_2O\}_n$ (**2**) obtained by using bismuth nitrate pentahydrate and dipicolinic acid. Compound **2** is a coordination polymer while **5** is a dimeric molecule. The structural drawings for the dimeric unit in **5** are given in Figure 5. In **5**, the coordination number at bismuth is nine and the geometry can be described as distorted tricapped trigonal prism.

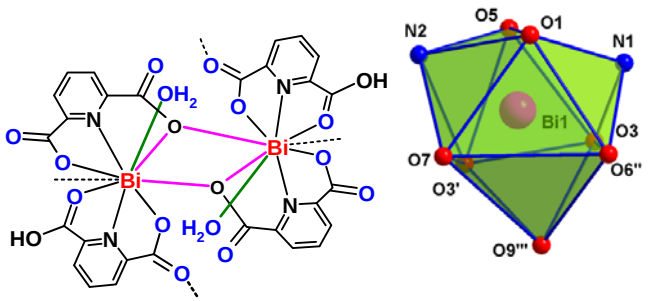

Figure 5. Left: Molecular structure of the dimeric unit in **5**. Right: Polyhedron showing the distorted tricapped trigonal prismatic geometry at bismuth.

(iii) Synthesis and structures of bismuth- pyridine carboxylates from $BiPh_3$

The reaction of $BiPh_3$ with 3-hydroxy picolinic acid (1:3 molar ratio) in ethanol resulted in $[PhBi(2\text{-}O_2C\text{-}3\text{-}(OH)C_5H_3N)_2(2\text{-}O_2C\text{-}3\text{-}OHC_5H_3NH)]$ (**6**). Compound **6** is monomeric in bismuth having a BiN_2O_4 skeleton with a pentagonal pyramidal geometry as shown in Figure 6. A closer look at the structure reveals that there is an additional weak but discernible ***secondary interaction*** between the coordinated O7 and bismuth atom of a second molecule [distance 3.449(5)Å, sum of van der Waals distances 3.9 Å], in the direction of the lone pair, leading to a weakly held dimer as shown in Figure 6 (right). Use of pyridine as the solvent in the 1:3 stoichiometric reaction of $BiPh_3$ and 3-hydroxy picolinic acid at room temperature resulted in an entirely different product, [(Bi(2-O_2C-3-

$(OH)C_5H_3N)_4)(C_5H_5NH)(C_5H_5N)]$ (**8**). The coordination number around bismuth is eight and we may describe the geometry as distorted dodecahedron as shown in Figure 7.

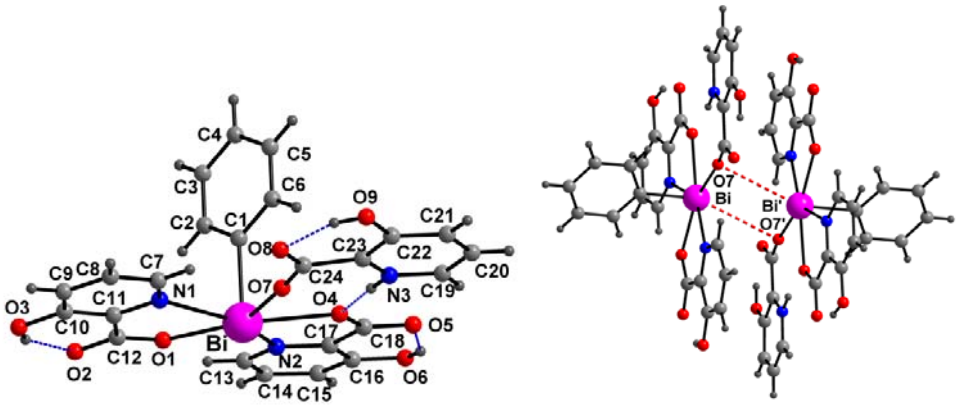

Figure 6. Left**:** Molecular structure of compound **6**. Right: Structure of **6** showing weak dimer formation *via* additional Bi…O interactions**.** The Bi-O8 distance is 4.592 (6) Å.

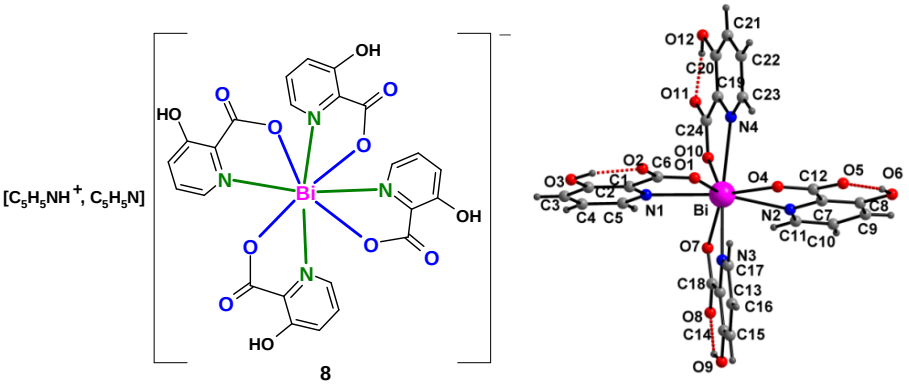

Figure 7. Left: Molecular structure of the anion in compound **8**. Right: Intramolecular O-H…O hydrogen bonding is also shown.

The compound $[PhBi(2\text{-}O_2C\text{-}C_4H_3N_2)_2(2\text{-}O_2C\text{-}C_4H_4N_2).H_2O]$ (**9**) was obtained by the 1:3 reaction of $BiPh_3$ and pyrazine-2-carboxylic acid in refluxing ethanol. To our knowledge, this is the first structural report on bismuth pyrazine-2-carboxylate. Taking into consideration only the stronger interactions, the geometry at bismuth may still be treated as pentagonal pyramid [Fig. 8]. What is unique in the system however, is that the bismuth atoms of two molecules come close to N2' of a second molecule [distance 3.509(8) Å; sum of van der Waals distances 4.0 Å]

resulting in a weak dimer. Although this distance is not in the realm of any significant bonding interactions, the fact that the nitrogen atom is located on the same side as the expected region for the lone pair of electrons on bismuth is unusual.

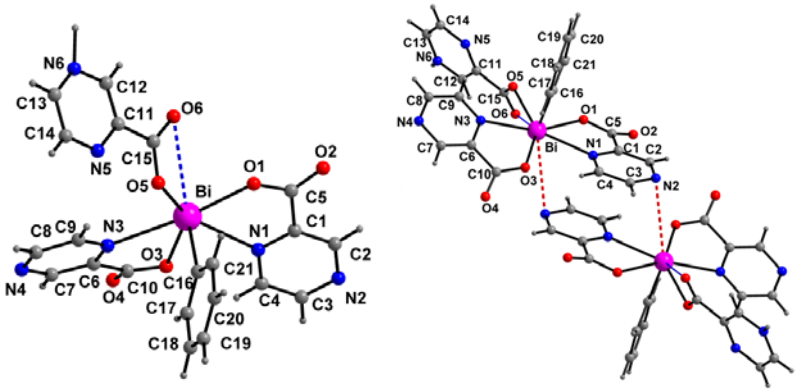

Figure. 8. Left**:** Molecular structure of compound **9**. Right: Dimer formation via weak Bi…N interaction in **9**.

Quinoline-2-carboxylic (quinaldic) acid is expected to react in a manner analogous to picolinic acid. However, the 1:3 stoichiometric reaction of $BiPh_3$ with this acid, conducted in refluxing ethanol afforded the bis-carboxylated product $[PhBi(2\text{-}O_2C\text{-}C_9H_6N)_2.H_2O]$ (**10**). The primary coordination number of bismuth is 5 [Fig. 9]. This basic geometry can be construed as square pyramid with quinaldate N/O at the base of the pyramid. Curiously though, compound **10** forms a weakly held ***dimer*** with two additional Bi-O interactions involving O3 and O4 [Bi1...O3' 3.347(5)Å; Bi...O4' 3.495(7) Å; symm. equiv.: –x, 1-y, 2-z] in the direction of the lone pair of electrons, as shown in Figure 9.

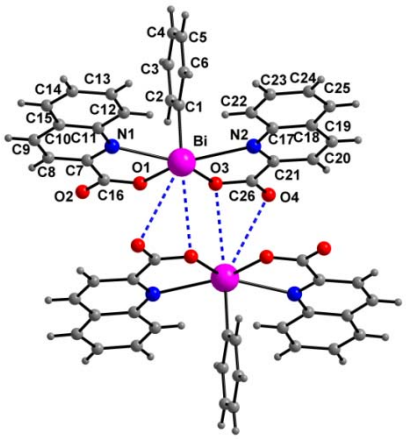

Figure 9. Molecular structure of compound **10** excluding the non-coordinated water molecule.

To our knowledge, structural chemistry of Bi(III) compounds of furan-2-carboxylic (furoic) acid and thiophene-2-carboxylic acids is not reported prior to our work. We have isolated crystalline [$Ph_2Bi(O_2C\text{-}C_4H_3O)$] (**11**) by the reaction of $BiPh_3$ and 2-furoic acid (used 1:3 molar ratio) in ethanol at room temperature (25 ^oC). Bismuth-thiophene carboxylates [$Ph_2Bi(O_2C\text{-}C_4H_3S)$] (**12**) and [$PhBi(O_2C\text{-}C_4H_3S)_2]_2$ (**13**) were obtained from a procedure similar to that for compound **11**.

In compound **11** [Fig. 10], primary coordination number of bismuth can be considered to be five with the longest Bi-O1' bond being 2.981(5)Å. Excluding the weaker Bi...O3 interaction [3.32(2) Å] to the furoate oxygen, the geometry at bismuth can be considered to square pyramidal with C7 as the apical bond and the remaining atoms C1, O1, O1' and O2' at the base. It can be noted that the carboxylate acts as both a bridging and a chelating ligand. The resulting entity is a coordination polymer. Unlike compound **11**, compound **12** was obtained only in trace quantities in a pure state. There are three molecules in the asymmetric unit (not shown here). As observed in the structure of **11**, the carboxylate moiety acts both as a chelating and as a bridging ligand leading to a polymeric chain. The coordination geometry at bismuth in **12** is rather irregular, but may be approximated as square pyramid with C1 (for Bi1), C8 (for Bi2) and C41 (for Bi3) at the apices of the corresponding bismuth atom.

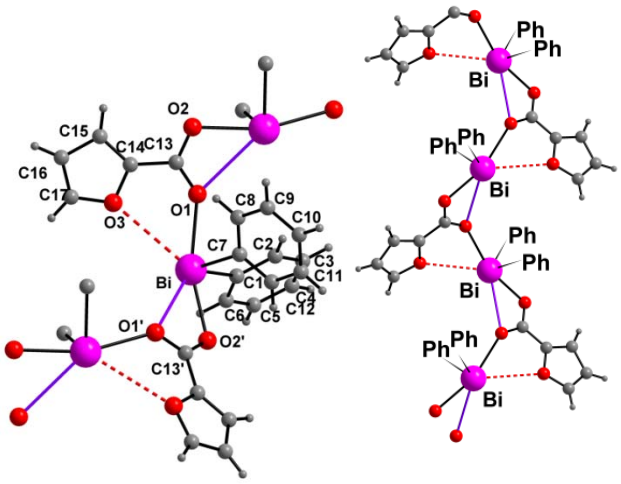

Figure 10. Left: Molecular structure of compound **11**, showing the weaker Bi…O interaction also. Right: The polymeric chain in **11**.

Compound **13** compound has two carboxylates per bismuth. One carboxylate is purely chelating while the other is involved in both chelation and bridging [Fig. 12]. The molecule thus can be considered to be a dimer of [PhBi(O_2C-$C_4H_3S)_2$]. The primary coordination sphere around bismuth has five oxygen atoms and one carbon atom but the geometry is non-octahedral. The overall geometry involving these groups is pentagonal pyramid [Fig. 12, right]; however there are interesting secondary Bi…S interactions in the structure (not shown here).

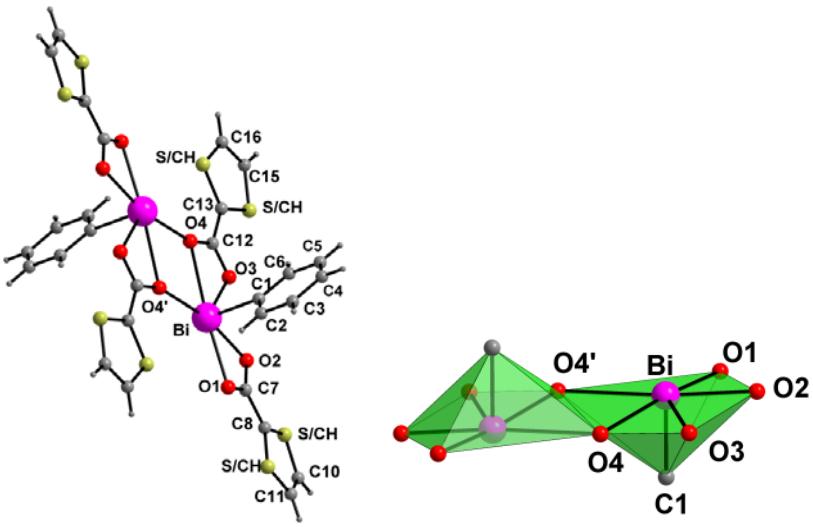

Figure 12. Molecular structure of compound **13.** Left: labelled structure showing the dimeric unit. Right: Polyhedra depicting the primary coordination sphere of pentagonal pyramid around bismuth.

The TGA data of compound **6** is stable up to ~210 °C and complete decomposition occurs near to 400°C. For compound **8** at 150 °C, pyridine and protonated pyridine are eliminated. Remaining decomposition pattern is similar to **6**. Compound **9** behaves differently, with the non-coordinated water molecules coming off and decomposition for this molecule starts at 270 °C and completes at 350 °C. In all the cases the final product of decomposition is most likely Bi_2O_3.

(iv) Bismuth vanadate ($BiVO_4$): A new simple synthetic route

Bismuth vanadate ($BiVO_4$; **14**) is prepared from bismuth nitrate and ammonium (**14a**) or sodium vanadate (**14b**) in water under reflux conditions. The phase purity of the sample was confirmed by powder X-ray (Fig. 13, left). The energy-dispersive X-ray spectrum (EDS) analysis confirms the formation of the

stoichiometric $BiVO_4$. The Raman spectra of the compounds between 10 and 1400 cm^{-1} are shown in Figure 13 (right). Each spectrum is dominated by an intense Raman band at 828 cm^{-1} assigned to ν_s(V–O), along with other peaks. Both the materials **14a** and **14b** are found to have nearly same E_g of 2.58 eV [calculated using the plot of $\alpha h\nu^2$ vs. photon energy ($h\nu$)] which is slightly higher than 2.4 eV reported from other groups.

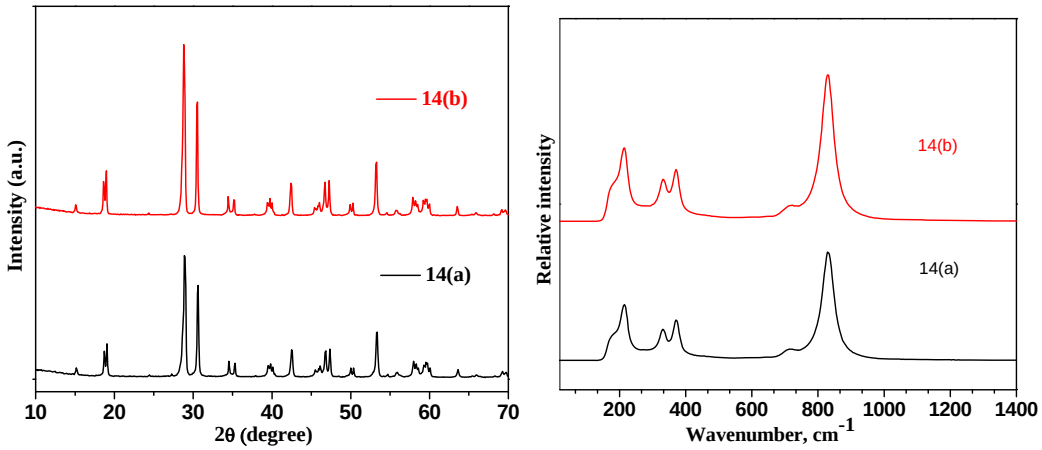

Figure 13. Left: Powder X-ray pattern, Right: Raman Spectra of $BiVO_4$ (**14a** and **14b**)

PART-B

Chapter 4 pertains to the literature on lanthanide oxopyridinum/ dipicolinate complexes. Chapter 5 describes the results obtained in the present study. Chapter 6 is the experimental section. Important results are outlined below.

(i) Synthesis and spectral data of lanthanide-4-hydroxy pyridine complexes

Synthesis of the lanthanide hydroxypyridine compounds [$M(4\text{-}O\text{-}C_6H_4NH)_3(NO_3)_2(H_2O)_2][NO_3]$ {M = La (**3**), Ce (**4**), Pr (**5**), Nd (**6**), Eu (**7**) and Gd (**8**)} was accomplished by the simple reaction of the corresponding nitrates with three mole equivalents of 4-hydroxypyridine in ethanol or water. All the compounds **3-8** crystallized in the chiral space group $P2_12_12_1$. Molecular structures of the representative compounds **6** and **7** are shown in Figure 14. One of the interesting features in these structures is the reversal of stereochemistry between the structures of the neodymium compound **6** and the europium compound **7** (as well as **3-5**) [Fig. 14, bottom]. Since each of these structures is in a chiral space group, this result

appears to be a case of spontaneous resolution. As per TGA, complete removal of organic residues did not occur till 400 ^{o}C.

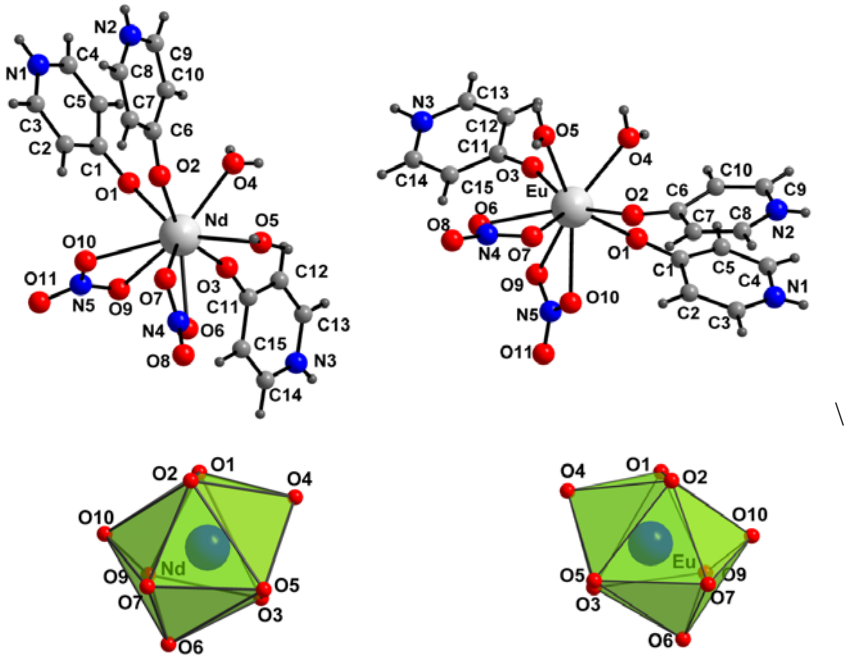

Figure 15. Top: Molecular structures of the cationic part in **6** and **7**; the anion is nitrate (not shown). Bottom: Polyhedral representation around the central atom in **6** and **7** showing the opposite stereochemistry.

(ii) Lanthanide dipicolinates: Simplified synthetic route and X-ray structures

As a continuation of our studies on bismuth dipicolinates, which also has a large size and exhibits +3 oxidation state, we became interested in lanthanide dipicolinates of the formula $\{Ln[(2\text{-}HO_2C\text{-}6\text{-}O_2C)C_5H_3N]_3\}$ $1.5H_2O$ [Ln = Sm (**9**), Gd (**10**), Eu (**11**), Dy (**12**), Tb (**13**) and Tm (**14**)]. These were synthesized by the reaction of $Ln(NO_3)_3.xH_2O$ with pyridine-2,6-dicarboxylic acid in water under reflux conditions for 4 h. All these compounds crystallize in the same space group ($P\bar{1}$) with essentially the same structure and for this reason; we shall concentrate on only the gadolinium complex **10**. There are two molecules in the asymmetric unit. In each case, gadolinium ion is surrounded by three dipicolinate ligands (Fig. 16). The ligand coordinates to the gadolinium ion through pyridine nitrogen and carboxylate oxygen in a five-membered chelating manner such that coordination number of lanthanide ion is 9. The bulk purity of the crystals obtained is compared by single crystal data and powder data thus obtained are in good agreement with each other.

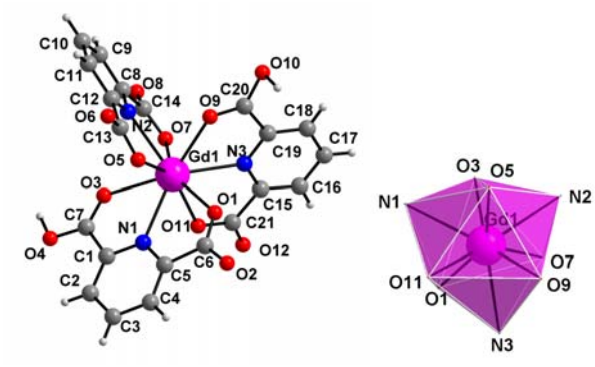

Figure 16. Molecule 1 (in the asymmetric unit) and polyhedron showing distorted tricapped trigonal prism geometry around Gd(III) in the structure of **10**.

(iii) Antitumor activity of the Gadolinium dipicolinate (compound 10)

Preliminary screening was done on cancer cell lines of different origins. Compound **10** showed significant effect on the proliferation of Hepatocellular carcinoma cells (HepG2). HepG2 cells were treated with **10** (10, 25, 50,100, 250, 500, 1000 μM) for 48 h and cell proliferation was determined by the MTT assay. A 50% inhibition in HepG2 cell proliferation was observed at 250 μM concentration of **10** in 48 h.

Western-blot analysis was performed with cytoplasmic extracts devoid of mitochondria, with anti-cytochrome *c* mouse monoclonal antibodies to detect cytochrome *c* release. We observed a time dependent increase in cytochrome *c* release in the cells treated with **10** (250 μM) and no release was observed in control cells (Fig. 17a). Upon treatment with **10** (250 μM) changes in the expression of Bcl-2 and BAX were observed. Bcl-2 protein expression decreased and pro-apoptotic protein BAX levels increased in a time dependent manner in **10** treated cells compared with the untreated controls (Figures 17b, 17c). Increase in the cell number in sub G0/G1 phase with treatemnt is characteristic feature of apoptosis induction. HepG2 cells treated with **10** (100 and 250 μM) for 48 h were analysed on FACS for the cell cycle alterations. Typical sub-diploid apoptotic peaks were observed in **10** treated cells. Control cells showed a G1, followed by S and G2/M-phases. Only 1.17% of the control cells showed hypodiploid DNA (Fig. 18a). Cells with hypodiploid DNA increased in **10** treated cells. Hypodiploid cells were 23.96% in 100 μM and 47.76% 250 μM in treated cells (Figures 18b and 18c). Thus this gadolinium dipicolinate compound has shown promising effect on the proliferation of hepatocellular carcinoma cells.

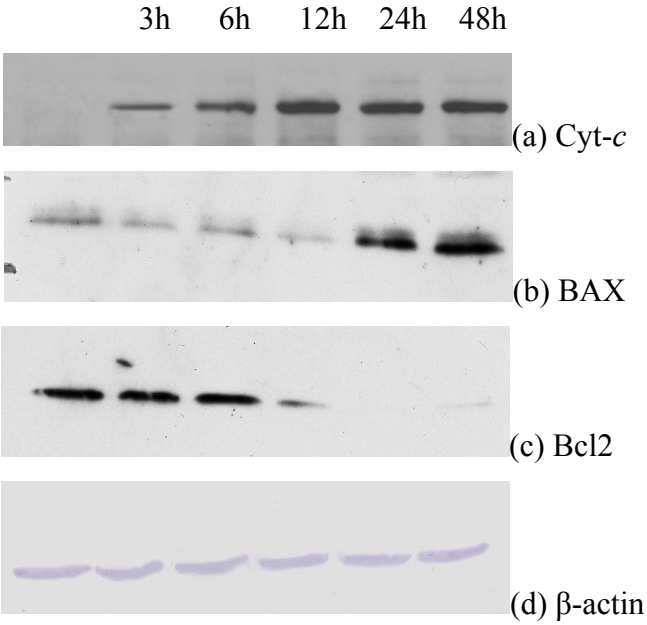

Figure 17. Time dependent expression of proteins involved in cell death process in compound **10** treated HepG2 cells (Western blot analysis)

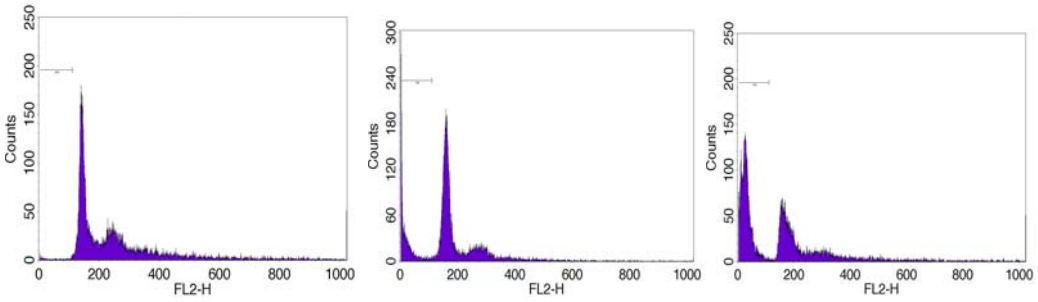

(a) (b) (c)

Figure 18. Cell cycle alterations of **10** treated HepG2 cells (see txt for details).

(iv) Attempted preparation of lanthanide zinc pyrophosphates, $Ln_{2/3}ZnP_2O_7$ [Ln = Pr (15), Sm (16), Nd (17), Dy (18) and Gd (19)]

In our earlier experiments using domestic microwave oven, we were able to obtain pure samples of $Ln_{2/3}ZnP_2O_7$ [Ln = Pr (**15**), Sm (**16**), Nd (**17**), Dy (**18**) and Gd (**19**)] by treating $Na_2ZnP_2O_7$ with the *in situ* prepared lanthanide chlorides. However, since the microwave oven used was a domestic one, for reproducibility, later investigations were performed by using a muffle furnace [600 ^oC/ 6 h]. To our dismay, the results obtained using the microwave were not very much reproducible by using the furnace in terms of the purity of the samples as evidenced by powder X-ray for the samples.

==========

PART A

BISMUTH(III) HETEROCYCLIC CARBOXYLATES-COORDINATION POLYMERS, MONOMERS, SECONDARY INTERACTIONS AND BISMUTH VANADATE ($BiVO_4$)

Chapter 1

INTRODUCTION

1.1 General Introduction: About Bismuth

Bismuth was first discovered in early 15th century and was established as an element by Potts and Bergmann in 1739.[1] Bismuth is the heaviest member of group 15 and the heaviest stable element in the periodic table. Although it belongs to the group 15, decreasing availability and increasing diffuseness of the outermost 's' electrons makes the +5 oxidation state less stable for bismuth when compared to phosphorus, arsenic and antimony.[2,3] Thus, the chemistry of bismuth is dominated by +3 oxidation state.

1.2 Bio-utility of Bismuth Compounds

Despite being compounds of a heavy metal, several bismuth derivatives have been used in medicine for more than two centuries.[4] Louis Odier in 1786 reported the first account for internal administration of bismuth compound to treat dyspepsia.[4b] Felix Balzer in 1889 first discovered that bismuth might be useful as an antisyphilitic agent.[4c] In 20th century, several bismuth compounds (subnitrate, subgallate, subcitrate, tartrate, subcarbonate and subsalicylate) were used to treat syphilis, hypertension, infections, skin conditions and gastrointestinal disorders.[4d,e] During the last four decades, bismuth compounds have been used medicinally in two major areas: antimicrobial and anticancer. They have also been used for the treatment of various gastrointestinal disorders, including gastric and duodenal ulcers, dyspepsia, diarrhoea, SARS and colitis.[5,6] Three compounds of bismuth, bismuth subsalicylate (BSS, Pepto-Bismol, 1.**1**), colloidal bismuth subcitrate (CBS, De-Nol, 1.**2**) and ranitidine bismuth citrate (RBC or Tritec, 1.**3**) are used around the globe for the treatment of gastrointestinal disorders which are related to the infection by the bacterium *Helicobacter pylori (H. pylori). H. pylori* produces nickel containing enzyme urease which catalyses the hydrolysis of urea to ammonia and carbon dioxide (Scheme 1.1). Thus produced urea has cytotoxic effects on the mammalian cells within the gastric epithelium. However, the mechanism of inhibition of ulcer by bismuth compounds is not clear as yet.[4g,h]

Scheme 1.1

1.3 Bismuth Carboxylates Relevant to Medicine

Bismuth carboxylates and their partially hydrolysed products have long been recognized as important compounds in chemotherapy. In order to understand their activity, a sizeable number of reports on structural as well as biochemical aspects have emerged during the past couple of decades.[4f,7] Bismuth subsalicylate and colloidal bismuth subcitrate are two important pharmaceutical agents. Bismuth subsalicylate (BSS) can be formulated approximately as $C_7H_5BiO_4$ and is rather insoluble in water. It is a colloidal substance obtained by hydrolysis of bismuth salicylate $[Bi\{C_6H_4(OH)CO_2\}_3]$. For BSS, only $[Bi_{38}O_{44}(Hsal)_{26}(Me_2CO)_{16}(H_2O)_2]\cdot(Me_2CO)_4$ (1.**4**) and $[Bi_9O_7(Hsal)_{13}(Me_2CO)_5]\cdot(Me_2CO)_{1.5}$ (1.**5**) are good structural models.[8] Colloidal bismuth subcitrate (CBS) has relatively higher solubility in water. In the gastric juice, it is converted to bismuth oxychloride and citric acid.[9] Most of the subcitrate complexes contain the stable $[Bi(cit)_2Bi]^{2-}$ dimer/s with additional O^{2-}, OH^- and H_2O ligands (Fig. 1.1; cit = $C_6H_4O_7^-$). Ranitidine bismuth citrate (RBC) is a relatively more recent addition with higher water solubility but the details on its complete structure are not available. However, the acidity (p*K*a1 of *ca* 1.5 for Bi^{3+}) and ability of the metal centre to readily expand the coordination sphere makes rationalization of the biological action quite challenging. These factors, in conjunction with the lability of the ligands, often lead to difficulties in controlling hydrolysis of molecular complexes. The net result is formation of the "BiO^+" cation and/or coordination oligomers or polymers, which are difficult to characterize.[10,11] The sensitivity of bismuth carboxylate complexes to water has been assuaged in many instances by the incorporation of N, O or S donor atoms into the ligands, which may mimic bismuth binding sites in biologically active surroundings.[4f,6]

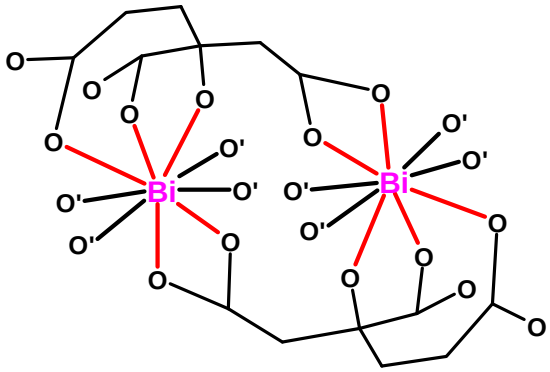

Figure 1.1 $[Bi(cit)_2Bi]^{2-}$ Dinuclear subunit normally found in bismuth citrate compounds; O' represents oxygen atom from citrate or water molecule. The terminal 'O' atoms of the citrate group are further connected to form the coordination polymer chain. The bismuth centre can also have coordination number of 8 with one of the acyclic ligands being absent.

1.3.1 Bismuth subsalicylate (BSS)

In the early 1900's, two of every 10 children used to die before the age of four from the illness "Cholera infantum". Characteristics of this disease are diarrhea and stomach upset. In the year 1900, a physician in New York prepared a medicine from bismuth subsalicylate (BSS), zinc salts, oil extracts of the winter green and a red dye. This preparation was called "Mixture Cholera Infantum." This became successful for the treatment of above illness. Norwich Pharmacal Company (Norwich, NY) started the manufacture of this drug and demand has increased for this. They have changed the name to bismosal and then to Pepto-Bismol.[8,12] Salicylic acid (1.**6**) plays an important role in the preparation of peptobismol and hence we need to know various coordination modes of this, after deprotonation, with metal [cf. Fig .1.2].

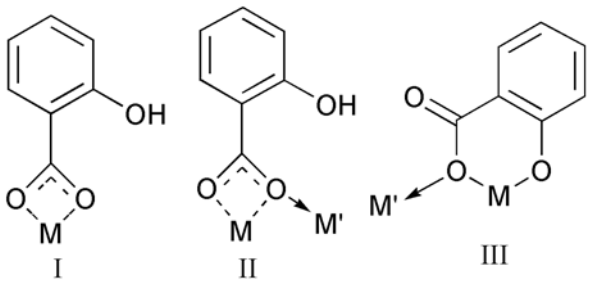

Figure 1.2. Different coordination modes of salicylate anion/dianion

Many researchers have tried to obtain mimics of the structure of BSS. Andrews *et al* reported the synthesis and structural elucidation of two bismuth salicylates $[Bi_{38}O_{44}(HSal)_{26}(Me_2CO)_{16}(H_2O)_2]\cdot(Me_2CO)_4$ (1.**4**) and $[Bi_9O_7(HSal)_{13}(Me_2CO)_5]\cdot(Me_2CO)_{1.5}$ (1.**5**).[8] As described by the authors, at the heart of the cluster in 1.**4** is a central Bi_6 octahedron in which the six Bi atoms and symmetry equivalents, are bound to only oxide ions. Surrounding this are four further Bi_6 octahedra, which share edges with each of the four equatorial edges of the central Bi_6, thus forming a planar cross of five octahedra. Above and below this plane are four further Bi_6 octahedra, joined at a single vertex which is also one of the axial Bi atoms of the central Bi_6 octahedron. Thus, each of these four octahedra shares four edges with neighboring Bi_6 octahedra. This accounts for all 38 Bi atoms (24 external and 14 internal). The Bi_9 clusters in compound 1.**5** comprise a central Bi_6 octahedron but with only seven of the eight trigonal faces capped by an O atom, as shown in Figure 1.3. Three additional Bi atoms protrude from the core and are connected through a bridging μ_4-O atom. The cores of 1.**4** and 1.**5** are surrounded by 26 and 13 salicylate ligands respectively. The bonding to the outlying Bi(III) centres corresponds to highly complex bridging modes (Fig. 1.3) with no evidence of any interaction with the *ortho*-hydroxy oxygen atoms.

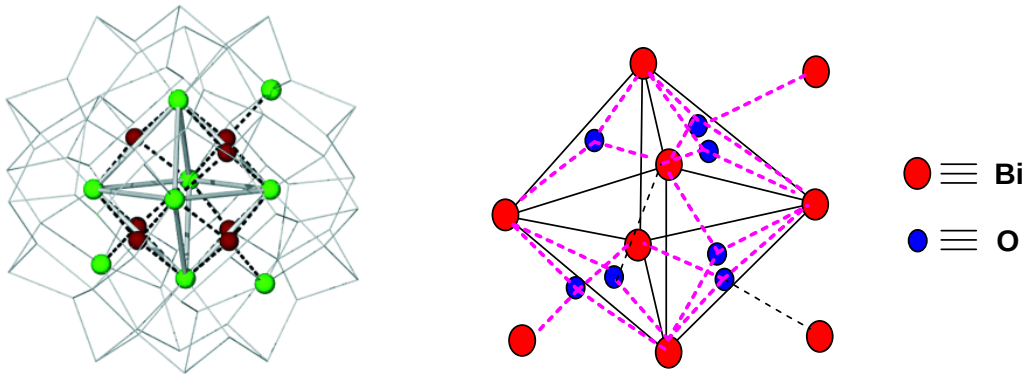

Figure 1.3. Left: Structure of the $Bi_{38}O_{44}$ core of $[Bi_{38}O_{44}(HSal)_{26}(Me_2CO)_{16}(H_2O)_2]$ (1.**4**), with Bi_9O_7 at the heart of the core [cf. ref. 8]. Right: Structure of the Bi_9O_7 core of $[Bi_9O_7(HSal)_{13}(Me_2CO)_5]$ (1.**5**), showing the octahedral arrangement of the Bi atoms with seven octahedral faces capped by an oxygen atom. Three Bi atoms extend the core bound to a capping O atom (green sphere = Bi, red sphere = O). Redrawn using data from ref. 8.

Whitmire's group reported the bismuth salicylate $[Bi(Hsal)_3]_n$ (Hsal = O_2C-C_6H_4-2-OH), (1.**7**) which was prepared from the stoichiometric reaction between triphenylbismuth and salicylic acid in refluxing toluene. To avoid hydrolysis, these complexes were trapped with ligands like 2,2'-bipyridine (bipy) or 1,10-phenanthroline (phen) leading to the complexes $[Bi(Hsal)_3(bipy)\cdot C_7H_8]_2$ (1.**8**) and $[Bi(Hsal)$-$(sal)(phen)\cdot C_7H_8]_2$ (1.**9**), respectively.[6d] In compound 1.**8**, each bismuth contains three salicylates, two of them coordinate to metal through 4-membered chelate ring and one acts as bridging ligand. Thus the coordination number of Bi is 9. In contrast to 1.**8**, in compound 1.**9**, one salicylate is coordinated to the metal centre through the carboxylate group and another salicylate coordinates through both phenolic and carboxylic oxygen atoms to form a five membered chelate ring. The carboxylate group of the doubly deprotonated salicylate ligand bridges between two metal centres, bringing the coordination number of the metal to seven (Fig. 1.4).

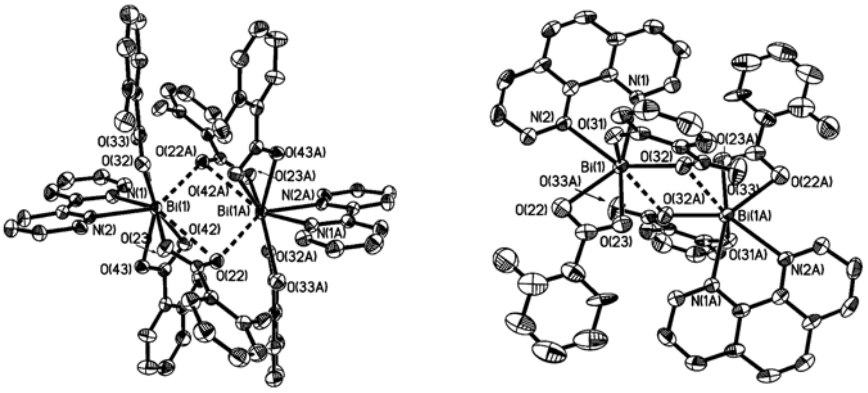

Figure 1.4. ORTEP representations of compounds 1.**8** (Left) and 1.**9** (Right) [cf. ref. 6d]. Bridging interactions are represented by broken lines.

Andre *et al* have reported the mechanochemical synthesis of bismuth subsalicylate from Bi_2O_3 and salicylic acid through ion- and liquid-assisted grinding (ILAG) method.[13] Rectangular crystals of BSS with formula $C_{14}H_{11}BiO_7$ (1.**10**) (Fig. 1.5) were obtained by the recrystallisation of precipitate from *N,N*-dimethylformamide (DMF). Thus obtained compound is isostructural with the cluster obtained from wet acetone by Andrews *et al*.[8]

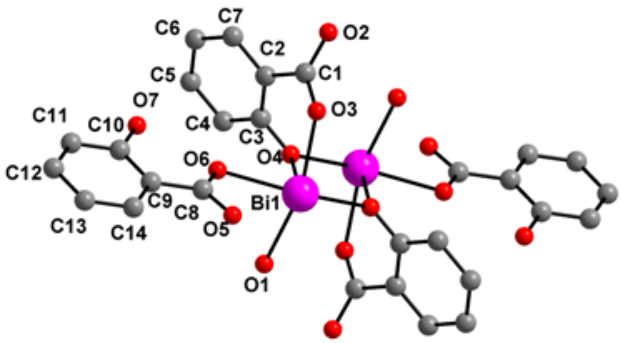

Figure 1.5 A fragment of a compound 1.**10** highlighting different bonding modes of sal^{2-} and $Hsal^{-}$ anions. Bi = purple, O = red, C = grey. Redrawn using coordinates from ref. 13.

Burford *et al* have given a detailed account on the bismuth thiosalicylate with the formula $C_{24}H_{21}BiO_6S_3$ (1.**11**).[6g] This compound was prepared using $BiCl_3$, KOH and methyl thiosalicylate (MTS) in ethanol. In this compound, each bismuth is surrounded by three thiosalicylate ligands in a chelating 6-membered ring fashion. However, sulfur end of one of the ligands bridges a second bismuth centre to lead to the dimeric unit with Bi_2S_2 core (Fig. 1.6). Gilman *et al* reported synthesis of phenylbismuth thiosalicylate from triphenylbismuth and thiosalicylic acid.[14] In this case, two phenyl groups are replaced by one thiosalicylate and according to the structure assigned, a cyclic derivative is obtained. However, the X-ray structure is not reported.

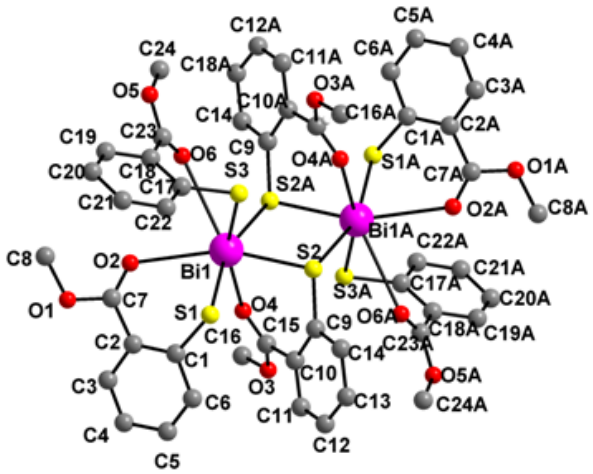

Figure 1.6 The molecular structure of compound 1.**11 (**Bi = purple, O = red, C = grey, S = yellow). Redrawn by using the coordinates from ref. 6g.

1.3.2 Colloidal Bismuth Subcitrate (CBS)

Colloidal bismuth subcitrate (CBS) is one of the complex bismuth salts of citric acid (H_4cit) and is an effective ulcer healing agent. According to the Merck index, it is described by the empirical formula $K_3(NH_4)_2Bi_6O_3(OH)_5(Hcit)_4$ (1.**12**).[15-17] To know the exact pharmacokinetics and dynamics of bismuth drugs in the stomach, Sun *et al* made an attempt to delineate the three dimensional structure of CBS under acidic conditions (pH - 3). A few tiny crystals of formula $K(NH_4)[Bi_2(cit)_2(H_2O)_2]$ $4H_2O$ (1.**13**) were obtained by adding dil. HCl to CBS. There are three dimeric units in the structure. The coordination at each bismuth in dimer **I** is complemented by a monodentate oxygen from a citrate belonging to the adjacent dimer [Bi-O 2.788(9) Å; Fig. 1.7] and one water molecule [Bi-O 2.445(15) Å]. Dimers **II** and **III** are structurally very similar to one another, with the coordination at Bi(III) complemented by a bidentate carboxylate from a third citrate and an oxygen either from a water molecule (dimer **II**) or from a citrate (dimer **III**).[10]

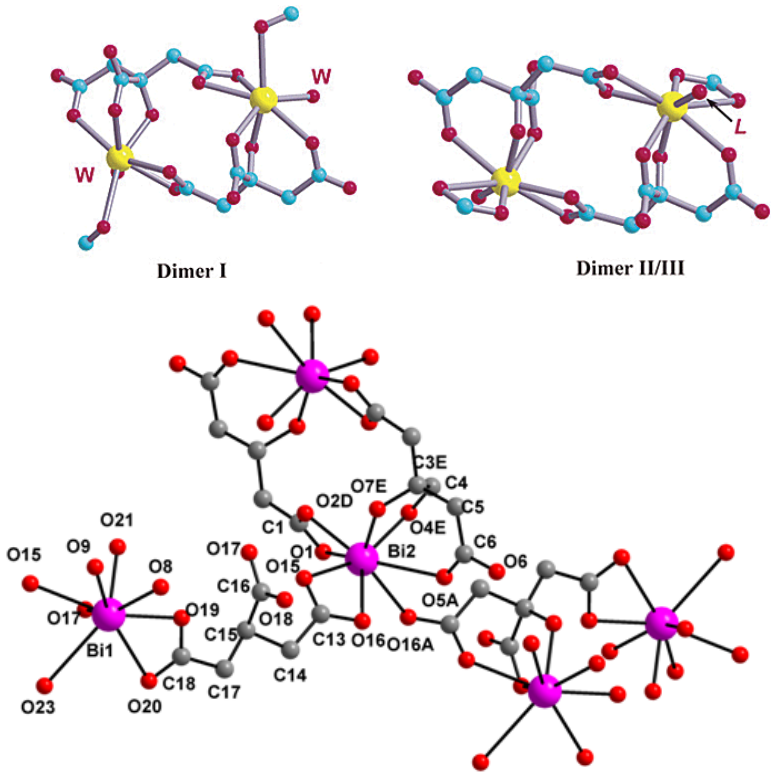

Figure 1.7 Basic dimeric units $[Bi(cit)_2Bi]^{2-}$ found in 1.**13** with a C_2 symmetry (dimer **I**) and an inversion centre (dimer **II**/**III**). W = water molecule, L = an oxygen from a water molecule (dimer **II**) or a citrate carboxylate (dimer **III**) [cf. ref. 10]. Bottom drawing was done using the coordinates available from CCDC.

There are several other structural varieties available for bismuth citrates. Most of the CBS compounds contain $[Bi(cit)_2Bi]^{2-}$ dimeric units with additional O^{2-}, OH^- and H_2O ligands. Citrate bridges help in dimeric unit to aggregate and form channels and sheets via hydrogen bonding with ammonium ions and water, which enhances the solubility of CBS. Channels (ca. 5×10 $Å^2$) present in citrate polymer may allow diffusion of molecules such as ranitidine.[5c]

1.4 Bismuth Complexes with Heterocyclic Carboxylic Acids

1.4.1 Bismuth–pyridine-2-carboxylate

Phenyl bismuth picolinate of the formula $[PhBi(2\text{-}(C_5H_4N)CO_2)_2]_4$ (1.**14**) is reported by Andrews *et al.*[7a] This is a tetrameric molecule [Fig. 1.8] in which each bismuth is coordinated to picolinate chelating through pyridyl-N atom, carboxylate O(-C) atom and by the remaining phenyl group. The geometry around bismuth resembles pentagonal pyramid with the vacant position *trans* to the phenyl group occupied by stereochemically active lone pair.

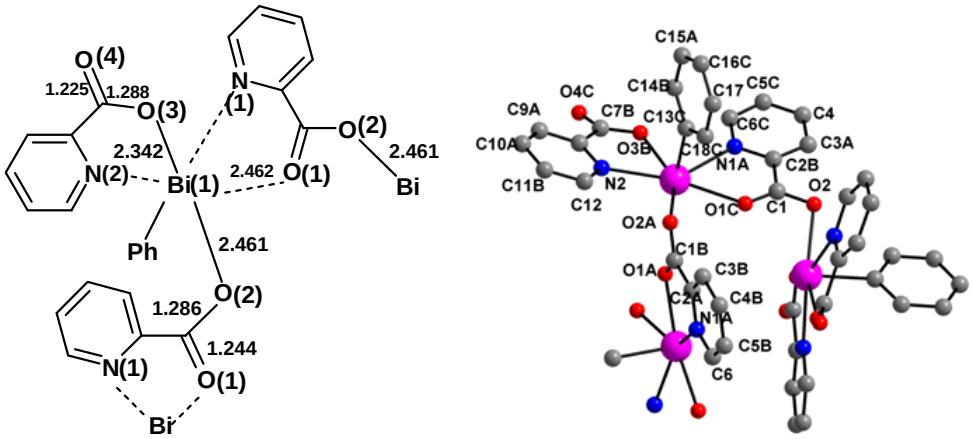

Figure 1.8. Asymmetric unit of $[PhBi(2\text{-}(C_5H_4N)CO_2)_2]_4$ (1.**14**) (in bold), showing the coordination environment around Bi and the mode of oligomerisation [cf. ref. 7a]. Bond lengths are in Å. Diagram on the right was drawn using coordinates from CCDC **(**Bi = purple, O = red, C = grey, N = blue).

Callens *et al* reported two bismuth picolinate complexes $(Na)[C_{24}H_{16}BiN_4O_8]$ $2.5H_2O$ (1.**15**) and $[C_{18}H_{12}BiN_3O_6]_n$ (1.**16**).[18] These were obtained while exploring benzylic oxidations by Bi(0) in the presence of *t*-BuOOH

and acetic acid. In compound 1.**15**, Bi(III) is having a coordination number of 8 (Fig. 1.9). Pyridine-N and carboxylate-O are coordinated to Bi in a 5-membered chelating ring fashion. Anionic part is having interaction with Na^+ ions along crystallographic *b* axis to form a chain polymer (Fig. 1.10). In 1.**16**, three picolinates are coordinated to Bi and the geometry around metal is bi-capped trigonal prismatic. Unlike 1.**15**, there is no need for any cation; ligand bridges have interactions with adjacent metal centres to form a coordination polymer.

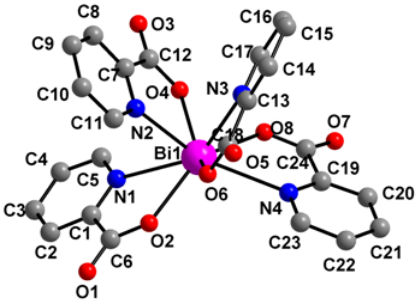

Figure 1.9 The molecular structure of the complex anion present in the crystals of 1.**15 (**Bi = purple, O = red, C = grey, N = blue). Redrawn from ref. 18 using the coordinates from CCDC.

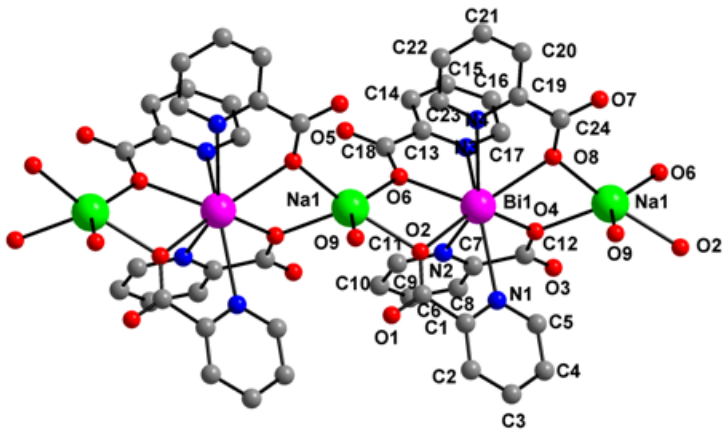

Figure 1.10 The sodium-linked chain polymer of bismuth complexes along the crystallographic *b* axis direction present in the crystals of 1.**15 (**Bi = purple, O = red, C = grey, N = Blue, Na = green). Redrawn from the coordinates [ref. 18] available in CCDC. Extension of the chain occurs via O2 and O4.

1.4.2 Bismuth–pyridine-2,6-dicarboxylates

Extensive work (after our reports) on bismuth pyridine-2,6-dicarboxylate (pydc) compounds has been reported very recently by Cheetham *et al.*[19] The compounds synthesized are [Bi(2,6-pydc)$_3$].3(dma) (1.**17)**, [Bi(2,6-pydc)$_3$].3(dma) 2(H_2O) (1.**18)**, [Bi(2,6-pydc)$_2$(dmf)].(dma) (1.**19)**, Bi(2,6-pydc)(2,6-pydcme).(MeOH) (1.**20)**, [LiBi(2,6-pydc)$_3$(H_2O)].2(dma) (1.**21)** and Li_5Bi(2,6-pydc)$_4$(H_2O)$_2$ (1.**22)** (dma = dimethyl ammonium cation, dmf = dimethylformamide and 2,6-pydcme = 6-methyl-oxycarbonyl pyridine 2-carboxylate). In compound 1.**17**, Bi(III) cation has ninefold coordination by three nitrogen and six oxygen atoms from three different pydc ligands, which chelate in a tridentate manner. Anionic part of pydc has non-covalent interactions with six dma cations via H-bonding. In compound 1.**18** also, each Bi(III) has nine-fold coordination. The asymmetric unit has half Bi(III) cation, one and a half 2,6-pydc dianions, one and a half dma cations and two water molecules each with a half occupancy, leading to a $[Bi(2,6\text{-pydc})_3]^{3-}$ unit that is similar to 1**.17**. The two half occupancy oxygen atoms of water lie adjacent to the methyl carbons of the half-occupancy dma molecule. Each anionic monomer interacts non-covalently with six dma cations through carboxylate–dma hydrogen bonding. In [Bi(2,6-pydc)$_2$(dmf)].(dma) (1.**19**), each Bi(III) cation is eightfold coordinated by five oxygen atoms from three different pydc anions, one oxygen from a terminal dmf molecule, and two nitrogen atoms from two different pydc anions (cf. Fig. 1.11). Two pydc anions coordinate to Bi(III) in a tridentate fashion through pyridyl nitrogen and carboxylate oxygen. Carboxylate oxygen of one pydc coordinates to another Bi(III) centre resulting in a dimeric molecule as $[Bi_2(2,6\text{-pydc})_4(dmf)_2]^{2-}$. Each anionic dimer is non-covalently connected to four dma cations through carboxylate–dma hydrogen bonding involving only the $Hpydc^{-1}$ anion. Thus each dimeric unit is connected to two other such units through the dma cations by hydrogen bonding, leading to the formation of an infinite one-dimensional H-bonded chain (Fig. 1.11).

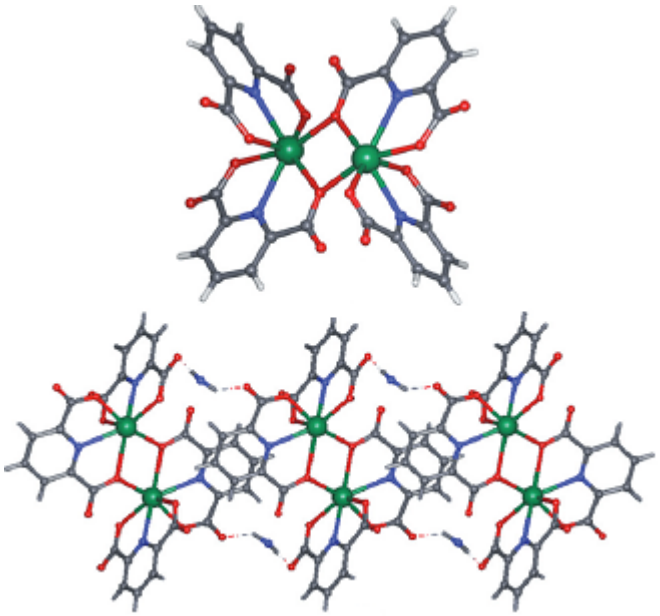

Figure 1.11. Top: The dimeric $Bi_2(2,6\text{-pydc})_4$ unit and Bottom: 1D H-bonding connectivity in 1.**19** (the dmf molecules and methyl groups in the dma cations are omitted for clarity) [cf. ref. 19].

In the compound $Bi_2(2,6\text{-pydc})_2(2,6\text{-pydcme})_2(MeOH)_2$ (1.**20**), each Bi(III) cation is eight-fold coordinated by five oxygen atoms from three different pydc anions, one oxygen from a terminal methanol molecule and two nitrogen atoms from two different pydc anions. In compound $[LiBi(2,6\text{-pydc})_3(H_2O)]_2(dma)$ (1.**21)**, each bismuth is nine fold coordinated by three nitrogens and six oxygens of three different pydc anions in a tridentate manner. In $Li_5Bi(2,6\text{-pydc})_4(H_2O)_2$ (1.**22**) [Fig. 1.12], each bismuth has nine fold coordination and geometry around Bi(III) is the same as in 1.**17**.

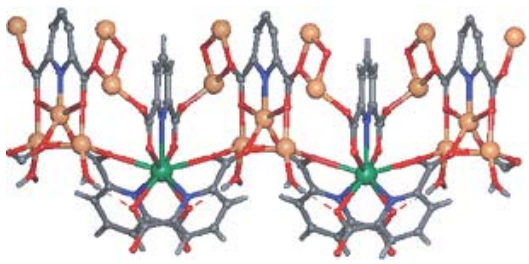

Figure 1.12. View of the one-dimensional connectivity between the monomeric $Bi(2,6\text{-pydc})_3$ coordination unit, $pydc^{-3}$ anion and the lithium cations in 1.**22** (hydrogen atoms in the $pydc^{-3}$ anion are not shown) [cf. ref. 19].

Ranjbar *et al* have reported the structure of a bismuth dipicolinate obtained by the reaction of bismuth subnitrate (in HCl) with pyridine-2,6-dicarboxylic acid (pydc) in water.[20] Light violet crystals of $[\{BiCl(H_2O)(pydc)\}_2]_n$ (1.**23**) were obtained at room temperature. The structure consists of dimeric units of the formula $\{BiCl(H_2O)(pydc)\}_2$. Each Bi(III) is seven fold coordinated with one water molecule, one chlorine atom, one tridentate bridging pydc, one carbonyl oxygen of the other pydc unit and one oxygen of bridging pydc. The dimeric units are combined together through Bi_2O_2 ring. The Bi-O linkages help in these dimeric units to connect and form an infinite system. Geometry around bismuth is distorted pentagonal bipyramidal (Fig. 1.13). Tridentate pydc (O2, N1, O4), O5 of water and Bi_2O_2 are present in the equatorial plane. The axial position is occupied by oxygen of pydc and chlorine atom.

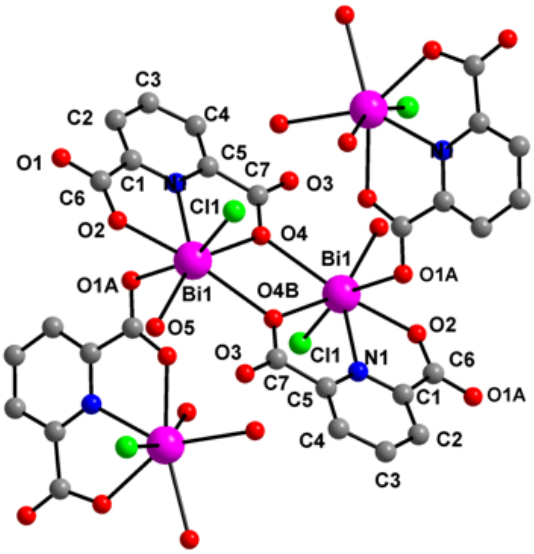

Figure 1.13 Molecular structure of 1.**23** (Bi = purple, O = red, C = grey, Cl = green). Redrawn using coordinates from ref. 20.

1.4.3 Bismuth –pyridine-2,5-dicarboxylate

Recently, zur Loye and co-workers reported bismuth dipicolinate of the formula $Bi_3(\mu_3\text{-}O)_2(pydc)_2(Hpydc)(H_2O)_2$ (1.**24)** obtained from the reaction of $Bi(NO_3)_3.5H_2O$ with pyridine-2,5-dicarboxylic acid in presence of a base using hydrothermal route.[21a] The asymmetric unit in this compound consists of three bismuth ions, three dicarboxylato ligands, two μ_3-oxide ligands, one coordinated and one uncoordinated water molecule. The overall structure is built around

centrosymmetric Bi_6O_4 clusters that contain the two μ_3-oxide ligands. The nitrogen and oxygen atoms of the $pydc^{2-}$ ligands and the oxygen atom of the coordinated water molecule complete the coordination sphere around the bismuth cations in the Bi_6O_4 clusters to form $Bi(1)O_5N_2$, $Bi(2)O_5$, and $Bi(3)O_5N$ polyhedra [Fig. 1.14]. The distorted polyhedra contain stereochemically active lone pairs of bismuth; the arrows indicate the approximate location of the lone pair [Fig. 1.15]. In another recent communication, zur Loye and Co-workers reported relevant bismuth dipicolinate of the formula $Bi(pydc)_2(H_3O^+)(H_2O)_{0.83}$**,** (where pydc is pyridine-2,5-dicarboxylic acid). This compound was prepared from pyridine-2,5-dicarboxylic acid and $Bi(NO_3)_3$ $5H_2O$ under solvo-thermal conditions.[21b]

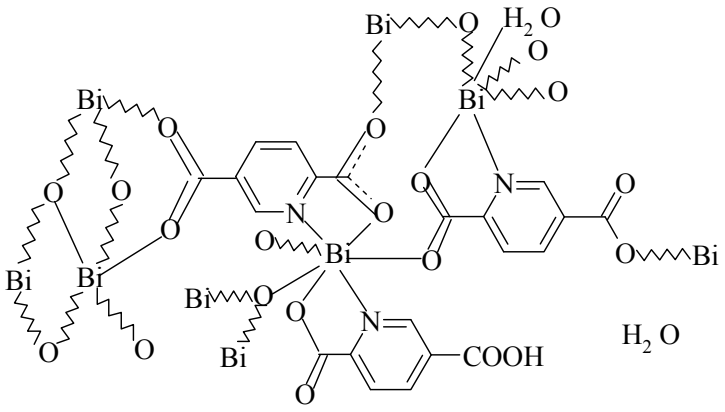

Figure 1.14. A line drawing of the connectivity in compound 1.**24** as given in ref. 21(a).

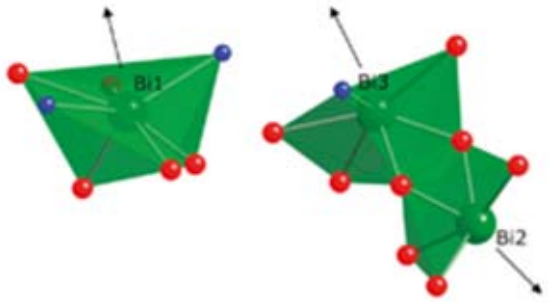

Figure 1.15. Stereochemically active lone pair formation of compound 1.**24**, the arrows show the approximate location of lone pair electrons. Bi = green, O = red, N = blue [cf. ref. 21(a)].

1.4.4 Bismuth –pyrazine and pyrazole carboxylates

Very few reports are available on Bi(III) pyrazine or pyrazole carboxylates. Wenkin *et al* reported the synthesis of Bi(III) derivatives with 3,5-dicarboxypyrazole (3,5-H_2Dcp) and 2,3-dicarboxypyrazine (2,3-H_2pzdc).[22] These compounds are obtained from $Bi(NO_3)_3$ $5H_2O$ and the respective ligand in water under reflux conditions. Bi_2(3,5-Dcp)$_2$ nH_2O (1.**25)** is characterized by the disappearance of absorption bands for the free carboxylic acid at 1696 cm^{-1} (carboxylic group), 3228, and 3436 cm^{-1} (associated with N-H) in the complex. In Bi(2,3-Hpzdc)$_3$ $2H_2O$ (1.**26**), the ligand has two carboxylic groups out of which one is coordinating to the metal and the other is free (Fig. 1.16). Compound Bi(2,3-Hpzdc)$_2$OH (1.**27)** is having an absorption band around 530 cm^{-1} that indicates the presence of Bi-O(H)-Bi bonds. Calcination of all these compounds at 500 ^oC led to α- Bi_2O_3.[22-24]

1.4.5 Other carboxylates of bismuth including those of Bi(V)

Domagala *et al* reported the crystal structure of bis[2-furoato]triphenylbismuth(V) (1.**28**) which was prepared from Ph_3BiCO_3 and furan-2-carboxylic acid in $CHC1_3$/methanol mixture.[25] Without considering the additional intramolecular interactions, two carboxylate oxygens and three phenyl carbons are coordinated to Bi to form trigonal bipyramid around it. Miloudi *et al* reported the structure of bis[2-thiophenecarboxylato]triphenylbismuth as a dichloromethane solvate (1.**29**).[26] This compound also has a structure similar to the bismuth furoate mentioned above. However, no corresponding Bi(III) compounds are known.

Bokhonov *et al* reported the synthesis and characterisation of bismuth(III) oxohydroxocarboxylates of the formula $Bi_6O_4(OH)_4(C_nH_{2n-1}O_2)_6$, where ($C_nH_{2n-1}O_2$) is a carboxylate ion and n = 2 (2–9, 11).[27a] Yukhin *et al* have obtained bismuth(III) oxohydroxolaurate by the reaction of lauric acid with bismuth nitrate (or) perchlorate solution.[27b] Since these are not pertinent to the topic of this thesis, they are not elaborated further.

1.4.6 Bimetallic carboxylates containing bismuth

Along with bismuth carboxylates, synthesis and structural charcterisation of bismuth-heterometallic carboxylates have attained equal importance as they can be sources of mixed metal oxide materials.[28a] With early transition metals, Whitmire

and co-workers have reported complexes with the formulae $Bi_2M_2(sal)_4(Hsal)_4(OCHMe_2)_4$ [M = Nb (1.**30**), Ta (1.**31**)], $Bi_2Ti_3(sal)_8(Hsal)_2$ (1.**32**) and $Bi_2Ti_4(OCHMe_2)(sal)_{10}$ (Hsal) (1.**33**) [sal = $O_2CC_6H_4$-2-O, Hsal = $O_2CC_6H_4$-2-OH]. These compounds were obtained from Ph_3Bi, salicylic acid and metal alkoxides.[28b] The structure of compound 1.**30** is given in Figure 1.16. The same research group has reported bismuth-heterometallic complexes of the formula $Bi_2(Hsal)_6{\cdot}M(acac)_3$ (M = Al, Cr, Fe, V, Co) (1.**34**) with diketonates.[28c] Whitmire and co-workers also reported a method to prepare the heterometallic complexes with divalent post-transition metals such as $Bi(Hsal)_3Cu(salen)$ and $Bi(Hsal)_3Ni(salen)$ (1.**35a** and **1.35b**) by using salen complexes of copper and nickel as precursors.[28d]

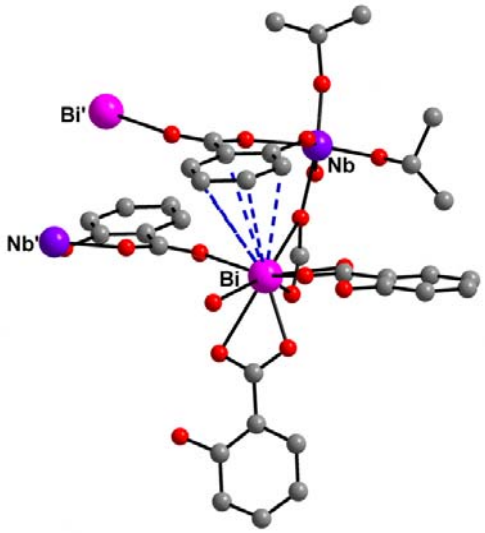

Figure 1.16. The π-interactions between bismuth and the salicylate ring (in 1.**30)** are represented by broken lines. (Bi = purple, Nb = violet, O = red, C = grey). Redrawn using coordinates from ref. 28(b).

1.5 Phenylbismuth Carboxylates

Along with bismuth salts, the precursor triphenylbismuth is widely used for the preparation of bismuth carboxylates. Recently (after our publications), Chandrasekhar and co-workers reported the synthesis of bismuth-ferrocene carboxylates (from Ph_3Bi and ferrocene carboxylic acid) of the formulae $[Bi_2(\mu_2\text{-}\eta^2\text{-}OOCFeCOO\text{-}\mu_2\text{-}\eta^2)(\eta^2\text{-}OOCFeCOO\text{-}\eta^2)(\mu_2\text{-}\eta^2\text{-}OOCFeCOO\text{-}\eta^2)]_n$ (1.**36**), $[Bi(\mu_2\text{-}\eta^2\text{-}FeCOO)(\eta^2\text{-}FcCOO)_2]_n$ (1.**37**) and $[Bi_2(\mu_2\text{-}\eta^2\text{-}FeCOO)_2(\eta^2\text{-}FeCOO)_4(H_2O)_4]{\cdot}(2FeCOOH)$ (1.**38**).[29a] The first two compounds 1.**36** and 1.**37** are

coordination polymers and (1.**38**) is a molecular dimer. Egorova *et al* obtained phenylbismuth bis(chloroacetate) by the reaction of chloroacetic acid with triphenylbismuth. Oxygen bridges of acetate coordinate to bismuth and form a polymer chain.[29b] Similarly, Sharutin *et al* reported the synthesis of tris(1-adamantanecarboxylato)bismuth(III), $\{Bi[OC(O)C_{10}H_{15}]_3\}_4$ (1.**39**) by the reaction of triphenylbismuth with 1-adamantanecarboxylic acid in toluene. All the four bismuth atoms are symmetrically equivalent in tetramer and are coordinated by 10 oxygen atoms of bidentate-chelating and two types of chelate-bridging adamantanecarboxylate ligands.[29c] Jain and co-workers reported the synthesis and characterisation of monoorganobismuth thiocarboxylates of the formula $[R'Bi(SOCR)_2]$ (R, R' = Ph or Me) (1.**40**). These were obtained by the reaction of methylbismuth dichloride or Ph_3Bi and thiocarboxylic acids RC(O)SH [R = Ph or Me] in the presence of a base (Et_3N) in benzene.[29d] Thus obtained bismuth thiocarboxylates are also useful precursors for the synthesis of Bi_2S_3. Andrews *et al* reported synthesis and crystal structure of bismuth tri-(*o*-methoxybenzoate) of the formula $[Bi(o\text{-}MeOC_6H_4CO_2)_3]_\infty$ (1.**41**) obtained by the reaction of Ph_3Bi and *ortho*-methoxy benzoic acid in toluene. The basic unit of the formula $Bi(o\text{-}MeOC_6H_4CO_2)_3$ [Fig. 1.17] is repeated through oxygen bridges to form the polymeric structure.[7a] Bismuth carboxylate complexes that can be used as lubricant additives[29e] and polyurethane catalysts in several commercial applications[29f] are also known in the literature.

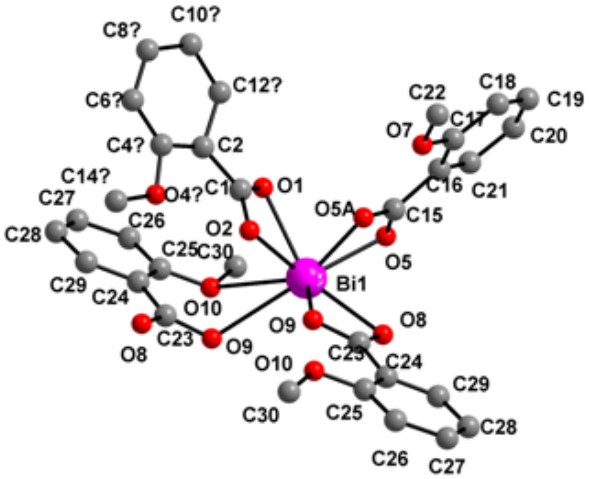

Figure 1.17. Asymmetric unit in $[Bi(o\text{-}MeOC_6H_4CO_2)_3]_\infty$ (Bi = purple, O = red, C = grey). Redrawn (ref. 7a) using coordinates from CCDC.

1.6 Stereochemically Active or Inactive Lone Pair of Electrons [LEP]?

In a molecule, for one particular atom, the lone pair of electrons [LEP] in an orbital that has directionality associated with it can be termed as stereochemically active. In case of heavy metals like Tl, Pb, Bi it may not be true every time i.e., the lone pair may or may not be stereochemically active. In compounds of these elements, the "s" electrons are more hidden and become less available for bonding. Hence the lone pair of electrons is sometimes stereochemically active and sometimes inactive. When the lone pair is stereochemically active, it will affect the structure by means of distortions in bond angles and in turn the properties. This is more important in materials. Other point is that the geometry may be influenced by stereochemically active lone pair in the presence of donor atoms or molecules or ions which may have additional weak intermolecular or intramolecular interactions. These weak interactions may be called as secondary bonds.[30a] It is known that the stereochemical activity of the lone electron pair decreases within the group from the top to down [in this case, from Sb(III) to Bi(III)].[30b,c] Bismuth aminocarboxylates confirm this thesis; most of the compounds characterized structurally do not exhibit the stereochemical activity of the lone electron pair.

1.6.1 Stereochemical activity of lone pair in Bi_2WO_6

Aurivillius phase of Bi_2WO_6[31a] finds applications in new ferroelectric random access memories,[31b,c] light-driven photocatalysts[31d,e] and electrolytes within solid oxide fuel cells (SOFCs).[31f-h] The structure of Bi_2WO_6 can be described as alternate layers of fluorite like Bi_2O_2 sheets and a perovskite like WO_4 layer of tilted corner sharing WO_6 octahedra. Recent neutron diffraction studies have shown that the ferroelectric transition is unusual among the Aurivillius phases and involves dramatic reconstructions[31i] from chains of edge and corners sharing WO_6 dimers. Also, the actual local oxygen arrangement around the bismuth in the high temperature phase is more asymmetric than that of the idealized high-temperature phase but characteristic for the presence of a stereochemically active lone pair of bismuth with short Bi-O bonds of ~2.4 Å to the apex oxygens within the WO_4 layer.[31j] Thus, elucidating the influence of the asymmetric lone-pair placement on the stabilization of the ferroelectric phases of Bi_2WO_6 appears more complex than expected based on a comparison with a prototypal high-temperature phase[31i] and calls for a reinvestigation. The nature of the lone pair also has important

consequences for the photocatalytic activity of Bi_2WO_6, in particular when bearing in mind that the conventional $6s^2$ lone-pair (textbook) model,[31k] frequently used to rationalize the distorted local oxygen environment around bismuth within bismuth-based oxides, has undergone recent revision.[31l-o] Whereas the conventional lone-pair model is explained by the formation of metal *np* and *ns* orbitals projected out into the void, recent bond analysis carried out on different binary post-transition metal oxides [31n-p] as well as ternary bismuth-based oxides $BiVO_4$[31q,r] have shown that the asymmetric lone pair is constructed from states with dominant contributions from the oxygen 2*p* orbitals and small contribution from Bi 6*s* and Bi 6*p* states. These antibonding states are located at the *top* of the valence band, whereas the majority of the Bi 6*s* states are located at the *bottom* of the valence shell.

1.6.2 Stereochemical activity of lone pair in bismuth and antimony halides

Wheeler and Pavan Kumar considered BiI_6^{3-}(1.**42)**, $BiCl_6^{3-}$(1.**43)**, BiI_3 (1.**44)**, and SbI_3 (1.**45)** as prototypical ions and molecules/ solids containing group 15 elements to study stereochemical activity of the lone pair of electrons.[32] The lone pair of electrons on the central Bi atoms of BiI_6^{3-} and BiI_3 is not evident in the structures. They are stereochemically inactive. The structure of SbI_3 (1.**45**) is similar to 1.**44** except that the Sb atoms are displaced by 0.320 Å along the hexagonal ***c*** axis. This results in a distortion from octahedral coordination, similar to that observed in $BiCl_6^{3-}$ (1.**43**) and resulting in three short (2.87 Å) and three long (3.32 Å) Sb-I distances in SbI_3. Like the molecular compounds described earlier, BiI_3 and SbI_3 contain Bi(III) and Sb(III), each with a lone pair of electrons. Like the lone pairs on Bi in the BiI_6^{3-} ion, the Bi lone pairs in solid BiI_3 are stereochemically inactive, inert pairs. Authors have presented simple frontier orbital arguments to provide a unified picture of the 'inert pair effect" in the species BiI_6^{3-} and $BiCl_6^{3-}$ and the extended solids BiI_3 and SbI_3. Extended Hückel molecular orbital calculations show that these compounds tend to exhibit a second-order Jahn-Teller distortion from octahedral to trigonal coordination. The result of the distortion is similar for the molecular and solid-state structures: stereochemically inactive lone pair electrons in the highest occupied orbitals of the octahedral structures (BiI_6^{3-} and BiI_3) occupy a spherically symmetric Bi '**s**' orbital which becomes, upon distortion to the $BiCl_6^{3-}$or SbI_3 structure types, a stereochemically active hybrid of s and p_z. In both cases, the hybridization is toward the longer bonds. Authors infer this from the

smaller Bi-I overlap populations along bonds in the direction of the hybrid for the MX_6^{3-} molecules and they demonstrated it directly in BiI_3 by moving the Bi atoms and noting that the hybrid points toward the longer Bi-I bonds. For the molecules studied, the lone pair is hybridized toward the nominally larger angles; for the MX_3 solids, the lone pair is hybridized toward the smaller angles. Thus, the fundamental assumption of VSEPR, i.e., that lone pair electrons demand angular space around the central atom is confounded in the solid state, and bond length rather than bond angle variations indicate the orientations of lone pair electrons in these compounds.[32]

1.7 Secondary Bonding Interactions in Bismuth Compounds

1.7.1 Weak Bi---N interactions in [Bi{$S_2CN(CH_3)(C_6H_{13})$}$_3$($C_{12}H_8N_2$)]

Trindade and coworkers reported the synthesis and characterisation of [Bi{$S_2CN(CH_3)(C_6H_{13})$}$_3$] (1.**46**) and [Bi{$S_2CN(CH_3)(C_6H_{13})$}$_3$($C_{12}H_8N_2$)] (1.**47**).[33a] These were prepared as precursors for nano and micro sized Bi_2S_3 particles. In complex 1.**47**, the Bi---N interactions can be considered as secondary bonds because they are longer than typical Bi-N covalent bond distances, but shorter than the sum of van der Waals radii.[33b] The Bi-S distances are in the range 2.700-2.966 Å and are close to the sum of the covalent radii of the elements (2.54 Å); therefore, the Bi-S interactions are considered as primary bonds. This is consistent with the trans influence observed for a number of bismuth complexes showing secondary and primary *Bi* to *E* bonds, in which *E* is a non metal[33b] (cf Fig. 1.18 for Bi---N secondary interactions). The distortion on the coordination geometry could also be due to the presence of stereochemically active electron lone pair on bismuth. Such an influence of the electron lone pair on the coordination geometry of bismuth is not so evident in the 1.**46**, which can be related to the expansion of the coordination number by introducing a bidentate ligand with a higher bite angle such as *o*-phenanthroline.[33b] In the case of 1.**47**, the distortion from a regular geometry is possibly due to stereochemical restrictions imposed by both types of bidentate ligands with distinct bite angles.

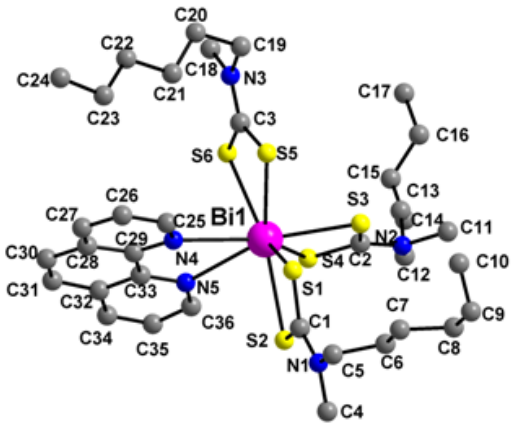

Figure 1.18. Molecular structure of $[Bi\{S_2CN(CH_3)(C_6H_{13})\}_3(C_{12}H_8N_2)]$ (1.**47**). **(**Bi = purple, O = red, C = grey, N = blue, S = yellow). Drawn [ref. 33(a)] using coordinates from CCDC.

1.7.2 Bi---S interactions in bismuth dithiocarbamate complexes

Teske and Bensch reported the crystal structures of two bismuth dithiocarbamate compounds $NH_4Bi(S_2CNH_2)_4{\cdot}H_2O$ (1.**48**) and $Bi(S_2CNH_2)_3$ (1.**49**).[34] In 1.**48**, authors have noted that the distance Bi---S(3) of 3.076(1) Å, which completes the polyhedron, is noticeably longer than the remaining Bi–S bonds [cf. Fig. 1.19]. The distortion of the polyhedron may be an obvious sign of stereochemically active lone electron pair which would generate asymmetric Bi–S interactions and therefore distorted polyhedra around Bi(III).

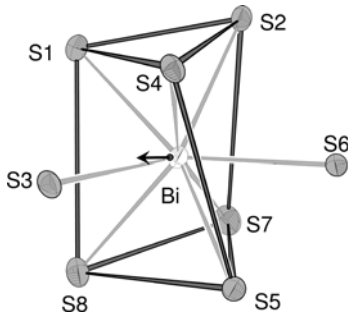

Figure 1.19. Coordination polyhedron [cf. ref. 34] around Bi(III) in $NH_4Bi(S_2CNH_2)_4{\cdot}H_2O$ (1.**48**). The displacement ellipsoids are drawn at the 60 % probability level.

1.7.3 Weak dimer formation in phenyl bismuth oxinate compounds

Campi *et al* reported the crystal structures and weak π-bonding in bismuth oxinate complexes, $[Bi(ox)_3(OH_2)]_2$ (1.**50)** and $[BiPh(ox)_2(O\text{-dmso})]_2$ (1.**51)**.[35a] In 1.**51**, the oxine ligands coordinate unsymmetrically; differences in the pairs of Bi-N and Bi-O distances possibly impacted by the very neat packing of the ligands, closely planar about the bismuth atom, despite close H...O inter-ligand contacts at the van der Waals distance. The pair of oxine ligands has a *transoid* disposition with the ligand 1 having the shorter Bi-O distance and ligand 2 having the shorter Bi-N distance. Close observation of the crystal packing shows an array of contacts (Fig. 1.20) from the bismuth atom to the six carbon atoms of the carbocyclic ring of the oxine ligand at distances ranging between 3.55-3.81(1) Å, suggestive of an effective η^6-interaction, so that the extended planes of the ligands about the coordination plane lie close and parallel. The Bi-N distances in the above pair of complexes are diverse, despite the non-bridging nature of the associated nitrogen atoms.[33b,35b-d]

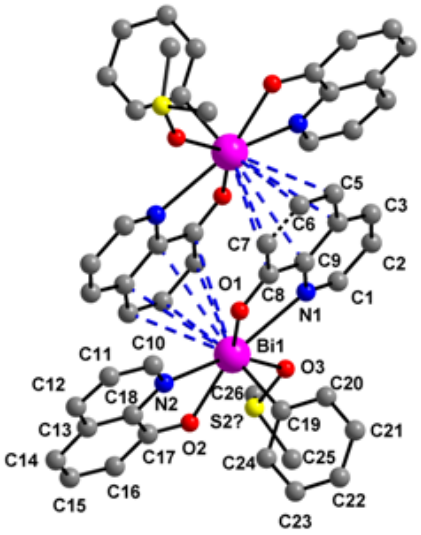

Figure 1.20. Projection of $[BiPh(ox)_2(O\text{-dmso})]_2$(1.**51)** onto its inversion image. (Bi = purple, O = red, C = grey, S = yellow). Diagram was drawn [ref. 35(a)] using coordinates from CCDC.

1.7.4 Weak secondary interactions in pyridine adducts of bismuth(III) halides

Norman and co workers reported several bismuth complexes.[36] Among these, bismuth in $[BiI_3(py)_3]$ (1.**52)** (py = pyridine) is octahedral with the iodide and pyridine ligands arranged in a *mer* configuration. A seven co-ordinate complex $[BiCl_3(py)_4]$ (1.**53**) is also described. The compounds $[BiCl_2Ph(4\text{-Mepy})_2]$ (1.**54**; 4-Mepy = 4-methylpyridine), $[BiBr_2Ph(4\text{-Mepy})_2]$ (1.**55**) $[BiBr_2Ph(4\text{-Bu}^t\text{py})_2]$ (1.**56**,

4-Bu^{t}py = 4-*tert*-butylpyridine) and [$BiBr_2Ph(py)_2$] (1.**57)** all have a five-co-ordinate, square-based pyramidal bismuth centre in which the phenyl group occupies the apical position with two *trans* halides and two *trans* pyridine ligands residing in the basal plane. It is observed that in all cases weak intermolecular interactions lead to dimers or polymers and specifically, these interactions involve a close contact between a halide and the bismuth centre approximately *trans* to the apical phenyl group. As is clear from the diagram and Fig 1.23, pairs of these monomeric units form weakly bonded dimers through very asymmetric halide bridging interactions, the longer secondary Bi---X bond being approximately *trans* to the phenyl group. For 1.**54**-1.**56**, the primary and secondary Bi–Cl/Br distances are, respectively, [2.701(2), 3.657(3)], [2.845(2), 3.772(2)] and [2.805(1), 3.691(2)] Å and the corresponding *trans* C–Bi---X angles are 151.2(2), 151.7(3) and 158.36(12)^o.[36a] Similar interactions are seen in [NEt_4][BiI_2Ph_2],[36b] [BiBr(2,4,6-$Me_3C_6H_2)_2.(Ph_2SO)$][36c] and in cationic complexes of the form [$BiAr_2(L)_2$].[36d]

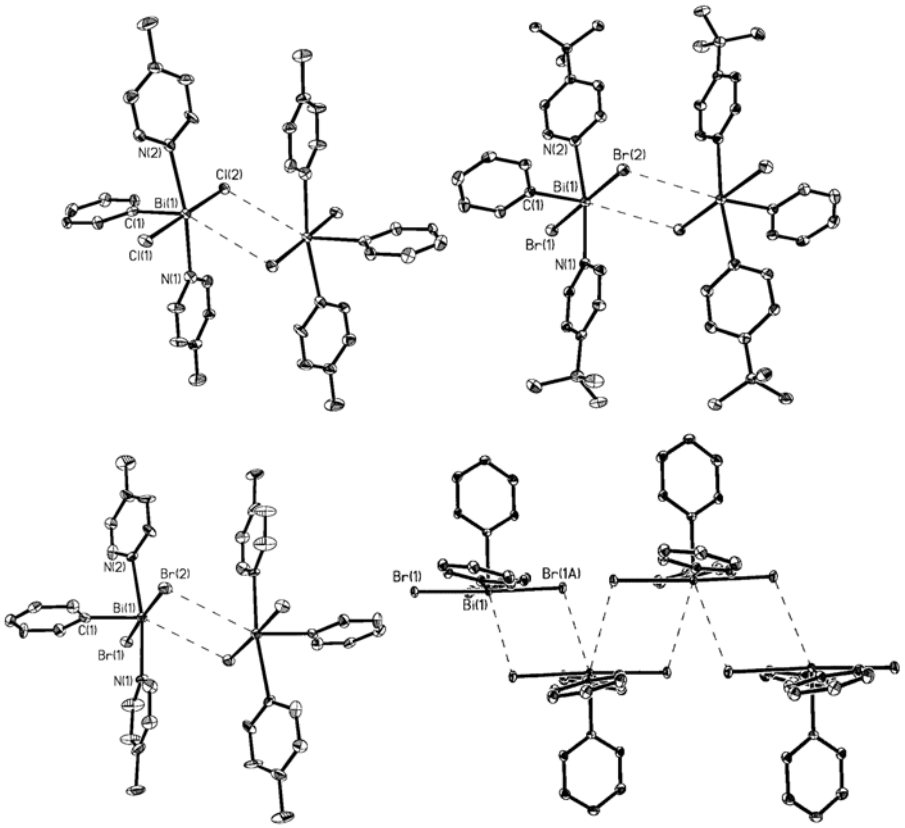

Figure 1.21. A view of the molecular structures of complexes showing the weakly bonded dimers [cf. ref. 36a]. Top left: 1.**54**. Top right: 1.**55**. Bottom left: 1.**56**. Bottom right: 1.**57**.

1.8 Bismuth Materials

Along with medicinal applications, bismuth and its derivatives find applications in materials chemistry. In materials, when the size is reduced from bulk to nano level they exhibit variety of interesting electronic, magnetic and optical properties.[37,38] Same is the case for bismuth. Bismuth has a small energy overlap between conduction and valence bands. With the decrease in size, the induced semimetal- semiconductor transition would be possible.[39] This transition and related quantum confinement effects are potentially useful for electrical and optoelectrical device applications. Bismuth materials with smaller size are known to exhibit enhanced thermoelectric properties at room temperature.[40] Some of the bismuth materials with their applications are mentioned below.

(i) Bismuth metal and its alloys

Bismuth exhibits many useful electronic properties due to the small effective mass, low density and the long mean free path of the carriers.[39b] Because of low toxicity, it is considered for replacing the lead in many applications. Commercial In19.1-Cd5.3-Pb22.6-Sn8.3-Bi44.7 alloy is a very good example of specialty fusible alloy with a melting point of just 47 ^{o}C that is useful in automatic sprinklers and electric fuses. Stripping voltammetric determination of Cd^{2+} can be done by a tin–bismuth alloy based electrode.[41]

(ii) Bismuth oxide

Harwig and Gerards reported four polymorphs of Bi_2O_3. Among them, monoclinic α phase is stable at room temperature. Upon heating at 729 ^{o}C transition occurs to give *fcc* δ-phase which is stable up to melting point temperature of 824 ^{o}C. Upon cooling from δ phase to α phase it transforms into tetragonal *β* and *bcc* γ phases at 650 and 639 ^{o}C respectively.[42] In electrochemistry, while constructing galvanic cells, oxygen ion conducting solid electrolytes have been utilised. Some of the successful oxide electrolytes studied are ZrO_2, HfO_2, CeO_2 and ThO_2 having additions of either an alkaline earth oxide, Sc_2O_3, Y_2O_3 or Bi_2O_3. By the addition of such di- or tri-valent ions, anion vacancies are created in these solid solutions to maintain electrical neutrality. The resulting increase in oxygen ion conductivity leads to ionic conduction.[43]

(iii) Bismuth sulfide

Semiconductor nanomaterials are of great interest because of their remarkable electronic, magnetic, optical, catalytic and mechanical properties and they find applications in nano devices. Among the metal sulfides, bismuth sulfide Bi_2S_3 is a direct band gap layered semiconductor. It crystallizes in orthorhombic system.[44a] Toxicity concerns of Pb and Cd sulfide nanomaterials have initiated the exploration of novel and environmentally benign nanomaterials Cu_2O,[44b] CZTS,[44c-d,] CIGS,[44e] Cu_2S,[44f] all these are p-type semiconductors and are employed in n-type oxide wide-band gap semiconductors. Bi_2S_3 is one of the alternatives due to its non-toxic constituents, high absorption coefficient of the order of 10^5 cm^{-1} and band gap of ~1.3 eV.[45] Bi_2S_3 is suitable for solar cell applications. Rath *et al* demonstrated the applicability of Bi_2S_3 nanostructured material as a novel n-type semiconductor that can be employed in solution-processed thin film solar cells as the electron acceptor.[46] Bismuth sulfide has a wide range of other applications that include photodiode arrays and photovoltaic converters,[46b-d] photodetectors,[46e] thermoelectrics,[46f] and electrochemical hydrogen storage,[46g,h] as imaging agent in X-ray computed tomography,[46i] in biomolecule detection,[46j] and H_2 sensing.[46k] .

(iv) Bismuth selenide

Bismuth selenide (Bi_2Se_3) has attracted considerable attention due to its characteristic anisotropic layered structure as well as its important applications in the field of optical recording system,[47a,b] strain gauges,[47c] narrow band-gap semiconductors[47d] and electromechanical and thermoelectrical devices.[47e–h] Nanostructured Bi_2Se_3 has high surface to volume ratio and hence enhances the visibility of surface states in transport measurements. Among the topological insulators that are predicted and experimentally verified, Bi_2Se_3 is like reference material with its simple band structure and wide band gap of ~0.3eV.[48a-c]

(v) Bismuth telluride

Thermoelectric materials are scalable, ideal and highly reliable for power generation. They are more advantageous than conventional energy technologies, the only problem is conversion efficiency of current devices is low (10%).

Thermoelectric devices are used to convert industrial waste heat into electricity and they could also make power generators in cars by utilizing heat from the exhaust gases. Bismuth-telluride (Bi_2Te_3) is commonly used in commercial Peltier cooling devices and has been proven to be one of the best thermoelectric materials with the highest figure of merit.[49a-d]

Theoretical predictions and experimental investigations suggest that compared to bulk, in nanosystems high density of states, increased phonon scattering or reduced lattice thermal conductivity are the factors which will enhance ZT. Therefore there is a need to prepare nano-Bi_2Te_3. Hence several methods to prepare nanorods, nanowires, nanoparticles and nanosheets of Bi_2Te_3 are reported.[49a]

(vi) Bismuth ferrate

Multiferroic materials find applications in electronic devices, such as multiple-state memories and new data-storage media. Among the multiferroic materials $BiFeO_3$ is well known to have simultaneous ferroelectric (T_C~ 830 °C) and G-type antiferromagnetic (T_N ~ 370 °C) properties above room temperature. It crystallises in rhombohedrally distorted perovskite structure.[50a] However, problems of low sinterability, low resistivity and persistent appearance of secondary phases have hindered the practical application of $BiFeO_3$ ceramics in electronic devices. To overcome these problems, various processing techniques have been pursued.[50b] To make $BiFeO_3$ as a device material, leakage current is the hindering factor; it results from defects. To overcome this problem, for making high quality samples with enhanced electric properties of $BiFeO_3$, partial substitution of Bi or Fe with other metal ions or metal- oxide is recommended.[50c]

(vi) Bismuth titanate

Bismuth based mixed oxide compounds with their unique crystal structures; high activity and band gap are widely investigated as photocatalysts. Bismuth titanates are known to have wide band gap and several crystal phases such as refractive sillenite phase $Bi_{12}TiO_{20}$ (1.**58**), dielectric pyrochlore phase $Bi_2Ti_2O_7$ (1.**59**), ferroelectric perovskite phase $Bi_4Ti_3O_{12}$ (1.**60)** and so on. These compounds are ferroelectrics and have high dielectric constant with excellent electro-optical and photoelectric properties.[51a]

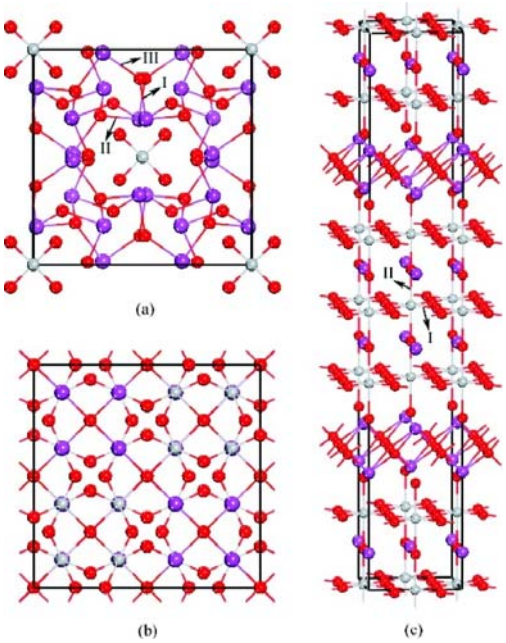

Figure 1.22. Bulk structures of (a) $Bi_{12}TiO_{20}$ (1.**58**) (b) $Bi_2Ti_2O_7$ (1.**59**) and (c) $Bi_4Ti_3O_{12}$ (1.**60**) (colour codes: Bi = purple, Ti = grey, O = red) (cf. ref. 51a).

$Bi_4Ti_3O_{12}$ [also written as $(Bi_2O_2)^{2+}(Bi_2Ti_3O_{10})^{2-}$] is a ferroelectric material with several useful properties for optical memory, piezoelectric and electro-optic devices. It can be viewed as having alternative stacking of a triple layer of TiO_6 octahedra (perovskite slab) and a monolayer of $(Bi_2O_2)^{2+}$ along the c axis. It has been found that $Bi_4Ti_3O_{12}$ has the high photocatalytic activity. Kudo *et al* reported the preparation of $Bi_4Ti_3O_{12}$ by a solid-state route and examined its photocatalytic activity for water splitting.[51b] Yao *et al* reported the preparation of $Bi_4Ti_3O_{12}$ by using the chemical solution decomposition (CSD) method and investigated the photocatalytic activity for oxidizing methyl orange.[51c] A few papers have also revealed the photocatalytic activity of $Bi_4Ti_3O_{12}$ for water splitting into hydrogen under visible light irradiation.[51d]

1.9 Bismuth Compounds as Catalysts/Reagents

Bismuth compounds and salts have also attracted much attention due to their low toxicity, low cost, good stability and excellent catalytic activity in many organic transformations. However, they have found limited application in organic synthesis. Bismuth(III) compounds act as Lewis acids due to the lack of shielding of the outer electron shells. A brief discussion on the catalytic behaviour is outlined in the following subsections.

1.9.1 Bismuth tribromide catalysed cascade electrophilic addition/ cycloisomerization

Polycyclic aromatic hydrocarbons (PAHs) are of great interest as they are used in the light-emitting diodes, field-effect transistors, and solar cells. Xiang-Chuan Wang *et al* reported the efficient synthesis of highly conjugated carbon-rich fluorene by isomerisation/ Friedel−Crafts type reaction of (*Z*)-1,3,5-triphenylpent-2-en-4-ynyl acetate in the presence of Lewis acid like $BiBr_3$ and base 2, 2'-bipyridine [Scheme 1.2].[52]

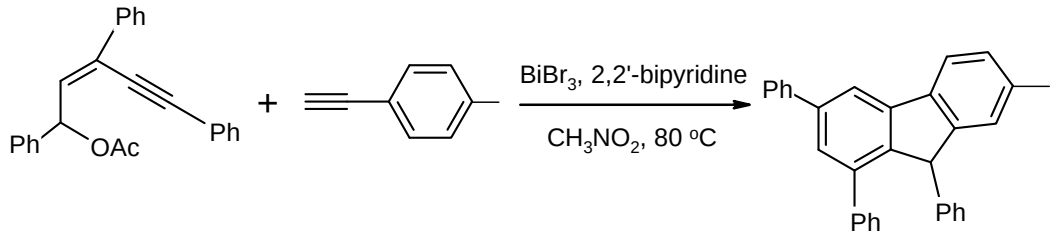

Scheme 1.2

1.9.2 Bismuth triflate catalyzed chemoselective conjugate reduction of α,β-unsaturated ketones

Chemoselective hydrogenation or conjugate reduction of α,β-unsaturated ketones is a useful and important method in organic synthesis. Suitably substituted ketones are important starting materials, especially for the synthesis of complex molecules and natural products. In comparison to other Lewis acids, bismuth triflate [$Bi(OTf)_3$] is known to chemoselectively reduce enones in presence of poly(methylhydro)siloxane (PMHS) [Scheme 1.3].[53]

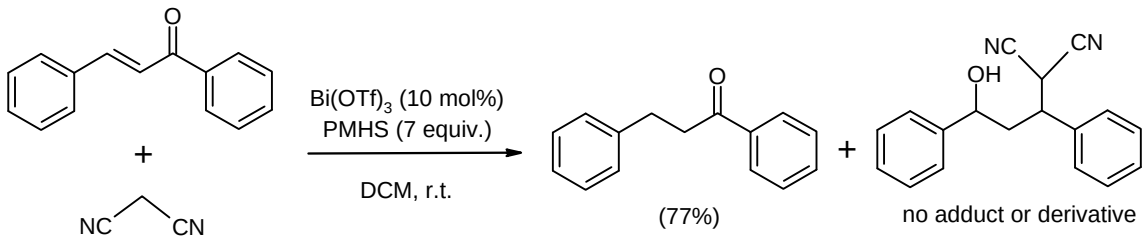

Scheme 1.3

1.9.3 Bismuth nitrate catalysed ipso-nitration of arylboronic acids

Nitration of aromatic compounds is one of the well studied reactions in organic chemistry as nitroaromatics are important intermediates in the synthesis of dyes, plastics and pharmaceuticals. Most commonly used nitrating reagent for nitration is nitration mixture (HNO_3/H_2SO_4). Very recently, Maiti and co-workers reported the nitration of aryl boronic acids using $Bi(NO_3)_3.5H_2O$ and $K_2S_2O_8$ affording good yields of the product [Scheme 1.4].[54]

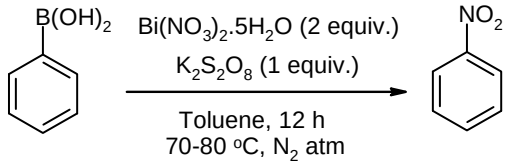

Scheme 1.4

1.9.4 $BiCl_3$-catalyzed three component reactions of anilines and aliphatic aldehydes in the presence (or lack) of N-vinyl amides

Bismuth salts are also known to catalyse the multicomponent reactions. Kouznetsov *et al* reported a general protocol for the simple and efficient synthesis of 2-alkyl-1,2,3,4-tetrahydro- quinolines and 2,3-dialkylquinolines. Commercial and inexpensive substituted anilines, valeraldehyde, and *N*-vinylpyrrolidin-2-one (NVP), N-vinylformamide (NVF) or N-vinylacetamide (NVA) were chosen as suitable reagents for their study.[55] Taking into consideration that bismuth trichloride is (i) a less toxic compound than other heavy metal salts that can effectively catalyze imino Diels–Alder cycloaddition, (ii) more stable and easy handling catalyst, (iii) water tolerant, they used it in their experiments. Thus, three component Povarov reactions between anilines, the valeraldehyde and the amides (molar ratio1:1, 1:1.2) in the presence of $BiCl_3$ (10 mol%) in MeCN at room temperature afforded the products in good yields [Scheme 1.5].

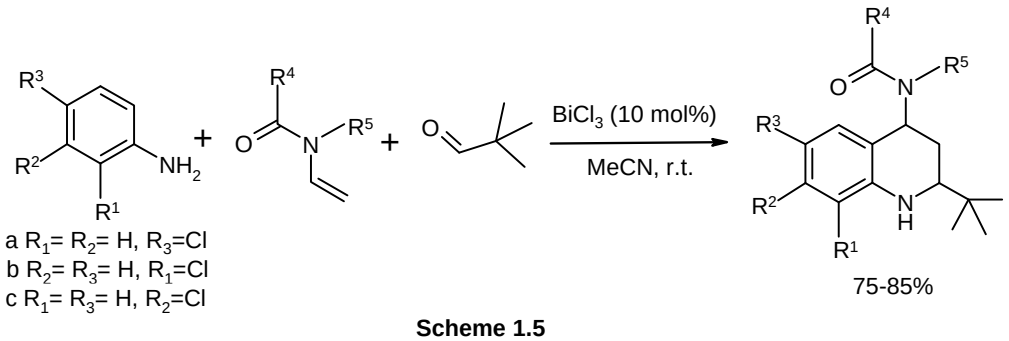

Scheme 1.5

1.9.5 Triphenyl bismuth as an arylating agent

There are several reports involving triphenylbismuth as arylating agent in organic reactions. In a recent study, Rao *et al* reported the coupling reaction of 2-bromobenzofuran with triphenylbismuth as organometallic nucleophile and palladium compounds as catalysts.[56] The screening was performed with 3.3 equiv. of 2-bromobenzofuran and 1 equiv of triphenylbismuth to cross couple three phenyls from bismuth reagent to obtain 3 equiv of 2-phenylbenzofuran stoichiometrically [Scheme 1.6].

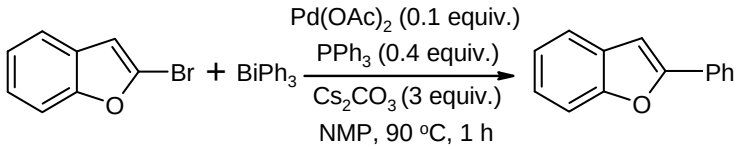

Scheme 1.6

OBJECTIVES OF THE PRESENT WORK - PART A

The main objective of this part of the present work was to develop the area of bismuth carboxylates and related bismuth chemistry. Specifically, it was planned to investigate following aspects:

(i) Synthesis and structural characterization of new bismuth pyridine carboxylates (coordination polymers and monomeric species) using bismuth nitrate and ammonium bismuth citrate,

(ii) Exploring the synthesis of phenyl bismuth heterocyclic carboxylates using $BiPh_3$, and subsequent investigations on the role of stereochemical activity, if any, of the lone pair of electrons on bismuth and on secondary bonding interactions in the products and,

(iii) Simpler routes to prepare micron-sized $BiVO_4$ and then extension of these routes to nano-$BiVO_4$, if possible.

Chapter 2

RESULTS AND DISCUSSION

2.1 General Comments on Bismuth Pyridine Carboxylates

Pyridine carboxylic acids are known to form stable chelate complexes with a large number of metals. On the basis of Pearson's hard–soft acid–base theory, Bi(III) can be considered to be a borderline acid, but it does bind fairly strongly with multidentate ligands possessing O and N donor atoms. Thus, it may be expected that anions of aminopolycarboxylic and polyaminopolycarboxylic acids form stable complexes with Bi(III). Several structural studies on iminodiacetic and nitrilotriacetic acid derivatives have been reported but those on picolinates (pyridine carboxylates) are scanty. Since Bi(III) ion is large, we can naturally expect coordination numbers of greater than six in most of its complexes. In the present work, pyridine-2-carboxylic acid, pyridine-2,6-dicarboxylic acid, quinoline-2-carboxylic acid, 3-hydroxy-picolinic acid, pyrazine-2-carboxylic acid, furan-2-carboxylic acid and thiophene-2-carboxylic acid were chosen as carboxylate reactants. All these acids are fairly soluble in hot water and hence the reactions were performed in hot water by using appropriate molar stoichiometry of the bismuth precursor to the acid. We must emphasise here that due to solubility restrictions, our studies are mostly restricted to X-ray structures and themogravimetric analysis (TGA).

2.1.1 Bismuth- pyridine carboxylates from bismuth nitrate

By using bismuth nitrate, we have prepared three compounds $[Bi(2\text{-}O_2C\text{-}C_5H_4N)_3]_n$ (**1**), $\{Bi[(2,6\text{-}O_2C)_2C_5H_3N)][(2\text{-}HO_2C\text{-}6\text{-}O_2C)C_5H_3N].H_2O\}_n$ (**2**) and $Bi(O_2CC_9H_6N)_2(O_3N)(O_2CC_9H_6NH).2H_2O$ (**3**) [Fig. 1]. They were synthesized by adding the corresponding carboxylic acid to a boiling aqueous solution of bismuth nitrate pentahydrate. When we tried to evaporate the reaction mixture at room temperature, very thin needle shaped crystals were obtained. They were not suitable for single crystal X-ray crystallography. Hence the reaction mixture was cooled slowly in a programmable hot air oven to obtain single crystals suitable

for X-ray crystallography. Compound **1** has been obtained previously while exploring benzylic oxidations by oxidizing Bi(0) in the presence of *t*-BuOOH and then reacting with picolinic acid,[18] but our route is more straightforward and simpler. Although in both the cases an aqueous medium was used, interestingly, the resulting complex did not contain any water of crystallisation. This was also shown by the absence of O-H band in the IR spectrum and the correct elemental analyses. By contrast, in the structures of **2** and **3**, non-coordinated water is present in the crystal lattice. In **3**, there is a sharper band at 3110 cm^{-1} ascribable to the protonated quinoline N-H (see X-ray structure below). These structures are described in subsequent sections. We have performed similar reactions with nicotinic acid, 2-hydroxy-nicotinic acid, 3-hydroxy-picolinic acid and pyridine-2,3-dicarboxylic acid and obtained only water-insoluble materials. From the reaction of bismuth nitrate with the amino acid L-proline, the only bismuth compound that we could isolate in small quantities was its oxonitrate cluster $Bi_6O_6(NO_3)_6$ (**4**) that does not contain the proline residue; we were able to get only the partial skeleton and not the full structure for these crystals [see below].

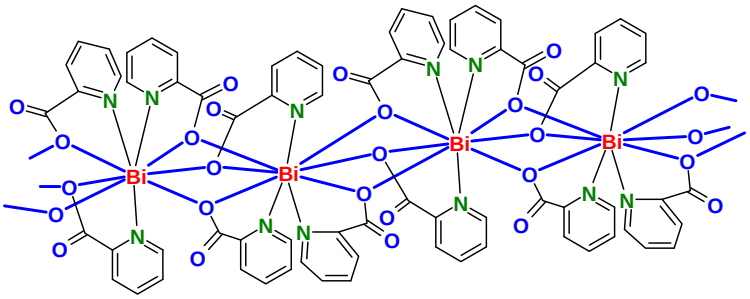

(1)

3 Bi-O covalent bonds
3 Bi-O coordinate bonds (one weak)
3 Bi-N coordinate bonds

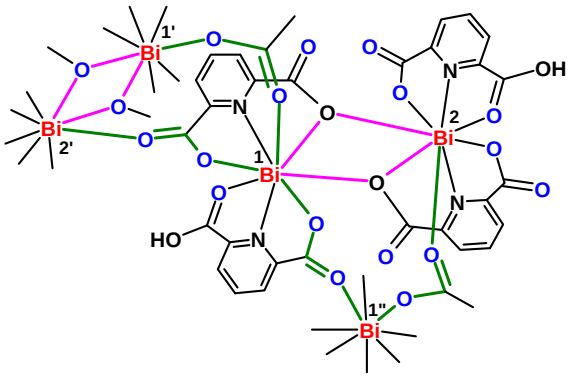

(2) [water molecules not shown]

Bi^1 and Bi^2 are in different environments
3 Bi-O covalent bonds
3 Bi-O coordinate bonds
2 Bi-N coordinate bonds

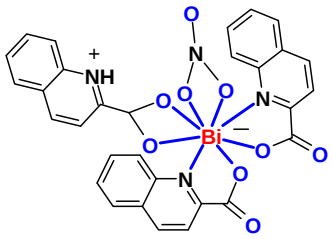

(3) [water molecule not shown]

3 Bi-O covalent bonds
3 Bi-O coordinate bonds (see text)
2 Bi-N coordinate bonds

Figure 1. Structures of **1**-**3** highlighting the coordination around bismuth atoms.

2.1.2 Crystal structure of bismuth pyridine-2-carboxylate (1)

Compound **1** [Fig. 2a].crystallised in the space group $P2_1/n$.[57] The relevant bond parameters are given in Table I. We assign a tricapped trigonal prismatic coordination sphere around bismuth with O(3'), O(5), O(1'), O(1), N(3) and O(3) forming the trigonal prism and N(1), O(5") and N(2) capping the three sides; this is shown in Figure 2b. The lone pair of electrons on bismuth appears to be stereochemically inactive. The bond distances are in the normal range for the covalent as well as coordinatively covalent linkages involving bismuth, with one of the Bi-O bonds being the longest, but within 0.8 Å of the sum of the van der Waals radii. Overall, the compound is a coordination polymer with three bridging oxygen atoms between adjacent bismuth centres. Each pyridine carboxylate forms five-membered rings using the nitrogen and one of the carboxylate oxygen atoms with the other oxygen being free. This type of structure is different from the tetrameric picolinate $[PhBi(2\text{-}(C_5H_4N)CO_2)_2]_4$,[7a] perhaps due to the presence of more number of oxygen atoms around bismuth in **1** It is also worth noting that a normal carboxylate like $[Bi(O_2CC_6H_4CH_3\text{-}3)_3]_\infty$ is also coordinatively polymeric but such complexes are composed of chelate carboxylates only.[58]

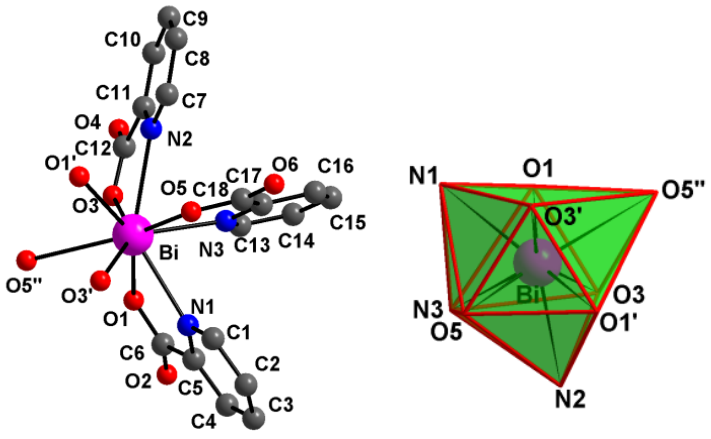

Figure 2a. Drawings representing the X-ray structure of **1**. Hydrogen atoms are not shown for clarity. Left: asymmetric unit + O(1'), O(3') and O(5') to show the coordination around bismuth. Right: polyhedron showing tricapped trigonal prismatic geometry around bismuth.

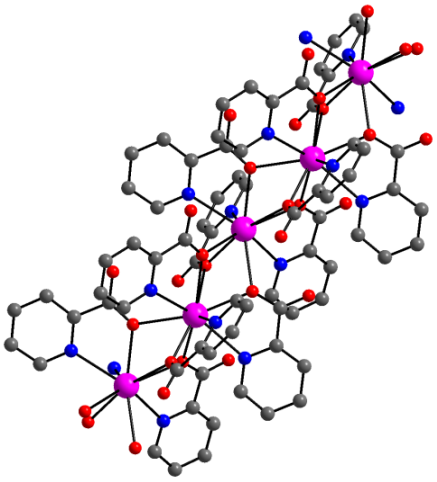

Figure 2b. Coordination polymeric motif in **1**. Colour code: Bi = magenta, O = red, N = blue and C = black. Symmetry operators: (i) 0.5-x, -0.5+y, 0.5-z; (ii) 0.5-x, 0.5+y, 0.5-z.

Table I. Selected geometric parameters (Å, ^{o}) in **1**[a]

Bi—O1	2.446(4)	Bi—N3	2.425(5)
Bi—O3	2.484(4)	Bi—O1’	2.662(4)
Bi—O5	2.315(4)	Bi—O3’	2.636(4)
Bi—N1	2.588(5)	Bi—O5“	2.935(4)
Bi—N2	2.627(5)		
O1—Bi—O3	63.70(13)	O5—Bi—O1’	69.87(14)
O1—Bi—O5	136.49(14)	O5—Bi—O3’	69.13(13)
O1—Bi—N1	63.83(13)	O5—Bi—O5“	154.91(12)
O1—Bi—N2	121.99(14)	N1—Bi—N2	138.89(16)
O1—Bi—N3	80.02(15)	N1—Bi—N3	71.31(17)
O1—Bi—O1^{1}	150.78(7)	N1—Bi—O1’	127.28(13)
O1—Bi—O3’	112.66(13)	N1—Bi—O3’	71.53(14)
O1—Bi—O5“	63.57(12)	N1—Bi—O5”	109.90(14)
O3—Bi—O5	135.06(14)	N2—Bi—N3	70.29(17)
O3—Bi—N1	123.34(14)	N2—Bi—O1’	69.91(14)
O3—Bi—N2	62.88(13)	N2—Bi—O3’	124.94(13)
O3—Bi—N3	80.12(15)	N2—Bi—O5“	107.58(14)

O3—Bi—O1’	108.98(13)	N3—Bi—O1’	128.12(15)
O3—Bi—O3’	150.89(6)	N3—Bi—O3’	128.76(15)
O3—Bi—O5“	62.08(12)	N3—Bi—O5“	135.74(15)
O5—Bi—N1	77.28(15)	O1’—Bi—O3’	58.83(13)
O5—Bi—N2	75.96(15)	O1’—Bi—O5“	87.73(11)
O5—Bi—N3	69.26(15)	O3’—Bi—O5“	89.91(12)

[a]Symmetry operators: (i) 0.5-x, -0.5+y, 0.5-z; (ii) 0.5-x, 0.5+y, 0.5-z.

Parameters involving O(5”) were taken by the Diamond program.

2.1.3 Crystal structure of bismuth pyridine-2,6-dicarboxylate (2)

Compound **2** [Fig. 3, Table II] is also a coordination polymer but the structural motif is quite different from that observed in **1**. There is a fused dinuclear [Bi(1)-O(2)-Bi(2)-O(9)-] polyhedral unit as well as a trinuclear [Bi(1)-O(9)-Bi(2)-O(4”)-C(1”)-O(1”)-Bi(1”)-O(8)-C(8)-O(5)-] motif. These features lead to a branched, rather than a linear, polymer. Since each bismuth is trivalent, between the two dipicolinates per bismuth, one free carboxylic acid -OH residue is still present in the compound. Although there are two distinct bismuth atoms in the asymmetric unit, both exhibit eight coordination with dodecahedral geometry. A major difference between the two bismuth atoms lies in the longest bond length: While for Bi(1), it is the coordinate bond to the carboxylic acid C=O [i.e. Bi(1)-O(6)], for Bi(2) it is a bridging oxygen of the [Bi_2O_2] skeleton [Bi(2)-O(2)]. Also, two Bi(1) and only one Bi(2) form a larger ring as mentioned before. Primarily, these differences make the two bismuth centres different.

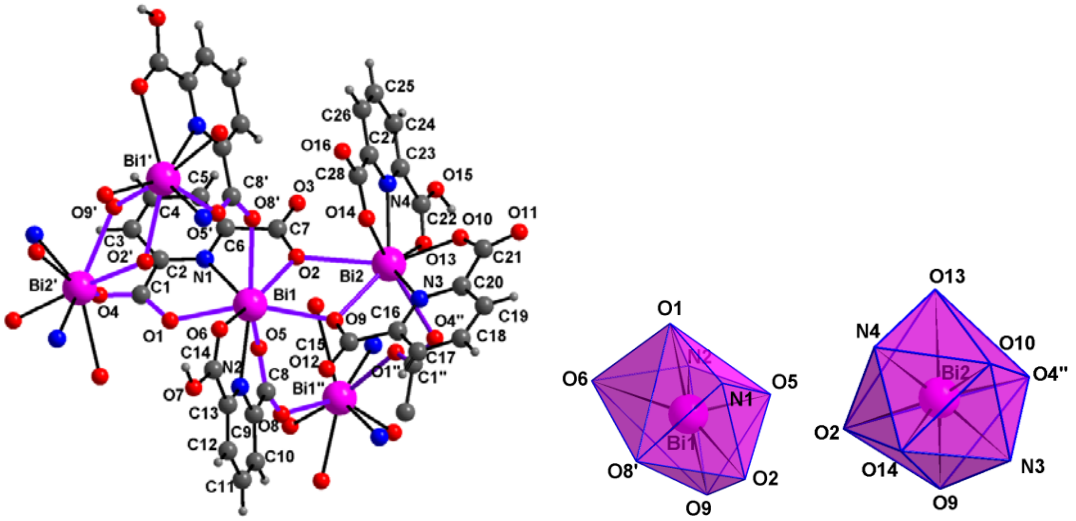

Figure 3a. Drawings representing the X-ray structure of **2**. Water molecules are not shown for clarity. Left: Asymmetric unit along with parts of other units to show the overall skeleton. Only selected atoms are labelled. Right: Polyhedra showing dodecahedral geometry around the two bismuth atoms of the asymmetric unit. Bi(1), N(1), N(2) as well as Bi(2). Colour code: Bi = magenta, O = red, N = blue, C = black, hydrogen = light grey.

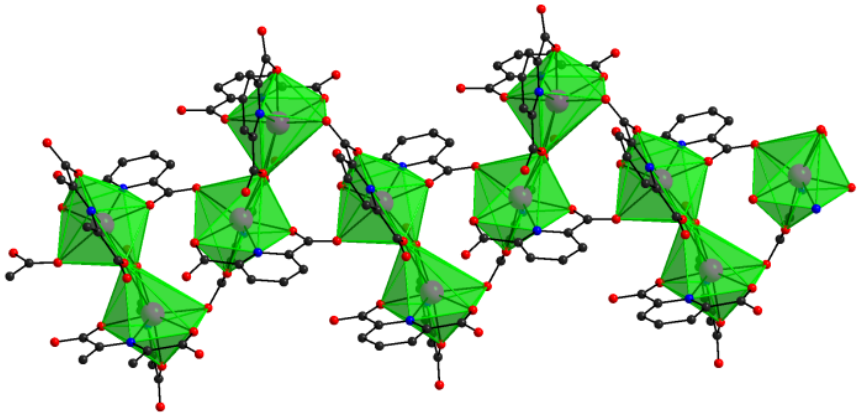

Figure 3b. A representation showing the dinuclear (fused polyhedra) and trinuclear units in **2**; hydrogen atoms and water molecules are omitted. Colour code: Bi = magenta, O = red, N = blue, C = black, hydrogen = light grey.

Table II. Selected geometric parameters (Å, °) in **2**[a]

Bi1—O1	2.391(5)	Bi2—O2	2.763(4)
Bi1—O2	2.483(4)	Bi2—O4”	2.625(5)
Bi1—O5	2.230(5)	Bi2—O9	2.584(5)
Bi1—O6	2.793(5)	Bi2—O10	2.268(5)
Bi1—O8’	2.635(5)	Bi2—O13	2.672(5)
Bi1—O9	2.524(5)	Bi2—O14	2.239(5)
Bi1—N1	2.429(5)	Bi2—N3	2.398(5)
Bi1—N2	2.478(5)	Bi2—N4	2.449(5)
O1—Bi1—O2	131.36(15)	O2—Bi2—O4”	121.13(15)
O1—Bi1—O5	91.1(2)	O2—Bi2—O9	62.39(13)
O1—Bi1—O6	67.16(17)	O2—Bi2—O10	155.67(16)
O1— Bi1—O8’	101.6(2)	O2—Bi2—O13	100.54(15)
O1— Bi1—O9	157.46(16)	O2—Bi2—O14	79.01(16)
O1— Bi1—N1	65.72(17)	O2—Bi2—N3	123.59(15)
O1— Bi1—N2	71.86(18)	O2 —Bi2—N4	81.83(16)
O2— Bi1—O5	75.57(18)	O4”—Bi2—O9	84.21(16)
O2—Bi1—O6	152.38(16)	O4”—Bi2—O10	81.87(16)
O2—Bi1—O8’	68.58(17)	O4—Bi2—O13	76.87(16)
O2—Bi1—O9	67.28(14)	O4”—Bi2—O14	145.27(16)
O2—Bi1—N1	66.13(16)	O4”—Bi2—N3	70.01(16)
O2—Bi1—N2	137.82(18)	O4”—Bi2—N4	137.51(18)
O5—Bi1—O6	129.35(16)	O9—Bi2—O10	133.75(15)
O5—Bi1—O8’	141.30(18)	O9—Bi2—O13	142.37(17)
O5—Bi1—O9	81.23(18)	O9—Bi2—O14	81.49(18)
O5—Bi1—N1	81.68(18)	O9—Bi2—N3	64.72(16)
O5—Bi1—N2	68.56(18)	O9—Bi2—N4	136.85(18)
O6—Bi1—O8’	89.02(16)	O10—Bi2—O13	75.56(17)
O6—Bi1—O9	101.55(16)	O10—Bi2—O14	85.50(18)
O6—Bi1—N1	122.91(17)	O10—Bi2—N3	69.06(17)

O6—Bi1—N2	61.37(17)	O10—Bi2—N4	74.97(18)
O8'—Bi1—O9	97.52(18)	O13—Bi2—O14	130.61(17)
O8'—Bi1—N1	71.04(18)	O13—Bi2—N3	134.02(17)
O8'—Bi1—N2	150.13(19)	O13—Bi2—N4	63.20(18)
O9—Bi1—N1	132.99(16)	O14—Bi2—N3	75.26(17)
O9—Bi1—N2	85.62(17)	O14—Bi2—N4	67.96(18)
N1—Bi1—N2	126.96(18)	N3—Bi2—N4	129.78(18)

[a]Symmetry operators: (i) -x+1, y+1/2, -z+1/2; (ii) -x+1, y-1/2, -z+1/2.

2.1.4 Crystal structure of bismuth quinoline-2-carboxylate (3)

Unlike **1** and **2**, compound **3** is monomeric [Fig. 4, Table III], most likely because of the sterically bulkier quinoline carboxylate moiety not permitting the oligomerization/polymerization. Under the conditions employed, the third nitrate could not be exchanged for quinaldate (qunioline 2-carboxylate). Overall, two quinoline carboxylates coordinate *via* [N,O] five-membered chelate, while the nitrate and the zwitterionic quinoline carboxylic acid coordinate *via* [O,O] four-membered chelate rings. Thus three types of chelating ligands surround the metal. Also, as can be seen from the diagram, the quinoline caboxyl nitrogen N(3) is protonated. The distortion in geometry from the more regular dodecahedron may, at least in part, be due to the lone pair of electrons on bismuth. The two water molecules in the asymmetric unit of **3** are hydrogen bonded to each other, to other oxygen atoms and the protonated nitrogen {N(3)…O(10) 2.704(8), O(10)…O(11) 2.749(6), O(10)…O(4) [sym: 0.5+x, 1.5-y, 0.5+z] 2.846(8), O(11)…O(2) [symm: -0.5+x, 0.5+y, z] 2.939(8), O(11)…O(6) 2.928(9) Å}. The water molecule is retained at least up to 200 ^{o}C (as shown by TGA).

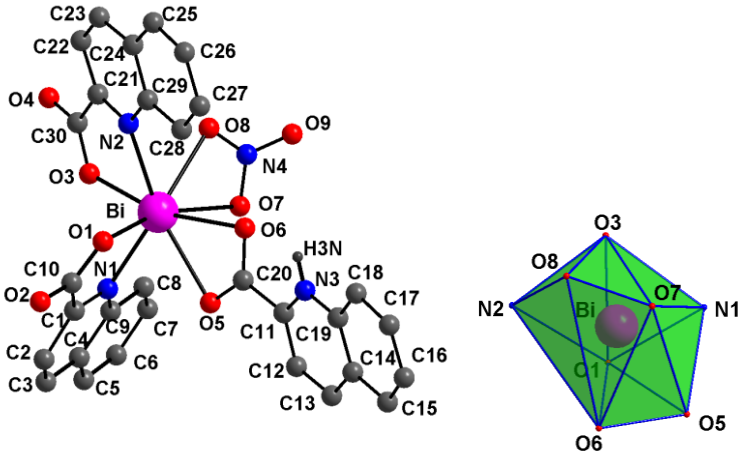

Figure 4. Drawings representing the X-ray structure of **3**. Hydrogen atoms are not shown for clarity. Left: asymmetric unit. Right: polyhedron showing slightly distorted dodecahedral geometry. Colour code: Bi = magenta, O = red, N = blue and C = grey-black.

Table III. Selected geometric parameters (Å, °) in **3**

Bi—O1	2.195(6)	Bi—N2	2.535(8)
Bi—O3	2.250(7)	Bi—O6	2.654(7)
Bi—O5	2.627(6)	Bi—O7	2.721(7)
Bi—N1	2.407(8)	Bi—O8	2.671(7)
O1—Bi—O3	91.93(19)	O5—Bi—O7	80.4(2)
O1—Bi—O5	82.5(2)	O5—Bi—O8	121.0(2)
O1—Bi—O6	92.3(3)	O5—Bi—N1	71.1(2)
O1—Bi—O7	162.8(2)	O5—Bi—N2	140.1(2)
O1—Bi—O8	148.3(2)	O6—Bi—O7	78.32(19)
O1—Bi—N1	71.5(3)	O6—Bi—O8	89.0(2)
O1—Bi—N2	78.1(2)	O6—Bi—N1	120.6(2
O3—Bi—O5	146.5(2)	O6—Bi—N2	96.2(2)
O3—Bi—O6	163.5(2)	O7—Bi—O8	47.2(2)
O3—Bi—O7	101.1(3)	O7—Bi—N1	100.7(2)
O3—Bi—O8	79.1(2)	O7—Bi—N2	117.0(2)

O3—Bi—N1	75.8(2)	O8—Bi—N1	133.4(2)
O3—Bi—N2	69.1(2)	O8—Bi—N2	70.3(2)
O5—Bi—O6	49.92(19)	N1—Bi—N2	132.12(19)

2.1.5 Crystal structure (partial) of bismuth oxonitrate $Bi_6O_6(NO_3)_6$ (4)

Although this is not a carboxylate complex, it is obtained in such a reaction (bismuth nitrate and L-proline) and hence is included here. The quality of data was not good enough to solve/refine the structure completely; however, it appears to contain interlinked Bi_6O_8 core [Fig. 5] with both chelating and bridging nitrate ligands [cell parameters: Monoclinic, $P2_1/n$; a = 15.342(5), b = 9.177(3), c = 17.132(6) Å, β = 113.989 (5)^o, V = 2203.7(12) Å^3; for similar structures, see ref. 4f]. Since the structure could not be refined well, it is thought not prudent to make further comments on the bond parameters.

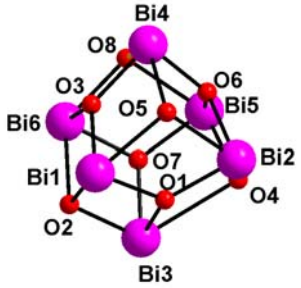

Figure 5. Core of the bismuth oxonitrate **4** obtained from the reaction of bismuth nitrate with L-proline. There are 6 nitrate anions that are not shown.

Table IV: Partial bond distance (Å) data in the bismuth oxonitrate **4**[a]

Bi1-O1	2.14(3)		Bi3-O1	2.23(3)		Bi5-O7	2.12(2)
Bi1-O2	2.30(3)		Bi3-O2	2.19(3)		Bi5-O6	2.17(3)
Bi1-O3	2.16(3)		Bi3-O4	2.90(3)		Bi5-O4	2.21(3)
Bi1-O5	2.45(3)		Bi3-O7	2.21(3)		Bi5-O8	2.50(3)
Bi2-O1	2.12(3)		Bi4-O6	2.12(3)		Bi6-O3	2.13(3)
Bi2-O4	2.29(3)		Bi4-O3	2.13(3)		Bi6-O7	2.17(3)
Bi2-O5	2.47(3)		Bi4-O5	2.35(3)		Bi6-O8	2.27(3)
Bi2-O6	2.21(3)		Bi4-O8	2.38(3)		Bi6-O2	2.43(3)

[a] The data presented here is only to indicate that a multinuclear bismuth cluster is obtained; there are several nitrate anions present that could not be fully refined.

2.1.6 Thermogravimetric analysis of compounds 1-3

The TGA data [Fig. 6] show that compound **1** is perfectly stable up to ~360 ^{o}C, after which decomposition occurs to lead to Bi_2O_3. Such a behaviour is observed for some other bismuth compounds also.[22] Compound **2** behaves differently, with the non-coordinated water molecules coming off before the decomposition sets in. Compound **3** shows a more interesting behaviour with its melting point almost coinciding with decomposition/sublimation at ca ~220 ^{o}C (consistent with its lower melting point). Foaming was also observed during melting of **3** that suggests the removal of water, but it decomposed nearly at the same temperature leaving a black residue.

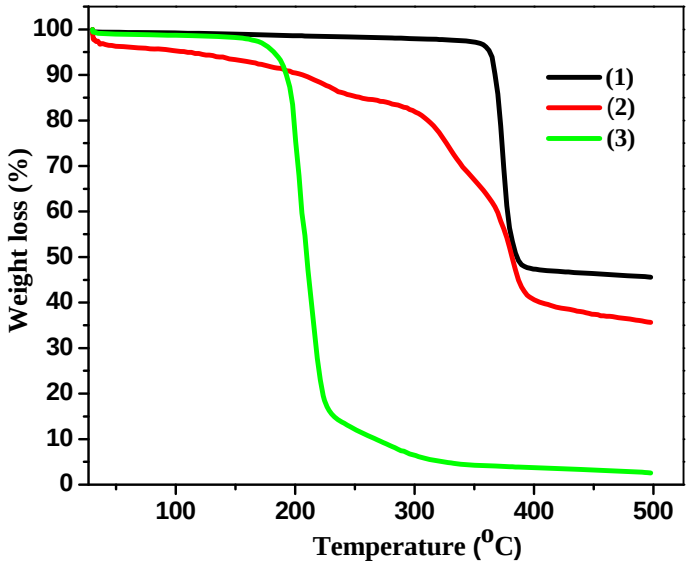

Figure 6. Drawing showing the TGA behaviour of compounds **1-3**

2.2 Bismuth Pyridine Carboxylates Prepared from Ammonium Bismuth Citrate

Ammonium bismuth citrate is not much explored as a starting material in bismuth chemistry. In this work, bismuth picolinate of the formula $[Bi(2\text{-}O_2C\text{-}C_5H_4N)_3]_n$ in another polymorphic form of **1'** (space group $P2_1$), was prepared by treating ammonium bismuth citrate with picolinic acid, but in this case the reaction was too fast and the product was obtained only as a microcrystalline precipitate. However, while attempting to isolate a bimetallic complex using $Gd(NO_3)_3\ 5H_2O$, $Bi(NO_3)_3.5H_2O$ and picolinic acid, we obtained crystalline $[Bi(2\text{-}O_2C\text{-}C_5H_4N)_3]_n$ in

the second polymorphic form **1'** (Fig. 7) for which an X-ray structure could be determined. The reaction of ammonium bismuth citrate with dipicolinic acid in water led to compound $\{[Bi((2,6\text{-}O_2C)_2C_5H_3N)((2\text{-}HO_2C\text{-}6\text{-}O_2C)C_5H_3N)(H_2O)]_2.5H_2O\}_n$ (**5**) which is different from $\{Bi[(2,6\text{-}O_2C)_2C_5H_3N)][(2\text{-}HO_2C\text{-}6\text{-}O_2C)C_5H_3N].H_2O\}_n$ (**2**) obtained by using bismuth nitrate pentahydrate and dipicolinic acid. Compound **5** was also obtained when a mixture of bismuth nitrate pentahydrate and gadolinium nitrate pentahydrate were treated with dipicolinic acid in water. In the latter case, it is likely that competition (albeit weaker) for the ligand by gadolinium resulted in the formation of **5** (rather than **2**).

2.2.1 Comparison of structures of bismuth pyridine-2-carboxylates 1 and 1'

Molecular structure of **1'** is shown in Figure 7. The bond distances in the two crystalline modifications are shown in Table V along with that reported by Callens *et al.*[18] There are moderate differences in the bond distances in the two modifications **1** and **1'**. However, the main point arising out of the present study is that even in the modification **1'**, the coordination number of bismuth is nine and the geometry can be described as tricapped trigonal prism. There are three Bi-O covalent bonds, three Bi-N coordinate covalent bonds and three Bi-O coordinate covalent bonds (with one of them weaker than the other two). Coordination number of only 8 is ascribed to **1'** in the literature.[18]

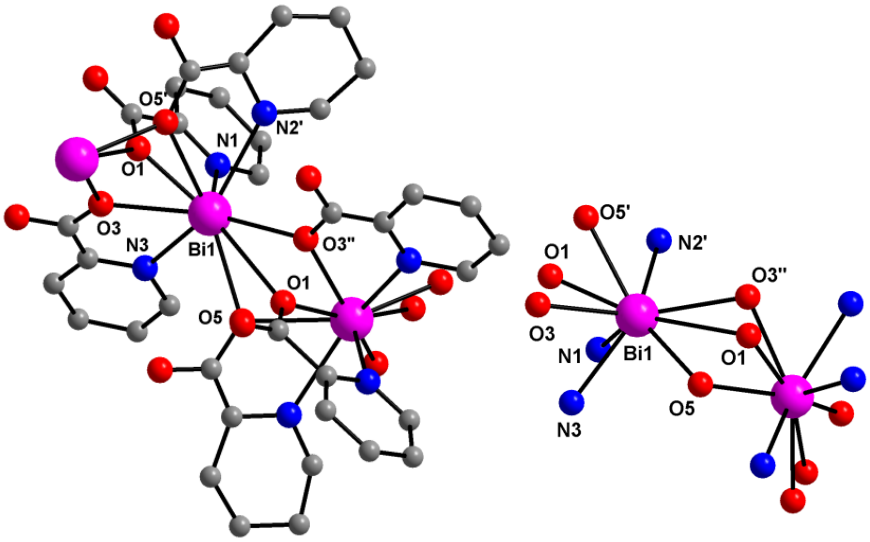

Figure 7. Molecular structure of **1'**. Only the bismuth and the corresponding coordinated atoms are shown. Symmetry codes (i) –x, -0.5+y, 2-z; (ii) –x, 0.5+y, 2-z.

Table V. Comparison of the bond distances in the two polymorphs **1** and **1'** (Å)[a]

Polymorph	**1**	**1'**
Space group	$P2_1/n$	$P2_1$[b,c]
Bi-N	2.425(5)	2.438(8)
	2.588(5)	2.571(6)
	2.627(5)	2.620(7)
Bi-O	2.314(4)	2.242(7)
	2.425(4)	2.533(7)
	2.446(4)	2.559(7)
	2.484(4)	2.563(7)
	2.636(4)	2.614(7)
	2.935(4)	2.987(9)

[b] Refinement of thermal parameters except for bismuth could be done only isotropically. In the .cif data available in the CCDC database corresponding to ref. 18 also, only isotropic refinement is reported. In our case, although the structure could be solved in the higher symmetry space group $P2_1/m$, there were too many short O…O contacts and a rather questionable coordination number of 13 on bismuth. Hence this space group was not considered further.

[c] Corresponding distances (except the last entry) as reported in the literature:[18] 2.430 (9), 2.588 (7), 2.633(7), 2.296 (6), 2.473(6), 2.531(6), 2.574(6) and 2.648(6) Å.

2.2.2 Crystal structure of bismuth pyridine-2,6-dicarboxylate (5)

A glance at the formula of **2** and **5** would indicate that there is only a difference in the number of molecules of water, but structurally, the two compounds are quite different. As described above, in **2**, the water molecules are not coordinated to bismuth while in **5**, each bismuth is coordinated to a water molecule thus leaving one of the carboxylate oxygen atoms for hydrogen bonding interactions. The structural drawings for the dimeric unit in **5** are given in Figure 8; the supramolecular structure leading to the coordination polymer is shown in Figure 9. Bond distances in **2** (repeated for comparison) and **5** are compiled in Table VI. There are two types of bismuth environments in **2**. Also, there are both dimeric

[Bi_2O_2] and trimeric [BiOCOBiOBiOCO] moieties in the overall structure. By contrast, in **5**, only one type of bismuth environment with a Bi_2O_2 skeleton is seen; these units are linked further to form an extended tetranuclear cage. The Bi1-O6" and Bi1-O9"' distances involving the bridging oxygen atom of dimeric unit and the coordinated water are much longer than the other Bi-O distances in **5**, as expected. The Bi-N distances in the two compounds are in a similar range. Since bismuth is trivalent in both the compounds, between the two dipicolinates per bismuth, one free carboxylic acid -OH residue is still present in each. Although there are two distinct bismuth atoms in the asymmetric unit of **2** both exhibit eight coordination with dodecahedral geometry at bismuth. However in **5**, the coordination number at bismuth is nine and the geometry can be described as distorted tricapped trigonal prism. In both the compounds, the supramolecular structure can be construed to have resulted in coordination polymers.

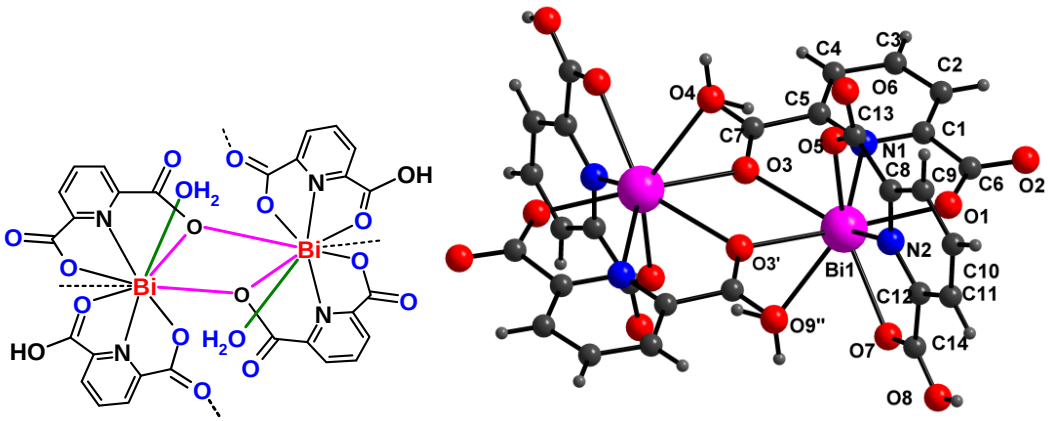

Figure 8. Molecular structure of the dimeric unit in **5**. The ninth weaker coordination involving O6" is not expanded in this drawing, but is shown in Figure 9.

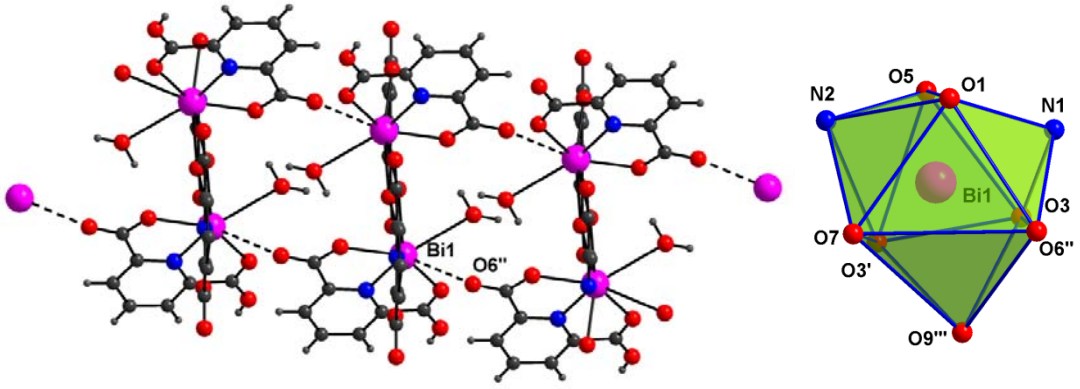

Figure 9. Left: Drawing showing the supramolecular motif via additional Bi…O interactions in **5**. Right: Polyhedron showing the distorted tricapped trigonal prismatic geometry at bismuth. Symmetry codes: (i) –x, -y, -z; (ii) 1+x, y, z; (iii) x, -1+y, z.

Table VI. Selected bond distances (Å) in **2** and **5** [a,b]

Compound	**2**			**5**	
Space group	$P2_1/c$			$P\bar{1}$	
Bi1—O1	2.391(5)	Bi2—O2	2.763(4)	Bi1 O1	2.298(3)
Bi1—O2	2.483(4)	Bi2—O4”	2.625(5)	Bi1 O3	2.670(4)
Bi1—O5	2.230(5)	Bi2—O9	2.584(5)	Bi1 O3'	2.583(3)
Bi1—O6	2.793(5)	Bi2—O10	2.268(5)	Bi1 O5	2.281(4)
Bi1—O8’	2.635(5)	Bi2—O13	2.672(5)	Bi1 O7	2.530(4)
Bi1—O9	2.524(5)	Bi2—O14	2.239(5)	Bi1-O6”	3.101(7)
Bi1—N1	2.429(5)	Bi2—N3	2.398(5)	Bi1-O9'''	2.891(11)
Bi1—N2	2.478(5)	Bi2—N4	2.449(5)	Bi1 N1	2.475(4)
				Bi1 N2	2.417(4)

[a]Symmetry codes for compound **2**: (i) -x+1, y+1/2, -z+1/2; (ii) -x+1, y-1/2, -z+1/2

[b]Symmetry codes for compound **5**: (i) –x, -y, -z; (ii) 1+x, y, z; (iii) x, -1+y, z.

There are several hydrogen bonding interactions in both **2** and **5**. While the water molecules are not coordinated to bismuth in **2**, both coordinated and non-coordinated water molecules are found in **5**. Also, there are more water molecules per bismuth in **5** which contributes to the difference in the two structures. Two water

molecules in the asymmetric unit of **2** [i.e., one per bismuth] form a "dimer" but are involved in hydrogen bonding to other atoms also. The hydrogen atom positions are not refined here; the relevant O…O distances are (i) O(15)…O(17) [symm: x, y-1, z] 2.520(10), (ii) O(17)…O(18) 2.714(17), (iii) O(18)…O(16) 2.792(9) and (iv) O(18)…O(13) [symm: x, 1+y, z] 3.385(1) Å. There is also one discernible C(4)-H…O interaction, with a C…O [symm: -x, y-0.5, 0.5-z] distance of 3.124(10)Å. In **5**, both the hydrogen atoms of the coordinated water are involved in hydrogen bonding, one to an oxygen atom of carboxylate moiety and the other to the oxygen of a non-coordinated water molecule. The oxygen atom O(9) corresponding to the coordinated water molecule is hydrogen bonded to the carboxylate oxygen O(5) and O(10) of a non-coordinated water molecule. The water molecules corresponding to O(10), O(11) and O(12) form a hydrogen bonded cyclic system. These are shown in Figure 10.

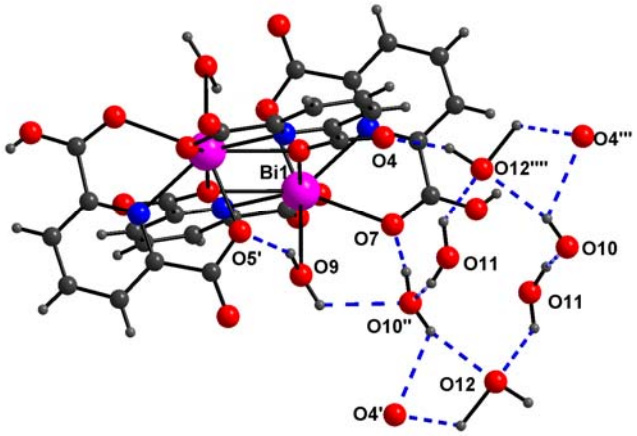

Figure 10. A diagram showing hydrogen bonding interactions in compound **5**. Hydrogen bonding parameters (Å, °): O(9)-H(9AO)...O(5') 0.927(5), 1.969(5), 2.826(5) Å, 152.7(6)°; O(9)-H(9BO)...O(10") 0.922(6), 2.336(9), 2.898(1) Å, 119.0(5)°; O(10)-H(10AO)...O(7) 0.906(7), 1.833(8), 2.706(8) Å, 161.0(6)°; O(10)-H(10BO)...O(4"') 0.905(6), 2.351(7), 2.891(9) Å, 118.3(4)°; O(10)-H(10BO)...O(12"") 0.905(6), 2.170(9), 2.995(1) Å, 151.3(5)°; O(11)-H(11AO)...O(12) 0.923(3), 2.024(9), 2.721(1) Å, 131.1(3)°; O(11)-H(11BO)...O(10") 0.922(6), 2.336(9), 2.898(1) Å, 119.0(5)°; O(12)-H(12O)...O(4') 0.994(7), 1.801(8), 2.728(1) Å, 153.7(6)°. Symmetry codes: (i) -x,1-y,-z, (ii) x,y+1,z, (iii) 1-x,-y,-z, (iv) -x+1,-y+1,-z+1.

It may be noted that the two forms **2** and **5** are prepared under slightly different conditions by using different precursors. Compound **2** is obtained under reflux conditions using bismuth nitrate because of the poor solubility of the nitrate. Compound **5** is formed at room temperature using the soluble ammonium bismuth citrate. We believe that the difference in temperature has resulted in the different structures and the use of a lower temperature to prepare **5** has led to a higher stoichiometry of water being retained in the lattice.

2.2.3 Comparison of thermogravimetric analysis of compounds 2 and 5

The thermal behaviour of **2** and **5** is also markedly different and compound **5** undergoes decomposition at an earlier stage than compound **2** [Fig. 11]. This is perhaps understandable since the interaction among different dimeric units in **5** is rather weak as discussed above. The final residue in each case, as evidenced by the percentage weight loss is Bi_2O_3.

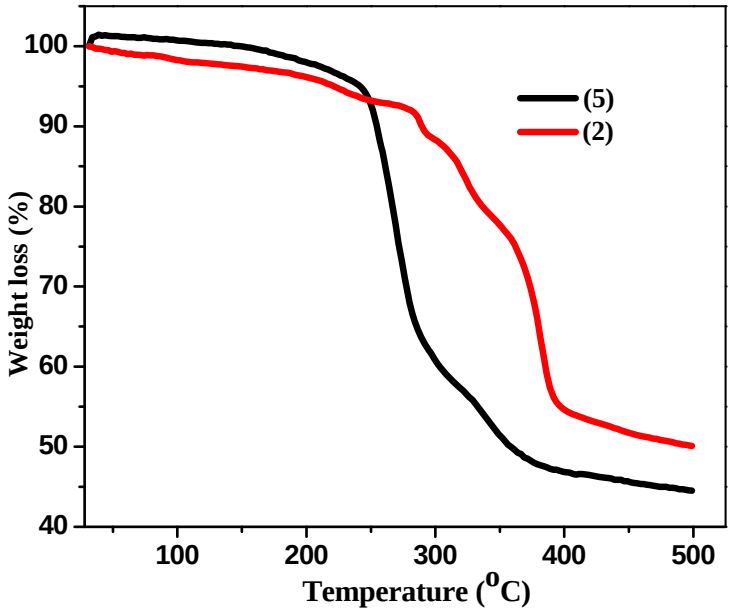

Figure 11. Drawing showing the TGA of compound **5** as compared to compound **2**.

2.3 Bismuth Pyridine Carboxylates prepared from Triphenylbismuth

2.3.1 Phenylbismuth 3-hydroxy pyridine-2-carboxylate (6)

Triphenylbismuth ($BiPh_3$) was prepared using the Grignard reaction of $BiCl_3$ with phenylmagnesium bromide.[59] The reaction of $BiPh_3$ with 3-hydroxy-picolinic acid (1:3 molar ratio) in ethanol at room temperature (25 °C) resulted in [PhBi(2-

O_2C-3-$(OH)C_5H_3N)_2$(2-O_2C-3-$OHC_5H_3NH)$] (**6**). When the same reaction was conducted under reflux conditions, an insoluble precipitate was obtained. Andrews *et al* have obtained the tetramer [PhBi(2-$(C_5H_4N)CO_2)_2]_4$ (**7**) by using $BiPh_3$ and picolinic acid in refluxing toluene as well as under solvent free conditions.[7a] It may be noted that there is one additional N-protonated carboxylate per bismuth in compound **6** that is monodentate and not present in compound **7**. Our new compound **6** is essentially monomeric in bismuth having a BiN_2O_4 skeleton with a pentagonal pyramidal geometry as shown in Figure 12; bond parameters are given in Table VII. While the phenyl carbon is at the apical position, the three oxygen and two nitrogen atoms form the base of the pyramid. The bond distances are in the same range as that observed in **7**. Thus, for the first look, it appears that the bismuth lone pair of electrons is stereochemically active. However, a closer look at the structure reveals that there is an additional weak but discernible interaction between the coordinated O7 and bismuth atom of a second molecule [distance 3.449(5)Å, sum of van der Waals distances 3.9 Å[37b]], in the direction of the lone pair, leading to a weakly held dimer as shown in Fig. 12 (Right). Similar dimeric formulation in bismuth oxinates have also been reported.[8] Both intra- and inter-molecular hydrogen bonding are present in **6**, but they do not appear to have influenced the coordination on bismuth. Moderately strong C-H...O interactions involving aromatic C-H and phenolic/carboxylic oxygen atoms are also found in the structure. A drawing showing more details on inter- and intra-molecular hydrogen bonding is depcited in Figure 13.

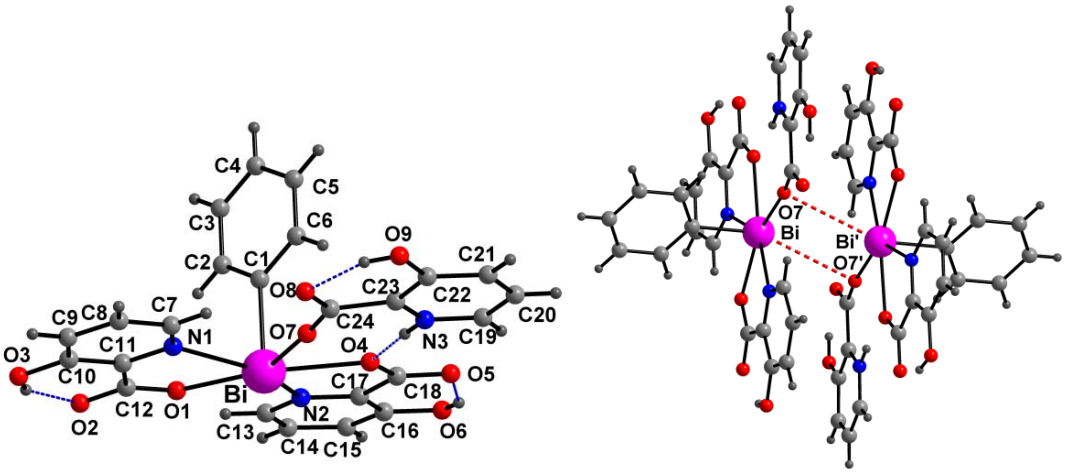

Figure 12. Left: Molecular structure of compound **6**. Right: Structure of **6** showing weak dimer formation *via* additional Bi…O interactions [Bi-O8 = 4.592 (6) Å].

Table VII. Selected geometric parameters (Å, ◦) in **6**

Bi-C1	2.233(3)	O1-Bi-O7	144.45(8)
Bi-O1	2.323(2)	O4-Bi-O7	70.88(8)
Bi-O4	2.442(2)	C1-Bi-N2	85.89(10)
Bi-O7	2.478(2)	O1-Bi-N2	78.58(9)
Bi-N1	2.568(3)	O4-Bi-N2	65.69(9)
Bi-N2	2.513(3)	O7-Bi-N2	136.51(9)
Bi...O7’	3.449(5)*	C1-Bi-N1	86.88(10)
		O1-Bi-N1	67.49(8)
C1-Bi-O1	88.72(10)	O4-Bi-N1	147.06(9)
C1-Bi-O4	85.48(10)	O7-Bi-N1	76.97(8)
O1-Bi-O4	144.10(8)	N2-Bi-N1	145.42(9)
C1-Bi-O7	88.74(11)		

*Symm. Equiv. 1-x, -y, -z

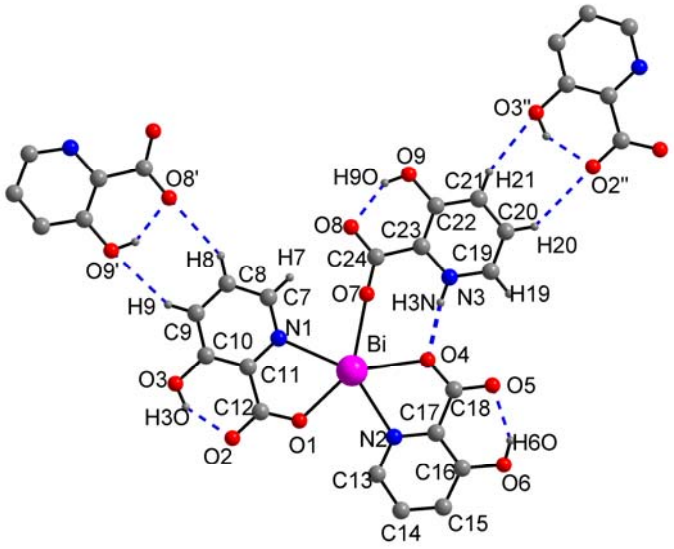

Figure 13. A diagram showing detailed hydrogen bonding interactions in compound **6**. Hydrogen bonding parameters (Å, °): C(8)-H(8)...O(8’) 0.930(5) 2.481(3), 3.320(6), 150.1(3); C(9)-H(9)...O(9’) 0.930(4), 2.529(4), 3.382(6), 152.68(28); C(20)-H(20)...O(2’’) 0.930(4), 2.680(3), 3.474(5), 143.8(3); C(21)-H(21)...O(3’’) 0.930(4), 2.434(3), 3.319(5), 159.1(3); N(3)-H(3)...O(4) 0.860(3), 1.863(3), 2.717(4), 172.3(2); O(3)-H(3O)...O(2) 0.820(4), 1.787(3), 2.514(5), 146.9(3); O(6)-H(6O)...O(5) 0.820(4), 1.852(4), 2.571(6), 145.6(3); O(9)-H(9O)...O(8) 0.820(3), 1.792(3), 2.524(4), 147.8(2). Symmetry codes: (i) -x,-y,-z, (ii) x, y-1, z+1.

2.3.2 Bismuth 3-hydroxy pyridine-2-carboxylate (8)

Interestingly, use of pyridine as the solvent in the 1:3 stoichiometric reaction of $BiPh_3$ and 3-hydroxy picolinic acid at room temperature resulted in an entirely different product, $[(Bi(2\text{-}O_2C\text{-}3\text{-}(OH)C_5H_3N)_4)(C_5H_5NH)(C_5H_5N)]$ (**8**).[18] The yield of this product could be maximized by increasing the amount of the acid. Single crystals of **8** were directly obtained from the reaction mixture after slow evaporation of most of the solvent (pyridine). The coordination number around bismuth is eight and we may describe the geometry as distorted dodecahedron as shown in Figure 14. Although bond distances are in the expected normal range, the Bi-O10 distance is slightly longer (by *ca* 0.1 Å) than the rest of the Bi-O distances (Table VIII). Inter and intramolecular hydrogen bonding in compound **8** are shown in Figure 15.

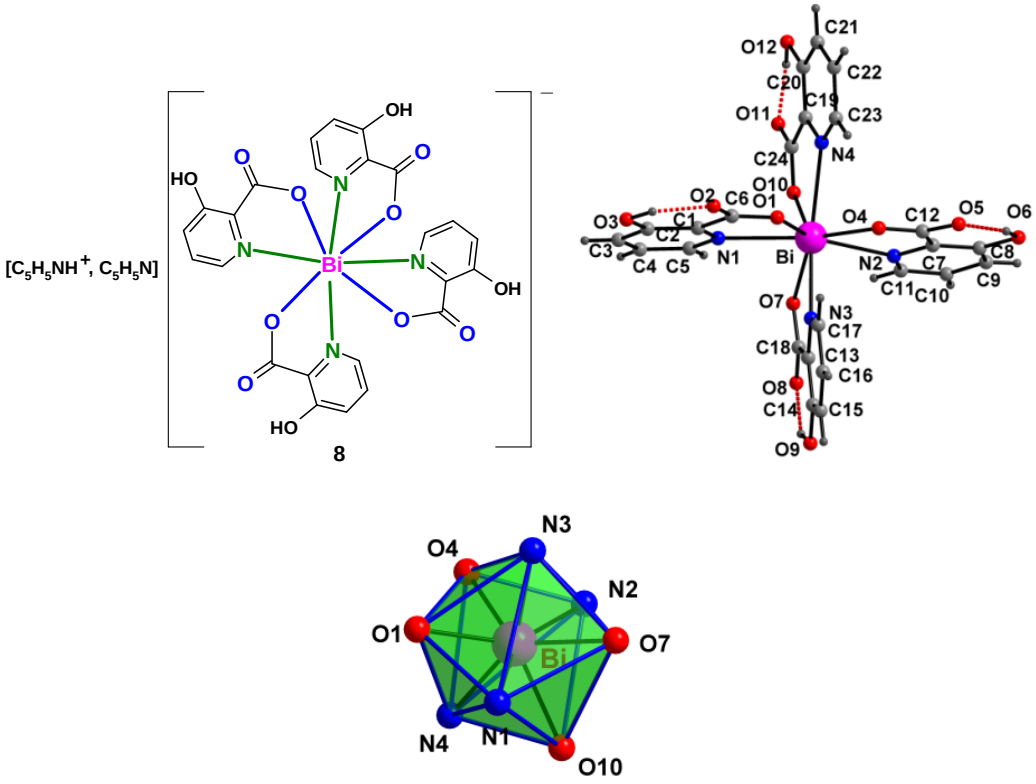

Figure 14. Top left**:** Molecular structure of the anion in compound **8**. Top right: Intramolecular O-H…O hydrogen bonding is also shown. Bottom: A polyhedral representation around bismuth.

Table VIII. Selected geometric parameters (Å, ◦) in **8**

Bi- O1	2.343(2)	O4 -Bi- N2	66.04(9)
Bi- O4	2.380(3)	O4- Bi- N3	80.75(10)
Bi- O7	2.447(3)	O4- Bi- N4	78.66(9)
Bi- O10	2.587(2)	O7- Bi- O10	76.21(8)
Bi- N1	2.559(3)	O7- Bi- N1	78.11(9)
Bi- N2	2.583(3)	O7- Bi- N2	76.00(9)
Bi- N3	2.449(3)	O7- Bi- N3	66.98(9)
Bi- N4	2.630(3)	O7- Bi- N4	138.97(9)
		O10- Bi- N1	79.34(9)
O1- Bi- O4	74.99(9)	O10- Bi- N2	83.56(9)
O1- Bi- O7	131.82(8)	O10- Bi- N3	143.04(9)
O1- Bi- O10	125.05(9)	O10- Bi- N4	62.89(8)
O1- Bi- N1	66.81(9)	N1- Bi- N2	151.69(9)
O1- Bi- N2	140.94(9)	N1- Bi- N3	89.82(10)
O1- Bi- N3	80.54(10)	N1- Bi- N4	96.58(10)
O1- Bi- N4	78.98(9)	N2- Bi- N3	90.46(10)
O4- Bi- O7	129.41(9)	N2- Bi- N4	95.45(10)
O4- Bi- O10	128.12(9)	N3- Bi- N4	154.03(10)
O4- Bi- N1	141.67(9)		

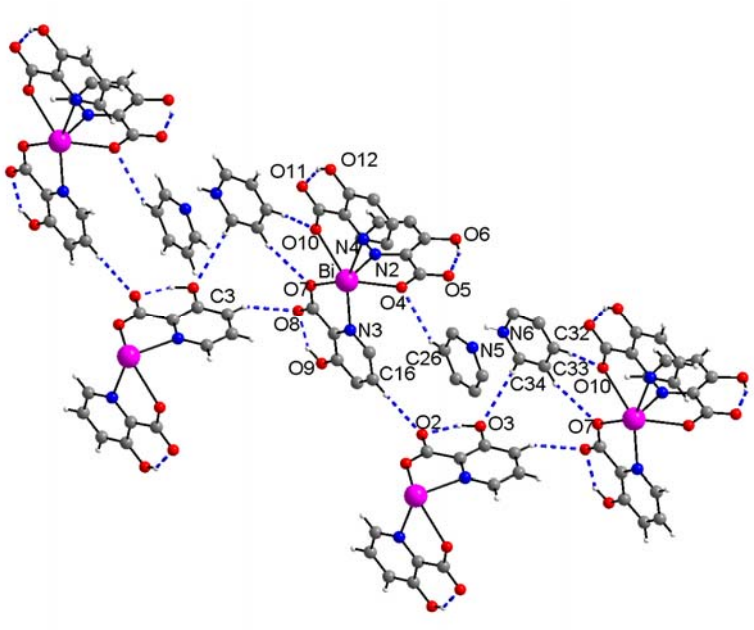

Figure 15. A diagram showing hydrogen bonding interactions in compound **8**. Hydrogen bond parameters (Å, °): O(6)-H(6O)...O(5) 0.891(6), 1.712(5), 2.536(5) Å, 152.8(5)°; O(9)-H(9O)...O(8) 0.867(5), 1.771(4), 2.552(5) Å, 148.6(4)°; O(12)-H(12O)...O(11) 0. 933(8), 1.683(7), 2.536(6) Å, 150.5 (6)°; C(26)-H(26)...O(4) 0.930(9), 2.741(3), 3.463(8) Å, 135.2(4)°; C(32)-H(32)...O(10') 0.930(5), 1.809(4), 2.736(6) Å, 173.9(3)°; C(33)-H(33)...O(7') 0.930(4), 2.616(3), 3.442(6) Å, 148.3(3)°; C(16)-H(16)...O(2'') 0.930(9), 2.741(3), 3.463(8) Å,135.2(4)°; C(3)-H(3)...O(8''') 0.930(4), 2.410(3), 3.236(5) Å, 147.9(3)°; C(34)-H(34)...O(3'') 0.930(6), 2.732(3), 3.316(6) Å,121.6(3)°. Symmetry codes: (i) x, +y, z+1; (ii) -x, -y+1, -z+1; (iii) -x, -y+1, -z+2; (iv) -x, -y+1, -z+1.

2.3.3 Phenylbismuth pyrazine-2-carboxylate (9): Weak secondary interactions

The compound $[PhBi(2\text{-}O_2C\text{-}C_4H_3N_2)_2(2\text{-}O_2C\text{-}C_4H_4N_2).H_2O]$ (**9**) was obtained by the 1:3 reaction of $BiPh_3$ and pyrazine-2-carboxylic acid in refluxing ethanol. To our knowledge, this is the first structural report on bismuth pyrazine-2-carboxylate. Wenkin *et al* and Zevaco *et al* have earlier reported the synthesis of only insoluble materials of bismuth pyrazine- and pyrazole carboxylates.[22-24] Taking into consideration only the stronger interactions, the geometry at bismuth may still be treated as pentagonal pyramid. Although the structure [Fig. 16a-b, Table IX] is somewhat analogous to that of compound **6**, the Bi(1)...O(6) distance [3.332(5)Å] is significantly shorter than that observed for the corresponding Bi...O(8) distance of 4.592 (6) Å in **5**. The water molecule present in the structure does not interact with

bismuth; it is involved only in hydrogen bonding interactions with the oxygen atoms O1, O4 and O6. Of the two nitrogen atoms N5 and N6 in the unique carboxylate, N6 which is farther away from the carboxylate moiety is protonated and hydrogen bonded to O1 and O2 (not shown in Fig. 16). What is unique in the system however, is that the bismuth atoms of two molecules come close to N2' of a second molecule [distance 3.509(8) Å; sum of van der Waals distances 4.0 Å[33b]] resulting in a weak dimer. Although this distance is not in the realm of any significant bonding interactions, the fact that the nitrogen atom is located on the same side as the expected region for the lone pair of electrons on bismuth is unusual (or fascinating). Intermolecular hydrogen bonding in compound **9** is shown in Figure 17.

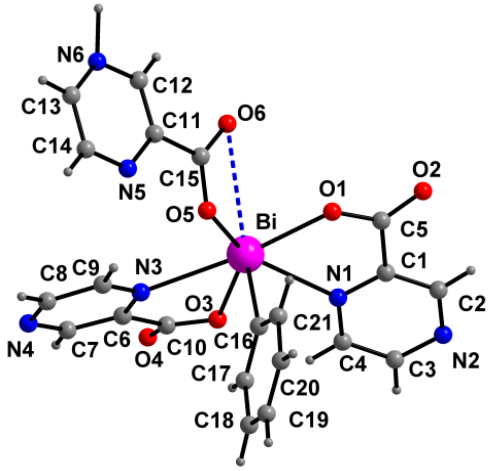

Figure 16a. Molecular structure of compound **9**.

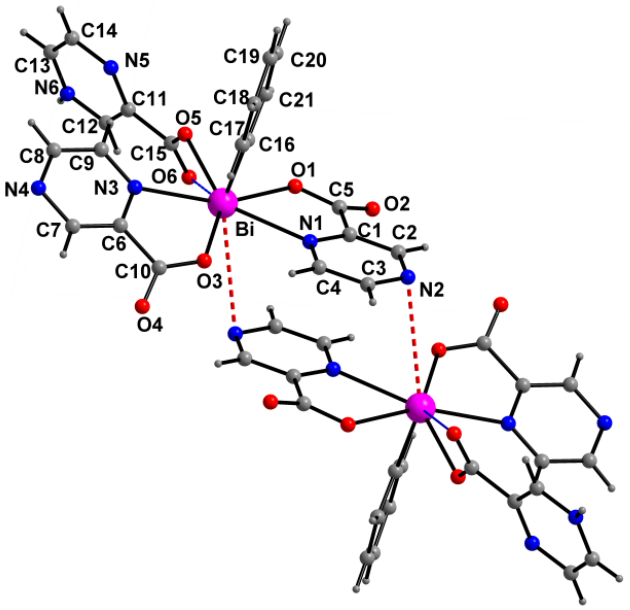

Figure 16b. Dimer formation via weak Bi…N interaction in **9**.

Table IX. Selected geometric parameters (Å, ◦) in **9**

Bi- C16	2.233(8)	C16- Bi- N1	80.4(2)
Bi- O1	2.398(5)	C16- Bi- N3	81.4(2)
Bi- O3	2.472(6)	O1- Bi- O3	136.08(16)
Bi- O5	2.368(5)	O1- Bi- O5	83.36(15)
Bi- N1	2.613(5)	O1- Bi- N1	65.27(16)
Bi- N3	2.625(6)	O1-Bi- N3	158.67(18)
Bi...N2'	3.509(8)[a]	O3- Bi1- O5	140.33(17)
Bi...O6	3.333(5)	O3-Bi- N1	71.80(18)
		O3- Bi- N3	64.13(17)
C16-Bi- O1	90.1(2)	O5- Bi- N1	144.12(17)
C16- Bi- O3	91.6(2)	O5- Bi- N3	76.21(18)
C16- Bi- O5	82.8(2)	N1- Bi- N3	131.42(17)

[a]Symm. equiv.: –x, -y, 1-z

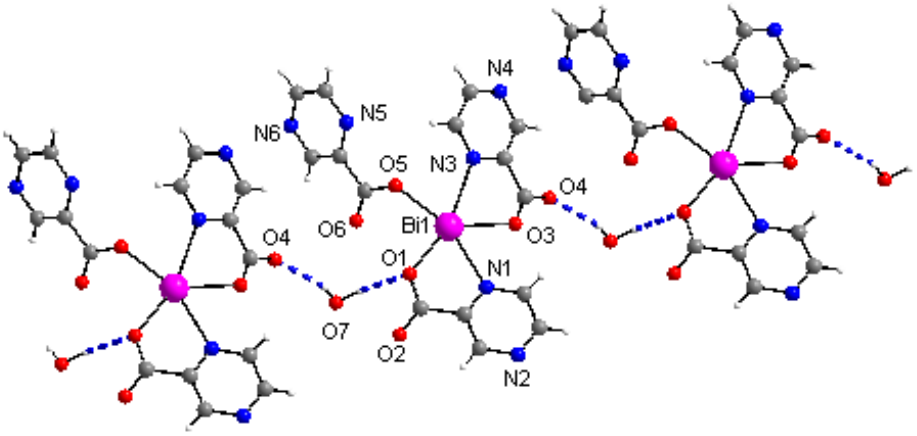

Figure 17. A drawing showing hydrogen bonding interactions in compound **9**. Hydrogen bond parameters: O(7)-H(7A)...O(4') 0.853(7), 1.929(7), 2.748(9) Å, 160.8(7)°; O(7)-H(7b)...O(1") 0.900(6), 2.273, 3.011 Å, 138.9(5)°. Symmetry codes: (i) 1-x, y+1,1.5-z; (ii) 1-x, y, 1.5-z.

2.3.4 Phenylbismuth quinoline-2-carboxylate (10): Weak secondary interactions

Quinoline-2-carboxylic (quinaldic) acid is expected to react in a manner analogous to picolinic acid. However, the 1:3 stoichiometric reaction of $BiPh_3$ with this acid, conducted in refluxing ethanol afforded the bis-carboxylated product

[PhBi(2-O_2C-$C_9H_6N)_2.H_2O$] (**10**) in fair yields. It crystallises in the monoclinic space group $P2_1/n$, wherein the primary coordination number of bismuth is 5 [Fig. 18, Table X]. This basic geometry can be construed as square pyramid with quinaldate N/O at the base of the pyramid. The lower coordination number relative to compound **3** may be directly correlated with the expected lower Lewis acidity of bismuth in **10** due to the Bi-C bond in lieu of a Bi-O bond in **3**. The structure differs from the tetramer [PhBi(2-(C_5H_4N)CO_2)$_2$]$_4$ (**7**), reported by Andrews *et al*[7a] in that the latter is a tetramer with primarily a pentagonal pyramidal geometry around bismuth. Curiously though, compound **10** forms a weakly held ***dimer*** with two additional Bi-O interactions involving O3 and O4 [Bi1...O3' 3.347(5) Å; Bi...O4' 3.495(7) Å; symm. equiv.: –x, 1-y, 2-z] in the direction of the lone pair of electrons, as shown in Figure 18.

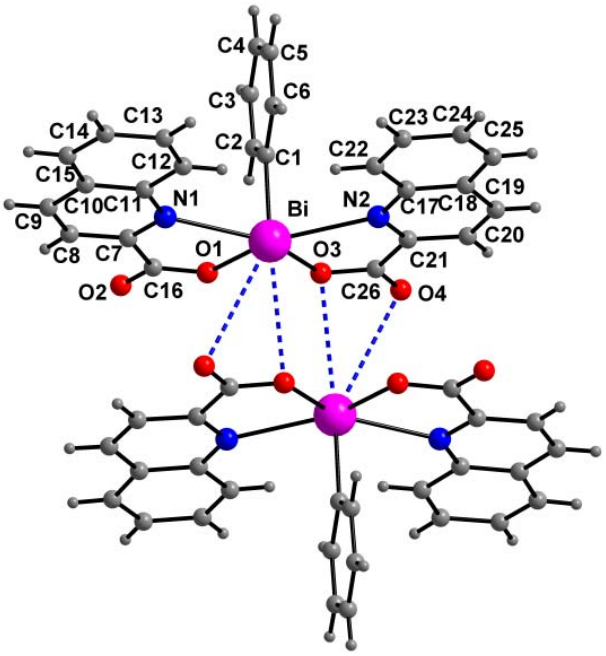

Figure 18. Molecular structure of compound **10** excluding the non-coordinated water molecule.

Table X. Selected geometric parameters (Å, ◦) in **10**

Bi- C1	2.237(7)	C1- Bi- O3	90.5(2)
Bi- O1	2.213(5)	C1- Bi- N1	82.46(18)
Bi- O3	2.241(4)	C1- Bi1- N2	83.32(18)
Bi- N1	2.610(5)	O1- Bi- O3	74.04(16)
Bi- N2	2.619(5)	O1- Bi- N1	67.48(16)
Bi...O3'	3.347(5)[a]	O1- Bi1- N2	141.21(18)
Bi...O4'	3.495 (7)[a]	O3- Bi1- N1	140.81(17)
		O3- Bi1- N2	67.90(19)
C1-Bi- O1	89.9(2)	N1- Bi1- N2	147.76(19)

[a]Symm. equiv.: –x, 1-y, 2-z

2.3.5 Phenylbismuth furan-2-carboxylate (11) and thiophene-2-carboxylates (12 and 13)

Furan-2-carboxylic (furoic) acid and thiophene-2-carboxylic acids feature potentially coordinating ring oxygen or sulphur in addition to the carboxylate group, in a manner analogous to picolinic acids. To our knowledge, structural chemistry of Bi(III) compounds of these acids is not reported. Examples of only Bi(V) compounds are, however, known.[25,26] We have isolated crystalline [$Ph_2Bi(O_2C$-$C_4H_3O)$] (**11**) by the reaction of $BiPh_3$ and 2-furoic acid (used 1:3 molar ratio) in ethanol at room temperature (25 ^oC). Bismuth-thiophene carboxylates [$Ph_2Bi(O_2C$-$C_4H_3S)$] (**12**) and [$PhBi(O_2C$-$C_4H_3S)_2]_2$ (**13**) were obtained from a procedure similar to that for compound **11**. Compound **12** was obtained only in very small quantities, but a few crystals suitable for X-ray structure were available; compound **13** was the major product.

Compound **11** [Fig. 19; Table XI] crystallises in monoclinic $P2_1/n$ space group, wherein primary coordination number of bismuth can be considered to be five with the longest Bi-O1' bond being 2.981(5) Å. The structure is shown in Figure 19. Excluding the weaker Bi...O3 interaction [3.32(2) Å] to the furoate oxygen, the geometry at bismuth can be considered to square pyramidal with C7 as the apical bond and the remaining atoms C1, O1, O1' and O2' at the base. It can be

noted that the carboxylate acts as both a bridging and a chelating ligand. The resulting entity is a coordination polymer.

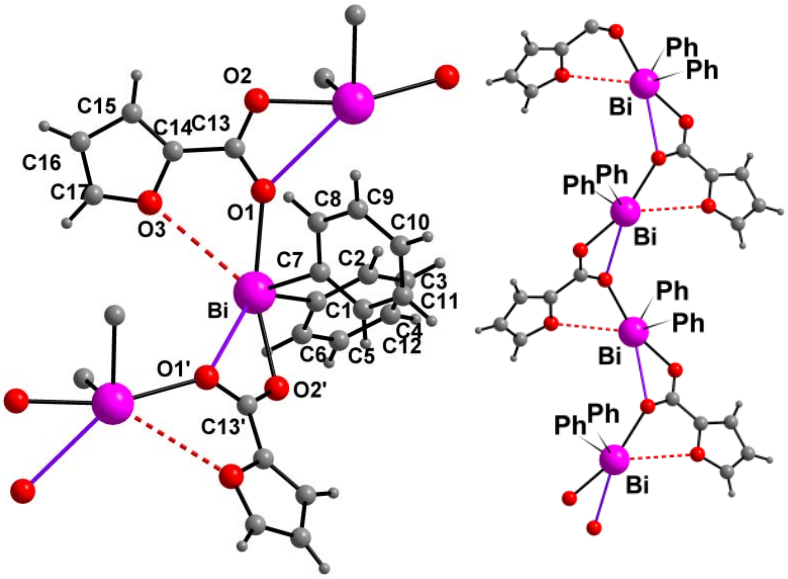

Figure 19. Left: Molecular structure of compound **11**, showing the weaker Bi…O interaction also. Right: The polymeric chain in **11**.

Table XI. Selected geometric parameters (Å, ◦) in **11**

Bi- C1	2.235(3)	C1- Bi- C7	94.60(13)
Bi- C7	2.243(4)	C1- Bi- O1	82.86(10)
Bi- O1	2.479(2)	C1- Bi- O2’	84.68(10)
Bi- O2’	2.368(5)[a]	C7- Bi- O1	83.02(12)
Bi.-O1’	2.982(5)[a]	C7- Bi- O2’	85.71(12)
Bi...O3	3.32(2)	O1- Bi- O2’	162.45(8)

[a]Symm. equiv. 0.5–x, 0.5+y, 0.5-z

Unlike compound **11**, compound **12** was obtained only in trace quantities in a pure state. Although we made an attempt to maximize the yield of this compound, due to simlar solubility characteristics, more quantities of the pure material could not be obtained. The X-ray structure [Fig. 20, Table XII], gratifyingly, could be obtained. The compound crystallises in the orthorhombic $P2_12_12_1$ space group. There are three molecules in the asymmetric unit. As observed in the structure of **11**, the carboxylate moiety acts both as a chelating

and as a bridging ligand leading to a polymeric chain. The main difference though is that Bi1 and Bi2 are involved in one chain while Bi3 is involved in a second chain. One Bi-O distance is longer and is in the range 2.95-3.05 Å. Although bismuth is considered to be thiophilic also,[6f, i] there are no apparent Bi...S interactions of < 4 Å in the molecule. The coordination geometry at bismuth is rather irregular, but may be approximated as square pyramid with C1 (for Bi1), C8 (for Bi2) and C41 (for Bi3) at the apices of the corresponding bismuth atom.

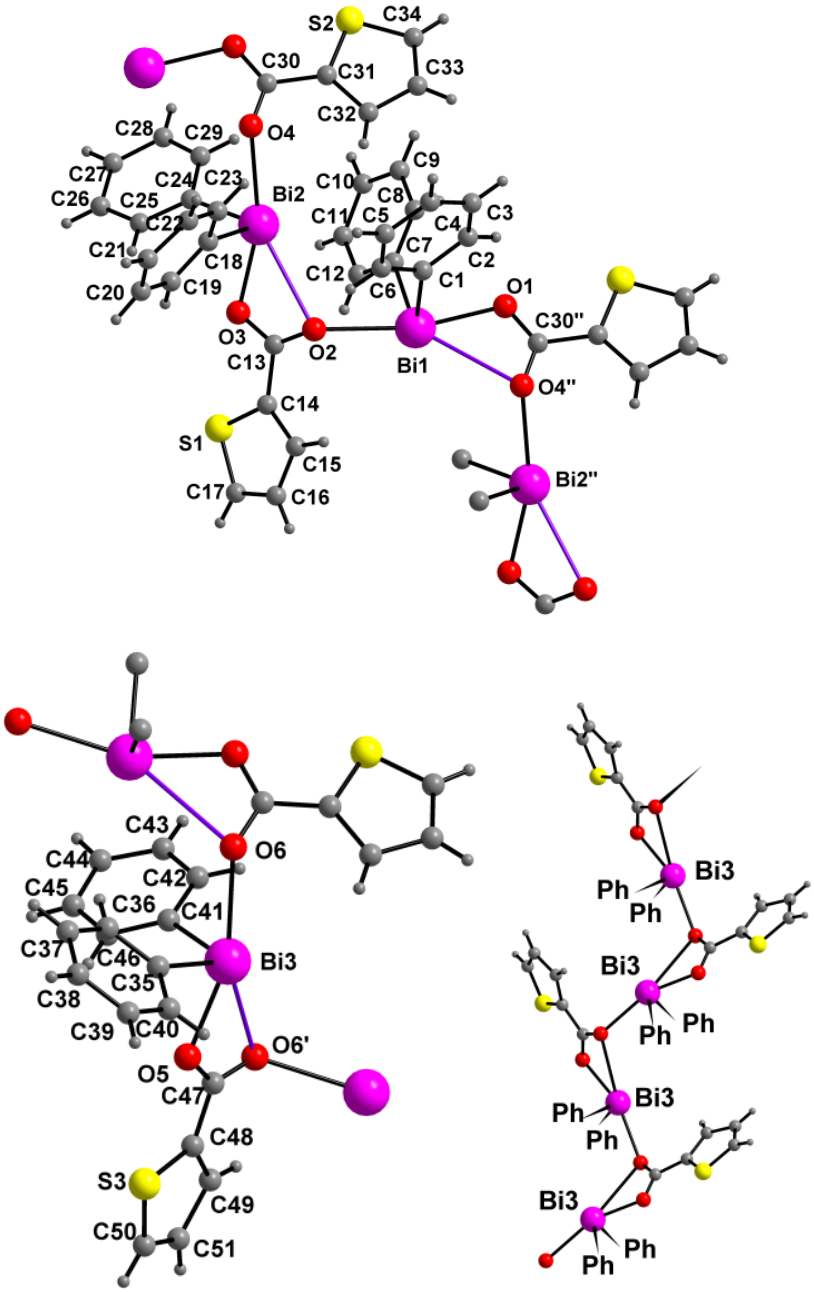

Figure 20. Molecular structure of compound **12.** Top: Chain involving Bi1 ad Bi2. Bottom left: Structure around Bi3. Bottom right: Chain involving Bi3.

Table XII. Selected geometric parameters (Å, ◦) in **12**

Bi1-C1	2.244(8)	C1-Bi1-C7	94.2(3)
Bi1-C7	2.236(8)	C1-Bi1-O1	86.9(2)
Bi1-O1	2.317(6)	C1-Bi1-O2	84.1(2)
Bi1-O2	2.564(6)	C7-Bi1-O1	85.5(2)
Bi1-O4	3.005(6)	C7-Bi1-O2	86.6(2)
		O1-Bi1-O2	167.6(2)
Bi2-C18	2.223(8)	C18-Bi2-C24	97.5(3)
Bi2-C24	2.239(9)	C18-Bi2-O3	87.3(3)
Bi2-O3	2.324(6)	C18-Bi2-O4	82.2(3)
Bi2-O4	2.580(6)	C24-Bi2-O3	85.0(2)
Bi2-O2	2.941(6)	C24-Bi2-O4	83.5(2)
		O3-Bi2-O4	163.3(2)
Bi3-C35	2.238(8)	C41-Bi3-C35	99.7(3)
Bi3-C41	2.235(8)	C35-Bi3-O5	81.8(2)
Bi3-O5	2.290(6)	C35-Bi3-O6	83.0(2)
Bi3-O6	2.568(6)	C41-Bi3-O5	89.0(3)
Bi3-O6	3.045(6)	C41-Bi3 O6	81.3(2)
		O5-Bi3-O6	160.3(2)

Compound **13** crystallises in triclinic [$P\bar{1}$] space group. This compound has two carboxylates per bismuth. One carboxylate is purely chelating while the other is involved in both chelation and bridging [Fig. 21, Table XIII]. The molecule thus can be considered to be a dimer of [$PhBi(O_2C\text{-}C_4H_3S)_2$] and is again a new structural type for bismuth. The primary coordination sphere around bismuth has five oxygen atoms and one carbon atom but the geometry is non-octahedral. The overall geometry involving these groups is pentagonal pyramid [Fig. 21, right]. The Bi-O4' (symm. code: 1-x, -y, 1-z) distance is the longest [2.818(3) Å] but still in the range expected for such compounds; thus all these Bi-O and Bi–C bond lengths are in normal range.

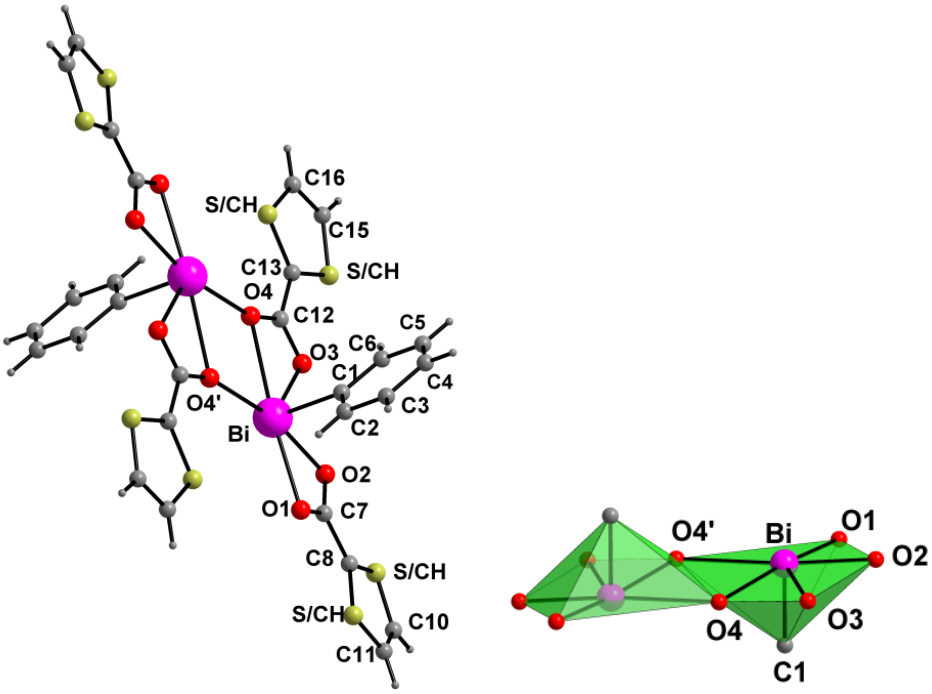

Figure 21. Molecular structure of compound **13.** Left: labelled structure showing the dimeric unit. Right: Polyhedra depicting the primary coordination sphere of pentagonal pyramid around bismuth.

The structure of **13**, though, shows another interesting crystallographic feature that is not very common and is not exhibited by compound **12**. The *carbon* adjacent to C8/C13 and *sulphur* exchange positions in the packing, resulting in essentially half occupancy by S and C-H moieties at each position.[60] However, one of these positions is close to bismuth [distance: 3.597(3) Å, sum of van der Waals distances 4.2 Å; symm. equiv. –x, 1-y, 1-z] as shown in Figure 22. This interaction is again in the direction of the lone pair of electrons on bismuth.

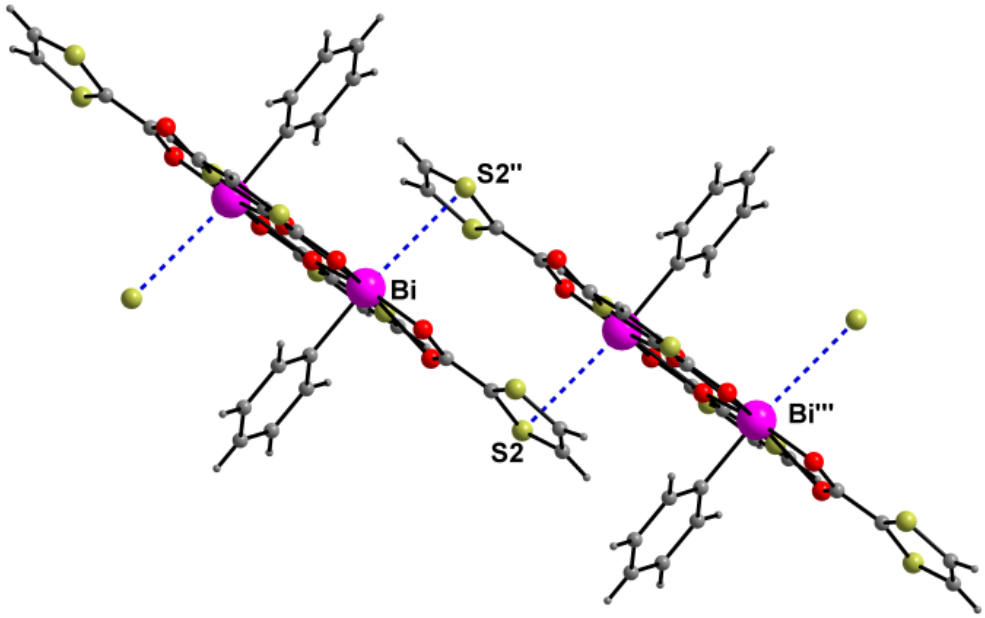

Figure 22. A diagram depicting weak Bi…S interactions in the crystal packing in compound **13**.

Table XIII. Selected geometric parameters (Å, ◦) in **13**

Bi- C1	2.222(4)	C1- Bi- O3	90.5(2)
Bi- O1	2.535(3)	C1- Bi- N1	82.46(18)
Bi- O2	2.282(3)	C1- Bi1- N2	83.32(18)
Bi- O3	2.266(3)	O1- Bi- O3	74.04(16)
Bi- O4	2.635(3)	O1- Bi- N1	67.48(16)
Bi-O4’	2.818 (4)[a]	O1- Bi1- N2	141.21(18)
Bi...S2”	3.597 (3)[a]	O3- Bi1- N1	140.81(17)
		O3- Bi1- N2	67.90(19)
C1-Bi- O1	89.9(2)	N1- Bi1- N2	147.76(19)

[a]Symm. equiv.: (i) 1–x, -y, 1-z, (ii) –x, 1-y, 1-z

2.3.6 Thermogravimetric analysis of compounds 6, 8-11 and 13

The TGA data [Fig. 23] show that compound **6** is stable up to ~210 °C, after which initially phenyl group is eliminated. Remaining ligands are let off from 250 to 350 °C and complete decomposition occurs near to 400°C. For compound **8** at 150 °C, pyridine and protonated pyridine are eliminated. Remaining decomposition pattern is similar to **6** as the ligand used is same for both. Compound **9** behaves differently, with the non-coordinated water molecules coming off before the decomposition sets in. Decomposition for this molecule starts at 270 °C and completes at 350 °C. Compounds **11** and **13** are thermally less stable and decompose more readily probably because of the ease of cleavage of the phenyl group. For **11**, decomposition starts at 210 °C and for **13** at 240 °C; it is complete at ~360°C. In all the cases the final product of decomposition is most likely Bi_2O_3.[18, 22, 33b]

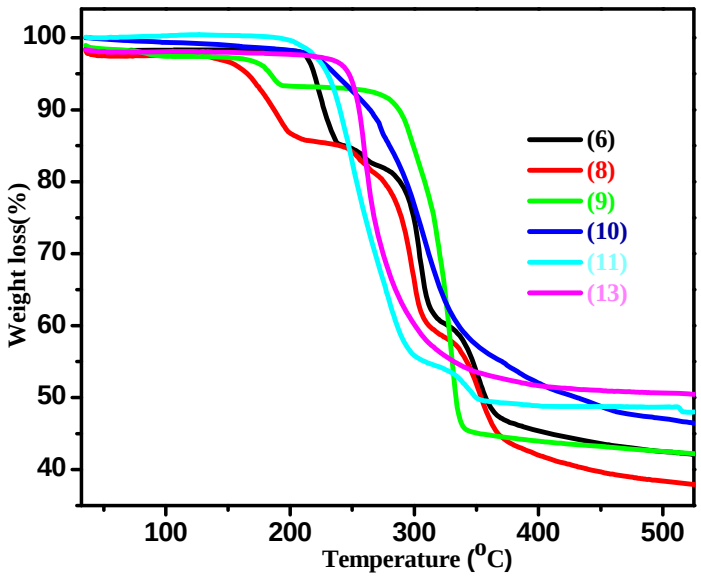

Figure 23. A drawing showing the TGA behaviour of compounds **6, 8-11** and **13**.

2.4 Antiulcer Activity of Ammonium Bismuth Citrate and Related Compounds

Some preliminary studies were conducted in Prof. Lalitha Guruprasad's (UoH) laboratory and the results are summarized here. The human gastric carcinoma epithelial cell line (AGS) was studied as an alternative in vitro model for evaluating the cytoprotective effects of antiulcer agents. Cytoprotection was measured by cleavage of 3-(4,5-dimehyl-2-thiazoyl)-2,5-diphenyl-2H-tetrazolium bromide (MTT) by surviving AGS cells following the exposure to selected antiulcer agents

and ethanol. After the 15% ethanol treatment for 30 min resulted in cytotoxicity with no appreciable cytoprotection by the possible anti-ulcer drug ammonium bismuth citrate as shown in Figure 24. It is however satisfying to see that ammonium bismuth citrate exhibits cytoprotection similar to ranitidine or copper aspirinate that have already shown anti-ulcer property. Compound **1** was checked for this purpose by dissolving it in dilute hydrochloric acid. However no tangible result could be obtained probably because of the exchange of carboxylate with the chloride ion. Therefore this part of the work was not continued further.

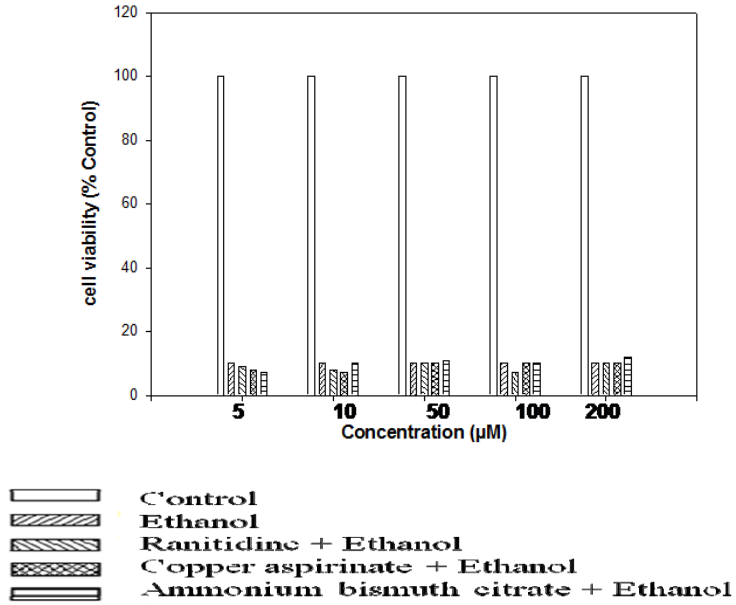

Figure 24. Cytoprotective effects of antiulcer drugs. Surviving of AGS cells treated with ethanol following a pre-treatment with Ranitidine, copper aspirinate and ammonium bismuth citrate. The cells were incubated with drugs for one hour and then with 15% ethanol for 30 min. before determining the cell survival with the MTT assay.

2.5 Bismuth Vanadate ($BiVO_4$; 14)- A New Simple Synthetic Route

Bismuth vanadate ($BiVO_4$; **14**) is one of the well explored materials in recent times and has been identified as photocatalyst.[61] This bright yellow compound with its nontoxic nature and relatively narrow band gap (2.4 eV) is a promising semiconductor material.[62] A study of the synthetic routes to this materials was one of our earlier objectives in the present work. We have prepared micron-sized $BiVO_4$ from bismuth nitrate (product labelled as **14a**) and ammonium or sodium vanadate

(product labelled as **14b**) in water under reflux conditions. The reaction mixture after filtration gives yellow precipitate of $BiVO_4$.

$BiVO_4$ appears in three main crystalline forms: monoclinic scheelite structure, tetragonal zircon structure and tetragonal scheelite structure. Yet only monoclinic $BiVO_4$ shows photocatalytic activity under visible light irradiation due to its specific electronic structure. The phase purity of the sample was confirmed by powder X-ray (Fig. 25) and the authenticity is proven by the well-indexed peaks corresponding to a pure monoclinic phase (with lattice constants a = 5.185, b = 11.713 and c = 5.102) of $BiVO_4$ (JCPDS No. 83-1699). No peaks of any other phases or impurities were detected, indicating that all samples were phase pure.[63] The energy-dispersive X-ray spectrum (EDS) analysis confirms the formation of the stoichiometric $BiVO_4$ compound (Fig. 26). Several research groups have reported the synthesis of $BiVO_4$ using methods like hydrothermal or use of an added base.[64] Our method is much simpler and more straightforward; this reaction of bismuth nitrate with vanadate salts is quite fast such that precipitate of the required compound was obtained immediately. The Raman spectra of the compounds between 10 and 1400 cm^{-1} are shown in Figure 27. Each spectrum is dominated by an intense Raman band at 828 cm^{-1} assigned to ν_s(V–O) and with a weak shoulder at about 709 cm^{-1} assigned to ν_{as}(V–O). The $\delta_s(VO_4^{3-})$ and $\delta_{as}(VO_4^{3-})$ modes are at 369 and 328 cm^{-1}, respectively.[63d,65]

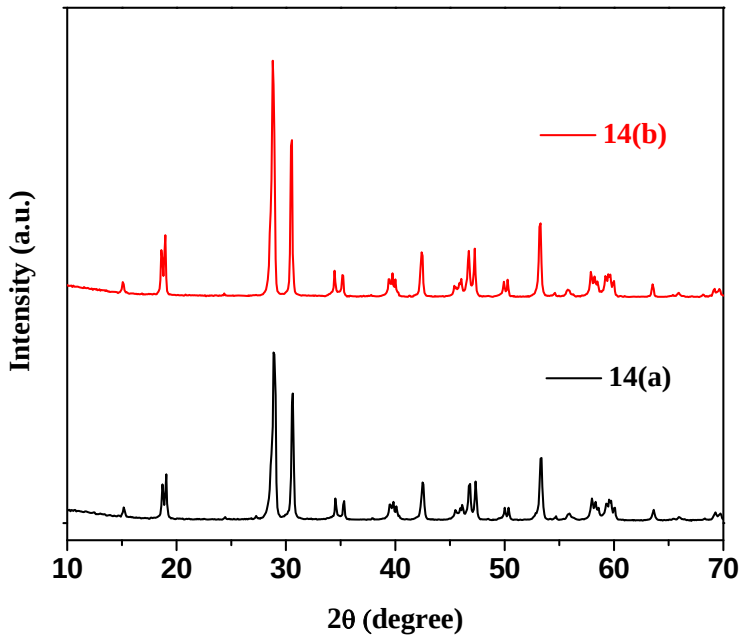

Figure 25. Powder X-ray pattern of $BiVO_4$ (**14a/14b**)

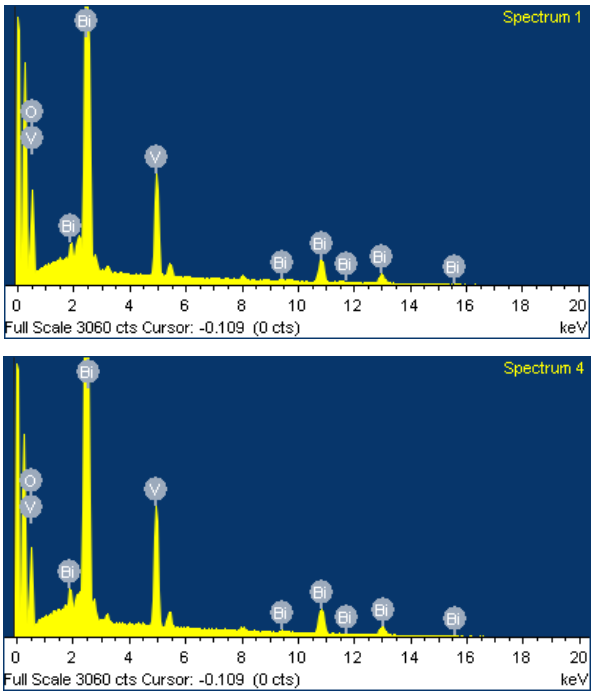

Figure 26. Energy dispersive spectra (EDS) of the $BiVO_4$. Left: **14a**, Right: **14b**.

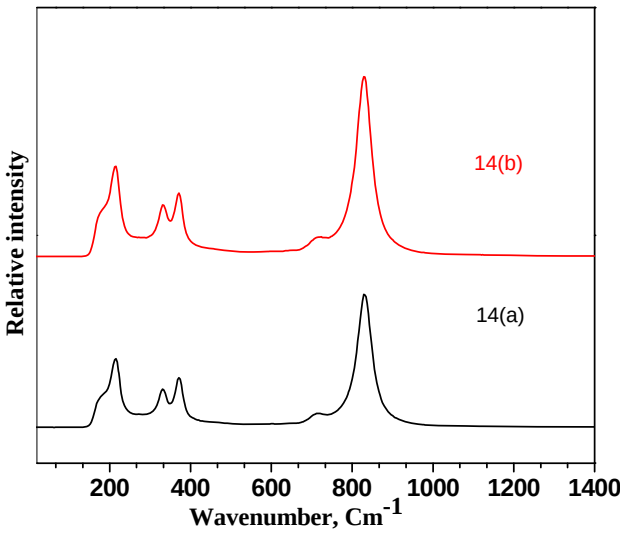

Figure 27. Raman Spectra of $BiVO_4$ (**14a** and **14b**)

The morphology and particle size are examined by SEM. Figure 28 presents scanning electron microscopy (SEM) images of **14a/14b**, which show that the products are composed of plate-like structures that are 1–2 μm long and 200 –600 nm width. It could also be found that irregular particles were formed.

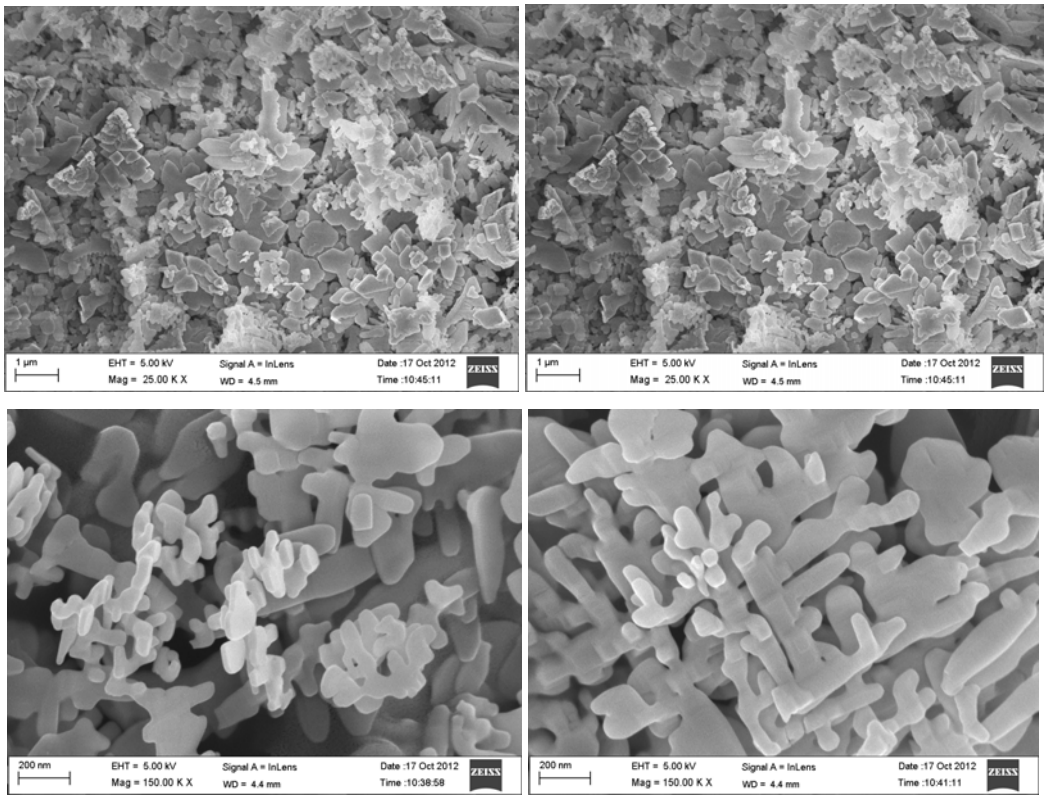

Figure 28. SEM images of $BiVO_4$ Left: **14a**, Right: **14b**.

The valence band (VB) of monoclinic $BiVO_4$ is composed of hybridized Bi 6s and O 2p orbitals, whereas the conduction band is composed of V 3d orbitals.[66] The UV absorption is due to the charge-transfer transition between O 2p and V 3d orbitals, while the visible absorption is assigned to the band transition from Bi 6s to V 3d. The absorption in visible zone is responsible for the high photocatalytic activity of monoclinic $BiVO_4$ under visible light irradiation. The UV-Vis diffuse reflectance spectra of **14a/14b** are shown in Figure 29. The band gap of a semiconductor can be estimated from the formula[67] $\alpha h\nu = A(h\nu - Eg)^{n/2}$, where α, ν, Eg and A are absorption coefficient, incident light frequency, bandgap and a constant respectively. For $BiVO_4$, the value of n is 1.[61b,68] The plots of $(\alpha h\nu)^2$ *vs* photon energy ($h\nu$) are shown in Figure 30, from which we could estimate the energy of the band gap of $BiVO_4$ sample. Both the materials **14a** and **14b** are found to have nearly same E_g of (from the intercept of the tangents to the plots) 2.58 eV which is slightly higher than 2.4 eV reported from other groups.[62]

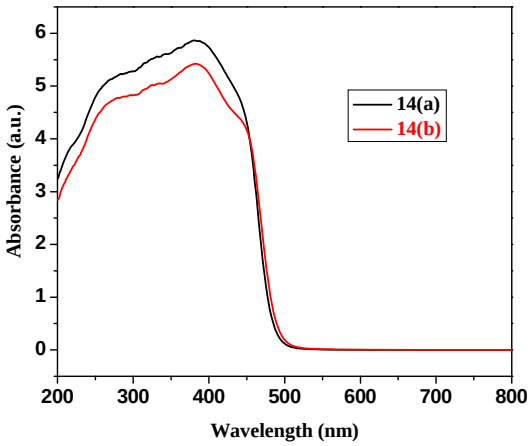

Figure 29. UV-Vis. diffuse reflectance spectra of $BiVO_4$ (**14a/14b**)

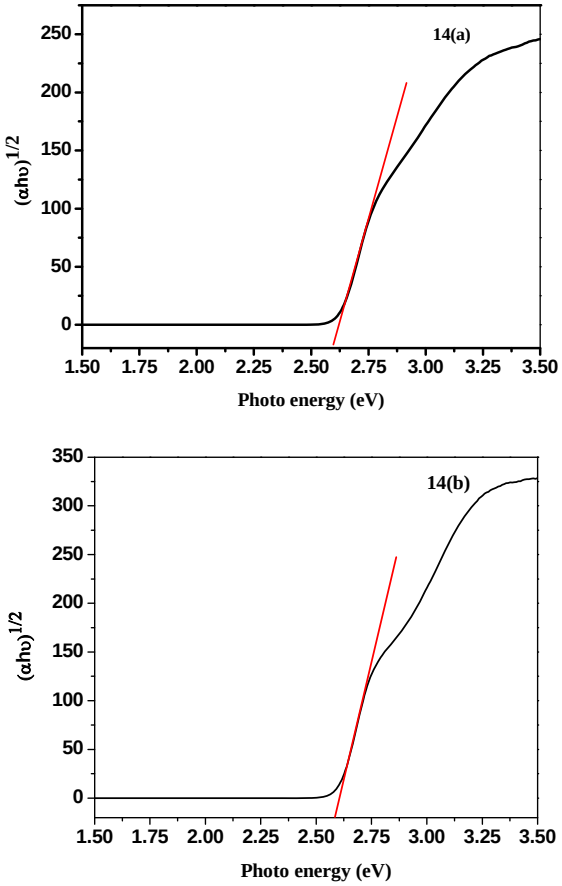

Figure 30. Plots of $(\alpha h\upsilon)^{1/2}$ versus $h\upsilon$, by which the values of the energy band gaps of the products could be estimated, corresponding to those in Figure **29**.

Compared to bulk material, nanosized material has better photocatalytic activity,[63d,65a] and thus we wanted to prepare nanoparticles of $BiVO_4$. We used several surfactants like polyethylene glycol (PEG-400), polyvinyl alcohol (PVA),

polyvinyl pyrrolidone (PVP) and sodium dodecyl sulfate (SDS). So far, we have not succeded in our attempts to prepare nano particles of $BiVO_4$. Further work in this direction is still in progress.

SUMMARY – PART A

1) The reaction of bismuth nitrate with picolinic, dipicolinic and quinoline carboxylic acids in water resulted in the formation of $[Bi(2\text{-}O_2C\text{-}C_5H_4N)_3]_n$ (**1**), $\{Bi[(2,6\text{-}O_2C)_2C_5H_3N)][(2\text{-}HO_2C\text{-}6\text{-}O_2C)C_5H_3N].H_2O\}_n$ (**2**) and $Bi(O_2CC_9H_6N)_2(O_3N)(O_2CC_9H_6NH).2H_2O$ (**3**). These compounds were characterized by single crystal X-ray crystallography and thermogravimetric analysis. Whereas compounds **1** and **2** are coordination polymers, complex **3** is monomeric. The lone pair of electrons on bismuth was stereochemically inactive in all the compounds. Although compounds **1** and **2** were rather insoluble in most of the solvents, the dissolution was quite fast in 2N HCl. This solubility factor was a problem in checking the bioactivity of these compounds.
2) Ammonium bismuth citrate as a water-soluble bismuth precursor was utilized in a reaction with dipicolinic acid, resulting in the new compound $\{[Bi((2,6\text{-}O_2C)_2C_5H_3N)((2\text{-}HO_2C\text{-}6\text{-}O_2C)C_5H_3N)(H_2O)]_2.5H_2O\}_n$ (**5**), which is a dimer unlike the coordination polymer **2**.
3) Reaction of triphenylbismuth ($BiPh_3$) with 3-hydroxy picolinic acid in ethanol resulted in $[PhBi(2\text{-}O_2C\text{-}3\text{-}(OH)C_5H_3N)_2(2\text{-}O_2C\text{-}3\text{-}OHC_5H_3NH)]$ (**6**), whereas the use of pyridine as the solvent resulted in an entirely different product, $[(Bi(2\text{-}O_2C\text{-}3\text{-}(OH)C_5H_3N)_4)(C_5H_5NH)(C_5H_5N)]$ (**8**). Bismuth has a coordination number of 6 in compound **6** and 8 in compound **8**.
4) The first example of a bismuth pyrazine caboxylate, i.e. $[PhBi(2\text{-}O_2C\text{-}C_4H_3N_2)_2(2\text{-}O_2C\text{-}C_4H_4N_2).H_2O]$ (**9**), is reported. Quinaldic acid reacts differently with $BiPh_3$ resulting in $[PhBi(2\text{-}O_2C\text{-}C_9H_6N)_2.H_2O]$ (**10**) that does not contain the additional carboxylate. By using $BiPh_3$, we have also isolated first examples of bismuth furoates and thiophene-carboxylates. Thus crystalline $[Ph_2Bi(O_2C\text{-}C_4H_3O)]$ (**11**) $[Ph_2Bi(O_2C\text{-}C_4H_3S)]$ (**12**) and $[PhBi(O_2C\text{-}C_4H_3S)_2]_2$ (**13**) that show novel structural features are

5) Phase pure $BiVO_4$ was prepared by a simple aqueous method without using base or hydrothermal route. This compound was characterized by P-XRD, Diffuse reflectance spectra, EDAX and SEM. We could get only bulk material and attempts to prepare nanosize $BiVO_4$ were unsuccessful (but are being pursued).

EXPERIMENTAL SECTION

General: Chemicals and solvents were procured from Aldrich/ Fluka or local manufacturers. Further purification was done according to standard procedures wherever required.[69]

Melting point: Melting points were determined using a SUPERFIT hot stage apparatus and are uncorrected.

Elemental analyses: Elemental analyses were carried out on a Perkin-Elmer 240C CHN or Thermo Finnigan EA1112 CHNS analyzer.

Infrared spectroscopy: IR spectra were recorded on a JASCO FT/IR 5300 spectrophotometer.

Absorbance and Fluorescence Spectroscopy: Steady state absorption and fluorescence spectra were recorded on UV-Vis-NIR scanning spectrophotometer (Shimadzu, model no. UV-3101PC) and SPEX FLUOROMAX-3 spectrofluorometer, respectively.

NMR spectroscopy: ^{1}H NMR spectra were recorded using 5 mm tubes on a Bruker 400 MHz NMR spectrometer [field strength: 400 (^{1}H), 100 (^{13}C)] in $CDCl_3$ and DMSO-d_6 solution (unless specified otherwise) with shifts referenced to $SiMe_4$ (^{1}H, $\delta = 0$).

Thermogravimetric analysis: Thermogravimetric and differential thermal analysis (TG-DTA) were carried out on a (Netzsch STA 409 Pc) TG-DTA instrument from 30 to 500 ^{o}C with a scanning rate of 10 deg/min. under nitrogen flow.

3.1 Synthesis of Bismuth Pyridine Carboxylates from Bismuth Nitrate

(a) Synthesis of $[Bi(2\text{-}O_2C\text{–}C_5H_4N)_3]_n$ (1)

To a boiling solution of $Bi(NO_3)_3.5H_2O$ (0.485 g, 1 mmol) in water (50 cm^3) was added the carboxylic acid (0.246 g, 3 mmol) and the clear solution obtained was heated under reflux for 2 h. The solution was filtered to remove any suspended

impurities and the clear, colourless filtrate was allowed to cool slowly. After 2 d, colourless crystals suitable for X-ray single crystal analysis were formed.

Yield: 0.320 g (56%)

Mp: >320 ^{o}C

IR (KBr) (cm^{-1}): 3074(w), 2926(w), 1651(s), 1591(s), 1568(m), 1462(m), 1332(s), 1290(m), 1238(m), 1161(w), 1089(w), 1047(m), 1010(w), 833(s), 763(s), 694(s), 632(m).

Elemental analysis (calc): C, 37.45 (37.58); H, 2.17 (2.10); N, 7.41 (7.30).

This compound was insoluble in common organic solvents and hence NMR spectra were not recorded.

(b) Synthesis of $\{Bi[(2,6\text{-}O_2C)_2C_5H_3N)][(2\text{-}HO_2C\text{-}6\text{-}O_2C)C_5H_3N]\cdot H_2O\}_n$ (2)

The reaction was conducted at room temperature affording the product in >75% yield, but the crystallinity was not great. In a procedure similar to that for **1**, using 100 mg (0.206 mmol) of bismuth nitrate pentahydrate better crystalline material was obtained.

Yield: 0.092 g, (40%)

Mp: >320 ^{o}C

IR (KBr) (cm^{-1}) : 3074(w), 2926(w), 1651(s), 1591(s), 1568(m), 1462(m), 1332(s), 1290(m), 1238(m), 1161(w), 1089(w), 1047(m), 1010(w), 833(s), 763(s), 694(s), 632(m).

Elemental analysis (calc): C, 37.45 (37.58); H, 2.17 (2.10); N, 7.41 (7.30).

This compound was also insoluble in common organic solvents, but soluble in 2N HCl (ca 50 mg in 5 cm^3). However, it is possible that the dissolution is accompanied by dissociation.

(c) Synthesis of $Bi(O_2CC_9H_6N)_2(O_3N)(O_2CC_9H_6NH)\cdot 2H_2O$ (3)

The procedure was similar to that for **1** except that the mixture was heated under reflux for 12 h, using 100 mg (0.206 mmol) of bismuth nitrate pentahydrate.

Yield: 0.075 g, (44%).

Mp: 210 ^{o}C

IR (KBr) (cm^{-1}): 3450(br), 3110, 1749(w), 1732(w), 1628(s), 1595(m), 1539(m), 1454(s), 1350(m), 1222(m), 1157(w), 796(w), 536(m).

Elemental analysis (calc): C, 43.85 (43.70); H, 2.79 (2.81); N, 6.86 (6.79);

3.2 Reaction of $Bi(NO_3)_3.5H_2O$ with Nicotinic, 2-Hydroxynicotinic, 3-Hydroxypicolinic and Pyridine-2,3-dicarboxylic acids

To a boiling solution of 0.206 mmol of $Bi(NO_3)_3.5H_2O$ in 60 cm^3 of H_2O was added 0.618 mmol of carboxylic (nicotinic, 2-hydroxynicotinic, 3-hydroxypicolinic and pyridine 2,3-dicarboxylic) acid and the mixture was heated under reflux for 12 h. The turbid solution was filtered, the precipitate washed with water and dried in air.

(a) Solid from the reaction of bismuth nitrate with 2-hydroxynicotinic acid

Yield: 0.059 g, (60%).

Mp: >320 ^oC

IR (KBr) (cm^{-1}): 3084(w), 2914(w), 1873(w), 1699(w), 1628(s), 1601(w), 1572(m), 1450(s), 1388(s), 1246(m), 1213(s), 1109(m), 677(s), 557(m), 445(s).

Elemental analysis (calc): C, 45.37 (45.28); H, 1.89 (1.93); N, 8.82 (8.76).

(b) Solid from the reaction of bismuth nitrate with 3-hydroxypicolinic acid

Yield: 0.064 g, (65%).

Mp: >320 ^oC

IR (KBr) (cm^{-1}): 3092(w), 2915(w), 1697(w), 1631(m), 1572(m), 1452(s), 1390(s), 1323(s), 1246(s), 1215(s), 1111(m), 883(s), 677(s), 580(m), 557(m).

Elemental analysis (calc): C, 45.37 (45.50); H, 1.89 (1.81); N, 8.82 (8.76).

(c) Solid from the reaction of bismuth nitrate with pyridine-2,3-dicarboxylic acid

Yield: 0.053 g, (50%).

Mp: >320 ^oC

IR (KBr) (cm^{-1}): 3447(br), 3090(w), 1728(s), 1657(w), 1616(w), 1575(s), 1448(m), 1383(s), 1278(m), 1228(w), 1149(m), 1099(s), 839(w), 698(s), 667(w), 555(m), 447(s).

Elemental analysis (calc): C, 48.93 (48.81); H, 2.33 (2.38); N, 8.15 (8.23).

3.3 Synthesis of Bismuth Oxonitrate $Bi_6O_6(NO_3)_6$ (4; formula is only approximate and is based on X-ray structure)

To a suspension of $Bi(NO_3)_3.5H_2O$ (0.485 g, 1 mmol) in 60 cm^3 of H_2O L-proline (0.167 g, 3 mmol) was added and the mixture heated under reflux for 2 h. Subsequent to this, the turbid solution was filtered and the clear solution was kept aside when a small quantity (ca 20 mg) of compound **4** crystallized out. Since it did not contain carbon, no further analysis was performed.

3.4 Bismuth Pyridine Carboxylates from Ammonium Bismuth Citrate

(a) Synthesis of $[Bi(2\text{-}O_2C\text{-}C_5H_4N)_3]_n$ (1')

Ammonium bismuth citrate (mol.wt. taken as 1875; 0.100 g, 0.053 mmol) and picolinic acid (0.039 g, 0.318 mmol) were dissolved in water (10 cm^3) at 25 ^oC. This led to immediate precipitation of insoluble microcrystalline compound that corresponded to $[Bi(2\text{-}O_2C\text{-}C_5H_4N)_3]_n$.

Yield: 0.020 g, 65%

Mp: >320 ^oC.

IR (KBr) (cm^{-1}): 3204(w), 3074(w), 1651(s), 1591(s), 1568(m), 1460(w), 1332(s), 1290(s), 1238(m), 1161(s), 1089(m), 1047(s), 1010(w), 835(s), 763(s), 694(s), 634(m). This is the same as that obtained from the method 3.1(a).

Elemental analysis (calc): C, 37.45 (37.58); H, 2.17 (2.10); N, 7.41 (7.30).

(b) Synthesis of $\{[Bi((2,6\text{-}O_2C)_2C_5H_3N)((2\text{-}HO_2C\text{-}6\text{-}O_2C)C_5H_3N)(H_2O)]_2.5H_2O\}_n$ (5)

Ammonium bismuth citrate (mol. wt. taken as 1875; 0.100 g, 0.053 mmol) was dissolved in water (10 cm^3) and dipicolinic acid (0.053 g, 0.318 mmol) was added to the solution at room temperature. The resulting clear solution was allowed to evaporate at room temperature to obtain colourless crystals of **5** over a period of 5-6 d.

Yield: 0.045g, 70 % based on Bi

Mp: >320 ^oC.

IR (KBr) (cm^{-1}): 3393(w), 3169(w), 3082(w), 1641(s), 1612(w), 1581(m), 1425(s), 1377(s), 1269(m), 1178(s), 1078(s), 1018(s), 916(s), 916(s), 767(s), 727(s), 665(s).

Elemental analysis (calc): C, 27.87 (27.85); H, 2.33 (2.36); N, 4.64 (4.71).

This compound was also obtained (X-ray evidence) in 65% yield when a mixture of $Bi(NO_3)_3$ and $Gd(NO_3)_3$ was treated with dipicolinc acid in aqueous medium at reflux temperature and crystallizing the compound after cooling the solution to *ca* 25 ^oC.

(c) Other reactions using bismuth nitrate, bismuth acetate or ammonium bismuth citrate[a]

S.No.	Reactants	Condition	Result / Possible product[a]
1	Bi $(NO_3)_3.5H_2O$ (in water) + 2-thionicotinic acid and 2,2'-bipyridyl	EtOH, RT, stirred for 6 h	Yellow insoluble precipitate
2	$Bi(NO_3)_3.5H_2O$ + picolinic acid + 1,10-1,10-phenanthroline	Water, Reflux for 4 h	White insoluble precipitate
3	$Bi(NO_3)_3.5H_2O$ + acetylsalicylic acid	Water, Reflux for 6 h	No reaction
4	$Bi(OAc)_3$ + picolinic acid	Pyridine, RT, stirred for 10 min	Immediate precipitate $\{Bi(2\text{-picolinate})_3\}_n$ (**1**)
5	$Bi(OAc)_3$ + pyridine-2,6-dicarboxylic acid	Pyridine, RT, stirred for 10 min	Precipitate $\{Bi(2,6\text{-dipicolinate})_3\}_n$ (**2**)
6	$Bi(OAc)_3$ + 3-hydroxy picolinic acid	Pyridine, RT, stirred for 10 min	Precipitate (insoluble)
7	$Bi(OAc)_3$ + pyridine-2,4-dicarboxylic acid	Pyridine, RT, stirred for 10 min	Precipitate (insoluble)
8	$Bi(OAc)_3$ + pyridine-2,3-dicarboxylic acid	Pyridine, RT, stirred for 10 min	Precipitate (insoluble)
9	$Bi(OAc)_3$ + picolinic acid	Water, Reflux for 4h, allowed to cool	$\{Bi(2\text{-picolinate})_3\}_n$ Single crystals (**1**)

		slowly	
10	$Bi(OAc)_3$ + salicylic acid	Water, Reflux for 4h	{Bi(salicylate)$_3$} precipitate obtained[8]
11	$Bi(OAc)_3$ + acetylsalicylic acid	Water, Reflux for 4h	Precipitate (insoluble)
12	$Bi(NO_3)_3.5H_2O$ + $Gd(NO_3)_3.5H_2O$ + dipicolinic acid	Water, Reflux for 2 h	{Bi(2,6-dipicolinate)$_3$}$_2$ Single crystlas (**2**)
13	$Bi(NO_3)_3.5H_2O$ + $Cu(NO_3)_2.3H_2O$ + picolinic acid	Water, Reflux for 2 h	{Cu(2-picolinate)$_2$} Single crystlas obtained (repored)[70]
14	$Bi(NO_3)_3.5H_2O$ + $Cu(NO_3)_2.3H_2O$ + dipicolinic acid	Water, Reflux for 2 h	{Cu(2,6-dipicolinate)$_2$} Single crystals obtained (reported)[71]

[a] Although IR spectra were taken in all the cases wherein insoluble precipitate was obtained, the structural elucidation on this basis was not possible and hence these data are not given here. All the insoluble prodcuts has mp>300 ^oC.

[b] In case of reactions 1 and 2, all the reactants $Bi(NO_3)_3.5H_2O$, 2-thionicotinic acid, 2,2'-bipyridyl, picolinic acid and 1,10-phenanthhroline dissolved in hot water or ethanol. Hence a clear solution was obtained at the beginning. After continuing the reaction, precipitate formation was observed. This precipitate was insoluble in water or in any of the common organic solvents. Hence our attempts to crystallise these compounds was unsucessful.

3.5 Synthesis of Bismuth Pyridine Carboxylates from Triphenylbismuth

(a) Synthesis of $BiPh_3$: This compound was prepared by a modification to the literature procedure.[59] To a suspension of Mg turnings (1.903 g, 0.0783 mmol) in THF (70 cm^3) was added bromobenzene (11.18 g, 0.0712 mmol) in THF (20 cm^3) drop-wise (30 min) at 0 ^oC. The mixture was brought to room temperature, and then heated under reflux till the reaction was complete (disappearance of Mg). The mixture was then cooled to 0 ^oC and $BiCl_3$ (7.409 g, 0.0234 mmol) in dry THF (40 cm^3) was added drop-wise (30 min). This mixture was further heated under reflux

overnight, filtered and the solvent removed from the filtrate. Thus obtained solid was purified by column chromatography (hexane +ethyl acetate, 1:49 vol/vol ratio).
Yield: 4.00 g, 30 % based on bismuth.
Mp: 70-75 ^{o}C (lit. 70-75[91]).
IR (KBr) (cm^{-1}): 3055(m), 1944(w), 1874(w), 1813(w), 1631(m), 1566(s), 1471(s), 1425(s), 1325(m), 1298(m), 1259(w), 1055(s), 1012(s), 995(s), 850(w), 731(s), 723(s), 692(s).
Elemental analysis (calc): C, 49.09 (49.23); H, 3.4 (3.36).

(b) Synthesis of [PhBi(2-O_2C-3-(OH)$C_5H_3N)_2$(2-O_2C-3-(OH)C_5H_3NH)] (6)

To a solution of $BiPh_3$ (0.100 g, 0.227 mmol) in ethanol (10 cm^3) was added 3-hydoxypicolinic [3-hydoxy-pyridine-2-carboxylic] acid (0.094 g, 0.681 mmol) in ethanol (15 cm^3) all at once and the clear solution obtained was stirred for a further 12 h. The solution was filtered to remove any suspended impurities and the colourless filtrate was left for slow evaporation of the solvent at 4 ^{o}C. After 8 d, crystals suitable for X-ray single crystal analysis were formed.
Yield: 0.079 g, 56%.
Mp: >320 $^{\circ}$C
IR (KBr) (cm^{-1}): 3456(br), 3090 (w), 1633(s), 1610(w), 1572(w), 1452(s), 1390(s), 1325(s), 1248(s), 1215(s), 1143(w), 1111(m), 1059(w), 883(s), 825(s), 729(w), 677(w).
^{1}H NMR (400 MHz, $CDCl_3$+DMSO-d_6) δ = 13.71 (br, 3H), 8.34-8.33 (br, 3H, Ar-*H* + N*H*), 7.59-7.56 (m, ca 11H, Ar-*H*), 7.15-7.12 (m, 1H, Ar-*H*) [Fig. 31, the broadness of the peaks may indicate some decomposition].
Elemental analysis (calc): C, 41.15 (41.08); H, 2.51 (2.56); N, 5.91 (5.99).

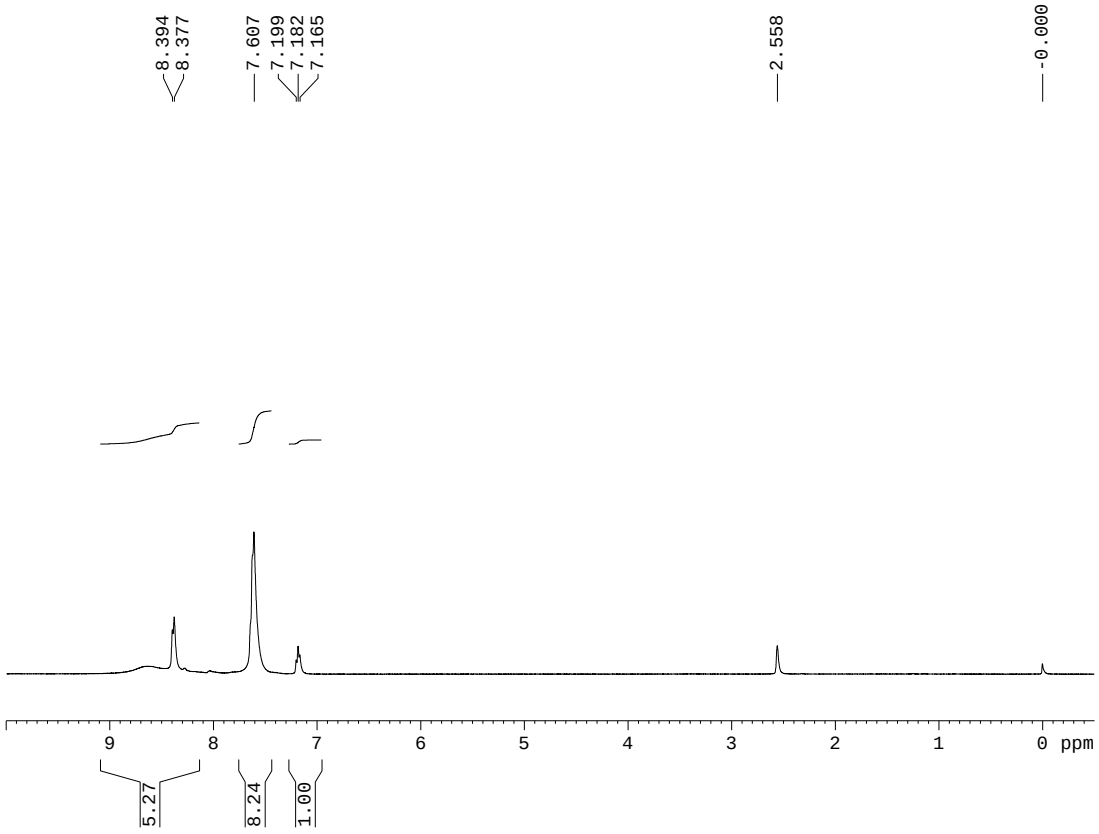

Figure 31. ^{1}H NMR spectrum of compound **6.**

(c) Synthesis of [(Bi(2-O_2C-3-(OH)$C_5H_3N)_4$)(C_5H_5NH)(C_5H_5N)] (8)

To a solution of $BiPh_3$ (0.100 g, 0.227 mmol) in pyridine (5 cm^3) was added 3-hydroxy-picolinic acid (0.094 g, 0.681 mmol) and the clear solution obtained was stirred for 12 h. The solution was filtered to remove any suspended impurities and the filtrate was left at room temperature. After 2 d, colourless crystals were obtained. Yield: 0.103 g, 48%.

Mp: >320 °C

IR (KBr) (cm^{-1}): 3427(w) 3057 (w), 2359(s) 1622(s), 1556(m), 1454(s), 1383(s),1307(s), 1244(m), 1143(w), 1057(w), 879(s), 806(s), 763(m), 677(s)

^{1}H NMR (400 MHz, DMSO-d_6) δ = 13.94 (br, ca 4H), 8.70-7.50 (br m, ca 21H, Ar-*H* + N*H*), 7.18 (~s, 2H, Ar-*H*) {Figure 32, the broadness of the peaks may indicate some decomposition].

Elemental analysis (calc): C, 44.26 (44.34); H, 2.85 (2.93); N, 9.21 (9.13)

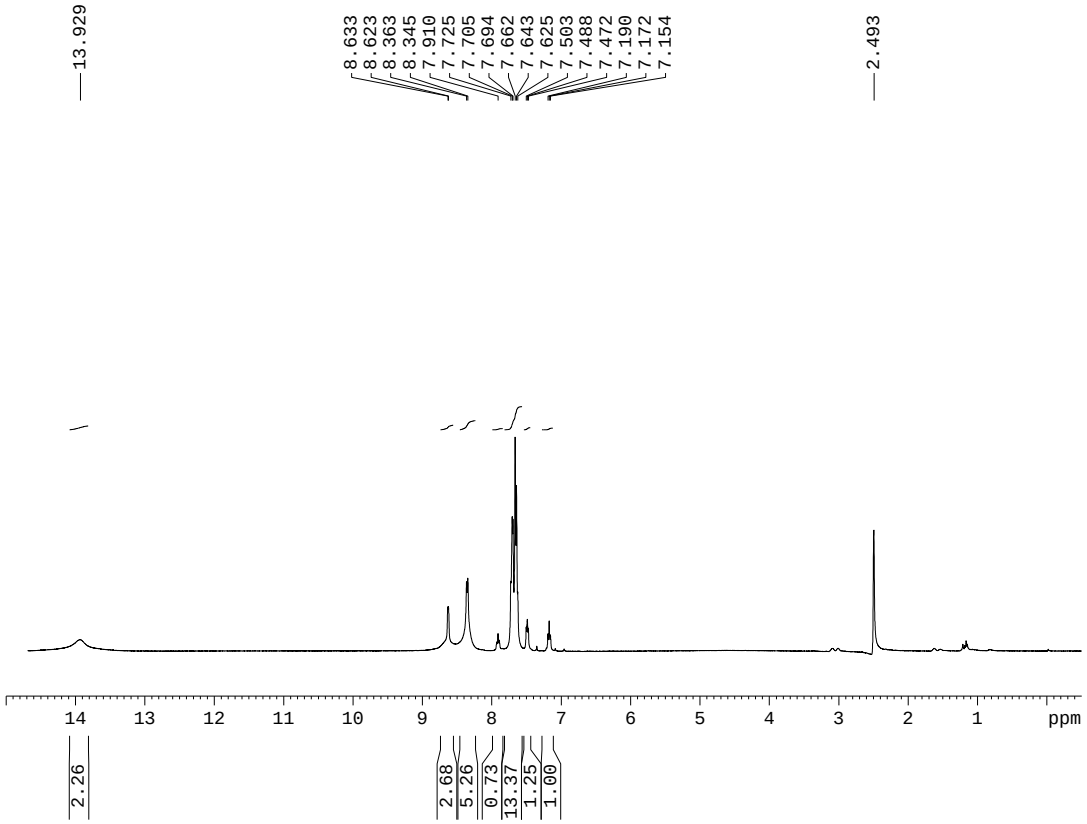

Figure 32. ^{1}H NMR spectrum of compound **8.**

(d) Synthesis of [PhBi(2-O_2C-$C_4H_3N_2$)$_2$(2-O_2C-$C_4H_4N_2$).H_2O] (9)

To a refluxing solution of $BiPh_3$ (0.100 g, 0.227 mmol) in dry ethanol (20 cm^3) under dry nitrogen atmosphere was added pyrazine-2-carboxylic acid (0.084 g, 0.681 mmol) and the clear solution obtained was heated under reflux for a further 6 h. The solution was filtered to remove any suspended impurities and the clear, colourless filtrate kept at 4 ^{o}C (open container). After 10-12 d, colourless crystals suitable for X-ray single crystal analysis were obtained.

Yield: 0.077 g, 50%.

Mp: >320 $^{\circ}$C.

IR (KBr) (cm^{-1}): 3474(br), 3057(w), 1645(s), 1599(m), 1558(m), 1471(w),1408(w), 1375(m), 1336(m), 1155(s), 1032(s), 846(s), 788(s), 729(s), 690(m), 632(m).

^{1}H NMR (400 MHz, $CDCl_3$+DMSO-d_6) δ = 9.33 (s, 2H, Ar-*H*), 9.07-9.00 (m, 4H, Ar-*H*), 8.44-8.42 (m, 2H, Ar-*H*), 7.60-7.57 (m, 2H, Ar-*H*), 7.14-7.11 (m, 1H, Ar-*H*).

Elemental analysis (calc): C, 37.51 (37.44); H, 2.31 (2.37); N, 12.35 (12.48).

(e) Synthesis of [PhBi(2-O_2C-$C_9H_6N)_2.H_2O$] (10)

The procedure was same as that for **9** using $BiPh_3$ (0.100 g, 0.227 mmol) and quinoline-2-carboxylic acid (0.118 g, 0.681 mmol).

Yield: 0.099 g, 67 %.

Mp: 234-238°C.

IR (KBr) (cm^{-1}): 3557(w), 3499(w) 3045(w), 1630(s), 1566(m), 1506(m), 1460(s), 1429(w), 1319(s), 1213(m), 1161(m), 958(w), 895(s), 798(s), 773(s), 733(s).

^{1}H NMR (400 MHz, $CDCl_3$+DMSO-d_6) δ = 8.52 (br, 5H, Ar-*H*), 8.07-7.99 (m, 7H, Ar-*H*), 7.64 (m, 5H, Ar-*H*), 4.50 (ca 2H, H_2O).

Elemental analysis (calc): C, 48.16 (48.51); H, 2.95 (2.45); N, 4.3 (4.32).

(f) Synthesis of [$Ph_2Bi(O_2C$-$C_4H_3O)$] (11)

To a solution of $BiPh_3$ (0.100 g, 0.227 mmol) in ethanol (25 cm^3) was added furan-2-carboxylic acid (0.076 g, 0.681 mmol) and the clear solution obtained was stirred at room temperature for a further 1 d. The solution was filtered and the filtrate kept at 4 °C. After 12-14 d, colourless crystals were obtained. When the reaction was conducted under reflux conditions, an insoluble precipitate was obtained.

Yield: 0.058 g, 54%.

Mp: 222-224 °C.

IR (KBr) (cm^{-1}): 3111(w), 3059 (w), 2920(w), 1583(s), 1537(m), 1516(m), 1469(m), 1412(s),1363(m), 1010(m), 812(s),775(s), 725(s).

^{1}H NMR (400 MHz, $CDCl_3$+DMSO-d_6) δ = 8.23-8.22 (d, J = 6.0 Hz, 3H, Ar-*H*), 7.69-7.67 (m, 1H, Ar-*H*), 7.56-7.55 (m, 3H, Ar-*H*), 7.51 (br, 1H, Ar-*H*), 7.34-7.24 (m, 3H, Ar-*H*), 6.91 (br, 1H, Ar-*H*), 6.41 (br, 1H, Ar-*H*).

Elemental analysis (calc): C, 43.12 (43.03); H, 2.68 (2.74).

(g) Synthesis of [$Ph_2Bi(O_2C$-$C_4H_3S)$] (12) and [$PhBi(O_2C$-$C_4H_3S)_2]_2$ (13)

Compound **12** (needle type, a few crystals, low solubility) was obtained in trace quantities along with compound **13** (rectangular blocks) by the same procedure as that for **6** using $BiPh_3$ (0.100 g, 0.227 mmol) and thiophene-2-carboxylic acid (0.076 g, 0.681 mmol). Attempted maximization of the yield of **12** by using ca 1:1

stoichiometry of the reactants under reflux conditions led to essentially insoluble material after washing off unreacted $BiPh_3$.

Compound **13**:

Yield: 0.078 g, 70%.

Mp: 224-228°C.

IR (KBr) (cm^{-1}): 3088(w), 2920(w), 2841(s), 1545(s), 1521(s), 1419(s), 1381(s), 1111(s), 862(s), 814(s), 767(s), 721(s), 653(m).

^1H NMR (400 MHz, $CDCl_3$+DMSO-d_6) δ = 8.73-8.72 (d, J = 11.2 Hz, 2H, Ar-*H*), 7.80-7.74 (m, 2H, Ar-*H*), 7.61-7.54 (m, 2H, Ar-*H*), 7.47-7.46 (m, 2H, Ar-*H*), 7.28-7.26 (m, 1H, Ar-*H*), 7.03-7.02 (m, 2H, Ar-*H*).

Elemental analysis (calc): C, 35.56 (35.62); H, 2.0 (1.71).

(h) Other reactions

To a boiling solution of 0.227 mmol of $BiPh_3$ in 25 cm^3 of ethanol was added 0.681 mmol of carboxylic (2-hydroxynicotinic, 2-thionicotinic or pyridine 2,6-dicarboxylic,) acid and the contents heated under reflux for 6 h to obtain a precipitate. The solution was filtered, the precipitate washed with ethanol and dried in air. All of these had melting points > 320 °C. Since characterization without an X-ray structure was not feasible no further analysis was performed. There was no reaction in refluxing toluene also. We could not effect a reaction with acetyl salicylic acid (aspirin) or cholic acid in EtOH or toluene or acetonitrile. However, dicyclohexyl phosphinic acid appeared to react and gave an insoluble powder that could not be characterized structurally and no further attempt was made to analyse the product.

3.6 Solubility Problem for the Bioactivity Studies

Solubility is an important parameter for checking the biological accessibility. Our target was to use the above compounds for pharmaceutical purposes.Although compounds **1** and **2** are rather insoluble in most of the solvents, the dissolution was quite fast in 2N HCl. Even in 0.1 N HCl, compound 1 could be solubilized after heating at 80 ◦C. However, no solid came out even after reducing the volume to *ca*. 0.5 ml/100 mg of 1. This is interesting because the compound as such is insoluble in

water. Further studies are required to learn the nature of the species present in dil. HCl.

3.7 Synthesis of Bismuth Vanadate, $BiVO_4$ (14)

To a boiling solution of $Bi(NO_3)_3.5H_2O$ (0.100g, 0.206 mmol) in water (50 cm^3) was added (a) NH_4VO_3 (0.024 g, 0.206 mmol) or (b) $NaVO_3$ (0.025g, 0.206mmol). A yellow precipitate was obtained. The mixture was filtered, the precipitate washed with hot water and then dried in air.

Yield: (a) 0.123 g (92.5%), (b) 0.106 g (80%).

Mp: >320 ^oC

IR (KBr; cm^{-1}): 3452(br), 823(s), 738(s), 682(s), 482(w).

The authenticity of the prodcut was confirmed by powder XRD (cf. Chapter 2, Results and Discussion].

3.8 X-ray Crystallography

X-ray data were collected on a Bruker AXS SMART diffractometer using Mo-K_α (λ = 0.71073 Å) radiation. The structures were solved by direct methods;[72] all non-hydrogen atoms were refined anisotropically unless stated otherwise. For the hydrogen atoms, the riding model was used; where possible, a Difference Fourier map was also used. The crystal data for compounds **1-3** are summarized in Table IV.

In the case of **1'** (this structure was reported earlier also but additional interactions were not checked)[18] all atoms except the bismuth were refined isotropically. Although a solution could be found in the space group $P2_1/m$ also, there were too many short contacts among different oxygen atoms with a large number (13) of Bi-O contacts and hence was not considered; this could also indicate a disordered structure. For **5**, hydrogen atoms were located by Fourier Difference maps and then were allowed ride on the respective non-hydrogen atom as appropriate. The crystal data for compounds **1'** and **5** are summarized in Table V.

The R_{int} was slightly higher in the case of **9**, but the refinement was smooth. Only in the case of **12**, the ring atoms (C22, C33) showed somewhat higher thermals, but the final R indices were quite good. In the case of compound **13**, the positions of S and CH groups adjacent to the carboxylate groups were essentially equally occupied. Hence the refinement was done by keeping both positions as

sulphur and giving it an occupancy of 0.71875 that corresponds to an electron count of 11.5 (S =16, CH = 7, average = 11.5, occupancy calculated for sulphur = 11.5/16 = 0.71875]. This procedure gives slightly different values of Mr, μ, density etc. The crystal data for the compounds **6** and **8-13** are summarized in Table VI.

Table IV. Crystallographic data for compounds **1-3**[a]

Compound	**1**	**2**	**3**
CCDC Number	749253	749254	749255
emp. formula	$C_{18}H_{12}BiN_3O_6$	$C_{28}H_{18}Bi_2N_4O_{18}$	$C_{30}H_{23}BiN_4O_{11}$
formula wt	575.29	1116.42	824.50
crystal system	Monoclinic	Monoclinic	Monoclinic
space group	$P2_1/n$	$P2_1/c$	Cc
a/Å	11.822(3)	12.341(3)	9.6810(6)
b/Å	7.738(2)	11.886(2)	18.5747(12)
c/Å	18.931(6)	21.485(4)	16.5929(11)
β/°	91.165(4)	103.96(3)	100.585(1)
V/Å^3	1731.3(9)	3058.6(11)	2933.0(3)
Z	4	4	4
D_{calcd}	2.207	2.424	1.867
μ	10.228	11.587	6.082
F_{000}	1088	2096	1608
Data/ restraints/ parameters	3371/0/ 253	6118/3/ 483	5182/8/427
S	1.116	1.101	1.091
R1	0.0349	0.0329	0.0240
wR2 (all data)	0.0852	0.0815	1.204
max./min. residual elec. dens. [eÅ^{-3}]	1.377/ -2.032	1.965/ -2.392	-0.420/ 0.106

[a] R1 = Σ||Fo| - |Fc||/Σ|Fo| and wR2 = [Σw(Fo2-Fc2)2/ΣwFo4]0.5

Table V. Crystallographic data for compounds **1'** and **5**[a]

Compound	**1'**[a]	**5**
CCDC Numbers	See ref. 93	759762
emp. formula	$C_{18}H_{12}BiN_3O_6$	$C_{28}H_{28}Bi_2N_4O_{23}$
formula wt	575.29	1206.50
crystal system	Monoclinic	Triclinic
space group	$P2_1$	$P\bar{1}$
a/Å	11.068(1)	7.1268(5)
b/Å	7.743(1)	11.0010(8)
c/Å	11.277(1)	12.1409(7)
α/°	90.0	111.841(6),
β/°	116.123(9)	96.555(5),
γ/°	90.0	90.320(6)
V/Å^3	867.73(10)	876.58(10)
Z	2	1
D_{calcd}	2.202	2.286
μ (mm^{-1})	10.203	10.126
F_{000}	544	574
Data/ restraints/ parameters	2655 / 28 / 118	2991 / 11 / 283
S	1.100	= 0.986
R1	0.0273	0.0239
wR2 (all data)	0.0744	0.0527
max./min. residual elec. dens. [eÅ^{-3}]	1.034/-1.069	1.088/-1.071

[a]Flack parameter 0.00(1), Literature[18] values of crystal dimensions (*a*, *b*, *c*, β) are: 11.010(1), 7.749(1), 11.227(1) Å and 116.361(7)°.

Table VIa. Crystallographic data for compounds **6** and **8-10**[a]

Compound	**6**	**8**	**9**	**10**
CCDC Number	825245	825246	825247	825248
emp. formula	$C_{24}H_{18}BiN_3O_9$	$C_{34}H_{27}BiN_6O_{12}$	$C_{21}H_{17}BiN_6O_7$	$C_{26}H_{19}BiN_2O_5$
formula wt	701.39	920.60	674.39	648.41
crystal system	Triclinic	Triclinic	Monoclinic	Monoclinic
space group	$P\bar{1}$	$P1$	$C2/c$	$P2_1/n$
a/Å	9.672(1)	9.982(1)	27.571(2)	10.120(2)
b/Å	11.413(1)	13.869(2)	10.287(1))	13.740(3)
c/Å	11.541(1)	13.908(2)	17.080(1)	16.630(3)
α/^{o}	77.802(2)	73.185(2)	90	90
β/^{o}	78.026(3)	70.121(2)	109.015(1)	101.00(3)
γ/^{o}	72.353(2)	70.084(2)	90	90
V/Å^3	1172.3(2)	1669.2(3)	4580.0(6)	2269.9(8)
Z	2	2	8	4
D_{calcd}	1.987	1.832	1.956	1.897
μ	7.581	5.358	7.755	7.809
F_{000}	676	904	2592	1248.0
Data/restraints/parameters	4774/0/337	5870/0/494 3	4001/4/325	3986/3/313
S	1.021	1.054	1.051	0.988
R1	0.0217	0.0247	0.0544	0.0359
wR2 (all data)	0.0500	0.0597	0.1355	0.0739
max./min. Residual elec. dens. [eÅ^{-3}]	0.825/-0.436	0.752/-0.537	3.703/-2.755	1.489/-0.806

[a]$R1 = \Sigma||Fo| - |Fc||/\Sigma|Fo|$ and $wR2 = [\Sigma w(Fo^2-Fc^2)^2/\Sigma wFo^4]^{0.5}$

Table VIb. Crystallographic data for compounds **11-13**[a]

Compound	**11**	**12**[a]	**13**
CCDC Number	825249	825250	825251
emp. formula	$C_{17}H_{13}BiO_3$	$C_{51}H_{39}Bi_3O_6S_3$	$C_{16}H_{11}BiO_4S_2$
formula wt	474.25	1470.94	540.35
crystal system	Monoclinic	Orthorhombic	Triclinic
space group	$P2_1/n$	$P2_12_12_1$	$P\bar{1}$
a/Å	10.340(2)	9.238(2)	8.645(1)
b/Å	9.725(2)	17.369(4)	9.601(1)
c/Å	15.679(3)	30.368(7)	10.697(1)
α/°	90	90	81.279(1)
β/°	101.02(3)	90	71.418(1)
γ/°	90	90	71.429(1)
V/Å^3	1547.6(5)	4873(2)	796.5(1)
Z	4	4	2
D_{calcd}	2.035	2.005	2.253
μ	11.399	10.984	11.346
F_{000}	888	2760	508
Data/restraints/ parameters	2726/0/190	8553/62/558	2802/0/208
S	1.086	1.051	1.055
R1	0.0191	0.0338	0.0221
wR2 (all data)	0.0471	0.0828	0.0556
max./min. residual elec. dens. [eÅ^{-3}]	0.758/-0.705	1.453/-0.667	1.318/-1.158

[a]Flack parameter: 0.005(8)

References

1) J. R. Partington, *A History of Chemistry,* MacMillan, London, 1961.

2) H. Suzuki and Y. Matano, Ed., *Organobismuth Chemistry*, Elsevier, Amsterdam, 2001.

3) J. Reglinski, *Chemistry of Arsenic*, *Antimony and Bismuth*; N. C. Norman, Ed.; Blackie Academic & Professional: London, 1998, 403.

4) (a) P. J. Sadler, H. Li and H. Sun*, Coord. Chem. Rev.,* 1999, **185**, 689.

(b) L. Odier, *J. Med. Chir. Pharm.,* 1986, **68**, 49.

(c) F. C. R. Balzer, *Soc. Biol.,* 1889, **41**, 537.

(d) A. Slikkerveer and F. A de Wolff, *Med. Toxicol. Adverse Drug Exp.,* 1989, **4**, 303.

(e) H. Menge, M. Gregor, B. Brosius, R. Hopert and A. Lang, *Eur. J. Gastroenterol. Hepatol.,* 1994, **4**, 1994.

(f) G.G. Briand and N. Burford, *Chem. Rev.*, 1999, **99**, 2601.

(g) J. R. Warren and B. Marshall*, Lancet,* 1983, 1273.

(h) H. L. T. Mobley, M. D. Island and R. P. Hausinger, *Microbiol. Rev.,* 1995, **59**, 451

5) (*a*) Z. Guo and P. J. Sadler, *Angew. Chem., Int. Ed.*, 1999, **38**, 1512.

(b) R. Ge and H. Sun, *Acc. Chem. Res.*, 2007, **40**, 267.

(c) N. Yang and H. Sun, *Coord. Chem. Rev.*, 2007, **251**, 2354.

(d) V. Stavila, R. L. Davidovich, A. Gulea and K. H. Whitmire, *Coord. Chem. Rev.*, 2006, **250**, 2782.

6) (a) N. Yang, J. A. Tanner, Z. Wang, J. D. Huang, B. J. Zheng, N. Zhu and H. Sun, *Chem. Commun.*, 2007, 4413.

(b) M. J. Abrams and B. A. Murrer, *Science*, 1993, **261**, 725.

(c) K. H. Thompson and C. Orvig, *Science*, 2003, **300**, 936.

(d) J. H. Thurston, E. M. Marlier and K. H.Whitmire, *Chem. Commun.*, 2002, 2834.

(e) P. C. Andrews,G. B. Deacon, W. R. Jackson, M. Maguire, N. M. Scott, B. W. Skelton and A. H.White, *J. Chem. Soc., Dalton Trans.*, 2002, 4634.

(f) G.G. Briand, N. Burford, M. D. Eelman, N. Aumeerally, L. Chen, T. S. Cameron and K. N. Robertson, *Inorg. Chem.*, 2004, **43**, 6495.

(g) N. Burford, M. D. Eelman and T. S. Cameron, *Chem. Commun.*, 2002, 1402.

(h) V. Stavila, J. C. Fettinger and K. H.Whitmire, *Organometallics*, 2007, **26**, 3321.

(i) H. A. Phillips, M. D. Eelman and N Burford, *J. Inorg. Biochem.,* 2007, **101**, 736;

7) (a) P. C. Andrews, G. B. Deacon, P. C. Junk, I. Kumar and M. Silberstein, *Dalton Trans.*, 2006, 4852.

(b) P. C. Andrews, G. B. Deacon, R. L. Ferrero, P. C. Junk, A. Kurrar, I. Kumar and J. G. MacLellan, *Dalton Trans.*, 2009, 6377.

(c) P. C. Andrews, G. B. Deacon, P. C. Junk, I. Kumar and J. G. MacLellan, *Organometallics*, 2009, **28**, 3999.

8) P. C. Andrews, G. B. Deacon, C. M. Forsyth, P. C. Junk, I. Kumar and M. Maguire, *Angew. Chem. Int. Ed.*, 2006, **45**, 5638.

9) J. R. Lambert and P. Midolo, *Aliment Pharmacol Ther* 1997, **11** (Suppl. 1), 27.

10) W. Li, L. Jin, N. Zhu, X. Hou, F. Deng and H. Sun, *J. Am. Chem. Soc.*, 2003, **125**, 12408.

11) G. G. Briand and N. Burford, *Adv. Inorg. Chem.*, 2000, **50**, 285.

12) D. Ws. Bierer, *Reviews of Infectious Diseases* 1990, **12,** S3.

13) (a) V. Andre, A. Hardeman, I. Halasz, R. S. Stein, G. J. Jackson, D. G. Reid, M. J.Duer, C. Curfs, M. T. Duarte and T. Friscic, *Angew. Chem. Int. Ed.,* 2011, **50**, 7858.

14) H. Gilman and H. L. Yale., *J. Am. Chem. Soc.,* 1951, **73,** 2880.

15) E. Asato,' W. L. Driessen, R. A. G. de Graaff, F. B. Hulsbergen, and J. Reedijk, *Inorg. Chem.,* 1991, **30**, 4210.

16) E. Asato, K. Katsura, M. Mikuriya, T. Fujii and J. Reedijk, *Inorg. Chem.*, 1993, **32**, 5322.

17) E. Asato, K. Katsura, M. Mikuriya, U. Turpeinen, I. Mutikainen and J. Reedijk, *Inorg. Chem.* 1995, **34**, 2447.

18) E. Callens, A. J. Burton, A. J. P. White and A. G. M. Barrett, *Tetrahedron Lett.*, 2008, **49**, 3709.

19) A. Thirumurugan, W. Li and A. K. Cheetham, *Dalton Trans.,* 2012, **41**, 4126.

20) M. Ranjbar, H. Aghabozorg, A. Moghimi and A. Yanovsky, *Anal. Sci.,* 2001, **17**, 1469.

21) (a) A. C. Wibowo, M. D. Smith and H.-C. zur Loye, *Inorg. Chem.*, 2010, **49**, 11001.

(b) A. C. Wibowo, M. D. Smith and H.-C. zur Loye, *Chem. Commun.,* 2011, **47**, 7371.

22) M. Wenkin, R. Touillaux and M. Devillers, *New J. Chem.*, 1998, **22**, 973.

23) T. Zevaco, M. Postel and N. Benalicherif, *Main Group Met. Chem.*, 1992, **15**, 217.

24) T. Zevaco, N. Guilhaume and M. Postel, *New J. Chem. (Nouv. J. Chemie)*, 1991, **15**, 927.

25) M. Domagala, H. Preut and F. Huber, *Acta Crystallogr. Sect. C: Cryst. Struct. Commun.*, 1988, **44**, 830.

26) A. Miloudi, G. Boyer, D. EI-Abed, J.-P. Finet and J.-P. Galy, *Main Group Met. Chem.*, 2001, **24**, 767.

27) (a) B. B. Bokhonov and Yu. M. Yukhin, *Russ. J. Inorg. Chem.,* 2010, **55**, 1381.

(b) Y. M. Yukhin, K. Yu. Milkhailov, B. S. Bokhonov and I. A. Vorsina, *Chem. for sustainable dev.*, 2004, **12**, 403.

28) (a) T. Ould-Ely, J. H. Thurston and K. H. Whitmire, *C. R. Chimie,* 2005, **8**, 1906.

(b) J. H. Thurston and K. H. Whitmire, *Inorg. Chem.,* 2002, **41**, 4194.

(c) J. H. Thurston, A. Kumar, C. Hofmann and K. H. Whitmire, *Inorg. Chem.,* 2004, **43**, 8427.

(d) J. H. Thurston, D. Trahan, T. Ould-Ely and K. H. Whitmire, *Inorg. Chem.,* 2004, **43**, 3299.

29) (a) V. Chandrasekhar and R. K. Metre, *Dalton Trans.,* 2012, **41**, 11684.

(b) I. V. Egorova, V. V. Sharutin, T. K. Ivanenko, N. A. Nikolaeva and A. A. Molokov, *Russ. J. Coord. Chem.,* 2006, **32**, 321.

(c) V. V. Sharutin, I. V. Egorova, O. K. Sharutina and L. A. Nevmeshkina, *Russ. J. Inorg. Chem.,* 2008, **53**, 1733.

(d) K. R. Chaudhari, A. P. Wadawale, V. K. Jain, N. Yadav and R. Bohra, *Indian J. Chem. Sec. A,* 2010, **49**, 34.

(e) R. T. Hart, A. A. Kerr and N. A. Eckert, *Tribology Trans.,* 2010, **53**, 22.

(f) J. D. Arenivar, 32nd Annual Polyurethane technical marketing conference 1989.

30) (a) A. B. Ilyukhin and A. L. Poznyak, *Crystallography Reports,* 2000, **45**, 56.

(b) G. Galy and G. Meunier, *J. Solid State Chem.,* 1975, **13**, 142.

(c) G. Galy and R. Enjalbert, *J. Solid State Chem.,* 1982, **44**, 1.

31) (a) C. E. Mohn and S. Stølen, *Phy. Rev. B,* 2011, **83**, 014103.

(b) R. W. Wolfe and R. E. Newnham, *Solid State Commun.,* 1969, **7**, 1797.

(c) Y. Noguchi, K. Murata, and M. Miyayama, *Appl. Phys. Lett.,* 2004, **89**, 242916.

(d) A. Kudo and S. Hijii, *Chem. Lett.,* 1999, 990568.

(e) J. Tang, Z. Zou and J. Ye, *Catal. Lett.,* 2004, **92**, 53.

(f) M. S. Islam, S. Lazure, R.-N. Vannier, G. Nowogrocko and G. Mairesse, *J. Mater. Chem.,* 1998, **8**, 655.

(g) C. Pirovano, M. S. Islam, R. N. Vannier, G. Nowogrocki, and G. Mairisse, *Solid State Ionics,* 2001, **140**, 115.

(h) S. Hull, *Rep. Prog. Phys.* 2004, **67**, 1233.

(i) A.Watenabe, Z. Inoue and T. Ohsaka, *J. Solid State Chem.,* 1982, **41**, 160.

(j) N. A. McDowell, K. S. Knight and P. Lightfoot, *Chem. A Eur. J.,* 2006, **12**, 1493.

(k) D. M. Adams, *Inorganic Solids,* John Wiley, London, 1974.

(l) P. Ravindran, R. Vidya, A. Kjekshus, H. Fjellvag and O. Eriksson, *Phys. Rev.B,* 2006, **74**, 224412.

(m) D. J. Payne, R. G. Egdell, A. Walsh, G. W. Watson, J. Guo, P. A. Glans, T. Learmonth and K. E. Smith, *Phys. Rev. Lett.*, 2006, **96**, 157403.

(n) A. Walsh, G. W. Watson, D. J. Payne, R. G. Egdell, J. Guo, P. A. Glans, T. Learmonth, and K. E. Smith, *Phys. Rev. B,* 2006, **73**, 235104.

(o) C. E. Mohn, S. Stølen, S. T. Norberg, and S. Hull, *Phys. Rev. B*, 2009, **80**, 024205.

(p) C. E. Mohn, S. Stølen, S. T. Norberg, and S. Hull, *Phys. Rev. Lett.,* 2009, **102**, 155502

(q) M. W. Stoltzfus, P. M. Woodward, R. Seshadri, J.-H. Klepeis, and B. Burnstein, *Inorg. Chem.,* 2007, **46**, 3839.

(r) A. Walsh, Y. Yan, M. N. Huda, M. M. Al-Jassim and S. H. Wei, *Chem. Mater.,* 2009, **21**, 547.

32) R. A. Wheeler and P. N. V. Pavan Kumar, *J. Am. Chem. Soc.,* 1992, **114**, 4776.

33) (a) O. C. Monteiro, H. I. S. Nogueira, T. Trindade, M. Motevalli, *Chem. Mater.,* 2001, **13**, 2103.

(b) C. Silvestru, H. J. Breunig, H. Althaus, *Chem. Rev*., 1999, **99,** 3277.

34) C. L. Teske and W. Bensch, *Z. Anorg. Allg. Chem.,* 2011, **637**, 406.

35) (a) E. M. Campi, G. B. Deacon, W. R. Jackson, B. W. Skelton, K. A. Smith and A. H. White, *Z. Anorg. Allg. Chem.,* 2006, **632**, 1483.

(b) A. Shier, J. M. Wallis, G. Müller and H. Schmidbaur, *Angew. Chem. Int. Ed.,* 1986, **25**, 757.

(c) W. Frank, J. Weber and E. Fuchs, *Angew. Chem. Int. Ed.,* 1987, **26**, 74.

(d) M. B. Ferrari, M. R. Cramarossa, D. Iarossi and G. Pelosi, *Inorg. Chem.,* 1998, **37**, 5681.

36) (a) S. C. James, N. C. Norman and A. G. Orpen, *J. Chem. Soc*., *Dalton Trans*., 1999, 2837.

(b) W. Clegg, R. J. Errington, G. A. Fisher, R. J. Flynn and N. C. Norman, *J. Chem. Soc.*, *Dalton Trans.*, 1993, 637.

(c) C. J. Carmalt, A. H. Cowley, A. Decken and N. C. Norman, *J. Organomet. Chem.*, 1995, **496**, 59.

(d) C. J. Carmalt, L. J. Farrugia and N. C. Norman, *J. Chem. Soc.*, *Dalton Trans.*, 1996, 443.

37) Y. W. Wang, B. H. Hong and K. S. Kim, *J. Phys. Chem. B,* 2005, **109**, 7067.

38) (a) C. T. Campbell, S. C. Parker and D. E. Starr, *Science*, 2002, **298**, 811.

(b) Z. Y. Tang, N. A. Kotov and M. Giersig, *Science*, 2002, **297**, 237.

(c) Y. Volokitin, J. Sinzig, L. J. deJongh, G. Schmid, M. N. Vargaftik and I. I. Moiseev, *Nature (London),* 1996, **384**, 621.

(d) B. H. Hong, S. C. Bae, C.-W. Lee, S. Jeong and K. S. Kim, *Science,* 2001, **294,** 348.

(e) S. B. Suh, B. H. Hong, P. Tarakeshwar, S. J. Youn, S. Jeong and K. S. Kim, *Phys. Rev. B,* 2003, **67**, 241402 (R).

39) (a) J. L. Costa-Kramer, N. Garcia and H. Olin, *Phys. Rev. Lett.,* 1997, **78**, 4990.

(b) K. Liu, C. L. Chien, P. C. Searson and Y. Z. Kui, *Appl. Phys. Lett.,* 1998, **73**, 1436.

(c) M. R. Black, Y. M. Lin, S. B. Cronin, O. Rabin and M. S. Dresselhaus, *Phys. Rev. B*, 2002, **65,** 195417.

(d) M. R. Black, P. L. Hagelstein, S. B. Cronin, Y. M. Lin and M. S. Dresselhaus, *Phys. Rev. B,* 2003, **68**, 235417.

40) (a) J. Heremans and C. M. Thrush, *Phys. Rev. B,* 1999, **59**, 12579.

(b) M. S. Dresselhaus, Y. M. Lin, O. Rabin and G. Dresselhaus, *Microscale Thermophys. Eng.,* 2003, **7**, 20

41) G. H. Hwang, W. K. Han, S. J. Kim, S. J. Hong, J. S. Park, H. J. Park and S. G. Kang, *J. Cer. Proc. Res.,* 2009, **10**, 190.

42) H. A. Harwig and A. G. Gerards, *J. Solid State. Chem.*, 1978, **26**, 265.

43) (a) P. Shuk, H –D. Weimhofer, U. Guth, W. Gopel and M. Greenblatt, *Solid State Ionics,* 1996, **89,** 179.

(b) T. H. Etsell and S. N. Flengas, *Chem. Rev.,* 1970, **70,** 339.

44) (a) Y. Yu, C. H. Jin, R. H. Wang, Q. Chen and L.-M. Peng, *J. Phys. Chem. B,* 2005, **109**, 18772.

(b) L. Hung, C. Tsung, W. Huang and P. Yang, *Adv. Mater.,* 2010, **22***,* 1910.

(c) Q. Guo, H. W. Hillhouse and R. Agrawal , *J. Am. Chem. Soc.,* 2009, **131**, 11672.

(d) C. Steinhagen, M. G. Panthani, V. Akhavan, B. Goodfellow, B. Koo and B. A. Korgel, *J. Am. Chem. Soc.,* 2009, **131**, 12554.

(e) M. G. Panthani, V. Akhavan, B. Goodfellow, J. P. Schmidtke, L. Dunn , A. Dodabalapur , P. F. Barbara and B. A. Korgel, *J. Am. Chem. Soc.,* 2008, **130**, 16770.

(f) Y. Wu, C. Wadia, W. Ma, B. Sadtler and A. P. Alivisatos, *Nano Lett.,* 2008, **8**, 2551.

45) L. Cademartiri , R. Malakooti , P. G. O'Brien, A. Migliori, S. Petrov, N. Kherani and G. A. Ozin, *Angew. Chem. Int. Ed.,* 2008, **47**, 3814.

46) (a) A. K. Rath, M. Bernechea, L. Martinez and G. Konstantatos, *Adv. Mater.*, 2011, **23**, 3712.

(b) J. Ma, Z. Liu, J. Lian, X. Duan, T. Kim, P. Peng, X. Liu, Q. Chen, G. Yao and W. Zheng *Cryst. Eng. Comm.,* 2011, **13**, 3072

(c) H. Wang, J. J. Zhu, J. M. Zhu and H. Y. Chen, *J. Phys. Chem. B,* 2002, **106**, 3848.

(d) H. F. Bao, C. M. Li, X. Q. Ciu, Y. Gan, Q. L. Song and J. Guo, *Small,* 2008, **4**, 1125.

(e) G. Konstantatos, L. Levina, J. Tang and E. H. Sargent, *Nano Lett.,* 2008, **8**, 4002.

(f) P. Boudjouk, M. P. Remington Jr., D. G. Grier, B. R. Jarabek and G. J. McCarthy, *Inorg. Chem.,* 1998, **37**, 3538.

(g) B. Zhang, X. C. Ye, W. Y. Hou, Y. Zhao and Y. Xie, *J. Phys. Chem. B*, 2006, **110**, 8978.

(h) L. S. Li, N. J. Sun, Y. Y. Huang, Y. Qin, N. N. Zhao, J. N. Gao, M. X. Li, H. H. Zhou and L.M. Qi, *Adv. Funct. Mater.,* 2008, **18**, 1194.

(i) O. Rabin, J. M. Perez, J. Grimm, G. Wojtkiewicz and R. Weissleder, *Nat. Mater.,* 2006, **5,** 118.

(j) L. Cademartiri, F. Scotognella, P. G. O'Brien, B. V. Lotsch, J. Thomson, S. Petrov, N. P. Kherani and G. A. Ozin, *Nano Lett.,* 2009, **9**, 1482.

(k) K. Yao, W. W. Gong, Y. F. Hu, X. L. Liang, Q. Chen and L. M. Peng, *J. Phys. Chem. C*, 2008, **112**, 8721.

47) (a) S. K. Batabyal, C. Basu, A. R. Das and G. S. Sanyal, *Mat. Lett.,* 2006, **60**, 2582.

(b) K. Watanabe, N. Sato and S. Miyaoka, *J. Appl. Phys,* 1983, **54**, 1256.

(c) S. B. Atkulov, T. Azimov and A. N. Shasiddonov, *Sov. Phys. Semicond.,* 1982, **16**, 1326.

(d) S. K. Mishra, S. Satpathy and O. Jepsen, *J. Phys. Condens. Matter*, 1997, **9**, 461.

(e) N. Sakai, T. Kajiwara, K. Takemura, S. Minomura and Y. Fujii, *Solid State Commun.,* 1981, **40,** 1045.

(f) N. G. Patel and P. G. Patel, *Solid State Electron.,* 1992, **35**, 1269.

(g) H. J. Goldsmid, J. E. Giutronich and M. M. Kaila, *Sol. Energy,* 1980, **24**, 435.

(h) B. Roy, B. R. Chakraborty, R. Bhattacharya and A. K. Dutta, *Solid State Commun.,* 1978, **25**, 937.

48) (a) J. J. Cha, J. R. Williams, D. Kong, S. Meister, H. Peng, A. J. Bestwick, P. Gallagher, D. G.-Gordon and Y.Cui, *Nano Lett.* 2010, **10**, 1076.

(b) H. Zhang, C.-X. Liu, X.-L.Qi, X. Dai, Z. Fang and S.-C. Zhang, *Nat. Phys.,* 2009, **5**, 438.

(c) G. Zhang, H. Qin, J. Teng, J. Guo, Q. Guo, X. Dai, Z. Fang and K. Wu, *Appl. Phys. Lett.,* 2009, **95**, 053114.

49) (a) G.-R. Li, F.-L. Zheng and Y.-X. Tong, *Cryst. Growth Des.,* 2008*,* **8**, 1226
(b) S. A. Sapp, B. B. Lakshmi and C. R. Martin, *Adv. Mater.,*1999, **11**, 402.
(c) J. J. Ritter and P. Maruthamuthu, *Inorg. Chem.,* 1995, **34**, 4278.
(d) E. J. Winder, A. B. Ellis and G. C. Lisensky, *J. Chem. Educ.,* 1996, **73**, 940.

50) (a) J. Chen, X. Xing, A. Watson, W. Wang, R. Yu, J. Deng, L. Yan, C. Sun and X. Chen, *Chem. Mater.,* 2007, **19**, 3598.
(b) N. Jeon, D. Rout, I. W. Kim and S.-J. L. Kang, *Appl. Phys. Lett.,* 2011, **98**, 072901.
(c) A. Huang and S. R. Shannigrahi, *J. Alloys and Comp.,* 2011, **509**, 2054.

51) (a) W. Wei, Y. Dai and B. Huang, *J. Phys. Chem. C,* 2009, **113***,* 5658.
(b) A. Kudo and S. Hijii, *Chem. Lett.,* 1999, **28**, 1103.
(c) W. F.Yao, H. Wang, X. H. Xu, J. T. Zhou, X. N. Yang, Y. Zhang and S. X. Shang, *Appl. Catal., A* 2004, **259**, 29.
(d) H. Zhang, G. Chen and X. Li, *Solid State Ionics,* 2009, **180**, 1599.

52) X –C. Wang, R –L. Yan, M –J. Zhong and Y-M. Liang, *J. Org. Chem.* 2012, **77,** 2064.

53) J.-Y. Shang, F. Li, X.-F. Bai, J.-X. Jiang, K-F. Yang, G.-Q. Lai and L.-W. Xu, *Eur. J. Org. Chem.,* 2012, 2809.

54) S. Manna, S. Maity, S. Rana, S. Agasti and D. Maiti, *Org. Lett.,* 2012, **14**, 1736.

55) V. V. Kouznetsov, C. M. Meléndez Gómez, F. A. Rojas Ruíz, E. del Olmo, *Tetrahedron Lett.,* 2012, **53**, 3115.

56) M. L. N. Rao, D. K. Awasthi and J. B. Talode, *Tetrahedron Lett.,* 2012, **53**, 2662.

57) The X-ray structure of crystals with the same molecular formula is also reported in ref. 18, $P2_1$ (no. 4), a = 11.0098(8), b = 7.7495(6), c = 11.2271(8) Å, β = 116.361(7)°, V = 858.29(11) Å^3, Z = 2. Note that it belongs to a chiral space group and thus the compound appears to be dimorphic. The deposited data suggest isotropic refinement for non-hydrogen atoms. The relevant bond distances for the assigned bicapped trigonal prismatic coordination (taken

from ref. 18) are: Bi–N 2.588(7), 2.430(9), 2.633(7) Å; Bi–O 2.473(6), Bi–2.531(6), 2.296(6), 2.648(6), 2.574(6) Å.

58) V. V. Sharutin, I. V. Egorova, T. K. Ivanenko, O. K. Sharutina, M. A. Pushilin, A. V. Gerasimenko, N. A. Adonin and V. F. Starichenko, *Russ. J. Coord. Chem.,* 2004, **30,** 309.

59) J. Supniewski and R. Adams, *J. Am. Chem. Soc.*, 1926, **48**, 507.

60) Such exchange of positions among certain moieties does occur in the crystal structures. For some examples from our work, see:

(a) C. Muthiah, K. Praveen Kumar, S. Kumaraswamy and K. C. Kumara Swamy, *Tetrahedron*, 1998, **54**, 14315 (CH_3 and Cl interchange).

(b) Manab Chakravarty, Praveen Kommana and K. C. Kumara Swamy, *Chem. Commun*., 2005, 5396 (oxygen and lone pair interchange).

(c) Manab Chakravarty, R. Rama Suresh and K. C. Kumara Swamy, *Inorg. Chem.,* 2007, **46**, 9819 (S and Se interchange).

(d) M. Phani Pavan, Manab Chakravarty and K. C. Kumara Swamy, *Eur. J. Org. Chem.,*2009, 5927 (CH and O interchange).

61) (a) Y. Zhao, Y. Xie, X. Zhu, S. Yan and S. Wang, *Chem. Eur. J*., 2008, **14**, 1601.

(b) A. Kudo, K. Omori and H. Kato, *J. Am. Chem. Soc.* 1999, **121***,* 11459.

(c) J. A. Seabold and K.-S. Choi, *J. Am. Chem.Soc.,* 2012, **134,** 2186.

(d) K. Sayama, A. Nomura, T. Arai, T. Sugita, R.Abe, M.Yanagida, T. Oi, Y. Iwasaki, Y.Abe and H. Sugihara, *J. Phys. Chem. B,* 2006, **110***,* 11352.

62) (a) A. Walsh, Y. Yan, M. N. Huda, M. M. Al-Jassim and S.H. Wei, *Chem. Mater.,* 2009, **21***,* 547.

(b) Y. K. Kho, W. Yang, T. A. Iwase, L. Madler, A. Kudo and R. Amal, *ACS Appl. Mater. Interfaces,* 2011, **3**, 1997.

63) (a) Y. Sun, C. Wu, R. Long, Y. Cui, S. Zhang and Yi Xie, *Chem. Commun*., 2009, 4542.

(b) G. Xi and J. Ye, *Chem. Commun.,* 2010, **46**, 1893.

(c) L. Zhou, W. Wang and H. Xu, *Crystal Growth & Design,* 2008*,* **8***,* 728.

(d) Z. Wang, W. Luo, S. Yan, J. Feng, Z. Zhao,Y. Zhu,Z/ Li and Z. Zou, *CrystEngComm*, 2011, **13**, 2500.

64) (a) Y. Zhou, K. Vuille, A. Heel, B. Probst , R. Kontic, G.R. Patzke *Applied Catalysis A: General* 2010, **375**, 140.

(b) D.Ke, T. Peng, L. Ma, P. Cai and K. Dai, *Inorg. Chem.* 2009, **48**, 4685.

(c) M.-L. Guan, D.-K. Ma, S.-W. Hu, Y.-J. Chen and S.-M. Huang, *Inorg. Chem*., 2011, **50**, 800.

(d) L. Zhang, Dairong Chen and X. Jiao, *J. Phys. Chem. B.,* 2006, **110***,* 2668.

(e) H. Li a, G. Liua and X. Duan, *Materials Chemistry and Physics*, 2009, **115**, 9.

65) (a) W. Yin, W. Wang, M. Shang, L. Zhou, S. Sun and L.Wang, *Eur. J. Inorg. Chem.,* 2009, 4379.

(b) A. Zhang and J. Zhang, *Mater. Sci.-Poland*, 2009, **27**, 1015.

(c) J. B. Liu, H. Wang, S. Wang., H. Yan, Mater. Sci. Eng. B, 2003, **104**, 36.

(d) A. Galembeck and O. L. Alves, *J. Mater. Sci.,* 2002, **37**, 1923.

66) K. Sayama, A. Nomura, Z. G. Zou, R. Abe, Y. Abe and H. Arakawa, *Chem. Commun*., 2003, 2908.

67) (a) X. Zhang, Z. H. Ai, F. L.Jia, L. Z. Zhang, X. X. Fan and Z. G. Zou, *Mater. Chem. Phys.*, 2007, **103**, 162.

(b) M. A. Butler, *J. Appl. Phys*., 1977, **48**, 1914.

68) M. Gotic, S. Music, M. Ivanda, M. Šoufeek, S. Popovic, *J. Mol. Struct*., 2005, **744**, 535.

69) D. D. Perrin, W. L. F. Armarego, , D. R. Perrin *Purification of Laboratory Chemicals*, Pergamon, Oxford, 1986.

(b) J. H. Thurston and K. H. Whitmire, *Inorg. Chem*., 2002, **41**, 4194.

70) P Segl'a, M. Jamnicky, M. Koman, J. Sima and T. Glowiak, *Polyhedron*, 1998, **17**, 4525.

71) E. E. Sileo, M. A. Blesa, G. Rigotti, B. E. Rivero and E. E. Castellano, *Polyhedron,* 1996, **15**, 4531.

72) (a) G. M. Sheldrick, *SHELX-97- A program for crystal structure solution and refinement,* University of Göttingen, 1997.

(b) G. M. Sheldrick, *SADABS, Siemens Area Detector Absorption Correction*, University of Göttingen, Germany, 1996.

(c) G. M. Sheldrick, *SHELXTL NT Crystal Structure Analysis Package*, Bruker AXS, Analytical X-ray System, WI, USA, 1999, version 5.10.

PART B

LANTHANIDE(III) OXO PYRIDINIUM, DIPICOLINATE COMPLEXES- STUDIES ON ANTICANCER ACTIVITY OF GADOLINIUM DIPICOLINATE

INTRODUCTION

4.1 Lanthanide Oxo-pyridinium or Hydroxy-pyridine Complexes

Lanthanide metal ions are hard acids and are known to form complexes with numerous ligands, mostly with hard donor centres like oxygen or nitrogen. The normal oxidation state of lanthanides is +3 [*Note*: Bismuth also has a stable +3 oxidation state, see Chapter 1]. The coordination number in most cases is more than six and the geometry around the metal centre is difficult to predict *a priori*. Lanthanide complexes with *O*-donor ligands are more numerous than those with other donor atoms and hence lanthanides are called 'oxophilic'. The compounds 2-hydroxy pyridine (2-HOPy) (4.**1**) and 4-hydroxy pyridine (4-HOPy) (4.**2**) constitute an interesting set of ligands because the coordination can occur *via* the nitrogen or oxygen subsequent to the proton shift to nitrogen or by complete deprotonation in the presence of a base (Scheme 4.1). 4-Hydroxypyridine is also bioactive and is known to inhibit photosystem II in plants;[1] some of its derivatives act as vasodilators.[2] In the case of deprotonated 2-hydroxypyridine, both chelation and bridging are possible while for deprotonated 4-hydroxypyridine, only bridging mode is possible. Several of these have been realized synthetically but interestingly it is also possible to have *O*-coordination or covalent bond formation via forms 4.**1'** or 4.**2'**. The different structural types are exemplified by compounds 4.**3**-4.**7** [Fig. 4.1][3-10] and also in the trinuclear clusters $[Fe_3(\mu_3\text{-}O)(\mu_2\text{-}CH_3COO)_6(C_5H_5NO)_2(H_2O)]ClO_4.nH_2O$ (n = 3, 4; C_5H_5NO = 2-pyridone).[11] Compound 4.**4** represents *O*-coordination after proton shift. The palladium and platinum complexes 4.**4a-b** as well as the iron complex 4.**6** of 4-hydroxypyridine are assigned *N*-coordination while the X-ray structure of compound 4.**7** shows *O*-coordination; the deprotonated ligand shows both *N*- and *O*-coordination in the tin complex 4.**5**. Some complexes of lanthanides including those of dysprosium and gadolinium with *O*-coordination are also known.[12]

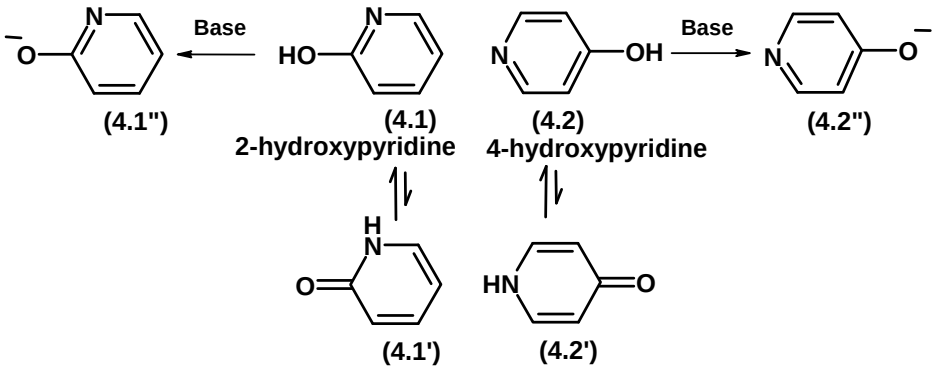

Scheme 4.**1**

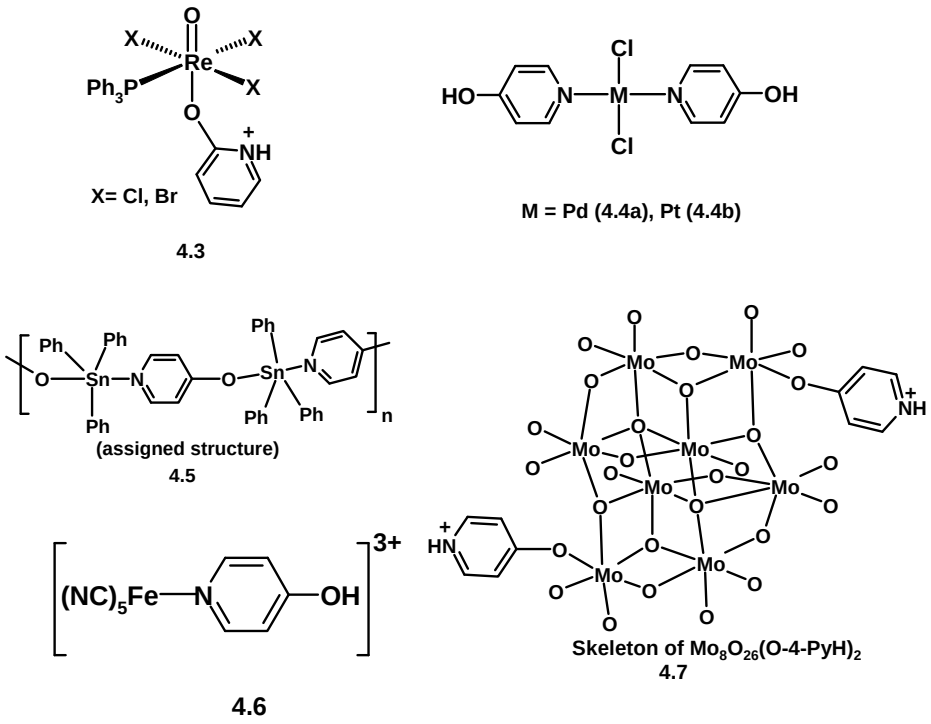

Figure 4.1. Different structural types of 2-hydroxy and 4-hydroxy pyridine complexes

Das and coworkers have made an interesting observation on water clusters that involves the loss/ gain (from atmospheric water vapour) of water molecules in several transition metal complexes of 2-hydroxy pyridine.[13] Among them, the Fe_3 cluster-containing compound $[Fe_3(\mu_3\text{-}O)(\mu_2\text{-}CH_3COO)_6(C_5H_5NO)_2(H_2O)]ClO_4.4H_2O$ is having 2-pyridone ligands coordinating through neutral oxo donor atoms to two Fe(III) centres.

4.1.1 4-Hydroxy pyridine or 4-pyridone-heterometallic complexes

Reaction of $Cu(OAc)_2$, 4-(1H)-pyridone and Dy(III) or Gd(III) nitrate in MeOH results in the formation of the heterometallic complexes $[Cu_2LnL_2(LH)_2(NO_3)(OH)_4\ xH_20]$, [Ln = Dy (4.**8**) or Gd (4.**9**), L = 4-(1H)-pyridone].[14] Reaction of $Cu(OH)_2$ with 4-(1H)-pyridone and $Dy(NO_3)_3$ in DMF results in the formation of the heterometallic compound $[Cu_2DyL_2(LH)_2(NO_3)_2(OH)_3DMF]$ (4.**10**). Due to the poor solubility in organic solvents, single crystals were not obtained. On the basis of the physico-chemical studies, different structures are tentatively proposed. It seems that lanthanide ions are coordinated to eight oxygen atoms, two from deprotonated 4-pyridone units, two from neutral pyridone ligands, two from a bidentate nitrate anion and two from hydroxyl anions. However, no conclusion could be made as to which structure is correct, since molar conductivity measurements are unattainable due to the insolubility of these complexes.

4.1.2 4-Pyridone- complexes with Gadolinium and Dysprosium

Goodgame *et al* reported the synthesis and crystal structures of $[DyL_4(NO_3)_2](NO_3)$ (4.**11**) and $[GdL(NO_3)_3(H_2O)].CH_3OH$ (4.**12**) [L = 4-(1H)-pyridone].[12] In compound 4.**11**, the dysprosium ion is eight-coordinate with a distorted dodecahedral coordination geometry. All four pyridone nitrogen atoms are involved in intermolecular hydrogen-bonding. The X-ray structural analysis of gadolinium complex (4.**12**) shows that this compound has a structure quite different from that of the dysprosium complex 4.**11**. In 4.**12**, dimers are formed in which pairs of Gd(III) ions are linked by two nitrate bridges. Each bridging nitrate binds in bidentate fashion to one Gd(III), but one of the coordinated nitrate oxygen atoms additionally adopts a binucleating role and bonds to the second Gd(III) ion, thus producing a Gd_2O_2 ring. Each gadolinium ion is further bonded to two pairs of oxygen atoms from bidentate but nonbridging nitrate groups, one pyridone oxygen atom and a water molecule. Each Gd(III) is thus nine-coordinate. All the available hydrogen bonding donors are involved in intermolecular bonding interactions.

4.2 Lanthanide Pyridine-2,6-dicarboxylic Acid Complexes

Among the O,N-ligands, pyridine carboxylic acids are very well known to coordinate to metals in a chelate fashion to form stable complexes. These carboxylic acids are biocompatible, soluble in water (most of them) and not so expensive. Pyridine-2,6-dicarboxylic acid (4.**13**) is a ligand with 5-coordinating centres.[15] Various coordination modes of this ligand are shown in Figure 4.2.

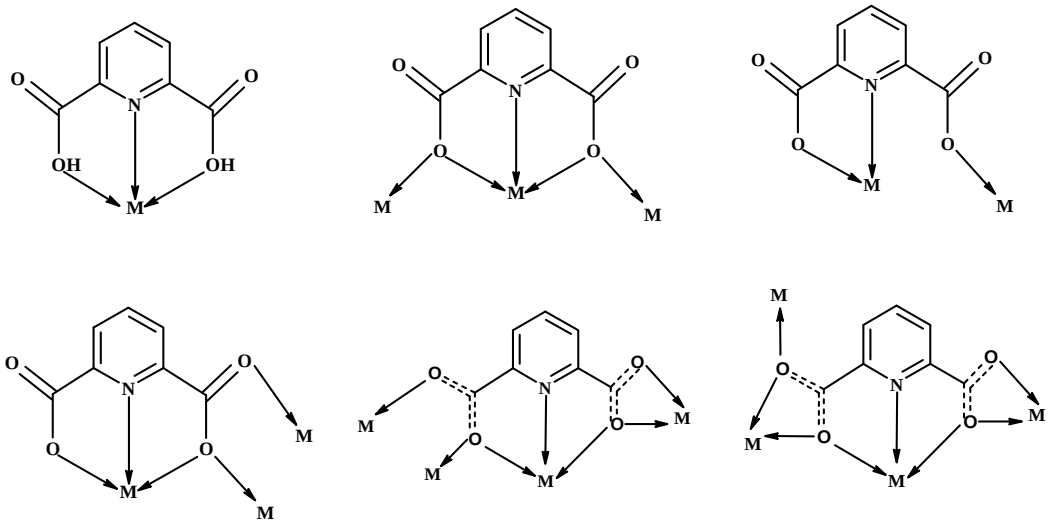

Figure 4.2. Various coordination modes observed in metal complexes of pyridine-2,6-dicarboxylic acid.

Bharadwaj and coworkers reported the synthesis of linear coordination polymers with lanthanides and pyridine-2,6-dicarboxylic acid under hydrothermal conditions. $[Pr(pdc)(pdcH)_2H_2O]0.4H_2O$ (4.**14**) $[Ce(pdc)(pdcH)_2H_2O]0.4H_2O$ (4.**15**) are the two structures in which hexameric water clusters join these linear chains through bonding to the metal ions (Fig. 4.3).[16] Other coordinated water and the carboxylate oxygen form an intricate array of hydrogen bonding resulting in a 3D network where each metal ion shows 9-coordination with an approximate *D*3 symmetry. The structure of each metal organic framework (MOF) consists of linear chains of M(III) ions where each metal ion shows 9-coordination binding two pdc^{2-} ligands, one bridging carboxylate O atom from a neighbour and two water molecules.

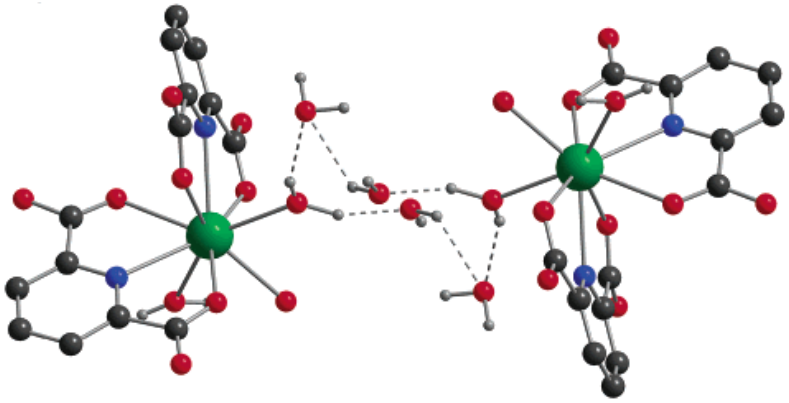

Figure 4.3. A view of the hexameric water cluster connecting two Pr(III) ions [cf. ref. 16]. C = black, H = grey, N = blue, O = red, Pr = green.

Brouca-Cabarrecq and coworkers reported the synthesis of three lanthanide dipicolinates of the formula $(CN_3H_6)_3[La(C_7H_3NO_4)_3]$ $3H_2O$ (4.**16**) $(C_4N_2H_{12})_{1.5}[Ce(C_7H_3NO_4)_3]$ $7H_2O$ (4.**17**) and $[Eu(C_7H_4NO_4)_3]_2$ $2.5H_2O$ (4.**18**).[17] Three complexes are zero dimensional structures with lanthanides being linked through dipicolinate groups. Each lanthanide is surrounded by three dipicolinic groups in the usual tridentate mode: two oxygen atoms pertaining to the two carboxylate functions and one nitrogen atom chelate the central Ln(III) (Fig. 4.4). In compounds 4.**16** and 4.**17**, each dipicolinate is nonprotonated and charge balance is maintained by the presence of guanidinium and piperazinium cations. In the structure of 4.**18**, the three-dipicolinic groups surrounding each Eu(III) are either unprotonated or one- and two-times protonated and so the entity is neutral.

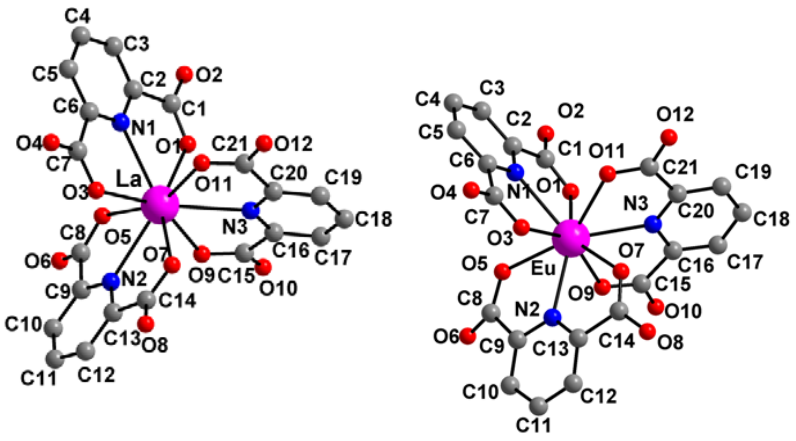

Figure 4.4 View of the molecular entity of (a) lanthanum in $(CN_3H_6)_3[La(C_7H_3NO_4)_3].3H_2O$ (4.**16**) and (b) europium in $[Eu(C_7H_4NO_4)_3]_2.2.5H_2O$ (4.**18**) [Redrawn using data from ref. 17].

Guerriero *et al* reported the synthesis of lanthanide dipicolinates of the formula $Na_3[Ln\ (pdc)_3]\ nH_2O$ and $[Ln(pdc)(Hpdc)]\ mH_2O$ (n = 5-10; m = 5-8) by the reaction of $Ln(NO_3)_3\ nH_2O$ [Ln = La, Gd, Dy] and pyridine-2,6-dicarboxylic acid [H_2pdc] in the presence of sodium hydroxide.[18] In each asymmetric unit, two dipicolinate ions are chelated to the metal ion through the nitrogen and two carboxylate oxygens and one of them links a further Ln(III) ion by a multidentate bridging bond with one remaining carboxylate oxygen. Sobolev and coworkers reported europium dipicolinate compound of the formula $(C_8H_{20}N)_3[Eu(C_7H_3NO_4)_3].4H_2O$ (4.**19**) as a tetraethylammonium salt. Eu(III) is bound with nine-coordination to six O- and three N-donor atoms of the ligands. Water molecules within the lattice are found sufficiently close to the uncoordinated dipicolinate O atoms to justify the postulation of hydrogen-bonding interactions.[19a] Extensive hydrogen-bonding interactions between the NH groups of the cations and the carboxylate O atoms of the anions in these salts may explain both the high lattice energy, which is reflected in low solubility, and the luminescence quenching.[19b]

Liu *et al* reported the structural details of samarium dipicolinate compound of the formula $[Sm(C_7H_3O_4)(C_7H_4O_4)(H_2O)_2]\ 4H_2O$ (4.**20**) in which pyridine-2,6-dicarboxylate ligand chelates to the Sm(III) and also bridges to the neighbouring Sm ions to form infinite chains along the c axis.[20] The asymmetric unit of (4.**20**) is composed of one Sm(III) ion, one $PydcH^{-1}$, one $Pydc^{2-}$ ligand, two coordinated water molecules and four water molecules of crystallization. Atom Sm1 is coordinated by $pydcH^-$ (atoms O1, N1 and O3), $pydc^{2-}$(O6, N2 and O7), and two aqua ligands (O9 and O10); the Sm atom is also bonded to one bridging O5 atom from a neighbouring $pydc^{2-}$ ligand, giving an overall nine-coordination [Fig. 4.5 (Top)]. The $pydc^{2-}$ group chelates to the Sm(III) ion and bridges to the neighbouring Sm(III)' ion, forming an infinite chain along the c axis [Fig. 4.5 (Bottom)]. Two neighbouring chains are linked to form a ladder-like band through O—H···O hydrogen bonds. The ladder-like bands form a layer structure parallel to (100) plane by hydrogen bonds with the uncoordinated water molecules, and adjacent layers are linked together through hydrogen bonds, resulting in a three-dimensional framework.

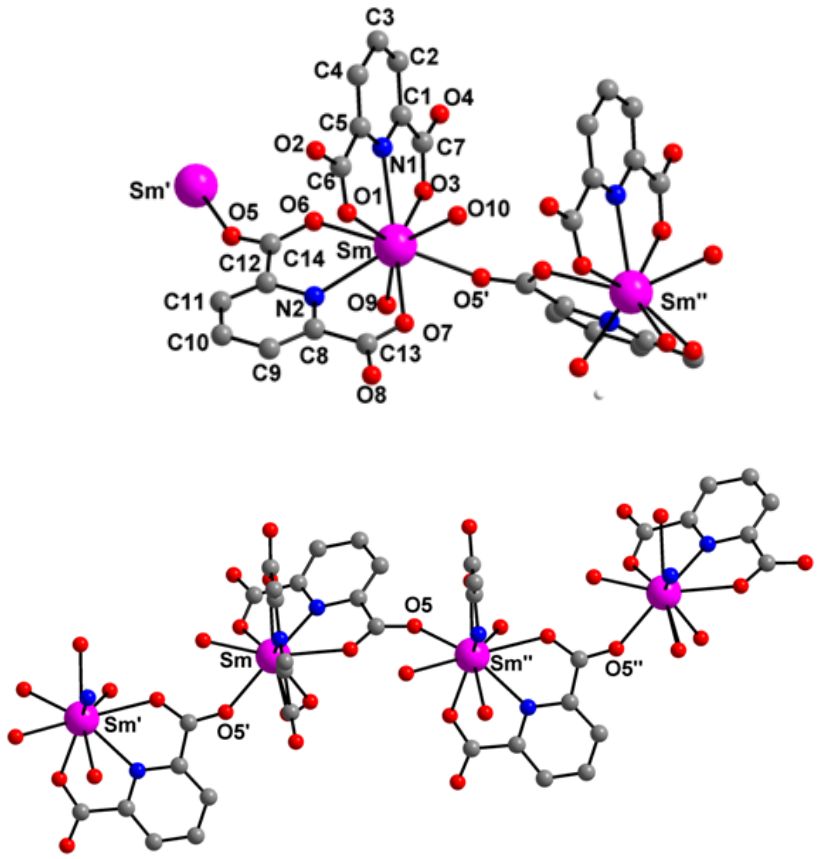

Figure 4.5. Top: The structure of 4.**20**. Bottom: The infinite chain along the *c* axis [Redrawn using data from ref. 20]

4.3 Lanthanide-Transition Metal Heterometallic Pyridine-2,6-dicarboxylic acid Complexes

A significant number of three-dimensional (3D) coordination polymers with well defined pores find applications in catalysis, gas storage, chemical separation, and ion exchange.[21-24] Zhao *et al* reported coordination polymers $\{[Ln(dipic)_3Mn_{1.5}(H_2O)_3]\cdot nH_2O\}_\infty$ [Ln = Pr, n = 2 (4.**21**); Ln = Gd, n = 3.5 (4.**22**); Ln = Er, n = 3 (4.**23**) through hydrothermal synthesis.[25] All these polymers crystallised in the hexagonal crystal system and the crystal structure is built up of two distinct types of building blocks, $Ln(dipic)_3$ and $MnO_4(H_2O)_2$ (Fig. 4.6**)**. The Ln(III) ion is coordinated by three tridentate (ONO) dipic anions, for which each carboxy group coordinates through one oxygen atom. Three N atoms and six O atoms complete the coordination sphere of the Ln(III) centre, which conforms most closely to a tricapped trigonal prism. The coordination geometry around Mn(II) centre is a slightly distorted octahedron, the equatorial plane of which comprises

four O atoms from the carboxy groups of the 2,6-dipicolinate molecules that are chelated to four neighboring Ln(III) centres; two water molecules occupy the remaining apical coordinate sites. There are three crystallographically independent 2,6-dipicolinate moities in the structure, each with the same coordination mode, i.e. chelation to one Ln(III) ion and linkage to two Mn(II) ions. One oxygen atom from a carboxyl group bonds to a Ln(III) centre and the other oxygen atom bonds to a Mn(II) centre; thus each Ln(III) centre has six Mn(II) ions as the nearest metal centres, while the Mn(II) centre has four Ln(III) ions in its vicinity (Fig. 4.6), as is consistent with the Mn:Ln molar ratio.

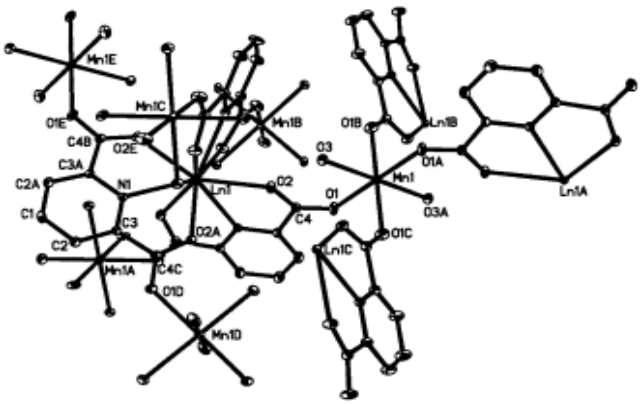

Figure 4.6. Diagram showing the two building units with atom labels of the Mn–Ln series [cf. ref. 25].

Prasad and Rajasekharan reported the heterometallic coordination polymers of dipicolinic acid (dipicH_2) containing Ce(IV) and Zn/Cd cations namely $[Zn(H_2O)_4Ce(dipic)_3]$ $8H_2O$ (4.**24**), $[Zn\text{-}(CH_3OH)_2(H_2O)_2Ce(dipic)_3]\cdot 3H_2O$ (4.**25**), $[Zn(CH_3CH_2OH)(H_2O)_3Ce(dipic)_3]$ $2CH_3CH_2OH\cdot 2H_2O$ (4.**26**), $[Cd(H_2O)_4Ce(dipic)_3][Ce\text{-}(dipic)(dipicH)_2]\cdot 24H_2O$(4.**27**), $[Cd(CH_3OH)_2(H_2O)_2Ce(dipic)_3]$ $3H_2O$ (4.**28**), and $[Cd(H_2O)_4Ce(dipic)_3]$ $3H_2O$ (4.**29**).[26] In compound 4.**24**, Ce(IV) is nine coordinate with a distorted tricapped trigonal prismatic geometry and Zn(II) has a distorted octahedral geometry. The polymeric chain is made up of alternating units of $[Ce(dipic)_3]^{2-}$ and two crystallographically unique $[Zn(H_2O)_4]^{2+}$ groups, situated on inversion centres and linked on either side by coordination through carbonyl oxygen atoms of two different dipicolinate ligands. Structure of $[Zn\text{-}(CH_3OH)_2(H_2O)_2Ce(dipic)_3]\cdot 3H_2O$ (4.**25**) is similar to 4.**24** except that only one unique Zn(II) ion situated on an

inversion centre with two of the four coordinated water molecules replaced by methanol molecules. Compound $[Zn(CH_3CH_2OH)(H_2O)_3Ce(dipic)_3]$ $CH_3CH_2OH{\cdot}2H_2O$ (4.**26**) differs from 4.**24** and 4.**25** in having two different zinc coordination polyhedra, one having four water molecules as terminal ligands and the other with two water molecules and two ethanol molecules. The polymeric part in $[Cd(H_2O)_4Ce\text{-}(dipic)_3]$ (4.**27**) is exactly similar to the chain in compound (4.**24**) except that Cd replaces Zn. The main difference is the presence of a free $[Ce(dipic)_2(dipicH_2)]$ molecule and 24 lattice–water molecules. The structure of $[Cd(CH_3OH)_2(H_2O)_2Ce(dipic)_3]$ $3H_2O$ (4.**28**) is very similar to that of 4.**25** with Zn replaced by Cd. The coordination environment in compound $[Cd(H_2O)_4Ce(dipic)_3]$ $3H_2O$ (4.**29**) is similar to that of 4.**25** and 4.**27**. The difference is only in the number of lattice–water molecules.[26]

4.4 Medicinal Importance of Lanthanide Compounds

Biomedical inorganic chemistry is an important area of chemistry. It offers the potential for the design of novel therapeutic and diagnostic agents and hence for the treatment and understanding of diseases which are currently intractable.[27-30] Many biological properties of the lanthanides are a function of their similarity to calcium.[31,32] One of the major physiological effects of the Ln(III) is to block both voltage operated and receptor operated calcium channels.[33] The Ln(III) can block the Na^+/Ca^{2+} synaptic plasma membrane exchange and inhibit skeletal, smooth and cardiac muscle contraction by blocking the Ca^{2+}-ATPase in the sarcoplasmic reticulum of muscle. The Ln(III) ions themselves are unable to cross cell membranes but act by blocking the exterior face of the calcium channel. Despite this difficulty, the Ln(III) have been used as biochemical probes to study calcium transport in mitochondria and other organelles. They can substitute for calcium in proteins,[32] though it should be noted that the Ln(III) can also substitute for other metal ions such as Mg(II), Fe(III) and Mn(II). Calcium dependent enzymes can either be inhibited by lanthanides or in some cases be activated to a similar or greater extent than by calcium. Generally the lanthanides are non-toxic, primarily because they cannot cross cell membranes and are therefore not absorbed if ingested orally. However, they are toxic if administered by the intravenous route where upon they can gain access to cells expressing calcium channels. Chelate such as Gd(DTPA), which is used as an NMR contrast imaging agent, is 50 times less toxic than $GdCl_3$

on a molar basis. It is rapidly cleared with a plasma half-life of 20 minutes and within 3 hours over 80% is excreted in the urine. This is in contrast to $GdCl_3$ where only 2% is excreted after 7 days. This emphasizes two important points when considering metal toxicity and pharmacology. The first is that the biochemical and physiological effects are dependent upon the chemical form and speciation of the metal, e.g. oxidation state, salt or complex. The second, more general, point is that toxicity is dependent upon the route of exposure.[34]

Magnetic resonance imaging (MRI) has become an important technique in modern diagnostic medicine, providing high-quality three-dimensional images of soft tissue without the need for harmful ionizing radiation.[35] Gadolinium (III), with its high magnetic moment and long electron spin relaxation time, is an ideal candidate for such a proton relaxation agent and is the most widely used metal centre for such purposes.[36,37] Free Gd(III) is toxic (LD_{50}=0.2 $mmolkg^{-1}$ in mice)[38] and must therefore be administered in the form of stable chelate complexes that will prevent the release of the metal ion *in vivo*. For these reasons, the development of ligands that are suitable for production of high-relaxivity agents with favorable properties for imaging applications remains an important goal. Lanthanide complexes have found a role in cancer treatment as contrast imaging agents such as Gd(III)-DTPA which is commonly used for MRI imaging of tumors.[36,39-40] One group of lanthanide complexes that has progressed into clinical trials is the texaphyrins.[41] Recently a redox active gadolinium texaphyrin complex has entered phase III clinical trials for the treatment of brain metastases of lung cancer. The Gd-texaphyrin complex, motexafin gadolinium (MGd, Xcytrin; Fig. 4.7) has been investigated and exploited as a radio- and chemo-sensitizer for cancer treatment based on its unique redox properties. Using pulse radiolysis it was shown that MGd can accept electrons from radicals including O_2^{2-} and also aquated electrons in the medium, resulting in reduction of the MGd complex.[41]

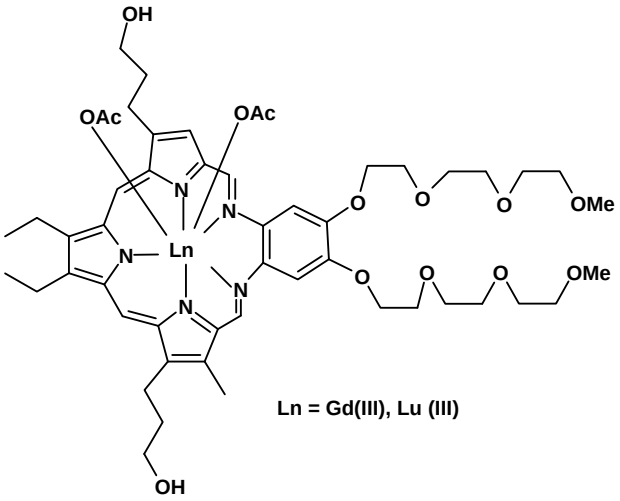

Figure 4.7. The structure of motexafin gadolinium (MGd, Xcytrin)

MGd contains the paramagnetic Gd ion in its central cavity and is detectable by magnetic resonance imaging (MRI).[42-43] Pre-clinical studies have shown that MGd localizes to tumor cells and enhances the efficacy of radiation and chemotherapy in tissue culture and in animal tumor models.[43–46] Lanthanides are able to inhibit calcium fluxes, required for cell cycle regulation, but they cannot substitute for calcium or other metal ions such as Mg(II), Fe(III) and Mn(II) in proteins, leading to the inhibition of their functions.[47-48] The tumor-inhibiting activity of lanthanum is considerably enhanced by complexation with various ligands such as phenanthroline.[49] The lanthanide complex tris(1,10-phenanthroline)tris(thiocyanato)lanthanum(III) (KP772; Figure 4.8) exerts potent activity against a wide range of tumor cell lines *in vitro* and a colon carcinoma xenograft model *in vivo* with properties comparable to cis-platin and methotrexate.[50]

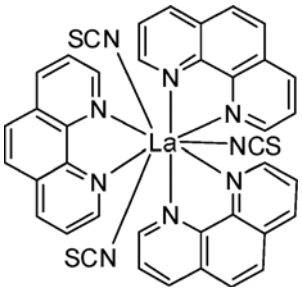

Figure 4.8. Structure of tris(1,10-phenanthroline)tris(thiocyanato-)lanthanum(III) (KP772).

4.5 Mixed Metal Pyrophosphates involving Lanthanides

Phosphate matrix is a good host for lasing ions both in crystalline and glassy states due to excellent transparency and good mechanical and thermal stabilities. They find applications in ultrafast switches and laser induced gratings.[51] The luminescence properties of doped ions (M) depend on the ionic nature of M-O bond in the parent lattice. This is achieved in phosphates in which the strong covalency of P-O bond induces an ionic M-O bond. Such a covalent P-O network is present in layer like structures of pyrophosphates.[52] Some pyrophosphates and their solid solutions are known to exhibit isotropic negative thermal expansion behaviour in the appropriate temperature intervals.[53] There are only limited reports on mixed lanthanide-(other) metal pyrophosphates that may possess useful optical properties. In the present work, attempts to investigate this aspect are made.

OBJECTIVES OF THE PRESENT WORK - PART B

The main objective of this part of the present work is to develop lanthanide oxopyridinim and lanthanide dipicolinate chemistry. In addition, it was planned to explore mixed metal pyrophosphates. Specifically, it was intended to investigate the following:

(i) Synthesis and structural characterization of new crystalline lanthanide oxopyridinium complexes using lanthanide nitrates and 4-hydroxypyridine,

(ii) Synthesis and anticancer activity of new lanthanide dipicolinate complexes through a simple route (non- hydrothermal), and

(iii) Methods for the synthesis of lanthanide(III)-zinc(II) pyrophosphates $Ln_{2/3}ZnP_2O_7$.

RESULTS AND DISCUSSION

5.1 General Comments on Lanthanide Hydroxypyridine/Pyridone Complexes

As mentioned in Chapter 4, the ligands 2-hydroxy and 4-hydroxypyridines [2-HOPy (**1**) and 4-HOPy (**2**)] constitute an interesting set of ligands because the coordination can occur via the nitrogen or oxygen subsequent to the proton shift to nitrogen or by complete deprotonation in the presence of a base. We were curious to know the nature of binding of these hydroxypyridine ligands in greater detail towards the lanthanide ions which are hard Lewis acids and hence preferentially coordinate through the oxygen.[54]

5.2 Synthesis and Spectral Data of Lanthanide-4-Hydroxy pyridine Complexes

Synthesis of the lanthanide hydroxypyridine compounds [M(4-O-$C_6H_4NH)_3(NO_3)_2(H_2O)_2][NO_3]$ {M = La (**3**), Ce (**4**), Pr (**5**), Nd (**6**), Eu (**7**) and Gd (**8**)} was accomplished by the simple reaction of the corresponding nitrates with three mole equivalents of 4-hydroxypyridine in ethanol or water. Depending on the solvent, crystallization occurs in 2-3 days (ethanol) or 7-8 days (water) upon slow evaporation of the solvent at room temperature (20-25 ^oC). The lanthanum compound **3**, although is isostructural to **4-5** or **7-8**, has a much higher melting point than rest of the compounds. UV-visible bands of these compounds are in the expected region;[55,56] there was no significant change between the solid state and solution state spectra. The europium compound **7** exhibited fairly strong emission bands at 590, 620 and 695 nm at room temperature upon excitation at 393 nm (Fig. 1); the decay profiles of both $Eu(NO_3)_3.5H_2O$ and compound **7** are overlapping which indicates similar lifetime for both (nearly 110 μs; Fig. 2).[57]

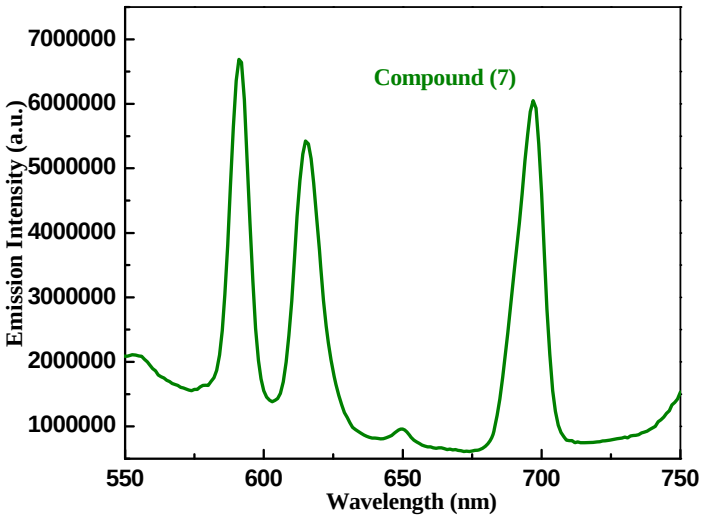

Figure 1. Emission spectrum of **7**.

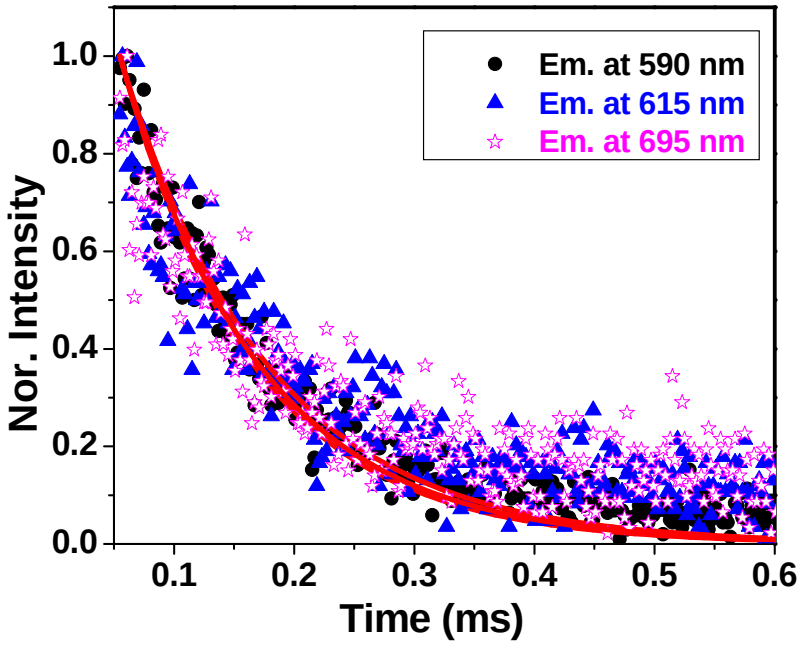

Figure 2. Fluorescence decay (normalized) curves for compound **7** (concentration 10^{-3}M) for the bands at 590, 615 and 695 nm.

The magnetic susceptibilities of the isolated compounds are consistent with those available in the literature.[55] The ^{13}C NMR spectrum (D_2O) of the lanthanide complex **3** showed resonances at δ 116.7, 139.3 and 180.4; these values are within 0.3 ppm of the corresponding values for 4-hydroxypyridine. The ^{1}H NMR spectrum of the ligand showed two peaks δ 6.43 and 7.73 [^{3}J(HH) = 7.2 Hz]. In compound **3**, these were shifted marginally to δ 6.50 and 7.79, but the shift was larger in the case of the cerium compound **4** [δ 7.07 and 8.00].

5.3 Crystal Structures of Lanthanide 4-Hydroxy-pyridine Complexes

All the compounds **3-8** crystallised in the chiral space group $P2_12_12_1$. In the case of **4-5** and **7-8**, the structures could be solved and refined readily by taking the coordinates of one and changing the corresponding lanthanide during the refinement. This was done in an effort to have consistent set of bond parameters for structural comparison. In the case of the neodymium compound **6**, however, the Flack parameter suggested that the stereochemistry had to be reversed and hence the refinement was done after taking care of this point. The structure of **3** was solved and refined independently, because of slight difference in the H-bonding between this and the rest of the compounds. Molecular structures of the representative compounds **6** and **7** are shown in Figure 3, while the polyhedral representations are shown in Figure 4. The bond distances are shown in Table I.

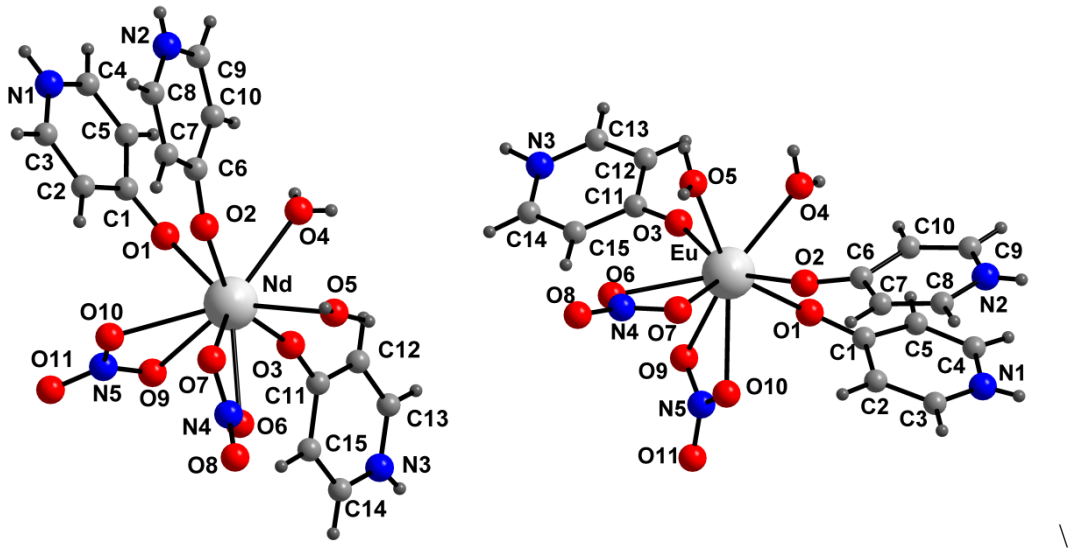

Figure 3. Molecular structures of the cationic part in **6** (left) and **7** (right); the anion is nitrate (not shown). Only non-hydrogen atoms are labeled.

Table I. Bond distances (Å) in compounds **3-8**.[a]

Compd	**3**	**4**	**5**	**6**	**7**	**8**
M-O1	2.493(3)	2.475(5)	2.452(5)	2.436(4)	2.400(2)	2.392(4)
M-O2	2.396(3)	2.376(5)	2.348(5)	2.344(4)	2.303(2)	2.309(3)
M-O3	2.358(3)	2.320(5)	2.297(5)	2.314(4)	2.272(2)	2.276(4)
M-O4	2.567(3)	2.538(6)	2.512(6)	2.512(5)	2.468(2)	2.453(5)
M-O5	2.529(3)	2.510(6)	2.499(5)	2.476(4)	2.445(2)	2.432(4)
M-O6	2.673(3)	2.643(5)	2.617(5)	2.610(4	2.573(2)	2.564(4)
M-O7	2.621(3)	2.591(6)	2.565(5)	2.568(5)	2.528(2)	2.518(4)
M-O9	2.661(3)	2.638(6)	2.629(5)	2.615(4)	2.593(2)	2.589(4)
M-O10	2.692(3)	2.666(6)	2.654(5)	2.632(4)	2.597(2)	2.590(4)

[a]We have also collected the data for the similar dysprosium compound but the quality of the data was poor; the structure was solved and refined independently. The relevant bond Dy-O distances are 2.366(13), 2.277(12), 2.237(13), 2.432(14), 2.42(2), 2.546(13), 2.510(14), 2.547(15) and 2.567(16) Å.

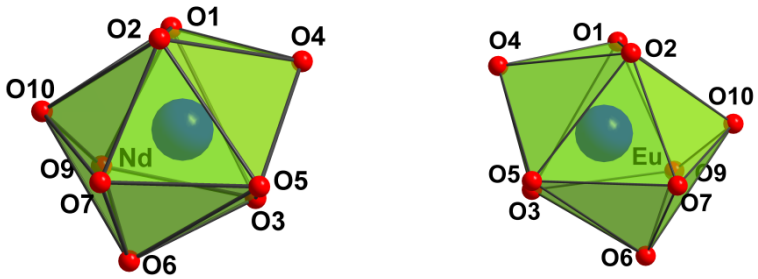

Figure 4. Polyhedral representation around the central atom in **6** (left) and **7** (right) showing the opposite stereochemistry.

As is evident from the structures, the coordination to the lanthanide ion occurs via the phenolate oxygen rather than the nitrogen atom. It should be noted here that the ligand is a neutral one with the proton relocated on the pyridine nitrogen. This type of ligation is consistent with the relatively hard acidity exhibited by the Ln(III) ions. Based on density functional molecular orbital calculations, Chen and Donnenberg have recently reported that the pyridone structure for the ligand is only marginally less stable (by ca 2.4 kcalmol^{-1}) than the phenolic structure **2**,[58] there is also crystallographic evidence to suggest that 4-pyridone molecule does

exist.[59,60] These data are in agreement with the *O*-bonded structures as observed by us in this study. The M-O bond distances are in the normal range expected for this set of compounds,[61,62] but the mean distances are in the order M-O(pyridone)<M-O(water)<M-O(nitrate) in all the six structures studied here. There is a subtle but clear-cut tendency for lower mean M-O bond lengths in the series La^{3+}>Ce^{3+}> Pr^{3+}> Nd^{3+}> Eu^{3+}> Gd^{3+} as expected from lanthanide contraction. This difference from La (III) to Gd (III) is about 0.1 Å.

One of the interesting features in these structures is the reversal of stereochemistry between the structures of the neodymium compound **6** and the europium compound **7** (as well as **3-5**) [see Fig. 3]. Since each of these structures is in a chiral space group, this appears to be a case of spontaneous resolution.[63] The other enantiomer of **6** or **7** might have been there in solution or as crystals but we could not identify them separately because of similar morphology of the crystals. The geometry around the metal in each case can be described as tricapped trigonal prism; this is different from the distorted dodecahedral geometry in [Dy(4-O-$C_6H_4NH)_4((NO_3)_2][NO_3]$.[10] The difference is probably related to the steric factors associated with the additional pyridone ligand in the latter compound.

In all the compounds studied here, there is extensive hydrogen bonding leading to a helical motif. The coordinated water molecules [corresponding to O4 and O5] are hydrogen bonded to either pyridone [O1] or nitrate [O13, O9, O12] oxygen atoms while the pyridine nitrogen atoms [N1, N2, N3] are hydrogen bonded only to the nitrate oxygen atoms [O7, O8, O11, O14]. The hydrogen bonding leads to eight as well as ten-membered motifs; the eight-membered ring motif is found between consecutive metal atoms (Fig. 5) The hydrogen bonding situation is similar in all the other cases including that of the lanthanum complex **3**. Hydrogen bond parameters are presnt in Table II.

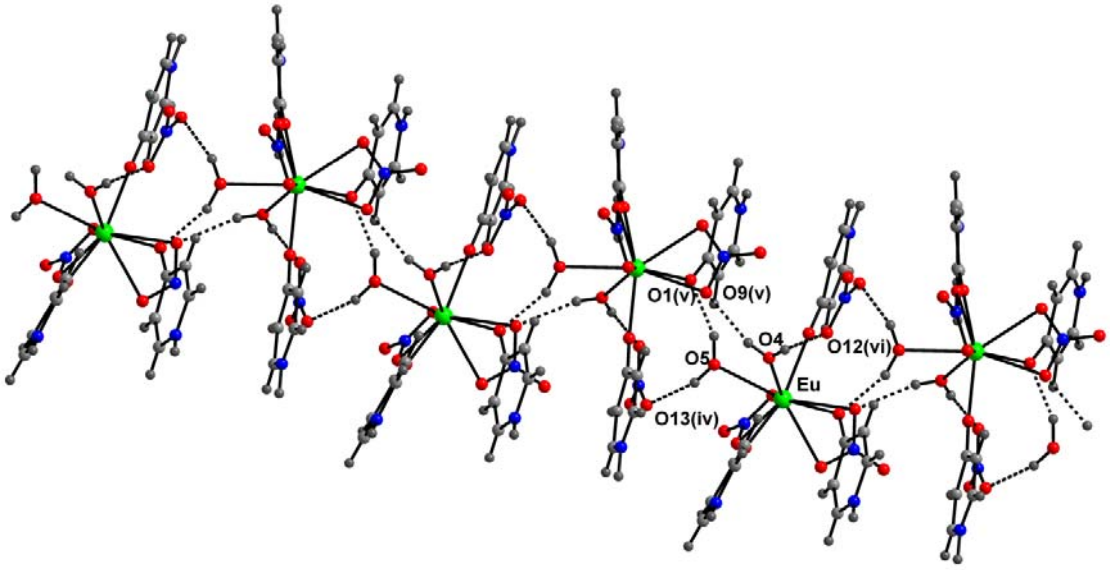

Figure 5. A diagram showing hydrogen bonding interactions (excluding those with the N-H protons) and the helical motif involving the coordinated water molecules in compound **7**. Hydrogen bond parameters (Å, °): N(3)-H(3A)…O(14^{i}) 1.05(5) 1.93(5) 2.931(4) 157(4); N(2)-H(2A)…O(8^{i}) 0.81(5) 2.23(5) 2.975(4) 153(5); N(2)-H(2A)…O(7^{i}) 0.81(5) 2.60(5) 2.996(4) 112(4); N(1)-H(1A)…O(11^{ii}) 0.83(4) 2.27(4) 2.975(4) 144(4); N(1)-H(1A)…O(8^{iii}) 0.83(4) 2.39(4) 2.984(4) 130(4); O(5)-H(5B)…O(13^{iv}) 0.918(10) 2.008(16) 2.893(3) 161(3); O(5)-H(5A)…O(1^{v}) 0.912(10) 1.929(19) 2.777(3) 154(3); O(4)-H(4A)…O(9^{v}) 0.81(4) 2.08(4) 2.872(3) 166(4); O(4)-H(4B)…O(12^{vi}) 0.76(4) 2.04(4) 2.788(4) 174(4). Symmetry codes: (i) 1-x, y-1/2, 1/2-z; (ii) -x, y-1/2, 1/2-z; (iii) 1/2-x, 1-y, 1/2+z; (iv) x, y, -1+z; (v) 1/2+x, 1/2-y, -z; (vi) x-1/2, 1/2-y, 1-z.

Table II: Hydrogen bond parameters in compounds **3-8**

Compd	H-bond	D-H (Å)	H…A (Å)	D…A (Å)	D-H…A (°)	Symm. of acceptor
3	O4 H4A O9	0.90(2)	2.09(4)	2.829(4)	139(4)	3_655
	O4 H4B O12	0.88(2)	1.94(3)	2.772(5)	156(4)	3_655
	O5 H5A O1	0.90(2)	1.90(3)	2.751(4)	157(4)	3_655
	O5 H5B O13	0.92(2)	1.96(3)	2.868(5)	171(4)	1_565

	N2 H2A O8	0.86	2.18	2.980(5)	153.9	4_465
	N1 H1A O11	0.86	2.25	2.960(5)	140.5	4_455
	N1 H1A O8	0.86	2.35	2.990(5)	131.2	2_664
	N3 H3A O14	0.86	2.11	2.947(6)	162.8	4_456
	N3 H3A O12	0.86	2.47	3.100(7)	130.6	4_456
4	N3 H3A O14	0.85(8)	2.12(8)	2.938(10)	160(7)	3_645
	N2 H2A O8	1.05(13)	2.24(13)	2.954(9)	123(10)	3_645
	N2 H2A O7	1.05(13)	2.38(14)	2.970(9)	114(10)	3_645
	N1 H1A O11	0.74(10)	2.34(11)	2.956(9)	143(11)	3_545
	N1 H1A O8	0.74(10)	2.43(10)	2.972(9)	132(10)	2_565
	O5 H5B O13	0.905(10)	2.04(5)	2.876(10)	153(9)	1_554
	O5 H5A O1	0.905(10)	1.89(4)	2.744(8)	156(9)	4
	O4 H4B O12	0.77(12)	2.03(12)	2.795(10)	172(12)	4_456
	O4 H4A O9	0.96(13)	1.89(13)	2.844(9)	173(9)	4
5	N3 H3A O14	0.72(12)	2.27(12)	2.934(11)	156(12)	3_645
	N2 H2A O8	1.04(13)	2.07(13)	2.958(9)	142(11)	3_645
	N2 H2A O7	1.04(13)	2.33(13)	2.986(9)	120(9)	3_645
	N1 H1A O11	0.83(9)	2.28(9)	2.948(10)	138(8)	3_545
	N1 H1A O8	0.83(9)	2.38(9)	2.968(9)	129(8)	2_565
	O5 H5B O13	0.902(10)	2.06(5)	2.866(9)	148(8)	1_554
	O5 H5A O1	0.902(10)	1.91(4)	2.750(7)	154(7)	4
	O4 H4B O12	0.75(10)	2.07(11)	2.785(9)	160(12)	4_456
	O4 H4A O9	0.62(11)	2.27(11)	2.859(8)	161(14)	4
6	O4 H4A O9	0.67(7)	2.18(7)	2.853(6)	172(10)	4_467
	O4 H4B O12	0.79(7)	2.00(7)	2.787(7)	168(8)	4_566
	O5 H5A O1	0.905(10)	1.93(3)	2.774(6)	154(5)	4_467
	O5 H5B O13	0.902(10)	2.15(5)	2.885(7)	139 (6)	1_556
	N1 H1A O8	0.85(6)	2.40(7)	2. 983(8)	127(6)	2_664

	N1 H1A O11	0.85(6)	2.25(7)	2.971(8)	143(6)	3_756
	N2 H2A O7	0.74(8)	2.55(8)	3.003(8)	121(8)	3_656
	N2 H2A O8	0.74(8)	2.29(8)	2.988(8)	157(9)	3_656
	N3 H3A O14	0.78(7)	2.20(7)	2.948(9)	161(7)	3_656
7	O4 H4A O9	0.81(4)	2.08(4)	2.872(3)	166(4)	4
	O4 H4B O12	0.76(4)	2.04(4)	2.788(4)	174(4)	4_456
	O5 H5A O1	0.912(10)	1.929(19)	2.777(3)	154(3)	4
	O5 H5B O13	0.918(10)	2.008(16)	2.893(3)	161(3)	1_554
	N1 H1A O8	0.83(4)	2.39(4)	2.984(4)	130(4)	2_565
	N1 H1A O11	0.83(4)	2.27(4)	2.975(4)	144(4)	3_545
	N2 H2A O7	0.81(5)	2.60(5)	2.996(4)	112(4)	3_645
	N2 H2A O8	0.81(5)	2.23(5)	2.975(4)	153(5)	3_645
	N3 H3A O14	1.05(5)	1.93(5)	2.931(4)	157(4)	3_645
8	N3 H3A O14	0.92(10)	2.18(10)	2.936(8)	138(8)	3_645
	N2 H2A O8	0.90(10)	2.12(11)	2.980(7)	158(11)	3_645
	N2 H2A O7	0.90(10)	2.56(13)	2.999(7)	111(9)	3_645
	N1 H1A O11	0.81(7)	2.25(8)	2.983(7)	150(8)	3_545
	N1 H1A O8	0.81(7)	2.44(8)	2.976(7)	125(7)	2_565
	O5 H5B O13	0.907(10)	2.04(3)	2.909(7)	159(6)	1_554
	O5 H5A O1	0.907(10)	1.98(4)	2.788(6)	148(6)	4
	O4 H4B O12	0.79(10)	2.02(9)	2.796(8)	169(8)	4_456
	O4 H4A O9	0.64(9)	2.25(9)	2.890(6)	174(11)	4

5.4 Thermogravimetric Analysis of Compounds 3-8

TGA studies also indicated the similarity among these structures. Water molecules were eliminated at temperatures below 150 ^{o}C, while the removal of hydroxypyridine (pyridone) residues took place at temperatures above 220 ^{o}C. However, complete removal of organic residues did not occur till ~400 ^{o}C (Fig. 6).

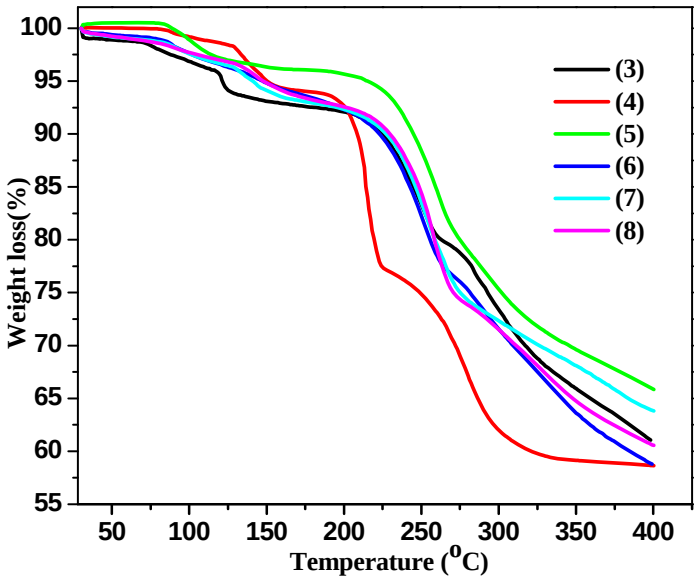

Figure 6. A drawing showing the TGA behaviour of compounds **3-8**.

5.5 Lanthanide Dipicolinates: Simplified Route and X-ray Structures

As a continuation of our studies on bismuth dipicolinates, which also has a large size and exhibits +3 oxidation state, we became interested in analogous/different dipicolinates. Additional interest in such compounds rested with the biocompatibility of these ligands. A fair number of reports on dipicolinate complexes of lanthanides are available,[15, 64] but there is room for further work. In a recent study, Chantal Brouca-Cabarrecq and coworkers reported that under hydrothermal conditions, only Eu(III) afforded the crystalline material suitable for X-ray study.[16] Even in the structure of the Eu(III) compound, there was a curious disorder in one of the dipicolinate moieties, and for this part as well as the lattice water molecules, only isotropic refinement could be used by the authors. In our study though, lanthanide dipicolinates of the formula {Ln[(2-HO_2C-6-O_2C)C_5H_3N]$_3$} 1.5H_2O [Ln = Sm (**9**), Gd (**10**), Eu (**11**), Dy (**12**), Tb (**13**) and Tm (**14**)] were synthesized by the reaction of $Ln(NO_3)_3.xH_2O$ with pyridine-2,6-dicarboxylic acid in water under reflux conditions for 4 h. We believe that the lesser

reaction time was the key to our success. Single crystals were obtained by slow cooling of the reaction mixture. All these compounds are isostructural and characterised by single crystal X-ray structure determination. The magnetic susceptibilities of the isolated compounds are consistent with that available in the literature.[55]

All the above compounds crystallise in the same space group ($P\bar{1}$) with essentially the same structure and for this reason, we shall concentrate on only the gadolinium complex **10**. One small difference between the literature report and ours is that we refined the structure as $\{Ln[(2\text{-}HO_2C\text{-}6\text{-}O_2C)C_5H_3N]_3\}_2.3H_2O$ while the literature gives it as $\{Ln[(2\text{-}HO_2C\text{-}6\text{-}O_2C)C_5H_3N]_3\}_2\ 2.5H_2O$. Also, we could refine all the non-hydrogen atoms anisotropically without any problem. However, only one of the carboxylate atoms [O16 split as O16A and O16B with the former having higher occupancy] in one of the two molecules in the asymmetric unit did show disorder. There are two molecules in the asymmetric unit. In each case, gadolinium ion is surrounded by three dipicolinate ligands (Fig. 7a, b). The ligand coordinates to the gadolinium ion through pyridine nitrogen and carboxylate oxygen in a five-membered chelating manner such that coordination number of lanthanide ion is 9. The relevant bond parameters are shown in Table III along with those for the reported Eu(III) complex. However, in the reported Eu(III) compound, one nitrogen and one oxygen coordinating to each of the two metal centers in the asymmetric unit are disordered and the refinement done was mostly isotropically. Such a problem does not exist in our compound **10**. All the Gd-O and Gd-N bond lengths are in the expected range; the only noteworthy point in this context is that one Gd-O distance [Gd1-O7/ Gd2-O21] is somewhat shorter than the rest. The geometry around each metal ion can be described as distorted tricapped trigonal prism (Fig. 7, bottom). The two trigonal faces corresponding to Gd1 are [O5, O9, O11] and [O1, O3, and O7] while those for Gd2 are [O13, O17, O19] and O15, O23, O23]. The nitrogen atoms cap the trigonal prsim on the square (approximate) faces. The bulk purity of the crystals obtained is compared by single crystal data and powder data thus obtained are in good agreement with each other (Fig. 8).

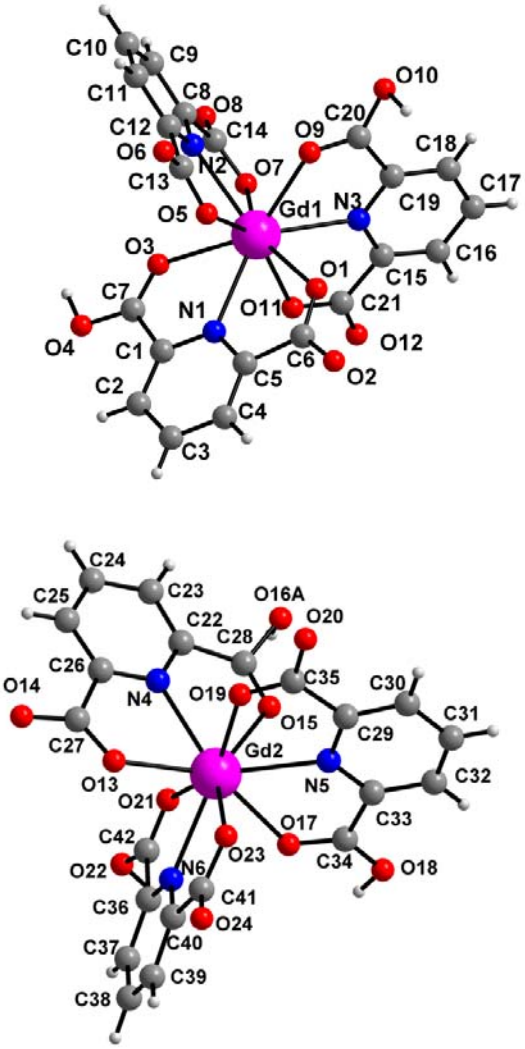

Figure 7a. Drawings representing the X-ray structure of **10**. Hydrogen atoms, the disordered O16B and water molecules are not shown. Top: Molecule 1 of the asymmetric unit. Bottom: Molecule 2 of the asymmetric unit. Colour code: Gd = purple, O = red, N = blue and C = grey-black.

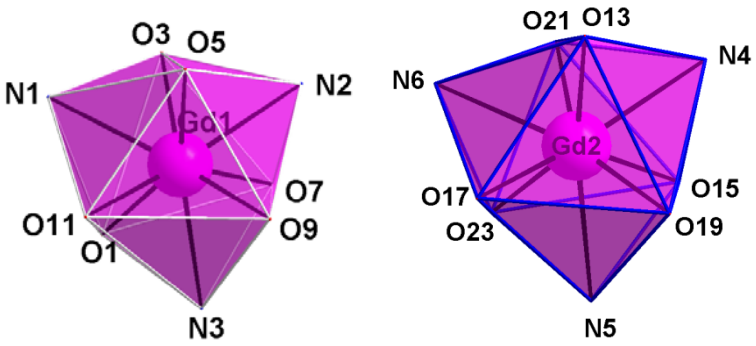

Figure 7b. Polyhedra showing distorted tricapped trigonal prism geometry around Gd(III).

Table III Bond distances (Å) in the Gd(III) complex **10** (this work) and in the (literature) reported Eu(III) complex[17]

Gd1-O1	2.401(3)		Gd2-O13	2.398(3)
Gd1-O3	2.476(3)		Gd2-O15	2.475(3)
Gd1-O5	2.426(3)		Gd2-O17	2.443(3)
Gd1-O7	2.387(3)		Gd2-O19	2.425(3)
Gd1-O9	2.434(3)		Gd2-O21	2.355(3)
Gd1-O11	2.426(3)		Gd2-O23	2.459(3)
Gd1- N1	2.547(3)		Gd2-N4	2.514(3)
Gd1-N2	2.508(3)		Gd2-N5	2.534(3)
Gd1-N3	2.502(3)		Gd2-N6	2.498(3)
Analogous Eu(III) compound from the literature[17]				
Eu1–O1	2.495(5)		Eu2–O13	2.373(5)
Eu1–O (disorder)	2.446		Eu2–O15	2.480(5)
Eu1–O3	2.448(6)		Eu2–O17	2.451(6)
Eu1–O5	2.442(6)		Eu2–O19	2.426(6)
Eu1–O7	2.446(6)		Eu2–O21	2.489(6)
Eu1–O9	2.402(6)		Eu2–O (disorder)	2.437
Eu1–O11	2.446(5)		Eu2–O23	2.406(6)
Eu1–N1	2.558(6)		Eu2–N4	2.519(7)
Eu1–N (disorder)	2.537		Eu2–N5	2.545(6)
Eu1–N2	2.520(6)		Eu2–N6	2.534(6)
Eu1–N3	2.532(7)		Eu2–N (disorder)	2.533

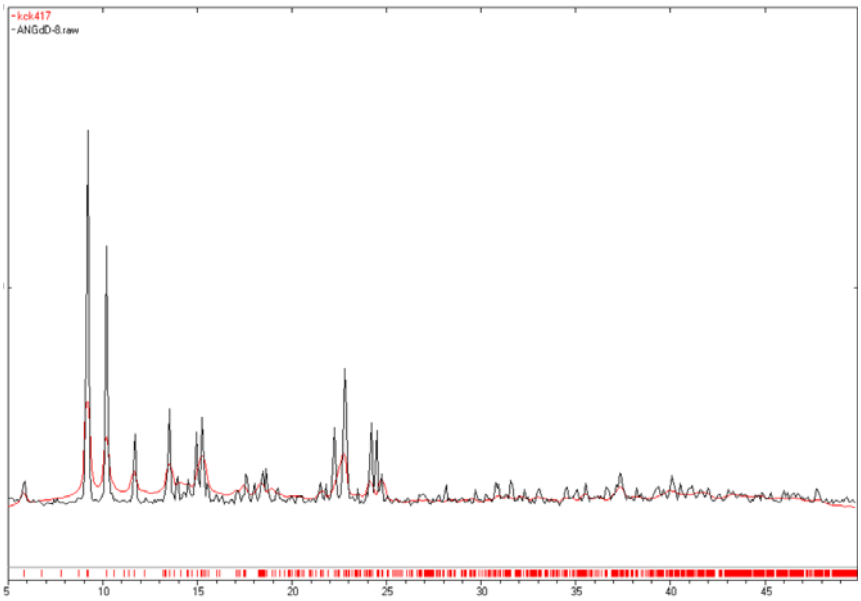

Figure 8. Comparison of single crystal data with powder pattern for compound **10**.

It can be noted that on each of the dipicolinate anion there is still one acidic (carboxylic) proton. In addition, for the two monomeric molecules present in asymmetric unit, there are three water molecules in the asymmetric unit. Thus there is extensive hydrogen bonding present in the system. For the question as to why there has been two molecules in the asymmetric unit the answer may lie in the hydrogen bonding interactions in conjunction with the disorder present in O16 that is part of the core containing Gd2.

The absorption spectra of lanthanide species are often characterised by line-like bands that result from forbidden intra f-f transitions.[65] Since we had difficulties in obtaining good spectra in solution, we have recorded the spectra in the solid state. The absorption bands are in the expected region (shown in Fig. 9) except a few minor shifts in the band positions. Eu(III) and Tb(III) ions are known to be highly fluorescent. The emission spectra of **11-13** (Fig. 10) also show a pattern similar that reported in the literature.[66]

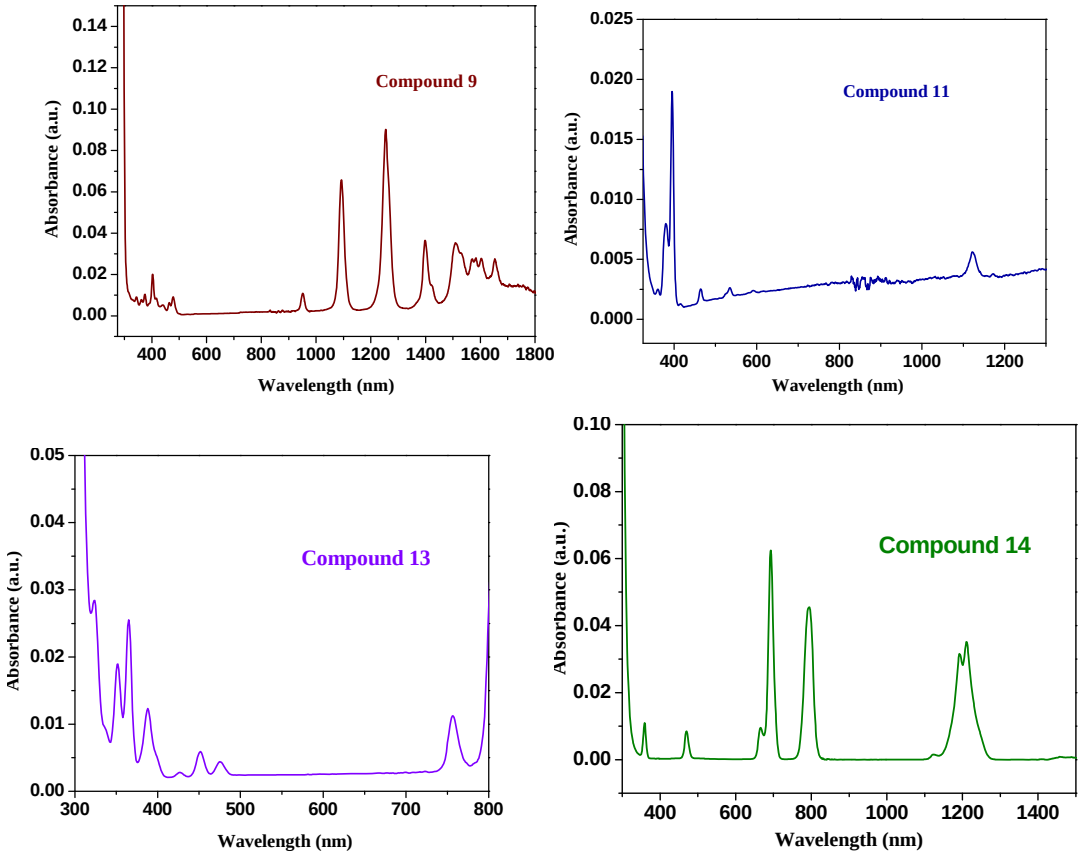

Figure 9. Solid state UV-Vis absorbance spectra of compounds **9**, **11, 13** and **14.**

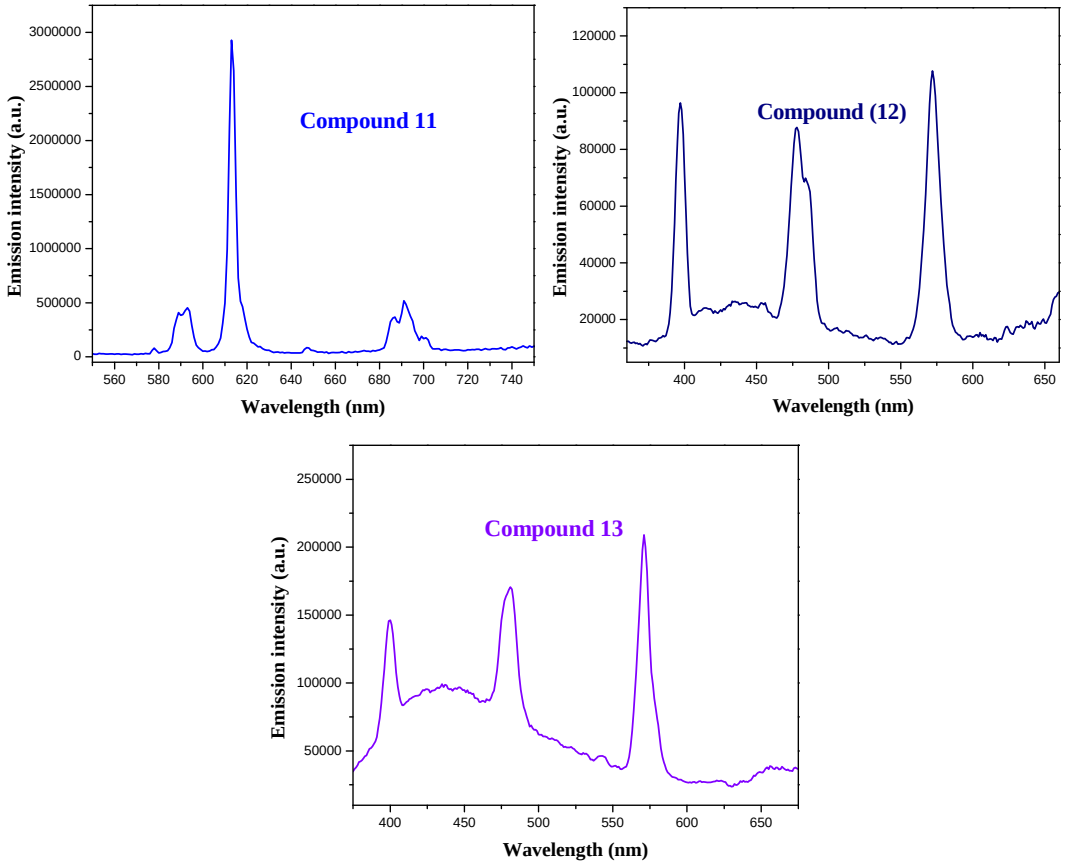

Figure 10. Emission spectra of compounds **11-13**.

5.5.1 Thermogravimetric analysis of compound 10

As a representative example, TGA of compound **10** is shown in Figure 11. All the other lanthanide dipicolinates are having similar thermal degradation pattern. Water molecules were eliminated at temperatures below 150 ^{o}C, while the removal of one of the dipicolinate ligand residues took place at temperatures above 280 ^{o}C. This situation corresponds to the stoichiometry Gd(dipicH)(dipic), wherein deprotonation has occurred at both the carboxylates on one ligand. Elimination of the other two dipicolinate molecules started above 320 ^{o}C, but even at 900 ^{o}C, complete removal of organic residues resulting in Gd_2O_3 is not complete.

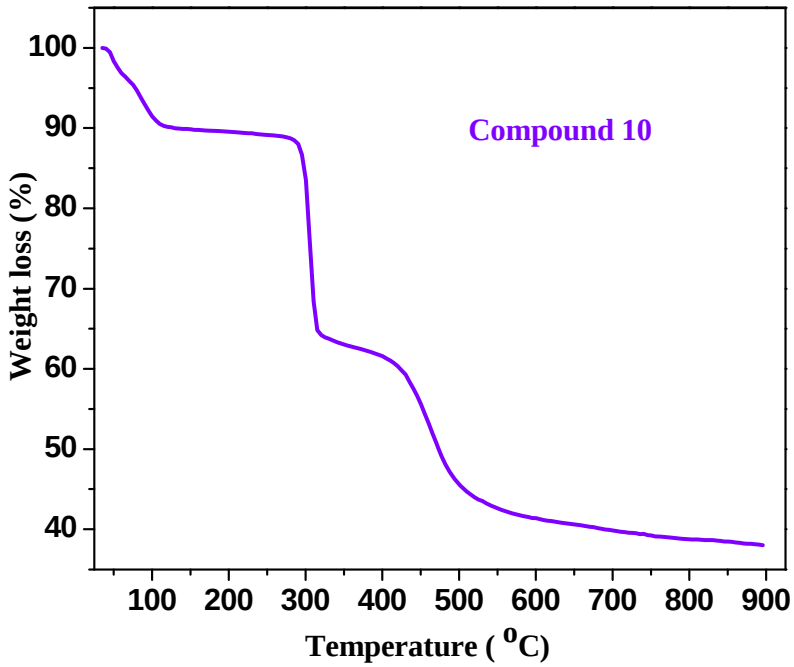

Figure 11. A drawing showing the TGA behaviour of compound **10**.

5.6 Antitumor Activity of the Gadolinium Dipicolinate (compound 10)

These studies were performed in the School of Life Sciences of our university in collaboration with Dr. Roy Karnati. Preliminary screening was done on cancer cell lines of different origins. Breast (MCF), Leukemia (K562), Skin (A341) and Liver (HepG2) cell lines were used. Compound **10** showed significant effect on the proliferation of Hepatocellular carcinoma cells (HepG2). So we continued further studies using this cell line. We also made an attempt to understand the molecular mechanisms. Motexafin gadolinium (MGd) was shown to induce apoptosis in B-cell derived tumor lines.[67] It was also shown to inhibit the

proliferation of highly resistant multiple myeloma cells.[68] Our study in similar lines shows that compound **10** inhibits the proliferation of HepG2 cells in a dose dependent manner.

(a) Effect of compound 10 on cell viability and morphology

HepG2 cells were treated with **10** (10, 25, 50,100, 250, 500, 1000 μM) for 48 h and cell proliferation was determined by the MTT assay. Under these experimental conditions, a dose-dependent decrease in proliferation of **10** treated HepG2 cells was observed. A 50% inhibition in HepG2 cell proliferation was observed at 250 μM concentration of **10** in 48 h (Fig. 12). The substrates, Gd(III) nitrate and other lanthanide nitrates/ dipicolinates (**9**, **11-14**) as well as dipiliconic acid did not show significant effect on the proliferation of HepG2 cells up to 1mM concentration. Since 50% inhibition of cell proliferation was observed at 250 μM of **10** in HepG2 cells, further experiments were carried out at 100 and 250 μM concentration.

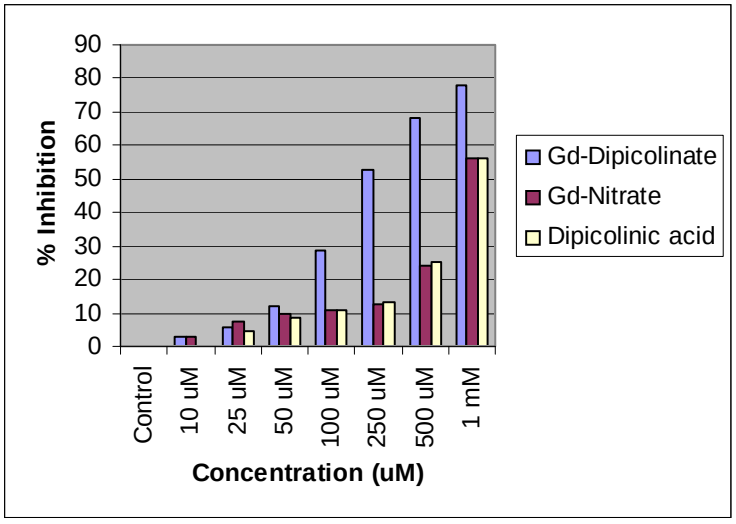

Figure 12. Effect of Gadolinium dipicolinate (**10**) on the proliferation of Hepatocellular Carcinoma Cell Line (HepG2) (48 Hrs).

Apoptosis or cell death can be understood by the morphology of the cell. Apoptotic cells exhibit very different morphological features. HepG2 cells treated with **10** (100 and 250 μM) showed significant membrane blebbing with distorted membranes, which is the characteristic morphological feature of the cells undergoing programmed cell death (Fig. 13).

(a) 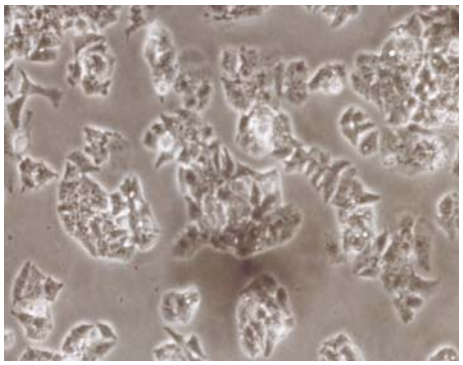 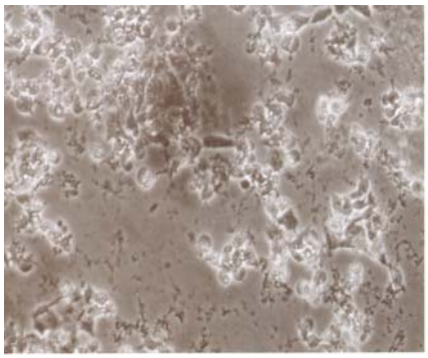 (b)

(c)

Figure 13. Phase-contrast micrographs showing the induction of cell death by compound **10** (48 Hrs). (a) Control, (b) Cells treated with 100 μM of compound **10**, (c) cells treated with 250 μM of compound **10**.

(b) Effect of compound 10 on cytochrome-*c* release and the expression of Bcl2 and BAX

Depolarized mitochondrial membrane potential is a common feature of apoptotic cells. Loss of the mitochondrial membrane potential might result in the release of the cytochrome-*c* in the cytosol. Translocation of cytochrome *c* from mitochondria into the cytosol is regulated by Bcl-2 family members. In the cytoplasm, cytochrome *c* becomes associated with caspase 9, Apaf-1 (apoptotic protease-activating factor 1) and dATP to form apoptosome complex, which activates caspases. Caspase activation results in the damage of cellular substrates leading to apoptosis. In our study we observed a time dependent increase in the release of cytochrome *c* into the cytosol with the compound **10** treatment.

Loss of mitochondrial membrane potential due to the initiation of apoptosis releases cytochrome *c* from the mitochondrial matrix. Release of cytochrome *c* into the cytosol is considered hallmark property of apoptotic cells. Western-blot analysis was performed with cytoplasmic extracts devoid of mitochondria, with anti-

cytochrome *c* mouse monoclonal antibodies to detect cytochrome *c* release. We observed a time dependent increase in cytochrome *c* release in the cells treated with **10** (250 μM) and no release was observed in control cells (Fig. 14a).

Bcl-2 family proteins are crucial in the cell death process. They are keys in deciding the form of cell death process. Ratio of Bcl-2 and BAX proteins determines the fate of the cell towards death or survival. Upon treatment with **10** (250 μM) changes in the expression of Bcl-2 and BAX were observed. Bcl-2 protein expression decreased and pro-apoptotic protein BAX levels increased in a time dependent manner in cells treated with **10**, compared with the untreated controls (Figure 14b, 14c).

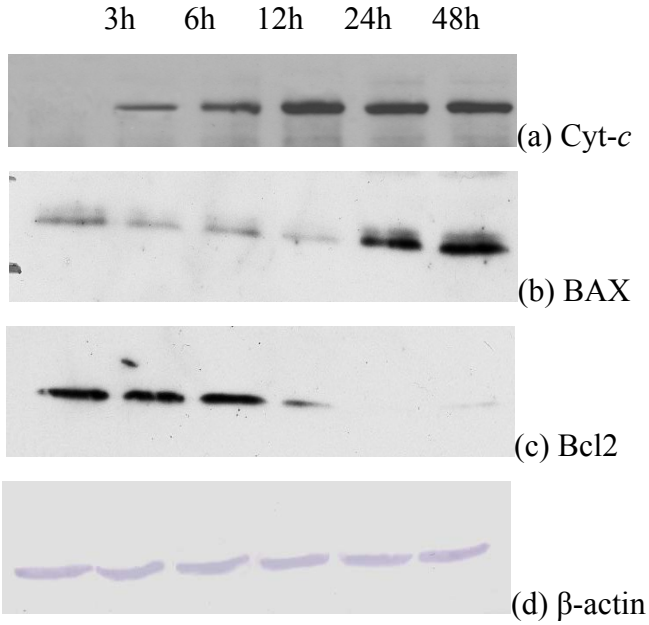

Figure 14. Time dependent expression of proteins involved in cell death process in compound **10** treated HepG2 cells (Western blot analysis).

(c) Effect of compound 10 on cell cycle

Flow cytometric cell cycle analysis using DNA-binding dye, propidium iodide, showed a concentration-dependent increase in the accumulation of cells in the sub Go/G1 phase. The cells in the sub G0/G1 are hypodiploid. This population of cells represents the cells undergoing apoptosis. We also observed a simultaneous decrease of cells in the other phases of cell cycle.

Increase in the cell number in sub G0/G1 phase with treatment is characteristic feature of apoptosis induction. HepG2 cells treated with **10** (100 and 250 μM) for 48 h were analysed on FACS for the cell cycle alterations. Typical sub-

diploid apoptotic peaks were observed in **10** treated cells. Control cells showed a G1, followed by S and G2/M-phases. Only 1.17% of the control cells showed hypodiploid DNA (Fig. 15a). Cells with hypodiploid DNA increased in **10** treated cells. Hypodiploid cells were 23.96% in 100 μM and 47.76% 250 μM in treated cells (Figs 15b and 15c).

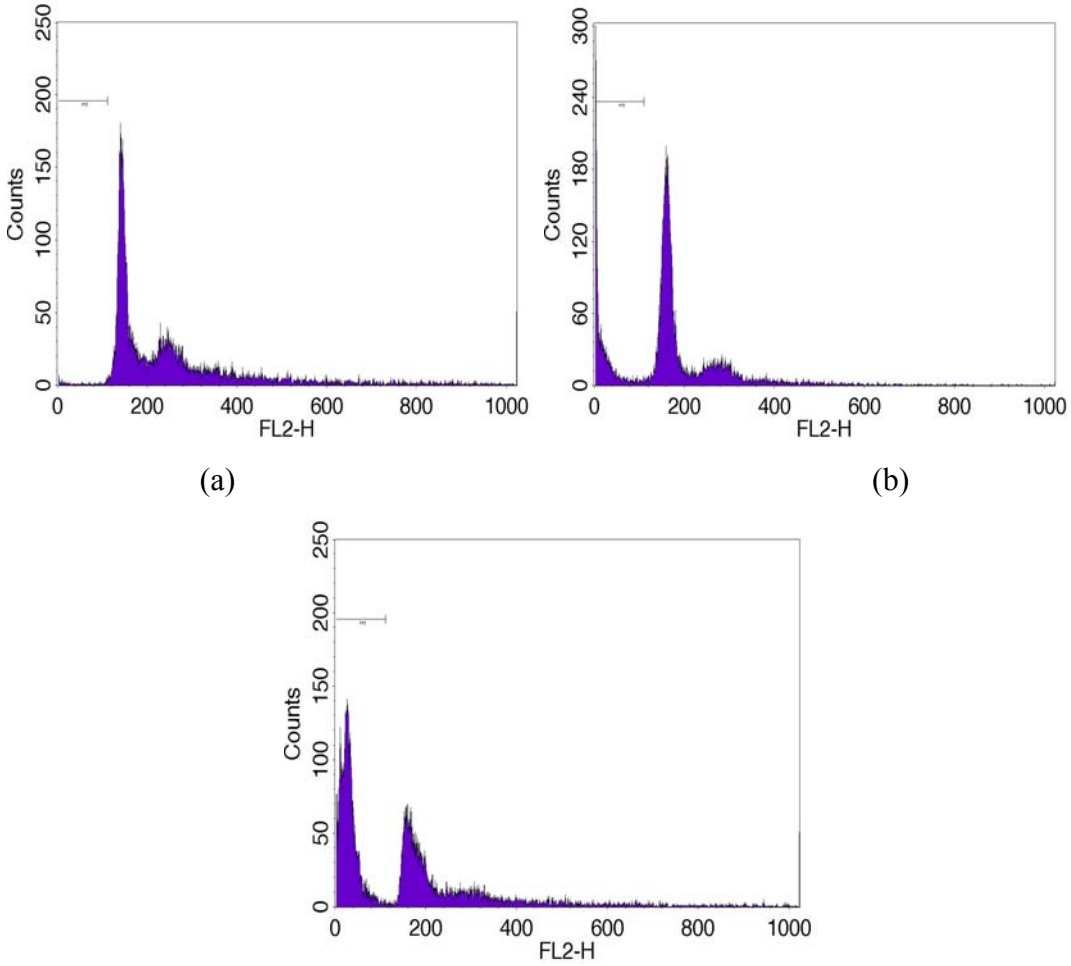

(a) (b)

(c)

Figure 15. Cell cycle alterations of **10** treated HepG2 cells (48 hrs; Flow-cytometric Analysis; see text for details).

As this gadolinium dipicolinate compound has shown promising effect on the proliferation of hepatocellular carcinoma cells, further studies will focus on synthesis of derivatives to these compounds which show more efficacy and developing these as promising drug candidates for the treatment of hepatocellular carcinoma.

5.7 Attempted Preparation of Lanthanide Zinc Pyrophosphates, $Ln_{2/3}ZnP_2O_7$ [Ln = Pr (15), Sm (16), Nd (17), Dy (18) and Gd (19)]

In some of the earlier experiments using domestic microwave oven, we were able to obtain pure samples of $Ln_{2/3}ZnP_2O_7$ (**15-19**) by treating $Na_2ZnP_2O_7$ with the *in situ* prepared lanthanide chlorides. The X-ray powder patterns of all the products that were thus obtained by microwave method are shown in Figure 16. However, since the microwave oven used was a domestic one, for reproducibility, later investigations were performed by using a muffle furnace [600 ^oC/ 6h]. To our dismay, the results obtained using the microwave were not very much reproducible by using the furnace in terms of the purity of the samples as evidenced by powder X-ray for the samples. The unit cell parameters derived from the least square fit analysis are given in Table IV for samples obtained using the microwave; these data are similar to that of $Na_2ZnP_2O_7$ which belongs to tetragonal system. The infrared spectra of pyrophosphates are characterised by bands corresponding to tetrahedral PO_4 group and P-O-P stretching vibration which occurs around 730 cm^{-1}. This band is observed in all the compositions in the present investigation. The metal composition was confirmed by ICP. We did not proceed further (although a considerable amount of time was devoted to standardise the furnace route) since a standard microwave reactor system was not available locally.

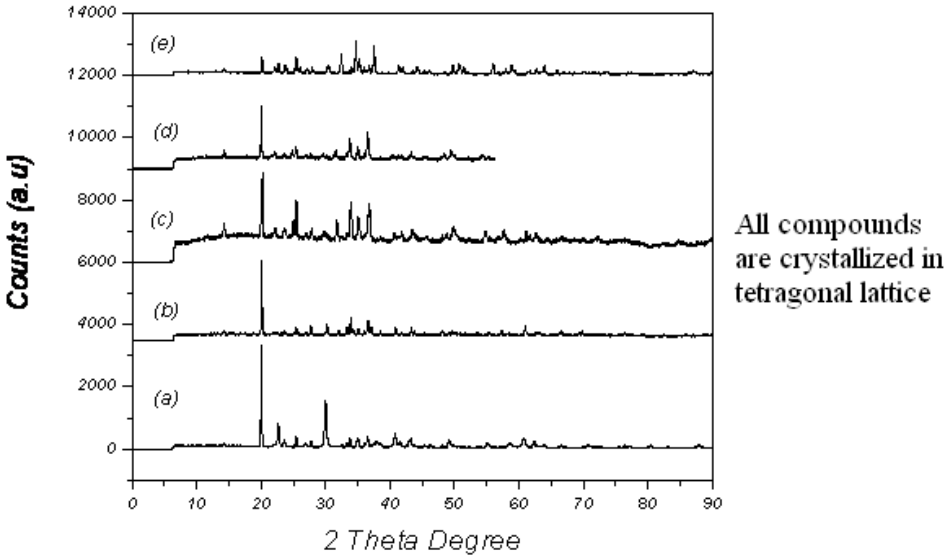

Figure 16. Powder XRD patterns of (a) $Dy_{2/3}ZnP_2O_7$, (b) $Sm_{2/3}ZnP_2O_7$, (c) $Nd_{2/3}ZnP_2O_7$, (d) $Pr_{2/3}ZnP_2O_7$ and (e) $Gd_{2/3}ZnP_2O_7$

Table IV. Unit cell parameters of $Ln_{2/3}ZnP_2O_7$ samples obtained by the microwave method.

Compound	a (Å) ± 0.005	c (Å) ± 0.005
$Dy_{2/3}ZnP_2O_7$	7.631	10.351
$Sm_{2/3}ZnP_2O_7$	7.685	10.281
$Nd_{2/3}ZnP_2O_7$	7.682	10.272
$Pr_{2/3}ZnP_2O_7$	7.733	10.334
$Gd_{2/3}ZnP_2O_7$		

SUMMARY – PART B

1) The reaction of lanthanide nitrates with 4-hydroxypyridine in water/EtOH resulted in the formation of crystalline $[M(4\text{-}O\text{-}C_6H_4NH)_3(NO_3)_2(H_2O)_2][NO_3]$ {M = La (**3**), Ce (**4**), Pr (**5**), Nd (**6**), Eu (**7**) and Gd (**8**)}. The lanthanide ion in these complexes shows a coordination number of nine with tricapped trigonal prismatic geometry and the coordination occurs through phenolate oxygen and water molecules. All these complexes crystallised in the chiral space group $P2_12_12_1$ suggesting spontaneous resolution. Interestingly, the neodymium compound **6** showed a stereochemistry opposite to that observed for others.
2) Reaction of lanthanide nitrates with pyridine-2,6-dicarboxylic acids in water resulted in crystalline monomeric complexes of the formula $\{Ln[(2\text{-}HO_2C\text{-}6\text{-}O_2C)C_5H_3N]_3\}.1.5H_2O$ [Ln = Sm (**9**), Gd (**10**), Eu (**11**), Dy (**12**), Tb (**13**) and Tm (**14**)]. This is unlike a literature report using hydrothermal method wherein crystalline samples could not be obtained. Even in the structure reported, there was a serious disorder; in our case, we could refine the structure more efficiently. Bulk purity of compounds was confirmed by the agreement of single crystal data with P-XRD.
3) Anti cancer actvity studies of **9-14** shown that only gadolinium dilpicolinate (**10**) has reasonable activity against *hepatocellular carcinoma* (HepG2; liver cancer cell line). MTT assay has shown that IC_{50} of compound **10** is 250 μM.

EXPERIMENTAL SECTION

Most of the details of equipment used have been given in Chapter 3. Steady state absorption and fluorescence spectra were recorded on a UV-Vis-NIR scanning spectrophotometer (Shimadzu, model no. UV-3101PC) and SPEX FLUOROMAX-3 spectrofluorometer, respectively.

6.1 Synthesis of $[M(4\text{-}O\text{-}C_6H_4NH)_3(NO_3)_2(H_2O)_2][NO_3]$ {M = La (3), Ce (4), Pr (5), Nd (6), Eu (7), Gd (8)}

To a solution of $Ln(NO_3)_3.xH_2O$ (1 mmol) dissolved in ethanol (10 cm^3) or water (7 cm^3) and 4-hydroxypyridine (3.0 mmol) was added. The resulting mixture was stirred for 1 h at room temperature to result in a clear solution. Solvent from this solution was allowed to evaporate at room temperature. Single crystals suitable for X-ray structural analysis were formed in 2-3 d (EtOH) or 7-8 d (water).

(a) $[La(4\text{-}O\text{-}C_6H_4NH)_3(NO_3)_2(H_2O)_2][NO_3]$ (3)

[Using $La(NO_3)_3.6H_2O$ (0.433 g) + 4-hydroxy pyridine (0.285 g)]: Colourless crystals.

Yield: 0.54g, 84 % based on the metal.

Mp: 196-200 ^oC; foaming was observed during melting of compound that suggested the expulsion of water.

IR (KBr, cm^{-1}): 3441(w), 3254(br), 3148(w), 3092(w), 2974(w), 1641(s), 1591(s). 1520(m), 1336(m), 1182(s), 1076(w), 1037(s), 999(s), 856(m), 733(s), 553(s), 501(m).

^1H NMR spectrum (400 MHz, D_2O): Two equal intensity doublets in the aromatic region at δ 6.50 and 7.79 [^3J(HH) = 7.2 Hz].

^{13}C NMR (100 MHz, D_2O): δ 116.67, 139.34 and 180.42.

Elemental analysis (calc): C, 27.87 (27.76); H, 2.96 (2.91); N, 13.00 (13.12).

Magnetic moment (μ_{eff}): 0.00 BM.

(b) $[Ce(4\text{-}O\text{-}C_6H_4NH)_3(NO_3)_2(H_2O)_2][NO_3]$ (4)

[Using $Ce(NO_3)_3.6H_2O$ (0.434 g) + 4-hydroxy pyridine (0.285 g)]: Colourless crystals.

Yield: 0.52 g, 82 % based on Ce

Mp: 80-84^oC (foaming at 125-135 ^oC)

IR (KBr, cm^{-1}): 3429(br), 3144(w), 3148(w), 2966(w), 1635(s), 1591(s). 1523(m), 1385(s), 1186(s), 1037(m), 1001(s), 858(m), 734(s), 553(s), 504(m).

Elemental analysis (calc): C, 27.82 (27.86); H, 2.95 (2.91); N, 12.98 (12.91).

Magnetic moment (μ_{eff}): 2.40 BM (Lit. $[Ce(PM)_2(NO_3)_2]NO_3$, 2.65 BM[55])

(c) $[Pr(4\text{-}O\text{-}C_6H_4NH)_3(NO_3)_2(H_2O)_2][NO_3]$ (5)

[Using $Pr(NO_3)_3.5H_2O$ (0.417 g) + 4-Hydroxy pyridine (0.285 g)]: Green crystals.

Yield: 0.50 g, 78 % based on Pr.

Mp: 90-92^oC (foaming at 125-135 ^oC)

IR (KBr, cm^{-1}): 3298(br), 3130(w), 2959(w), 1635(s), 1590(s). 1520(m), 1385(s), 1186(s), 1039(m), 1001(s), 858(m), 738(s), 555(s), 510(m).

The CD spectrum was too noisy and hence its analysis was not attempted.

UV-Vis (λ_{max}, nm): 444, 469, 482, 588

Elemental analysis (calc): C, 27.79 (27.91); H, 2.95 (2.92); N, 12.96 (12.92).

Magnetic moment (μ_{eff}): 3.40 BM (Lit. $[Pr(PM)_2(NO_3)_2]NO_3$, 3.62 BM[55])

(d) $[Nd(4\text{-}O\text{-}C_6H_4NH)_3(NO_3)_2(H_2O)_2][NO_3]$ (6)

[Using $Nd(NO_3)_3.6H_2O$ (0.438 g) + 4-hydroxy pyridine (0.285 g)]: Light pink crystals.

Yield: 0.53 g, 89 % based on Nd

Mp: 87-90^oC (foaming at 125-135 ^oC).

IR (KBr, cm^{-1}): 3435(br), 3271(w), 3148(w), 2966(w), 1639(s), 1595(s). 1529(m), 1454(s), 1385(s), 1184(m), 1001(s), 858(m), 736(s), 553(s), 510(m) cm^{-1}.

UV-Vis (λ_{max}, nm): 511 (minor), 522, 574, 730 (minor), 745, 800.

Elemental analysis (calc): C, 27.65 (27.56); H, 2.93 (2.90); N, 12.89 (12.78).

Magnetic moment (μ_{eff}): 3.50 BM (Lit. $[Nd(PM)_2(NO_3)_2]NO_3$, 3.78 BM[55])

(e) $[Eu(4\text{-}O\text{-}C_6H_4NH)_3(NO_3)_2(H_2O)_2][NO_3]$ (7)

[Using $Eu(NO_3)_3.5H_2O$ (0.428 g) + 4-hydroxy pyridine (0.285 g)]: Colourless crystals.

Yield: 0.51g, 81 % based on Eu.

Mp: 90-94^oC (foaming at 125-135 ^oC).

IR (KBr, cm^{-1}): 3472(br), 3294(w), 3138(w), 2964(w), 1639(s), 1531(s). 1529(m), 1385(s), 1186(s), 1045(m), 1001(s), 860(m), 742(s), 555(s).

UV-Vis (λ_{max}, nm): 394.

Elemental analysis (calc): C, 27.32 (27.26); H, 2.90 (2.88); N, 12.74 (12.81).

Magnetic moment (μ_{eff}): 3.35 BM (Lit. $[Eu(PM)_2(NO_3)_2]NO_3$ 3.39 BM[55])

(f) $[Gd(4\text{-}O\text{-}C_6H_4NH)_3(NO_3)_2(H_2O)_2][NO_3]$ (8)

[Using $Gd(NO_3)_3.5H_2O$ (0.434 g) + 4-Hydroxy pyridine (0.285 g)]: Colourless crystals.

Yield 0.24 g, 52 % based on Gd.

Mp: 86-88^oC (foaming at 125-135 ^oC).

IR (KBr, cm^{-1}): 3232(br), 3084(w), 2957(w), 1635(s), 1525(s). 1385(s), 1186(s), 1039(m), 999(s), 858(m), 736(s), 555(s) 499.

UV-Vis (λ_{max}, nm): 363, 387, 451.

Elemental analysis (calc): C, 27.11 (27.16); H, 2.88 (2.91); N, 12.64 (12.55).

Magnetic moment (μ_{eff}): 7.63 BM (Lit. $[Gd(PM)_2(NO_3)_2]NO_3$ 6.86 BM[55]).

6.2 Synthesis of Lanthanide Dipicolinates{M $[(2\text{-}HO_2C\text{-}6\text{-}O_2C)C_5H_3N]_3\cdot\}1.5\ H_2O$ [M = Sm (**9**), Gd (**10**), Eu (**11**), Dy (**12**), Tb (**13**), Tm (**14**)]

To a boiling solution of $Ln(NO_3)_3.xH_2O$ in water (50 cm^3) was added pyridine-2,6-dicarboxylic acid. A clear solution was obtained after refluxing further for 4 h. The mixture was filtered to remove any suspended impurities and the clear, colourless filtrate allowed to cool slowly. After 2 d, crystals suitable for X-ray single crystal analysis were formed.

(a) $\{Sm[(2\text{-}HO_2C\text{-}6\text{-}O_2C)C_5H_3N]_3\cdot\}.1.5\ H_2O$ (9)

[Using $Sm(NO_3)_3.5H_2O$ (0.150 g, 0.337 mmol) + pyridine-2,6-dicarboxylic acid (0.168g, 1.011 mmol)]: Colourless crystals.

Yield: 0.173 g, 79 % based on Sm.

Mp: >320 ^{o}C.

IR (KBr, cm^{-1}): 3503(br), 3366(w), 3285(w), 3090(m), 1672(s), 1589(s), 1444(s), 1375(s), 1278(s), 1078(m), 1020(m), 900(m), 767(m), 717(s), 661(w).

Solid state UV-Vis (λ_{max}, nm): 345, 371, 402, 437, 481.

Elemental analysis (calc): C, 38.88 (38.96); H, 1.85 (1.91); N, 6.48 (6.43).

Magnetic moment (μ_{eff}): 1.87 BM (Lit. $[Sm(PM)_2(NO_3)_2]NO_3$ 1.85 BM[55])

(b) {Gd[(2-HO$_2$C-6-O$_2$C)C$_5$H$_3$N]$_3$}1.5 H$_2$O (10)

[Using $Gd(NO_3)_3.5H_2O$ (0.150 g, 0.332 mmol) + pyridine-2,6-dicarboxylic acid (0.166 g, 0.996 mmol)]: Colourless crystals.

Yield: 0.148 g, 68 % based on Sm.

Mp: >320 ^{o}C.

IR (KBr, cm^{-1}): 3574(br), 3400(w), 3090(w), 1674(s), 1591(s), 1452(s), 1356(s), 1278(s), 1076(m), 1020(m), 902(m), 761(m), 717(s), 663(m).

Solid state UV-Vis (λ_{max}, nm): 363, 387, 451.

Elemental analysis (calc): C, 38.47 (38.52); H, 1.83 (1.76); N, 6.41 (6.48).

Magnetic moment (μ_{eff}): 7.60 BM [Lit. $[Gd(PM)_2(NO_3)_2]NO_3$ 6.86 BM[55]]

(c) {Eu[(2-HO$_2$C-6-O$_2$C)C$_5$H$_3$N]$_3$}.1.5 H$_2$O (11)

[Using $Eu(NO_3)_3.5H_2O$ (0.150 g, 0.336 mmol) + pyridine-2,6-dicarboxylic acid (0.168 g, 1.008 mmol)]: Colourless crystals.

Yield: 0.148 g, 65 % based on Eu.

Mp: >320 ^{o}C.

IR (KBr, cm^{-1}): 3572(br), 3504(w), 3090(w), 1672(s), 1589(s), 1452(s), 1350(s), 1261(s), 1076(m), 1020(m), 900(m), 760(m), 717(s), 661(m).

Solid state UV-Vis (λ_{max}, nm): 394.

Elemental analysis (calc): C, 38.82 (38.76); H, 1.84 (1.79); N, 6.47 (6.43).

Magnetic moment (μ_{eff}): 3.32 BM (Lit. $[Eu(PM)_2(NO_3)_2]NO_3$ 3.39 BM[55])

(d) {Dy[(2-HO$_2$C-6-O$_2$C)C$_5$H$_3$N]$_3$}.1.5 H$_2$O (12)

[Using $Dy(NO_3)_3.5H_2O$ (0.150 g, 0.430 mmol) + pyridine-2,6-dicarboxylic acid (0.215 g, 1.290 mmol)]: Colourless crystals.

Yield: 0.210 g, 74 % based on Dy.

Mp: >320 ^{o}C.

IR (KBr, cm^{-1}): 3576(br), 3506(w), 3090(w), 1674(s), 1591(s), 1452(s), 1354(s), 1278(m), 1076(m), 1020(m), 902(m), 761(m), 717(s), 663(m).

Solid state UV-Vis (λ_{max}, nm): 387, 451, 755.

Elemental analysis (calc): C, 38.18 (38.26); H, 1.81 (1.76); N, 6.36 (6.28).

Magnetic moment (μ_{eff}): 9.70 BM (Lit. $[Dy(PM)_2(NO_3)_2]NO_3$ 9.96 BM[55])

(e) {Tb $[(2\text{-}HO_2C\text{-}6\text{-}O_2C)C_5H_3N]_3$}.1.5 H_2O (13)

[Using $Tb(NO_3)_3.5H_2O$ (0.150 g, 0.344 mmol) + pyridine-2,6-dicarboxylic acid (0.172 g, 1.032 mmol)]: Colourless crystals.

Yield: 0.153 g, 68 % based on Tb.

Mp: >320 ^oC.

IR (KBr, cm^{-1}): 3576(br), 3506(w), 3090(m), 1674(s), 1591(s), 1454(s), 1356(s), 1278(m), 1076(m), 1020(m), 902(m), 767(m), 717(s), 663(m).

Solid state UV-Vis (λ_{max}, nm): 352, 364, 390, 427, 451, 476, 756.

Anal. Calc. for formula: C, 38.41 (38.49); H, 1.82 (1.76); N, 6.40 (6.48).

Magnetic moment (μ_{eff}): 8.66 BM (Lit. $[Tb(PM)_2(NO_3)_2]NO_3$, 9.35 BM[55])

(f) {Tm $[(2\text{-}HO_2C\text{-}6\text{-}O_2C)C_5H_3N]_3$}.1.5 H_2O (14)

[Using $Tm(NO_3)_3.6H_2O$ (0.150 g, 0.337 mmol) + pyridine-2,6-dicarboxylic acid (0.168 g, 1.011 mmol)]: Colourless crystals.

Yield: 0.148 g, 66 % based on Tm

Mp: >320 ^oC.

IR (KBr, cm^{-1}): 3582(br), 3512(w), 3094(w), 1674(s), 1593(s), 1462(s), 1358(s), 1280(m), 1076(m), 1022(m), 904(m), 761(m), 719(s), 663(m).

Solid state UV-Vis (λ_{max}, nm): 359, 470, 665, 693, 795.

Anal. Calc. for formula: C, 37.83 (37.71); H, 1.80 (1.89); N, 6.30 (6.21).

Magnetic moment (μ_{eff}): 6.96 BM (Lit. $[Tm(PM)_2(NO_3)_2]NO_3$, 6.90 BM[55])

6.3 Antitumour Activity of Compound 10

(a) Cell viability assay

The effect of Gd compounds on the cell proliferation was determined by the MTT assay. HepG2 cells (5×10^3 cells/well) were seeded on to a 96-well culture plate in the presence or absence of **10** (10, 25, 50,100, 250, 500, 1000 μM) for 48 h in a final volume of 100 μl. Gd $(NO_3)_3.5H_2O$ and dipicolinic acid were also used as

controls to understand whether the activity is specific to the **10** and not due to substrates. After treatment, the medium was removed and 20 μl of MTT (5 mg/cm^3 of PBS) was added to the fresh medium. The plates were incubated for 2 h at 37 ^{o}C. After incubation, 100 μl of DMSO was added to each well and plates were agitated for 1 min. Attenuance was read at 570 nm on a multi-well plate reader. The percentage inhibition of proliferation was calculated as a fraction of control (without compound **10**).

The effect of other lanthanide nitrate salts on the proliferation of HepG2 cells was also studied by MTT assay. The respective substrates were used as controls.

(b) Phase Contrast Micrographs

The morphology of HepG2 cells treated or untrated with **10** was assessed by phase contrast micrographs. HepG2 cells (1×10^5) were exposed to **10** at concentration of 100 μM and 250 μM for 48 h. After treatment, cells were observed for morphological changes under an inverted phase contrast microscope.

(c) Cell Cycle Analysis

Alteration in cell cycle of HepG2 treated with **10** was assessed by flow cytometric analysis. Cells were seeded at a density of 4×10^5 in 6-well culture plates, cultured in 10% FBS with or without compound **10** at concentration of 100 μM and 250 μM for 48 h. After treatment, cells were harvested and washed with 1X PBS. For cell cycle analysis, the treated and control cells were fixed in 70% ice cold ethanol, washed with 1X PBS, incubated with RNase A (0.1 mg/cm^3) and stained with Propidium iodide (50 mg/cm^3). Flow cytometric analysis was performed using a Becton Dickinson FACS Calibur (San Jose, CA, U.S.A.)

(d) Western Blotting

The changes in the expression of proteins involved in cell viability with **10** treatment were assessed by western blotting. HepG2 cells at a density of 6×10^6 were seeded in 90 mm culture dishes. They were incubated with compound **10** (250 μM) for 0, 3, 6, 12, 24 and 48 h. After treatment, cells harvested were washed with 1 X PBS and suspended in cell lysis buffer [20 mM Tris, 1 mM EDTA, 150 mM NaCl, 1% Nonidet P40, 0.5% sodium deoxycholate, 1 mM β-glycerophosphate, 1 mM Na_3VO_4 (sodium orthovanadate), 1 mM PMSF, 10 μg/cm^3 leupeptin, 20 μg/cm^3

aprotinin and phosphatase inhibitor cocktails 1 and 2 with 100-fold dilution]. The cell suspension was given intermittent vortexing every minute. After 30 min of vortexing at 4°C, the cell lysates were centrifuged (10 000g) for 30 min at 4°C. The resultant supernatants were used as the whole cell extracts. The protein content was determined by the Bradford method 100 μg of total protein from each time point was resolved on SDS/8–12% PAGE gels along with protein molecular mass standards and then transferred on to nitrocellulose membranes. Membranes were stained with 0.5% Ponceau *S* in 1% acetic acid to check the transfer. The membranes were blocked with 5% (w/v) non-fat dry milk and then incubated with the primary antibodies [BAX (1:250 dilution), Bcl-2 (1:500 dilution), Cyt C (1:1000 dilution), β actin (1:1000 dilution)] in 10 cm^3 of antibody-dilution buffer (1×Tris-buffered saline and 0.05% Tween 20 with 1% milk powder) with gentle shaking at 4°C for 8–12 h and then incubated with peroxidase-conjugated secondary antibodies. Signals were detected by using peroxidase substrate, TMB/H_2O_2.

6.4 Attempted Synthesis of Lanthanide Zinc Pyrophosphates $Ln_{2/3}ZnP_2O_7$ (Ln = Pr, Sm, Nd, Dy and Gd)

(a) Preparation of sodium zinc pyrophosphate $Na_2ZnP_2O_7$

Stoichiometric amounts of NaH_2PO_4 and ZnO were thoroughly ground and then heated in a muffle furnace at 720 °C. The reaction is according to the equation given below.

$$2NaH_2PO_4.2H_2O + ZnO \rightarrow Na_2ZnP_2O_7 + H_2O\uparrow$$

(b) Attempted preparation of $Ln_{2/3}ZnP_2O_7$

Rare earth oxide (Ln_2O_3, Ln = Pr, Sm, Nd, Dy and Gd) was first converted to its chloride by dissolving in conc. HCl. Excess acid was removed by slow heating to get $LnCl_3.xH_2O$ (x ~ 4-6) as a solid. Then stoichiometric amounts of the individual $LnCl_3.xH_2O$ (~ 4 mmol) and $Na_2ZnP_2O_7$ (6 mmol) were thoroughly mixed in a mortar. In the initial trials, a domestic microwave oven (full voltage, 5 min) was used to heat this mixture, wherein we obtained the desired compounds. In later experiments, the resultant powder was heated at 600 °C (6 h), then treated with hot distilled water (3 x 10 cm^3) and filtered. The insoluble powder was analyzed further for the lanthanide pyrophosphate [powder X-ray]. The filtrate obtained was slowly evaporated to dryness to get a solid [NaCl, powder X-ray].

6.5 X-ray Crystallography

The details on equipment and radiation are already presented in Chapter 3. In the case of compound **4**, reflections were weak but the structure could be refined well. The hydrogen atoms were fixed by geometry or located by Difference Fourier map; subsequently a riding model was used. Crystallographic data are presented in Table Va-b. In the case of lanthanide dipicolinates (e.g. **10**), one of the carbonyl oxygen atoms (O16) showed some disorder. Crystallographic data for **9-13** are presented in Table VIa-b.

Table Va. Crystallographic data for compounds **3-6**.

Compd	**3**	**4**	**5**	**6**
CCDC No.	761885	761886	761887	761888
formula	$C_{15}H_{19}LaN_6O_{14}$	$C_{15}H_{19}CeN_6O_{14}$	$C_{15}H_{19}PrN_6O_{14}$	$C_{15}H_{19}NdN_6O_{14}$
formula wt	646.27	647.48	648.27	651.60
crystal system	Orthorhombic	Orthorhombic	Orthorhombic	Orthorhombic
space group	$P2_12_12_1$	$P2_12_12_1$	$P2_12_12_1$	$P2_12_12_1$
a/Å	11.865(5)	11.066(5)	11.079(5)	11.026(6)
b/Å	11.089(4)	11.783(8)	11.732(6)	11.788(6)
c/Å	17.730(7)	17.694(11)	17.570(10)	17.659(9)
V/Å^3	2332.7(15)	2307(2)	2284(2)	2295(2)
Z	4	4	4	4
D_{calcd}	1.840	1.864	1.885	1.886
μ	1.913	2.056	2.217	2.345
F_{000}	1280	1284	1288	1292
Data/ restraints/ parameters	4615/6/337	3251/3/349	3881/3/349	4584/3/349
S	0.982	1.112	1.132	1.134
R1	0.0262	0.0435	0.0396	0.0347

wR2 (all data)	0.0554	0.1114	0.1011	0.0713
max./min. residual electron dens. [eÅ^{-3}]	0.729/-0.523	1.574/-1.546	1.882/-1.451	0.708/-0.763

Table Vb. Crystallographic data for compounds **7-8**.

Compd	**7**	**8**
CCDC number	761889	761890
formula	$C_{15}H_{19}EuN_6O_{14}$	$C_{15}H_{19}GdN_6O_{14}$
formula wt	659.32	664.61
crystal system	Orthorhombic	Orthorhombic
space group	$P2_12_12_1$	$P2_12_12_1$
a/Å	11.010(2)	11.015(3)
b/Å	11.714(2)	11.709(4)
c/Å	17.579(3)	17.639(5)
V/Å^3	2267.1(7)	2275.0(12)
Z	4	4
D_{calcd}	1.932	1.940
μ	2.851	2.999
F_{000}	1304	1308
Data/ restraints/ parameters	4370/3/349	4469/3/349
S	1.051	1.109
R1	0.0176	0.0333
wR2 (all data)	0.0424	0.0826
max./min. residual electron dens. [eÅ^{-3}]	0.390/-0.569	0.975/-1.010

Table VIa. Crystallographic data for compounds **9-11**.

Compd	**9**	**10**	**11**
formula	$C_{42}H_{24}Sm_2N_6O_{24}$.$3H_2O$	$C_{42}H_{24}Gd_2N_6O_{24}$.$3H_2O$	$C_{42}H_{24}Eu_2N_6O_{24}$.$3H_2O$
formula wt	1351.44	1365.22	1354.66
crystal system	Triclinic	Triclinic	Triclinic
space group	$P\bar{1}$	$P\bar{1}$	$P\bar{1}$
a/Å	11.8534(8)	11.7835(9)	11.8238(8)
b/Å	13.4084(10)	13.4768(10)	13.4508(9)
c/Å	15.3103(11)	15.2486(11)	15.2917(11)
V/Å^3	2354.8(3)	2344.3(3)	2353.7(3)
Z	2	2	2
D_{calcd}	1.906	1.934	1.911
μ	2.573	2.909	2.744
F_{000}	1328.0	1336	1332.0
Data/ restraints/ parameters	8258/25/7244	8221/18/739	8222/18/739
S	1.081	1.013	1.008
R1	0.0380	0.0335	0.0385
wR2 (all data)	0.0902	0.0870	0.0956
max./min. residual electron dens. [eÅ^{-3}]	1.297/-0.606	1.481/-1.185	1.666/-0.927

Table VIb. Crystallographic data for compounds **12-14**.

Compd	**12**	**13**	**14**
formula	$C_{42}H_{24}Dy_2N_6O_{24}$.$3H_2O$	$C_{42}H_{24}Tb_2N_6O_{24}$.$3H_2O$	$C_{42}H_{24}Tm_2N_6O_{24}$.$3H_2O$
formula wt	1375.72	1368.56	1388.58
crystal system	Triclinic	Triclinic	Triclinic
space group	$P\bar{1}$	$P\bar{1}$	$P\bar{1}$
a/Å	11.7237(8)	11.7510(8)	11.633(5)
b/Å	13.5618(10)	13.5221(10)	13.651(6)
c/Å	15.1975(11)	15.2257(11)	15.131(6)
V/Å^3	2338.2(3)	2342.0(3)	2324.4(17)
Z	2	2	2
D_{calcd}	1.954	1.941	1.984
μ	3.276	3.100	3.898
F_{000}	1344.0	1340.0	1356.0
Data/ restraints/ parameters	8204/25/6963	8221/25/7173	8165/18/739
S	1.000	1.017	0.985
R1	0.0405	0.0333	0.0385
wR2 (all data)	0.1016	0.0828	0.0882
max./min. residual electron dens. [eÅ^{-3}]	1.447/-1.383	1.314/-0.753	1.112/-0.653

References

1) M. Soskic and A. Sabljic, *Pesticide Science (Croatia)*, 1995, **45,** 133, *Chem. Abstr*., 1995, **123**, 281275.

2) S.-I. Hirano, Y. Watanabe, K. Kominato, N. Agata, Y. Hara, N. Shibamoto, T. Yoshioka, T. Kioka, H. Iguchi, M. Shirai, H. Tone and R. Okamoto, *USP,* 1993, 5223519 [EP (1992) 491281]; *Chem. Abstr.,* 1992, **117**, 232209.

3) F. A. Cotton and L. D. Gage, *Inorg. Chem.,* 1979, **18**, 1716.

4) S. Chattopadhyay, P. E. Fanwick and R. A. Walton, *Inorg. Chim. Acta,* 2004, **357**, 764.

5) E.J. de Souza, V.M. Deflon, A.G. de A. Fernandes, S.S. Lemos, A. Hagenbach and U. Abram, *Inorg. Chim. Acta* 2006, **359**, 1513.

6) M. A. Chowdhury, F. Huq, A. Abdullah, P. Beale and K. Fisher, *J. Inorg. Biochem.,* 2005, **99**, 1098.

7) F. Huq, H. Tayyem, P. Beale and J.Q.Yu, *J. Inorg. Biochem.,* 2007, **101**, 30

8) A. Szorcsik, L. Nagy, M. Scopelliti, A. Deák, L. Pellerito, G. Galbács and M. Hered, *J. Organomet. Chem.,* 2006, **691**, 1622.

9) G. Mahata and K. Biradha, *Inorg. Chim. Acta,* 2007, **360**, 281.

10) S. McConnell, M. Motevalli and P. Thornton, *Polyhedron,* 1995, **14**, 459.

11) (a) S. Supriya and S. K. Das, *New J. Chem.,* 2003, **27**, 1568.
(b) S. Supriya and S. K. Das, *J. Am. Chem. Soc.,* 2007, **129**, 3464.

12) D. M. L. Goodgame, M. Lalia-Kantouri and D. J. Williams, *J. Crystallogr. Spectroscopic Res.,* 1993, **23**, 373.

13) S. Supriya, S. Manikumari, P. Raghavaiah and S. K. Das, *New J. Chem.,* 2003, **27**, 218.

14) M. L-Kantouri, *Transition Met. Chem.,* 1996*,* **21**, 491.

15) (a) J. Albertsson, *Acta Chem. Scand*., 1972, **26**, 1005.
(b) J. Albertsson, *Acta Chem. Scand*., 1972, **26**, 1023.

16) S. K. Ghosh and P. K. Bharadwaj, *Inorg. Chem.,* 2003, **42**, 8250.

17) C. B-Cabarrecq, J. D-Ghys, A. Fernandes, J. Jaud and J. C. Trombe*, Inorg. Chim. Acta,* 2008, **361**, 2909.

18) P. Guerriero, U. Casellato, S. Sitran and P. A. Vigato, *Inorg. Chim. Acta,* 1987, **133**, 337.

19) (a) P. A. Brayshaw, J. M. Harrowfield and A. N. Sobolev, *Acta Cryst.,* 1995, **C51**, 1799.

(b) J. M. Harrowfield, Y. Kim, B. W. Skelton and A. H. White, *Aust. J. Chem.,* 1995, **48**, 807.

20) S-H. Liu, Y-Z. Li and Q-J. Meng, *Acta Cryst.,* 2005, **E61**, m1111.

21) Y-P. Ren, L-S. Long, B-W. Mao, Y-Z. Yuan, R-B. Huang and L-S. Zheng, *Angew. Chem. Int. Ed.,* 2003, **42**, 532.

22) (a) L.-S. Long, X.-M. Chen, M.-L. Tong, Z.-G. Sun, Y.-P. Ren, R.-B. Huang and L.-S. Zheng, *J. Chem. Soc. Dalton Trans.,* 2001, 2888.

(b) S.-Y. Yang, L.-S. Long, R.-B. Huang and L.-S. Zheng, *Chem. Commun.,* 2002, 472.

(c) S.-Y. Yang, L.-S. Long, Y.-B. Jiang, R.-B. Huang and L.-S. Zheng, *Chem. Mater.,* 2002, **14**, 3229.

(d) M. J. Zaworotko, *Nature,* 1997, **386**, 220.

23) (a) S. S.-Y. Chui, S. M.-F. Lo, J. P. H. Charmant, A. G. Orpen and I. D. Williams, *Science,* 1999, **283**, 1148.

b) C. R. Kagan, D. B. Mitzi and C. D. Dimitrakopoulos, *Science,* 1999, **286**, 954.

24) (a) B. L. Chen, M. Eddaoudi, S. T. Hyde, M. O'Keeffe and O. M. Yaghi,

(b) M. Eddaoudi, J. Kim, N. Rosi, D. Vodak, J. Wachter, M. O'Keeffe and O. M. Yaghi, *Science,* 2002, **295**, 469.

25) B. Zhao, P. Cheng, Y. Dai, C. Cheng, D- Z. Liao, S-P. Yan, Z-H. Jiang and G-L. Wang, *Angew*. *Chem. Int. Ed.,* 2003, **42**, 934.

26) T. K. Prasad and M. V. Rajasekharan, *Crystal Growth & Design,* 2008, **8**, 1346.

27) (a) Z. Guo and P. J. Sadler, *Angew. Chem. Int. Ed.,* 1999, **38**, 1512.

(b) P. J. Sadler, *Adv. Inorg. Chem.,* 1991, **36**, 1.

28) P. J. Sadler in *Lectures in Bioinorganic Chemistry* (Eds.: M. Nicolini, L. Sindellari), Cortina, Verona, 1991, pp. 1-24

29) M. J. Abrams and B. A. Murrer, *Science,* 1993, **261**, 725.

30) See reviews on Bioinorganic Enzymology: *Chem. Rev.,* 1996, **96**, 2237.

31) (a) S. P. Fricker, *Chem. Soc. Rev.,* 2006, **35**, 524.

(b) K. Wang, Y. Cheng, X. Yang and R. Li, *Met. Ions Biol. Syst.*, 2003, **40**, 707.

32) C. H. Evans, *Trends Biochem. Sci.,* 1983, 445.

33) M. A. Jakupec, P. Unfried and B. K. Keppler, *Rev. Physiol. Biochem. Pharmacol.,* 2005, **153**, 101.

34) T. J. Haley, *J. Pharm. Sci.,* 1965, **54**, 663.

35) (a) E. J. Werner, A. Datta, C. J. Jocher and K. N. Raymond, *Angew. Chem. Int. Ed.,* 2008, **47**, 8568.
(b) R. B. Lauffer, *Chem. Rev.,* 1987, **87**, 901.

36) P. Caravan, J. Ellison, T. McMurry and R. Lauffer, *Chem. Rev.,* 1999, **99**, 2293.

37) E. Toth, L. Helm and A. E. Merbach, *Top. Curr. Chem.*, 2002, **221**, 61.

38) R. Ranganathan, N. Raju, H. Fan, X. Zhang, M. Tweedle, J. Desreux and V. Jacques, *Inorg. Chem.,* 2002, **41**, 6856.

39) For reviews on lanthanides in medicine/MRI imaging see, M. Bottrill, L. Kwok and N. J. Long, *Chem. Soc. Rev.,* 2006, **35**, 557.

40) F. Rosch and E. F-Aronsson, *Met. Ions Biol. Syst.,* 2004, **42**, 77.

41) A. M. Evens, *Curr. Opin. Oncol.,* 2004, **16**, 576.

42) (a) J. Chen, J. Ramos, M. Sirisawad, R. Miller and L. Naumovski, *Apoptosis,* 2005, **10**, 1131.
(b) S. W. Young, M. K. Sidhu and F. Qing, *Invest Radiol.,* 1994, **29**, 330.

43) S. W. Young, F. Qing, A. Harriman, *Proc. Natl. Acad. Sci. USA,* 1996, **93**, 6610.

44) D. Magda, C. Lepp, N. Gerasimchuk, *Int. J. Radiat. Oncol. Biol. Phys.* 2001, **51**, 1025.

45) R. A. Miller, K. W. Woodburn and Q. Fan, *Clin. Cancer Res.,* 2001, **7**, 3215.

46) S. Xu, K. Zakian and H. Thaler, *Int. J. Radiat. Oncol. Biol. Phys.,* 2001, **49**, 1381.

47) T. Sato, M. Hashizume, Y. Hotta and Y. Okahata, *BioMetals,* 1998, **11**, 107.

48) L. J. Anghileri, *Eur. J. Cancer.,* 1979, **15**, 1459.

49) Z. M. Wang, H. K. Lin, S. R. Zhu, T. F. Liu, Z. F. Zhou and Y. T. Chen, *Anti-Cancer Drug Des.,* 2000, **15**, 405.

50) P. Heffeter, M. A. Jakupec, W. Koerner, S. Wild, N. G. Von Keyserlingk, L. Elbling, H. Zorbas, A. Korynevska, S. Knasmueller, H. Sutterluety, M. Micksche, B. K. Keppler and W. Berger, *Biochem. Pharmacol.,* 2006, **71**, 426.

51) E. G. Behrens, F. M. Durville, R. C. Powell and D. H. Blackburgn. *Phy. Rev*., 1989, **39**, 6076.

52) I. Belharouak, P. Gravereau, C. Parent, J. P. Chaminade, E. Lebraud and G. Le Flem, *J. Solid State Chem*., 2000, **152**, 466.

53) V. Korthuis, N. Khosrovani, A. W. Slieght, N. Roberts, R. Dupree and W. W. Warren, *Chem. Mater.,* 1995, **7**, 412.

54) (a) S. K. Langley, B. Moubaraki and K. S. Murray, *Inorg. Chem*., 2012, **51**, 3947.

(b) L. Pellegatti, J. Zhang, B. Drahos, S. Villette, F. Suzenet, G. Guillaumet, S.Petoud and E. Toth, *Chem. Commun*., 2008, 6591.

55) B. Keshavan, P.G. Chandrashekara and N.M. Made Gowda, *J. Mol. Struct*., 2000, **553**, 193.

56) G. Rijulal and P. Indrasenan, *J. Rare Earths*, 2008, **26**, 315.

57) F. Tanaka and S. Yamashita, *Inorg. Chem*., 1984, **23**, 2044.

58) Y.-f. Chen and J. J. Dannenberg, *J. Am. Chem. Soc*., 2006, **128**, 8100.

59) J. P. H. Charmant, N. Norman and J. Starbuck, *Acta Crystallogr*., 2002, **E58**, M144.

60) It has been reported that the equilibrium of the tautomerization in aqueous solution favors the pyridone isomer for the 4-hydroxypyridine. See: C.-n. Chen, M.-c. Wu, A. Yeh and T. Y. R. Tsai, *Inorg. Chm. Acta*, 1998, **267**, 81.

61) E. G. Moore, J. Xu, C. J. Jocher, I. Castro-Rodriguez and K. N. Raymond, *Inorg. Chem*., 2008, **47**, 3105.

62) N. Xu, W. Shi, D.-Z. Liao, S.-P. Yan and P. Cheng, *Inorg. Chem*., 2008, **47**, 8748.

63) For further details on spontaneous resolution, see: N. N. Bhuvan Kumar and K. C. Kumara Swamy, *Tetrahedron Lett*., 2008, **49**, 7135.

64) (a) P. A. Brayshaw, A. K. Hall, W. T. A. Harrison, J. M. Harrowfield, D. Pearce, T. M. Shand, B. W. Skelton, C. R. Whitaker and A. H. White, *Eur. J. Inorg. Chem.,* 2005, 1127.

(b) B. Zhao, L. Yi, Y. Dai, X.-Y. Chen, P. Cheng, D- Z. Liao, S –P. Yan and Z.-H. Jiang, *Inorg. Chem*., 2005, **44**, 911.

(c) C. Reinhard and H. U. Gudel, *Inorg. Chem*., 2002, **41**, 1048.

(d) A. D'Ale´o, A. Picot, A. Beeby, J. A. G. Williams, B. L. Guennic, C. Andraud and O. Maury, *Inorg. Chem*., 2008, **47**, 10258.

65) (a) W. T. Carnall, P. R. Fields and K. Rajnak, *J. Chem. Phys*., 1968, **49**, 4412.

(b) T. Moeller, *J. Chem. Ed*., 1970, **47**, 417.

(c) W. T. Carnall, *Anal. Chem*., *1962*. **34**, 786.

(d) Z. A. Tahaa, A. M. Ajlounia, W. Al Momanib, A. A. Al-Ghzawia, *Spectrochim. Acta Part A,* 2011, **81**, 570.

66) (a) A. L. Jenkins and G. M. Murray, *J. Chem.Ed*., 1998, **75**, 227.

(b) Z. Xia, Q. Wei, Q.Yang, C. Qiao, S.Chen, G. Xie, G. Zhang, C. Zhou and S. Gao, *Cryst. Eng. Comm*., 2012, DOI: 10.1039/c2ce26120k.

67) A. M. Evens, P. Lecane, D. Magda, S. Prachand, S. Singhal, J. Nelson, R. A. Miller, R. B. Gartenhaus and L. I. Gordon, *BLOOD*, 2005, **105**, 1265.

68) J. P. Evans, F. Xu, M. Sirisawad, R. Miller, L. Naumovski and P. R. Ortiz de Montellano, *Mol. Pharmacol,* 2007, **71**, 193.